AD-A194 461 AFRRI (ARMED FORCES RADIOBIOLOGY RESEARCH INSTITUTE) 1/3
REPORTS OCTOBER NOVEMBER AND DECEMBER 1987(U) ARMED
FORCES RADIOBIOLOGY RESEARCH INST BETHESDA MD MAR 88
UNCLASSIFIED F/G 22/1 NL

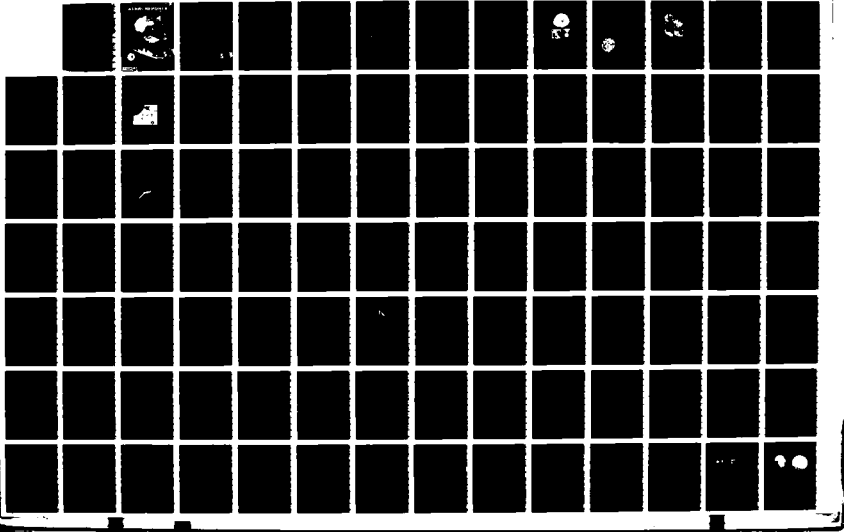

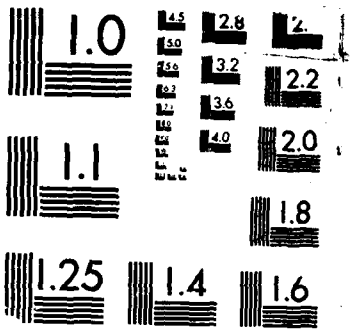

AFRRI REPORTS

AD-A194 461

October
November
December

1987

Defense Nuclear Agency

Armed Forces Radiobiology Research Institute

Bethesda, Maryland 20814-5145

REPORT DOCUMENTATION PAGE

1a. REPORT SECURITY CLASSIFICATION UNCLASSIFIED	1b. RESTRICTIVE MARKINGS
2a. SECURITY CLASSIFICATION AUTHORITY	3. DISTRIBUTION/AVAILABILITY OF REPORT Approved for public release; distribution unlimited.
2b. DECLASSIFICATION/DOWNGRADING SCHEDULE	
4. PERFORMING ORGANIZATION REPORT NUMBER(S) SR87-34 - SR87-49, TR87-1	5. MONITORING ORGANIZATION REPORT NUMBER(S)
6a. NAME OF PERFORMING ORGANIZATION Armed Forces Radiobiology Research Institute 6b. OFFICE SYMBOL (*If applicable*) AFRRI	7a. NAME OF MONITORING ORGANIZATION
6c. ADDRESS (*City, State and ZIP Code*) Defense Nuclear Agency Bethesda, Maryland 20814-5145	7b. ADDRESS (*City, State and ZIP Code*)
8a. NAME OF FUNDING/SPONSORING ORGANIZATION Defense Nuclear Agency 8b. OFFICE SYMBOL (*If applicable*) DNA	9. PROCUREMENT INSTRUMENT IDENTIFICATION NUMBER
8c. ADDRESS (*City, State and ZIP Code*) Washington, DC 20305	10. SOURCE OF FUNDING NOS. PROGRAM ELEMENT NO.: NWED QAXM PROJECT NO.: TASK NO.: WORK UNIT NO.:
11. TITLE (*Include Security Classification*) AFRRI Reports, Oct-Dec 1987	
12. PERSONAL AUTHOR(S)	
13a. TYPE OF REPORT Reprints/Technical 13b. TIME COVERED FROM _____ TO _____	14. DATE OF REPORT (*Yr., Mo., Day*) 1988 March 15. PAGE COUNT 205
16. SUPPLEMENTARY NOTATION	
17. COSATI CODES FIELD / GROUP / SUB. GR.	18. SUBJECT TERMS (*Continue on reverse if necessary and identify by block number*)

19. ABSTRACT (*Continue on reverse if necessary and identify by block number*)

This volume contains AFRRI Scientific Reports SR87-34 through SR87-49 and Technical Report TR87-1 for Oct-Dec 1987.

20. DISTRIBUTION/AVAILABILITY OF ABSTRACT UNCLASSIFIED/UNLIMITED ☐ SAME AS RPT. ☐ DTIC USERS ☐	21. ABSTRACT SECURITY CLASSIFICATION UNCLASSIFIED
22a. NAME OF RESPONSIBLE INDIVIDUAL Junith A. Van Deusen	22b. TELEPHONE NUMBER (*Include Area Code*) (202)295-3536 22c. OFFICE SYMBOL ISDP

Partial CONTENTS :

Scientific Reports

SR87-48: Tolliver, J. M., and Pellmar, T. C. Ionizing radiation alters neuronal excitability in hippocampal slices of the guinea pig.

SR87-49: Walden, T. L. A paradoxical role for eicosanoids: Radioprotectants and radiosensitizers.

Technical Reports

TR87-1: Dooley, M., and Zeman, G. H. Comparison of AFRRI and ETCA dosimetry measurements at AFRRI TRIGA reactor.

From: PROSTAGLANDIN AND LIPID METABOLISM IN RADIATION INJURY
Edited by Thomas L. Walden, Jr. and Haywood N. Hughes
(Plenum Publishing Corporation, 1987)

THE MAST CELL GRANULE: A PHOSPHOLIPID SOURCE FOR PROSTAGLANDIN SYNTHESIS

S. P. Chock and E. A. Schmauder-Chock

Experimental Hematology Department
Armed Forces Radiobiology Research Institute
Bethesda, Maryland 20814-5145

ABSTRACT

Phospholipid, the source of fatty-acid-derived mediators of the inflammatory response, such as prostaglandins, leukotrienes, thromboxanes, and other eicosanoids, has been localized in the mast cell secretory granule. This matrix-bound granule phospholipid accounts for about 50% of the total content of the mast cell phospholipid. Evidence for the presence of this phospholipid can be observed ultrastructurally in the form of micelles and vesicles when the granule is subjected to water infiltration. It is suggested that the spontaneous sequestration of phospholipid and other hydrophobic elements in response to water influx results in the formation of micelles of various sizes. The coalescence of micelles results in the formation of large spherical micellar aggregates and bilayer vesicles. Since granule matrix is extruded in conjunction with histamine release in radiation injury, this large quantity of matrix-bound phospholipid becomes an available source for eicosanoid synthesis.

INTRODUCTION

Many symptoms of radiation sickness are similar to the symptoms expressed in mast cell anaphylaxis. Histamine release has been implicated in radiation injury (1). The production of eicosanoids such as prostaglandins E_2 and $F_{2\alpha}$ and thromboxane B_2 have been detected in animals exposed to ionizing radiation (2). The formation of eicosanoids has also been observed following mast cell anaphylaxis (3). In spite of the coincidence, there has been no evidence directly linking the secretion of mast cells to the production of eicosanoids. Since arachidonic acid constitutes about 18.2% of the total mast cell phospholipid fatty acid (4), the release of phospholipid in conjunction with histamine release during radiation injury could serve as the source for the production of eicosanoids.

We recently found the presence of a large quantity of phospholipid in the mast cell secretory granule. This granule-bound phospholipid can be seen ultrastructurally in the forms of micellar structures and vesicles of various sizes when the granule is subjected to water infiltration. The extrusion of this huge phospholipid store into the interstitial space in conjunction with histamine release may provoke the synthesis of many fatty acid-derived eicosanoids and chemotactic factors by cells at the site of anaphylaxis.

MATERIALS AND METHODS

Rat peritoneal mast cells were purified according to Sullivan et al. (5). Granules were purified from mast cells by brief sonication pulses similar to those described by Amende and Donlon (6). The granule fraction was obtained by centrifugation of the 198 x g supernatant for 15 minutes at 1000 x g. After washing the granule twice with Hank's balanced salt solution without calcium and magnesium (HBSS), the granule pellet was resuspended in about 1 ml of HBSS. A 10-microliter aliquot was diluted for counting using a particle counter. The phospholipid was extracted exhaustively in a solvent mixture of chloroform:methanol:water (2:1:1). The phospholipid was measured using the micromethod of Vaskovsky et al. (7). Electron microscopy was carried out as described earlier (8). All reagents used were of analytical grade.

RESULTS AND DISCUSSION

Due to difficulty in obtaining purified quiescent mast cell granules, the phospholipid content of the granule has never been carefully evaluated. Purified mast cell granules usually exist in one of two forms: either the membrane-bound electron-dense quiescent form or the swollen dispersed "activated" form which usually contains no perigranular membrane (9). Activated granules have lost much of their matrix phospholipid due to the process known as *de novo* membrane generation (8). Based on ultrastructural observation, our granule preparation can contain up to 50% of activated granules. This preparation contained $1.97 \times 10^{-17} \pm 1 \times 10^{-17}$ (S.D.) mole phospholipid/granule as determined by method of Vaskovsky et al. (7). If we assume that the average phospholipid molecular weight is 800 daltons and that an average mast cell contains 1200 granules (10), the amount of phospholipid found in the granules would total 1.89×10^{-11} g/cell. This value compared to the total phospholipid value of 4.14×10^{-11} g/cell reported for the mast cell (4) means that about 50% of the total mast cell phospholipid was stored in the secretory granules. The presence of such a large amount of phospholipid in the granule was reflected in the large number of hydrophobic micellar structures seen with the electron microscope when the granule was subjected to water infiltration.

Figure 1 is an electron micrograph of a granule after its perigranular membrane has been removed by hypo-osmotic shock. Large bead-like micellar structures are

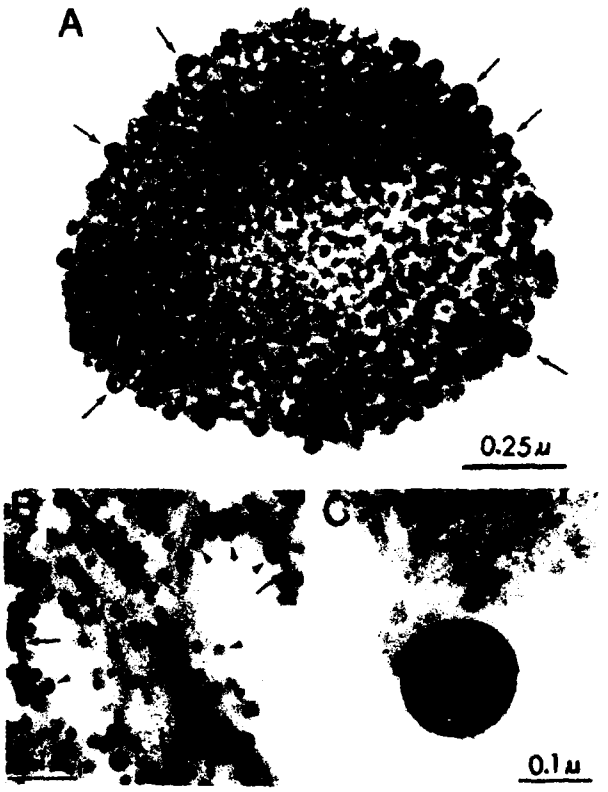

Fig. 1. Formation of micellar structures due to hydration. (A) Granule after membrane removal was exposed to water. Appearance of bead-like micellar structures (arrows) is most apparent at periphery. (B) Unraveling of demembraned granule by vortexing caused formation of small micellar structures (arrowheads) adhering to strands of proteoglycan backbone material (arrows). (C) Large bead-like structure, probably an aggregate of lipid material, can also be seen in close association with smaller micellar structures.

clearly seen in the periphery of the granule where water infiltration predominated (Fig. 1A). When a demembraned granule was further unraveled by vortexing in water, the appearance of small micellar structures was seen throughout and in association with the strand-like granule proteoglycan (or proteo-heparin) backbone material (Fig. 1B). The formation of these hydrophobic micellar structures was the result of the spontaneous sequestration of phospholipid into micelles in the presence of water. The coalescence of many small micelles into large bead-like spherical structures can be seen in Fig. 1C. When the coalescence of micelles results in the formation of bilayer vesicles, their insertion into the perigranular membrane enables the granule to enlarge during activation (8,11). When the granule was extracted with neutral detergent (Brij-56), all the micellar structures disappeared, leaving behind a spherical structure like a ball made of loose narrow ribbons (Fig.

2A). Further extraction of the granule with detergent caused the granule to unravel into strands of ribbon-like structure (Fig. 2B), which might be the proteo-heparin backbone material. This suggests that the granule was constructed by compressing strands of proteoglycan into a spherical structure to which phospholipid and other granule components were bound.

Figure 3A shows an activated granule unraveled after being extruded from a mast cell nearby during the process of rapid freezing and freeze-substitution. The presence of vesicles is also seen in association with the proteo-heparin strand. Under high magnification, small micellar structure can be seen decorating the proteo-heparin strand like a string of pearls (Fig. 3B). This structure might represent the same micellar structure found in the *in vitro* experiment described in Fig. 1B. This further supports our finding that phospholipid is a constituent of the mast cell granule.

Since the bulk of this granule-bound phospholipid was extruded with histamine during anaphylaxis and radiation injury, this large amount of phospholipid might provoke the synthesis of eicosanoids by the various cell types found near the site of anaphylaxis. The phagocytosis of the extruded mast cell granule by neutrophils, macrophages, or eosinophils could also lead to the production of various eicosanoids. The production of the different eicosanoids might serve as chemical mediators of the immune response process, or they might represent a system of cell communication.

Fig. 2. Removal of hydrophobic components with neutral detergent revealing basic structure of mast cell granule. (A) Granules extracted with 1% Brij-56 followed by brief heating resulted in removal of hydrophobic elements from dispersed granule structure. (B) Further heating and vortexing of detergent-extracted sample resulted in reducing granule matrix into strands of ribbon-like proteo-heparin.

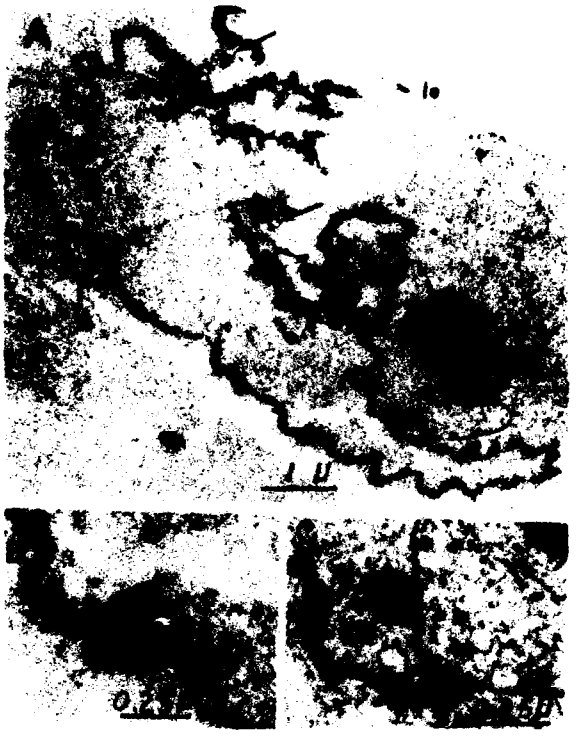

Fig. 3. Unraveling of a cold-activated granule following its extrusion from mast cell during rapid freezing and freeze-substitution. (A) Unraveling of an extruded granule also shows presence of vesicles (arrows) and smaller micellar structures in close association with strand of proteoglycan granule backbone. (B) Under higher magnification, small micellar structures (arrowheads) appear to adhere to strand of proteoglycan-like pearls on string. (C) Large electron-dense bead-like structure (b) of 170 nm can also be seen in association with backbone and a strand of electron-dense material (asterisk).

ACKNOWLEDGMENTS

Part of the data presented here have been submitted to the Department of Biology, The George Washington University, Washington, DC, as partial fulfillment for the degree of Doctor of Philosophy (E. A. S.-C.). Supported by the Armed Forces Radiobiology Research Institute, Defense Nuclear Agency, under work unit MJ00132. Views presented in this paper are those of the authors; no endorsement by the Defense Nuclear Agency has been given or should be inferred. Research was conducted according to the principles enunciated in the "Guide for the Care and Use of Laboratory Animals" prepared by the Institute of Laboratory Animal Resources, National Research Council.

REFERENCES

1. Doyle, T. F., and Strike, T. A. Radiation-released histamine in the rhesus monkey as modified by mast cell depletion and antihistamine. Scientific Report SR75-18. Armed Forces Radiobiology Research Institute, Bethesda, MD, 1975.
2. Donlon, M., Steel, L. K., Helgeson, E. A., Shipp, A., and Catravas, G. N. Radiation-induced alterations in prostaglandin excretion in the rat. Life Sci. 32: 2631-2639, 1983.

3. Metcalfe, D. D., Kaliner, M., and Donlon, M. A. The mast cell. CRC Crit. Rev. Immunol. 3: 23-74, 1981.
4. Strandberg, K., and Westerberg, S. Composition of phospholipids and phospholipid fatty acids in rat mast cells. Mol. Cell. Biochem. 11: 103-107, 1976.
5. Sullivan, T. J., Parker, K. L., Stenson, W., and Parker, C. W. Modulation of cyclic AMP in purified rat mast cells. J. Immunol. 114: 1473-1478, 1975.
6. Amende, L. M., and Donlon, M. A. Isolation of cellular membranes from rat mast cells. Biochim. Biophys. Acta 812: 713-720, 1985.
7. Vaskovsky, V. E., Kostetsky, E. Y., and Vasendin, I. M. A universal reagent for phospholipid analysis. J. Chromatogr. 114: 129-141, 1975.
8. Chock, S. P., and Schmauder-Chock, E. A. Evidence of *de novo* membrane generation in the mechanism of mast cell secretory granule activation. Biochem. Biophys. Res. Commun. 132: 134-139, 1985.
9. Uvnas, B. Mast cell granules. *In*: "The Secretory Granules." A. M. Poisner and J. M. Trifaro, eds. Elsevier Biomedical Press, Amsterdam, 1982, pp. 357-384.
10. Helander, F. H., and Bloom, G. D. Quantitative analysis of mast cell structure. J. Microsc. 100: 315-321, 1974.
11. Chock, S. P., and Chock, E. S. A two-stage fusion model for secretion. Fed. Proc. 44 (4): 1324, 1985.

Research Issues for Radiation Protection for Man during Prolonged Spaceflight[1]

JAMES J. CONKLIN[2]

ARMED FORCES RADIOBIOLOGY RESEARCH INSTITUTE
BETHESDA, MARYLAND 20814

AND

MICHAEL P. HAGAN

BAYLOR COLLEGE OF MEDICINE
HOUSTON, TEXAS

I. Introduction

It has been three decades since the Soviet cosmonaut Yuri Gagarin was rocketed into immortality as the first man in space. Remarkably, it has been nearly 20 years since Neal Armstrong and Buzz Aldrin demonstrated that man can explore near-Earth bodies, establishing the concept that planetary exploration is possible if man chooses to do so. Since then, groups of scientists from many nations have developed plans for manned orbital space stations.

[1]Views presented in this article are those of the authors. No endorsement by the Defense Nuclear Agency has been given or should be inferred.

[2]Present address: Centocor, Inc., Malvern, Pennsylvania 19355.

ADVANCES IN RADIATION BIOLOGY, VOL. 13

In July 1975, a successful Apollo–Soyuz Test Project (ASTP)[1] not only brought to a close the Apollo program but also inaugurated the era of international spaceflight. As the goals of the U.S. program then turned toward a permanent manned presence in space, the international commitment grew with it. To date, 96 astronauts, representing not only the United States but also Canada, France, Mexico, the Netherlands, Saudi Arabia, and West Germany, have flown shuttle missions. Arrested in 1986 by the disaster of *Challenger*, these flights will resume in the summer of 1988. By 1994, the construction of a space station will begin in low Earth orbit (LEO), and manned occupation is scheduled for 1995.

To operate successfully manned orbital space stations or to conduct planetary exploration requires an understanding of the radiation environment and the biological effects of space radiation. Since significant radiation hazards are known to exist in outer space in general and in certain orbits in particular, it is prudent to plan for the mitigation of these hazards. The biological significance of space radiation on astronaut performance and health must be understood. In addition, we must consider spaceflight conditions, both operational and physiological, which may exacerbate the effects of exposure to radiation.

Even as the radiobiology of space becomes known, other human factors continue to be of interest. It has been 7 years since Nelson and Andrews (1976) reviewed the potential protection of radiation accident victims in high-risk occupations (nuclear industry, nuclear Navy, astronauts) by autologous bone marrow transplants (ABMT). They raised several cogent objections to the use of ABMT in these accidental exposures. Among

[1]Abbreviations: ABMT, autologous bone marrow transplant(s); AD, autosomal dominant; AET, aminoethylisothiourea; AFB, Air Force Base; AL, anomalously large solar flare event; AR, autosomal recessive; ASTP, Apollo–Soyuz Test Project; BCG, Bacillus Calmette–Guérin; BMSC, bone marrow stem cells; BMT, bone marrow transplant; BRM, biologic response modifier; BrdUrd, bromodeoxyuridine; CFU, colony forming unit; cGy, centigray; CNS, central nervous system; CTZ, chemoreceptor trigger zone; DMF, dose modification factor; DNA, deoxyribonucleic acid; DRF, dose reduction factor; EACA, ε-aminocaproic acid; ED_{50}, 50% emesis dose; ET, endotoxin; ETI, early transient incapacitation; EVA, extravehicular activities; g/cm^2, gram of aluminum per square centimeter (a measure of shielding); GCR, galactic cosmic radiation; GEO, geosynchronous orbit; GI, gastrointestinal; GID, gastrointestinal dysfunction; GVHD, graft-versus-host disease; HLA, human leukocyte antigen; HZE, high charge and energy; IV, IP, intravenous, intraperitoneal; kW, kilowatt; LD_{50}, 50% lethal dose; LET, linear energy transfer; LPS, lipopolysaccharide; MDP, muramyldipeptide; MEA, mercaptoethylamine; MeV, million electron volts; NASA, National Aeronautics and Space Administration; OER, oxygen enhancement ratio; PD, performance decrement; PHA, phytohemagglutinin; PTH, parathyroid hormone; PvO_2, venous oxygen pressure; RBE, relative biological effectiveness; RCBP, regional cerebral blood flow; RES, reticuloendothelial system; RNA, ribose nucleic acid; SOLPRO, Solar Proton Model; SPE, solar particle event; STS, Space Transportation System; T65, 1965 dose estimate of Hiroshima/Nagasaki victims; XD, X-linked dominant; XR, X-linked recessive; Z, charge.

these objections were difficulty in certifying those at risk, cost of cryopreservation, discomfort and hazards of collection, anxiety in identified populations, and the fact that only a fraction of identified and subsequently exposed persons will use ABMT. Since then, much has been learned about bone marrow transplantation (BMT), as it has become a frequently performed clinical procedure. Significant changes have also occurred in the estimation of vulnerability and possible threat of exposure of U.S. astronauts to radiation in space, due to advances in our understanding of natural solar phenomena and to technological developments that pose man-made hazards. Although astronauts will still be few in number from an industrial standpoint, the extraordinary cost (economic, political, technological) of a manned space system requires that every method of protecting crews from hazards in space be evaluated. In this context, any technique that protects astronauts or allows the recovery or ensures the safety of the astronauts' spacecraft is potentially important. The protection of these invaluable resources requires adopting a truly holistic approach to radiation protection.

For the purpose of this article, we describe radiation protection provided by any physical, chemical, biological, or pharmacological modality that accomplishes the goal of protecting the astronaut from radiation hazard or increases his ability to assist other astronauts or spacecraft. Thoughtful examination of these largely operational considerations has led to identification of medical and radiobiological research required to support the industrialization of near-Earth space. The scope of these research efforts involves thematic issues that have been defined after review of the available preliminary research from several scientific disciplines that relate to the problem of radiation protection in space. The present article serves to highlight areas of research requiring further investigation. While certain of these needs for research are driven by the planned orbits involving small designated astronaut populations and well-defined durations that may be specific to the military, it is the use of geostationary orbits, permanent lunar basing, and the proposed Mars mission that form the primary basis for these operational considerations. The interested reader is referred to more comprehensive reviews of the biological significance of space radiation on manned spaceflights (Langham, 1967; Schambra *et al.*, 1967; Reetz and O'Brien, 1968; Tobias and Todd, 1974; and Calvin and Gazenko, 1975).

II. Space Radiation Environment

The radiation environment is a formidable challenge to man in his routine use of space. With much written about the potential exposure of man to space radiation (Langham, 1965; Reetz, 1965; Todd, 1983; Schimmerling

and Curtis, 1979; Benton and Henke, 1983), it is clear that the space radiation environment is complex. Between the launch of his craft and its attainment of geostationary orbit, an astronaut encounters trapped electrons and protons in the Earth's radiation belts; bremsstrahlung radiation from the interaction of particulate radiation with the spacecraft; the possibility of solar flares, which normally consist of protons, α particles, and particles of high charge and energy (HZE); galactic cosmic radiation (GCR), which includes protons and HZE particles; and man-made radiation such as an on-board nuclear reactor, other on-board radiation sources, and for military spacecraft the possibility of fast neutrons and γ rays from exoatmospheric nuclear weapons radiation (Hardy *et al.*, 1983). The hazards are schematically summarized in Fig. 1, while in Fig. 2 the near-Earth density of radiation flux is shown. The steady-state or constant radiation exposures from these sources have been reviewed; consequently, this article concentrates on mitigation of the acute effects of potentially high-dose exposures (Todd, 1983; Benton and Henke, 1983).

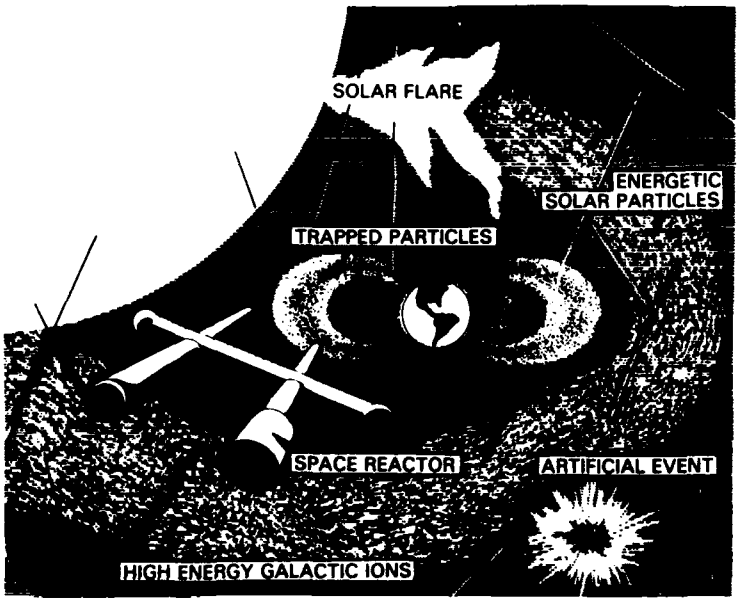

FIG. 1. Pictorial representation of the complex near-Earth radiation hazards to be faced by man in prolonged spaceflight. These hazards include particles produced by solar flares, space nuclear reactor irradiation (neutrons and photons), geomagnetically trapped particles (electrons and protons), artificial events (nuclear devices), and high-energy galactic cosmic rays.

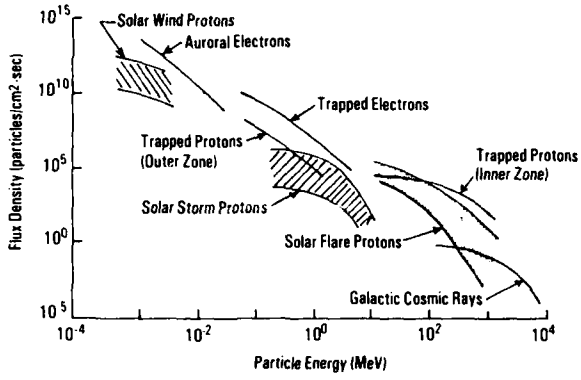

FIG. 2. Space radiation environment. Near-Earth particulate levels are shown in relation to incidence, energy, and source (Wilson, 1978.)

Figure 3 schematically shows the relationship of different Earth orbits for a space station to the strapped radiation belts. As you recall from Fig. 1, the radiation environment is even more complex than shown. Importantly, the low paraequatorial orbits can intersect the South American anomaly, but they are essentially protected from other natural radiation hazards. The polar orbits routinely intersect the horns of the geomagnetically trapped particles, as well as receiving 30–35% of the free space dose. Synchronous orbit spacecraft remain stationary over the same point on the Earth's surface. Here, a space station will see 100% of the free space dose (solar particles and GCR). Moreover, transit to and from the space station will be through the geomagnetically trapped radiation belts.

Historically, nearly all of the U.S. orbital space missions have flown in equatorial orbits, where radiation hazards are minimal. The exceptions to this have been the lunar missions, which ended a decade ago. By the late 1980s, the Space Shuttle, Space Transportation System (STS), will be launched into polar orbit from Vandenberg Air Force Base, California. Radiation exposure depends on altitude, inclination, shielding, and length of the mission. The polar orbit, involving decreased geomagnetic shielding, will expose crew members to approximately 30% of the free space radiation environment, more than 6-fold that seen at equatorial orbits (Hardy *et al.*, 1983). Future flights will increase the exposure even more as they involve increased altitude, inclination, and duration.

The exposure to a solar particle event (SPE) relative to free space varies with inclination, varying from 5% at 28.5° inclination to 35% at 90° inclination (Hardy *et al.*, 1983). On August 4, 1972, an unexpected SPE

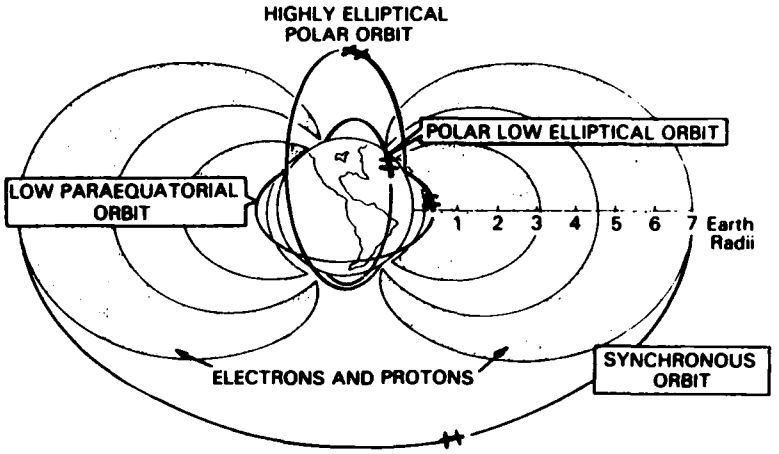

FIG. 3. Schematic representation of various types of orbits which have been flown by NASA or are planned by NASA during the next 20 years. Note that the intermediate altitude and low inclination (paraequatorial) orbits intersect primarily the geomagnetically trapped radiations. Polar orbits intersect the horns of the trapped radiation belts, and expose the spacecraft to the free space environment as well. The geosynchronous orbit is stationary over a fixed point on Earth and is exposed to 100% of the free space dose, as well as to the outermost geomagnetically trapped electrons and protons.

occurred, which would have exposed shuttle crew members in polar orbit to approximately 280 centigray (cGy) to the skin and 20 cGy to the bone marrow in less than 48 hr (Hardy *et al.*, 1983). If the United States had had a geosynchronous space station at that time, the radiation hazard would have been much greater. Current NASA plans are to have one space station in orbit by 1993 and three space stations by the year 2000, one of which will be in geosynchronous orbit (Loftus, 1983).

NASA plans also call for major increases in extravehicular activities (EVA) in space station missions for basic science and its applications, as well as for commercial and technological development activities (Loftus, 1983). EVA activities significantly increase the radiation hazard because of decreased shielding, vulnerability during the precursor irradiation associated with solar flares, and possible exposure to any space-station nuclear power source. Additionally, crews in geosynchronous orbit will not be able to be recovered immediately after a potential exposure.

To plan for long-duration spaceflight, Stassinopolous and his colleagues have developed a model to predict trends in solar flare activity. This model, called SOLPRO (Stassinopoulos and King, 1974; Stauber *et al.*, 1983), uses modified Poisson statistics to predict the probability of an anoma-

lously large solar flare event (AL) during solar maximum. Over the 5-year period during solar maximum, this model predicts four ALs with 89% confidence.

A. Solar Flares

Solar storms periodically emit bursts of energetic charged particles. These solar storms normally consist of protons (85%), α particles (5–10%), and HZE particles (5–10%) (Todd, 1983; Stauber *et al.*, 1983). The solar storm HZE flux around the Earth may increase by 3–4 orders of magnitude for hours or days. Over a 4-day period in July 1959, the total skin dose behind 1 cm^2 of shielding was estimated to be over 1000 cGy outside the Earth's magnetosphere (Curtis, 1974). Stassinopoulos (1979) has estimated that a 90-day stay in GEO during a large SPE could result in exposure to an HZE fluence of $3 \times 10^7/cm^2$. These anomalously large flares may have a proton flux of 10^{10} protons/cm^2 with energies above 20 MeV.

B. Geomagnetically Trapped Radiation

Outer-zone geomagnetically trapped protons are of low energy and thus of little importance for missions in geosynchronous orbits. This is not true for protons trapped in the inner zone (see Fig. 2). For several reasons, crew members in geosynchronous orbit are at more risk from the effects of radiation than those in other Earth orbits. At geosynchronous orbit, geomagnetically trapped electrons are a significant problem due to the continuous nature of the electron exposure and its short-term variability. Geomagnetically trapped electrons occupy an inner band (2.4 Earth radii) and outer band (2.8–12 Earth radii) (Stauber *et al.*, 1983). Because of solar activity, there is a strong dynamic character to the trapped particle fluxes in the outer band. Diurnal electron exposure intensity varies by a factor of 10, while 100-fold changes in electron flux occur from magnetic storm activity (Hardy *et al.*, 1983). The volatile nature of these geomagnetic changes can cause an order of magnitude change in flux within minutes (Lin and Anderson, 1966). In addition, a geosychronous orbit receives free space solar particle flux undeflected by Earth's geomagnetic shielding.

C. Galactic Cosmic Radiation

Radiation from outside the solar system is known as galactic cosmic radiation (GCR). It consists of protons (85%), α particles (14%), and HZE particles (1–2%) ranging in energy from 100 MeV to 10 GeV (Stauber *et*

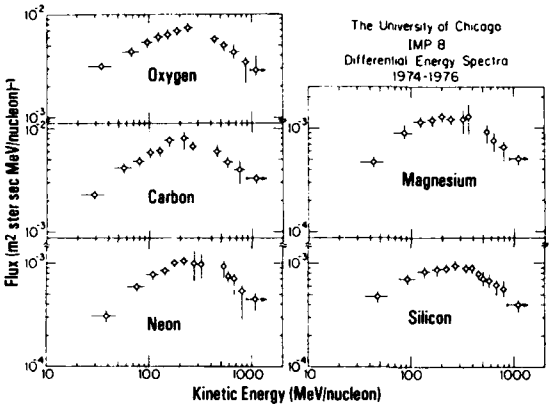

FIG. 4. Differential HZE spectra. Selected particulate spectra for HZE particles as measured by the IMP 8 telescope are shown (Wefel, 1978).

al., 1983). At geosynchronous orbit, the GCR is essentially isotropic. HZE particles (defined as those ions having a charge greater than 2 and an energy exceeding 50 MeV/nucleon) deposit energy as a function of the square of the charge (Z) and the inverse of the velocity (Todd, 1983). Consequently, even though they exist in low abundance, GCR particles with Z greater than 3 are responsible for an increasing percentage of dose (Curtis, 1974). Some of the data illustrating relative abundance of some of the more prevalent species are shown in Fig. 4. The flux–energy spectrum of GCR undergoes changes out of phase with the maximum peaks of activity in the solar cycle, doubling in intensity at solar minimum (Schaefer, 1968). This phenomenon is presumed to be caused by modulation of the interplanetary magnetic field from increased solar plasma flow, resulting in deflection of GCR at solar maximum. Although HZE particles normally are not a significant proportion of GCR fluence, they may have biological effects disproportionate to their total absorbed dose. They will be discussed in Section III, A.

Pion exposures are another potential problem at altitudes and geosynchronous orbits where human activities may be staged. As GCR enters the atmosphere, it collides with atmospheric nuclei and breaks into pions and protons (E. G. Stassinopoulos, personal communication). The pions subsequently decay into muons before striking the Earth (E. G. Stassinopoulos, personal communication). GCR traversing the shielding of the spacecraft will also produce secondary radiation consisting of HZE, pions, neutrons, and protons.

D. Man-Made Radiation Hazards

In 1962 the United States detonated a 1.4-megaton nuclear weapon exoatmospherically at 400 km over the Pacific Ocean (Teague and Stassinopoulos, 1972). Largely as a result of the β decay of fission fragments, 10^{27} electrons were released and geomagnetically captured at 3000–6000 km. The dose rate from these high-energy electrons was between 5 and 50 cGy/day. While the precise altitude of the electrons produced by a nuclear weapon depends on both the yield and the altitude of the burst, electron loading of the radiation belts can persist for months to years (Teague and Stassinopoulos, 1972).

Radioactive isotopes for experiments and nuclear reactors on board spacecraft for power may also represent serious radiation hazards. For example, the leakage radiation from a 100-kW fast nuclear reactor has been calculated to yield a total dose rate of 36×10^6 cGy/hr at 1 m from the core (Tobias and Grigor'yev, 1975; J. Sholtis, personal communication). Sufficient shielding via containment would require enormous masses; consequently, physical separation from the space station with several different geometry shields has been planned (Hardy *et al.*, 1983; J. Sholtis, personal communication). These fluences may result in significant hazards for certain EVA requirements and also present a hazard to the new EVA suit control-system microelectronics and to the astronaut. As an illustration, GCR has caused single-event upset phenomena in satellite microelectronics, resulting in errors and program failures in system microprocessors (Peterson, 1983).

E. Secondary Radiation

GCR, SPE protons, and geomagnetically trapped electrons and protons will interact with the spacecraft to produce secondary radiations (Schaefer, 1968; Tobias and Grigor'yev, 1975). The resulting dose buildup may be significant. For example, behind 2 cm^2 of aluminum spacecraft shielding, the dose is almost entirely due to bremsstrahlung radiation. In fact, in tissue the buildup factor for protons of 500 MeV is greater than 3 at a depth of 20 cm (Wilson and Khandelwals, 1976). The most significant radiation at GEO is the bremsstrahlung radiation caused by the interaction of outer-belt geomagnetic electrons with the spacecraft (Hardy *et al.*, 1983). Because of all of these facets, potential radiation exposure in geosynchronous orbit, polar low Earth orbit space stations, and future lunar or planetary missions, careful consideration must be given to radiation protection.

III. Response to Irradiation in Space

A. Cellular Radiobiology

For sparsely ionizing radiation, an understanding of the physiological consequences in irradiated mammals follows directly and relatively predictably from a knowledge of the underlying cellular damage. However, for the types of radiation encountered in space, this direct correlation may not exist or, at best, may be less obvious (as described below). For example, the distribution of cellular damage due to proton irradiation is highly energy dependent (Langham, 1967). In fact, both the total dose and the dose distribution within the proton-irradiated animal vary with the energy of the particle (Langham, 1967). As described above, the energy of protons of solar origin that are likely to be encountered in geostationary orbit can vary over several orders of magnitude. Further, HZE particles, although relatively few in number, can have physiological consequences far beyond a measure of their cell-killing properties. Although much of the evidence for these properties is incomplete by virtue of the newness of this field of study, trends have become apparent. In extrapolating the available data to man, the following introduction of the evidence for misrepair of lesions caused by high-linear energy transfer (LET) radiation and the disturbances in cell proliferation also associated with these lesions will undoubtedly be understated in some instances and overstated in others. In each case the details of the particle type, energy, flux, biological system investigated, and limited scope of available data should be noted, for it is these limitations that should drive current and future research.

1. Effects of High-LET Irradiation

HZE particles interact with tissue through a relatively uniform specific ionization until, slowing to a velocity permitting recombination, the particle experiences the sudden increase in specific ionization that gives rise to the "Bragg peak." In the region of this increase the aerobic relative biological effectiveness (RBE) for cell killing increases to a value between 3 and 5, depending on the level of the effect. The oxygen enhancement ratio (OER) decreases to a value typically between 1 and 2 (Blakely *et al.*, 1979). The particular values of RBE and OER at the Bragg peak are a function of the particle's charge, velocity, fragmentation pattern, and the oxygenic state of the cells encountered. However, along the plateau portion of the Bragg curve where ionization is related to a constant Z^2, the RBE for cell killing of several mammalian cell lines varies between 1 and 3 and the OER typically lies between 2 and 3 (Blakely *et al.*, 1984).

Once again, the specific values depend on the charge, velocity, and mass of the particle.

These variations in RBE and OER are quite important for the beams used for radiotherapy which initially are of a single species and are monoenergetic. In outer space, however, much of the specificity of the dose distribution will be lost, due to the spectrum of particle masses and energies. The net result will be an averaging of the individual physical beam characteristics and therefore also the associated RBE and OER values. However, for an exposure to HZE radiation it appears that not only the potential for cell killing is important but also the absence of recovery from that exposure.

For a specific particle, the RBE increases to a maximum as the linear energy transferred per unit particle track length (LET) increases. The RBE decreases with further increases in LET (Blakely *et al.*, 1979, 1984). When the same biological effect is plotted against the particle fluence instead of dose, evidence indicates that the biological effect increases asymptotically and then saturates with increasing LET (Kraft *et al.*, 1983, 1985; Wulf *et al.*, 1985).

For particles of high charge and energy, the physical manner in which the energy is deposited may be more significant than the average dose per gram of absorber. In addition to this lack of correlation between effect versus dose and effect versus particle fluence, two other biophysical properties of HZE irradiation are fundamentally important. First, the cross section for the killing of mammalian cells lies below the geometrical cross section, an indication of at least a subeffective lesion and perhaps, by extension, repair (Kiefer, 1984). Further, it has been shown that OER, which decreases at LET values near 100 keV/μm, increases again at much greater LET values, indicating that particle track structure may have unique effects at these extreme values of LET (Schopfer *et al.*, 1984; Blakely *et al.*, 1984; Barendsen *et al.*, 1966). Combined with physiological evidence for the recovery from cellular damage (evidence introduced below), these biophysical indications of subeffective lesions raise the possibilities that recovery from HZE irradiation occurs and may be due to the geometry of these lesions, qualitatively distinct from the recovery from sparsely ionizing radiation.

Cellular damage introduced by HZE irradiation is structurally correlated, a fact recognized as early as 1952 when Tobias *et al.* (1952) identified the "localized radiolesions" produced by high-energy particles. In the absence of cellular repair, this spatially correlated damage would be of principal interest at the tissue level of organization (e.g., fovea when considering vision). When the RBE could be estimated for the particular

spectrum of particle mass and energy the tissue damage would be completely described. However, in the presence of repair the actual extent of recovery of the cell may be significant. Currently, there is evidence not only for this recovery but also for the faulty repair of these lesions. As illustrated below, this faulty or misrepair may be of greater consequence than the original lesion.

2. *Evidence for Repair*

Much of our present-day understanding of the biological effects of particulate radiation that will be encountered in space has been developed from the study of cells in culture. This growing body of evidence involves the study of chromosome aberrations, mutational or transformational events, and cell killing, which are effects that result from exposure to HZE particles. Although radiobiological data involving proton irradiation are less abundant, evidence has been developed using monoenergetic proton beams as well as neutron irradiation. The neutron data are of direct interest for space in that the conversion of solar protons to neutrons is of special concern near the boundary of the ionosphere (Lundquist, 1979; Stassinopoulos, 1979). More importantly, for cellular effects, the data derived from neutron exposures of cells in liquid culture are of interest in that well over 90% of the dose under these conditions is produced from "knock-on" protons. As we shall see, the data from these experiments imply that biological repair—that is, repair or recovery that leads to increased cell survival—takes place after high-LET irradiation.

One classical demonstration of cellular repair has been the liquid holding recovery observed after incubating irradiated cells in a metabolically deprived state. The occurrence of this type of repair has been established after high-LET irradiation of either mammalian cells (Wheeler *et al.*, 1980; Guichard *et al.*, 1982) or yeast (Frankenberg-Schwager *et al.*, 1984). Indeed, a dose modification factor (DMF) greater than 1, the threshold for the demonstration of repair, has been observed even after eukaryotic cells were irradiated with uranium ions at an LET greater than 1600 keV/μm (Kiefer, 1984; Schopfer *et al.*, 1984). Chinese hamster cells (Ngo *et al.*, 1981), normal human lung fibroblasts (Ohno *et al.*, 1984), human T-1 cells (Blakely *et al.*, 1979), mouse BalbC 3T3 cells (Ngo *et al.*, 1981), cells grown in multicellular spheroids (Durand and Olive, 1976), *in situ* melanomas (Guichard *et al.*, 1982), and rhabdomyosarcoma cells carried "*in vivo*" (Afzal-Javad, 1985) have all shown indications of cellular recovery after high-LET irradiation. Moreover, under some circumstances, biological effects are amplified after low-dose or low-dose-rate exposures (we shall return to this point). Evidence for these effects, their implications

for the *in vivo* response to HZE or proton irradiation, and the corroborating *in vivo* data are detailed below.

In an elegant series of experiments involving high-LET irradiation (Frankenberg-Schwager *et al.*, 1984), it was demonstrated that cell survival in *Saccharomyces cerevisiae* was dependent on the ability of these cells to repair double-strand breaks. The survival curves in Fig. 5 illustrate the demonstrable reduction in survival observed when cells that were temperature-sensitive for the repair of double-strand breaks were incubated at the nonpermissive temperature. The repair of strand breaks after high-LET irradiation has also been demonstrated directly by Keng *et al.* (1983) through the use of sedimentation studies. Moreover, studying DNA damage at the level of the chromosome, Geard (1985) has shown that it is more likely that multiple aberrations will occur for a single high-LET particle than will cell killing for the same particle fluence, mass, and velocity.

At the cellular level, repair is indicated both by the presence of liquid holding recovery which can be inhibited by β-Ara-A (Iliakis, 1980) and by the synergism shown to occur during the combined treatment of mammalian cells with HZE and X-irradiations (Ngo *et al.*, 1981; Blakely *et al.*, 1985). Further, caffeine, an inhibitor of postreplication repair in mammalian cells, reduces the DMF resulting from liquid holding. Finally, concerning this question of interaction between low-LET and high-LET radiations, Yang and Tobias (1984) have observed that a conditioning dose

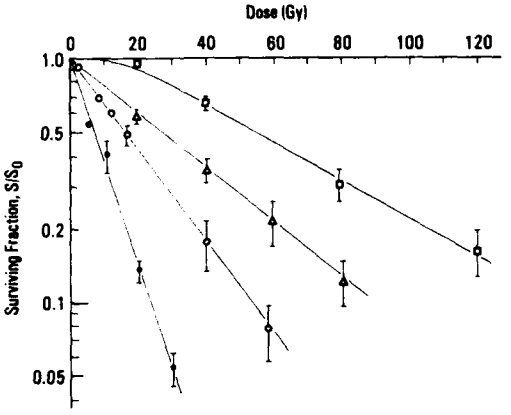

FIG. 5. Effects of inhibition of double-strand break (DSB) repair on recovery of yeast after irradiation with α particles. (●) No DSB repair; (○) DSB repair plus 0 hr of liquid holding; (△) DSB repair plus 24 hr liquid holding; (□) DSB repair plus 72 hr liquid holding (Frankenberg-Schwager *et al.*, 1984).

of X rays increases the capacity of C3H10T½ cells to survive and resist viral transformation after high-LET irradiation.

Part of the explanation of the mechanism by which these modest but definite indications of repair may translate into significant effects for an irradiated animal is revealed by comparing the induction by high-LET irradiation of chromosome aberrations, cell cycle delay, and cell survival. Cell cycle delay can be so marked after high-LET irradiation that at least one group has been prompted to title an article "Drastic G_2 Arrest . . ." (Lucke-Huhle *et al.*, 1979). In fact, Geard (1980) has argued that the traversal of a cell or nucleus by a single particle may induce significant progression delay. For sparsely ionizing radiation, division delay for mammalian cells in culture is roughly equal to 1 hr/Gy (Elkind *et al.*, 1963). However, for high-LET irradiation, α particles (for example, a 0.3-Gy dose) may induce a delay as long as 22–30 hr. Associated with this increased sensitivity is also a marked change in the age–response pattern. That is, the cell cycle pattern for division delay after high-LET irradiation appears to be qualitatively distinct from that observed after sparsely ionizing irradiation. Largely reflecting a more significant delay of cell irradiation during the G_2 phase, these differences in the age response for delay have been measured for Chinese hamster cells (Ngo, 1980), human T-1 cells (Blakely *et al.*, 1985), mouse L929 cells (Sasaki, 1984), and HeLa cells (Lucke-Huhle *et al.*, 1984).

Having previously noted that individual particles of high-LET radiation are more likely to produce multiple chromosome aberrations than cell death, we now have two qualitatively distinct forms of cell injury that are disproportionately increased after high-LET irradiation. Unfortunately, at present little is known of either the physiological consequences or the underlying molecular mechanisms of division delay.

3. Changes in Patterns of Proliferation

The coordination of cell proliferation in response to stress, however, is a precisely controlled event in regenerative tissues. For example, hydroxyurea, a powerful recruiter of quiescent cells within the bone marrow, is completely without effect if RNA synthesis is blocked for even a few hours after the hydroxyurea insult (Feher and Gidali, 1980). This control can be critical. For example, when proliferation is manipulated in a positive sense, as in the recruitment of granulocytes and macrophages by immunomodulators administered within a few hours of irradiation, a significant increase is produced in the subsequent peripheral population of these cells and the survival of the animal is enhanced (Patchen and MacVittie, 1983). The recruitment of stem cells into active proliferation appears to be im-

portant for the gut as well. Evidence has been presented by Potten and Hendry (1983) that subpopulations of gut stem cells exhibit differences in radiosensitivity and that resistant cells can be stimulated to enter the sensitive population.

Not only is proliferation highly controlled, but also this control appears to be particularly sensitive to irradiation with particles of high-LET. Hanson (1984), investigating the recruitment of stem cells in the gut, has shown that for 14-MeV neutron radiation, doses as low as 0.20 Gy will induce cycling in the small bowel. Changes in the relative numbers of specific subpopulations may also play a role in testes irradiated with charged particles. Investigating the effects of various HZE particle masses and energies, Alpen and Powers-Risius (1981) found that alterations in testis weight were dependent on particle mass even for constant-LET. Apropos to the consideration of radiation to be encountered in space, it has been recently observed that even though the induction of a chronic increase in proliferation of marrow stem cells requires high fluences, low fluences of high-LET radiation acutely stimulate normally quiescent marrow stem cells into cycle. Figure 6 shows that spleen colony-forming units (CFUs) derived from bone marrow may be acutely stimulated to cycle by 0.8–1.0 Gy of ^{60}Co γ-radiation. However, even the lowest doses of ^{56}Fe ion radiation

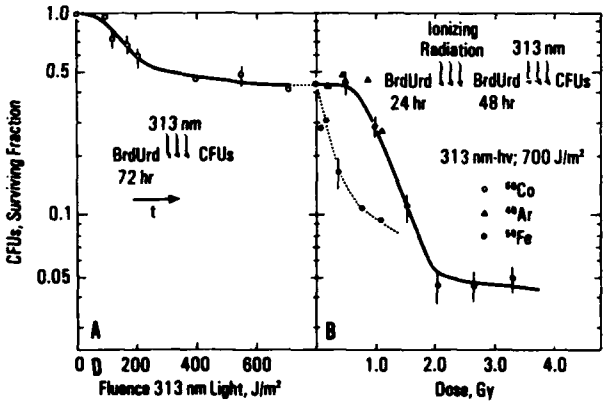

FIG. 6. Bone marrow proliferation stimulated with ionizing radiation. Increased cell killing results from incorporation of BrdUrd during normal proliferation (A). When proliferation is stimulated (B), the level of killing increases, reflecting the increase in the proliferative fraction. In each case, proliferation has been measured over a 72-hr period. For data in (B), an exposure to whole-body radiation preceded the final 48 hr.

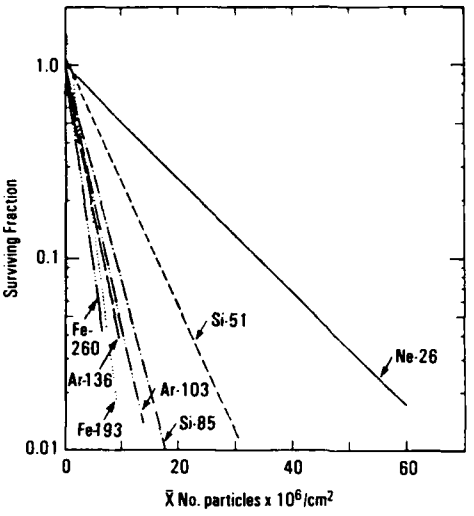

FIG. 7. Survival of CFUs after HZE irradiation. Survival curves for spleen colony forming units (CFUs) is plotted as a function of dose or particle flux (Ainsworth *et al.*, 1984).

induced the CFUs to cycle, shown here by an increase in the uptake of the DNA substituent bromodeoxyuridine (BrdUrd) (M. Hagan, unpublished results). However, the cell survival data shown in Fig. 7 (Ainsworth *et al.*, 1984; Afzaland and Ainsworth, 1987) demonstrate (as indicated above for chromosome aberrations and for cell cycle delay) that the mechanism which produces cell killing cannot account for this proliferative stimulus.

4. *Evidence for Misrepair*

Evidence for aberrant recovery, or "misrepair" of high-LET-induced cell damage, comes from several sources. Hill *et al.* (1982) have described conditions for low dose-rate exposure to fission neutrons under which neoplastic transformation is actually enhanced. These results are compared in Fig. 8 with similar effects reported by Ullrich for the induction of mammary lung adenocarcinomas (Ullrich, 1984). A similar low-dose phenomenon has also been reported for the induction of tumors of the Harderian gland (Fry *et al.*, 1983). As can be seen from the survival data in Fig. 9, once again cell survival cannot account for the effect. A paradoxical increased effect after fractionation has also been observed by Grahn and colleagues (Thomson *et al.*, 1981, 1985) and by Storer and Ullrich (1983) for life span shortening in mice, an end point that largely reflects the total increase in tumor incidence for a population. At present, these demon-

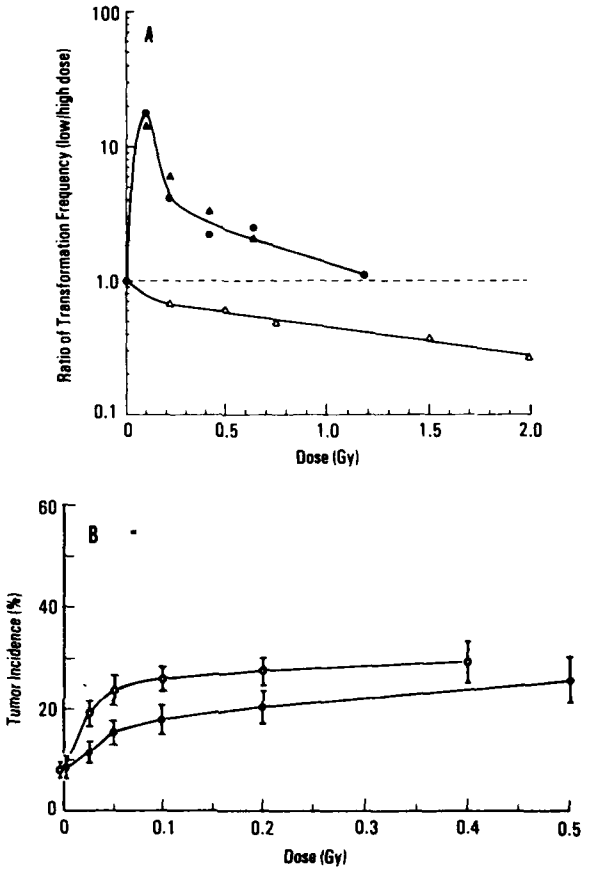

FIG. 8. (A) Increase in transformation of 10T½ cells after low-dose rate irradiation with fission-spectrum neutrons (Hill *et al.*, 1982). △, 0.1 cGy/min (^{60}Co-γ); ●, 0.086 cGy/min; ▲, 0.43 cGy/min. (B) Tumor incidence has also been shown to increase after low dose-rate neutron irradiation. Here mammary adenocarcinoma is shown to increase at low dose and low dose rate after neutron irradiation (Ullrich, 1984). ○, 0.00083 cGy/min; ●, 0.0083 cGy/min.

strations of increased likelihood of tumor induction at low doses and hence the paradoxical fractionation effect are understood only at the phenomenological level. No molecular mechanism has been shown or suggested.

5. Dose Distribution

As mentioned earlier, both the dose and the dose distribution in a proton-irradiated animal are highly dependent on the energy spectrum of the proton source (Langham, 1967). This situation is the basis for the use of

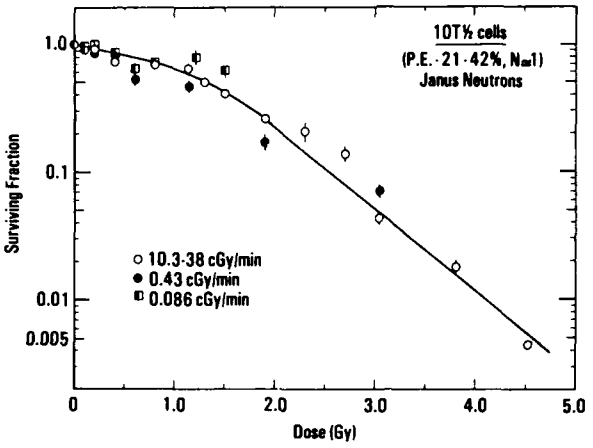

FIG. 9. Dose-rate independence of the survival of 10T½ cells after irradiation with fission-spectrum neutrons (Hill *et al.*, 1982).

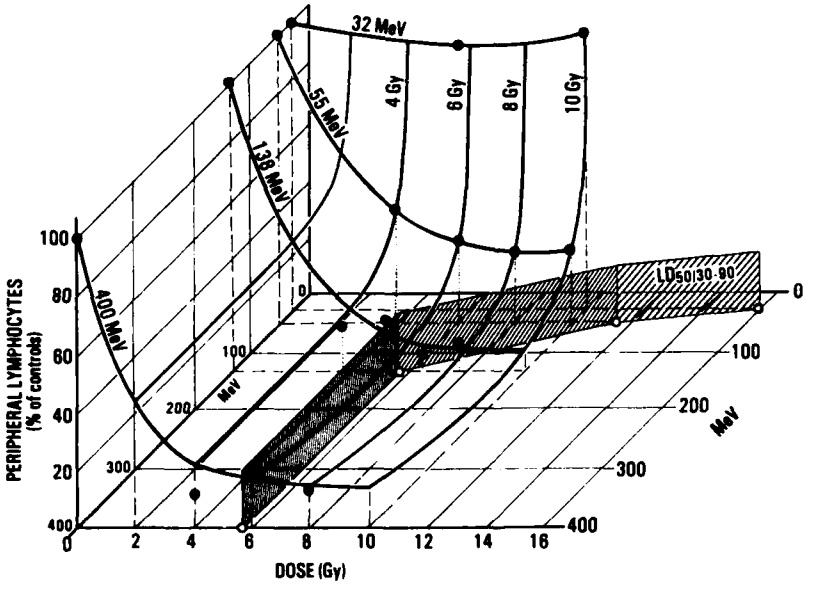

FIG. 10. Comparison of the peripheral lymphocyte count with $LD_{50/30-90}$ following proton irradiation. The peripheral count, taken at the nadir after exposure to a monoenergetic beam of protons is plotted as a function of dose and energy. The $LD_{50/30-90}$ data were taken from the same irradiated population (Dalrymple *et al.*, 1965).

proton beams in radiotherapy, and it is an equally important consideration for irradiation in space. Protons of solar origin (solar wind) or trapped in the outer zone are of such low energy that the spacesuit alone would provide adequate shielding. Protons emitted during an SPE or accelerated within the inner zone, however, are energetic enough to be of concern even through several g/cm^2 of Al equivalent shielding.

Studies performed at the U.S. Air Force School of Aerospace Medicine have revealed how the occurrence of bone marrow depression in primates responds to changes in fluence or energy. The data in Fig. 10 relate the LD_{50} to depression of peripheral lymphocytes. The sharply descending curve between 55 and 138 MeV coincides with an obvious change in mechanism for the LD_{50}, and it correlates well with the energy range in which full-thickness penetration occurs for these primates. The most likely conclusion is that, for large doses of proton irradiation, marrow involvement will dominate the response only for the hardest of spectra to be encountered in space. Corroboration of this result has been provided in part by the mortality studies reported by Ashikawa *et al.* (1964), who observed that mice irradiated with a 730-MeV proton source or with a degraded source (240 MeV) died disproportionately from gastrointestinal injury. The pattern of mortality compared with mortality after X-irradiation is shown in Fig. 11.

The cellular radiobiology described in the foregoing has been concerned with the sources of high-LET radiation found in space. In point of fact, normal spaceflight operations will encounter electron irradiation both in geostationary orbit and during the transfer between geostationary and low-

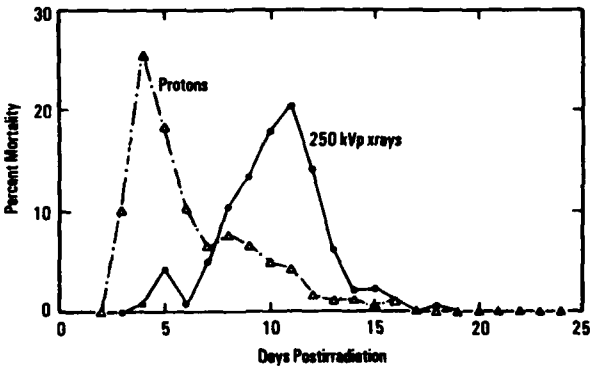

FIG. 11. The pattern of mortality after an exposure of mice to a 98% lethal dose of either proton or X-radiation (Ashikawa *et al.*, 1964).

Earth orbits. In these trajectories, incident radiation within the spacecraft will result primarily from the associated bremsstrahlung. While certainly nontrivial, these radiations are susceptible to routine shielding. HZE particles and high fluences of energetic protons will not be so easily eliminated. For HZE particles and protons of high energy, the significant cellular aspects are the misrepair of high-LET lesions, disturbances in cell proliferation, and energy dependence of the distribution of damaged cells after proton irradiation. Faulty repair may underly the increase in tumorigenesis, and it may be a major occupational concern. Increases in steady-state proliferation of the gut or marrow need to be explored. Certainly if these increases occur, their importance for the immune response, inflammatory processes, drug interactions, and aging must be examined. Also requiring examination is the dominance of gut injury due to the heterogeneity of the dose distributions likely to be encountered in space, which presents the interesting result that therapy for gut injury may be important (and immunomodulation less so). Of probable concern also will be the occurrence of microlesions in discrete sites of neurofunction or in single neuron pathways. Perhaps the single most apparent conclusion from examination of the available cellular data is that a vast amount of work is left to be done.

B. Hematopoietic System

1. Hemopoietic and Immune Responses to Sepsis following Irradiation

Ionizing radiation compromises the natural defenses against infectious disease, endogenous intestinal microflora, and associated toxins (Walker and Porvaznik, 1978). An early phase of nonspecific cell-mediated resistance plays a vital role in the first line of defense against bacterial disease. Numerous murine and canine models have been developed in which these defense mechanisms may be analyzed for radiosensitivity, enhancement of the cell-mediated resistance phase, and stimulation of the bone marrow-derived precursors that are responsible for replenishing the mature, functional end cells necessary for ultimate recovery from the effects of radiation and the infectious process. Our understanding of the mechanisms involved in these model systems will aid greatly in developing effective treatment regimens for the infectious processes resulting from combined injuries in the irradiated animal. Undoubtedly, the understanding of combined injuries will be important for spaceflight as well. Studies continue in the search for agents that will selectively enhance the recovery of the marrow stem-cell population and the cell-mediated immune system, both of which ultimately help determine the survival of the irradiated and/or combined-

injured animal. Of specific interest are biological response modifiers (BRMs) such as detoxified endotoxin, muramyldipeptide (MDP), interleukin-1, thymosin, and the yeast cell wall component glucan (a linked polyglycan).

2. *Modulation of Hemopoietic and Immune Function*

Many drugs and biological substances have been shown to stimulate hemopoiesis and/or the immune system in normal and in irradiated animals. Endotoxin (lipopolysaccharide), *Corynebacterium parvum*, Bacillus Calmette–Guérin (BCG), levamisole, and glucan are a few of the better characterized hemomodulating and/or immunomodulating agents. Although many agents have been shown to be effective in the murine model, their toxicity in the doses needed for therapeutic efficacy in the larger animals (dog, monkey, and human) has made them ineffective. Research continues on the detoxification methods for active BRMs as well as novel ways to present the substance to target cells. A possible approach is the use of liposomes, in which the encapsulated substance is directed to reactive target cells such as the monocytes and macrophages of the reticuloendothelial system (RES) while bypassing other reactive cells that would initiate the toxic reactions.

Glucan, a particularly interesting agent because of its ability to stimulate hemopoiesis as well as the RES, significantly enhances hemopoietic repopulation in irradiated mice (Patchen and MacVittie, 1983). A drawback to the use of glucan, namely, its particulate nature, has been recently eliminated with the availability of a soluble form (Patchen *et al.*, 1984). As can be seen from the data in Table I, either preadministration or

TABLE I

EFFECTS OF POLYGLYCANS ON ENDOGENOUS COLONY FORMATION (E-CFU) WHEN ADMINISTERED 1 hr BEFORE OR AFTER 6.5 Gy COBALT-60 RADIATION[a]

Sample	Compound	E-CFU[b]	Enhancement
Control	Saline	4.5 (1.2)	1.0
Rx preirradiation	Glucan-F[c]	21.1 (3.6)	4.7
	Glucan-P	17.8 (2.1)	4.0
Rx postirradiation	Glucan-F	17.6 (1.8)	3.9
	Glucan-P	14.8 (2.3)	3.3

[a] From Patchen *et al.* (1984).

[b] Standard deviations are shown in parentheses.

[c] Glucan-F is a soluble polyglycan, while Glucan-P refers to the particulate preparation.

administration after the radiation exposure enhances hemopoietic recovery. Further, the soluble form provides no less an enhancement. Another substance that has shown an unusual ability to stimulate hemopoietic activity in normal and irradiated mice is endotoxin bound with the antibiotic polymyxin B sulfate. The polymyxin binds the lipid A portion of the lipopolysaccharide (LPS) molecule, purportedly inhibiting the mitogenic effect of LPS. Preliminary experiments by Walker *et al.* (1984) demonstrated a stimulatory effect on hemopoietic precursors far above that induced by the native LPS molecule.

3. Infection

Infections, usually of intestinal origin, are often lethal when associated with radiation doses that cause hematopoietic depression. Hematopoietic depression also increases the likelihood of other opportunistic infections. For example, in the second week after exposure to nuclear weapons at Hiroshima and Nagasaki, exposed individuals showed heavily infected, ulcerated lesions of the skin, mucous membranes, and respiratory tract (Liebow *et al.*, 1949). Likewise, the increasing incidence of microorganisms in normally sterile tissues of irradiated animals was observed to occur in parallel with, but preceding, an increase in mortality (Miller *et al.*, 1950; Walker and Porvaznik, 1983). In fact, animals given midlethal doses of irradiation survived only when infections failed to develop. Microorganisms were also seen growing freely in postmortem histological specimens taken from victims of the atomic bombs at Hiroshima and Nagasaki.

Abnormal colonization, another effect of ionizing radiation, appears to be associated with lethality. Previous work (Porvaznik *et al.*, 1979) has shown that some populations of endogenous flora are quickly lost in rats given a lethal dose of radiation, and the flora are not regained before death. During this period of recolonization, opportunistic pathogens overgrow the ileum of moribund animals. In rats given sublethal radiation (5.0 Gy), however, endogenous flora are lost but return before overgrowth by pathogens (Walker and Porvaznik, 1983). Infection occurring after irradiation may be a consequence of this abnormal colonization of mucosal surfaces as well as the suppression of systemic immunological defenses. To target those immunological deficiencies noted as most readily amenable to corrective actions, it is essential to discover which immunological compromises and mucosal abnormalities most directly lead to infection. This information will be valuable not only in predicting the risk of infection but also in preventing and treating infection.

The role of various microorganisms present in the mixed infections

seen after irradiation is poorly understood. For example, little is known of the mechanisms through which some organisms produce enzymes that either protect otherwise susceptible pathogens against antibiotic therapy or impair the phagocytic removal of otherwise susceptible bacteria. Also poorly understood are the mechanisms by which pathogens occurring in the immunocompromised host use virulence factors to facilitate infection at particular times after injury. Some pathogens may have binding characteristics that enable them to colonize in greater numbers on the mucosal surfaces of radiation victims than on the nonirradiated mucosa (Walker *et al.*, 1985). In addition, it appears that the integrity of the mucous blanket is associated with radiation-induced infection (Walker *et al.*, 1985).

C. Gastrointestinal System

The crypt cells of the small intestine, which are nearly as radiosensitive as the stem cells of the bone marrow, play a significant role in determining survival after exposure to high doses of radiation. Although the proliferative status of the stem cells (crypt cells) of the intestine is uncertain (Potten *et al.*, 1984), there is agreement that alteration in this proliferative status may profoundly affect radiosensitivity. The size of the microlesion produced by HZE particles, the dose distribution resulting from an exposure to protons, and the proliferative effects of high-LET irradiation all point to the likelihood of increased gut injury. At doses of approximately 1 Gy, gastrointestinal (GI) disturbances result from decreased cell production in crypts of the small intestine, resulting in partial denudation of the intestinal lining (Conard *et al.*, 1956; Tori and Gasbarrini, 1963). If crypt cells are stimulated to cycle by low doses of either low-LET or high-LET radiation, the kinetics and relative proportions of the various radiosensitive components change (Potten *et al.*, 1984). The data presented in Fig. 12 clearly exemplify this stimulatory effect. Here, mice exposed to radiation doses below 1 Gy become increasingly more susceptible to vincristine, a cell cycle-specific toxic agent, reflecting the increased proportion of cycling clonogenic cells (Potten *et al.*, 1984). At higher doses, epithelial cell tight junctions may be disrupted, creating a portal by which bacterial endotoxins and gut microflora may gain entry to the systemic circulation (Walker and Porvaznik, 1983).

Radiation doses delivering more than approximately 8 Gy to the human gastrointestinal crypts cause significant destruction of the epithelium (Quastler, 1956). With the GI transport epithelium normally replaced on a 5- to 8-day cycle, radiation inactivation of intestinal stem cells prevents the replacement of mature transport epithelium as cells are sloughed off from the tips of the villi. Complete destruction of the crypt stem cells will

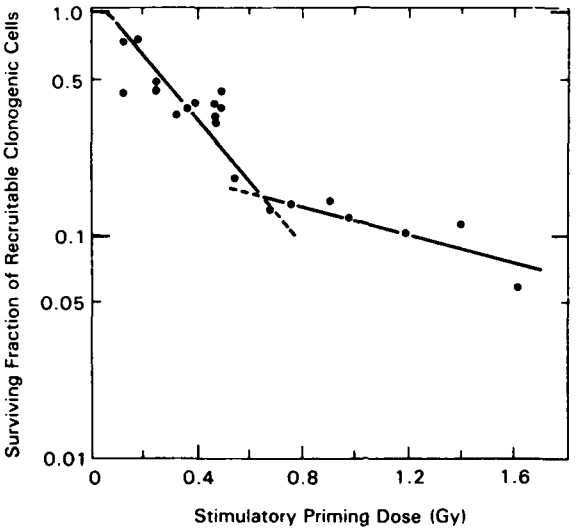

FIG. 12. Surviving fraction of 14% of cells not killed by vincristine treatment (12 hr) and 11 Gy of γ rays (^{137}Cs, about 4.4 Gy/min) is plotted against dose of radiation required to recruit them into cycle and so be killed by vincristine treatment. (After Potten *et al.*, 1984.)

result in total loss of GI transport capability within the first week after exposure to radiation. Clinically, this loss of transport epithelium function results in diarrhea and loss of fluid and electrolytes. Other stigmata include severe vomiting, hemorrhagic diarrhea, malabsorption, paralytic ileus, and renal insufficiency. At these doses of radiation, which are sufficient to cause the gastrointestinal syndrome (5-day lethality), bacteremia and endotoxemia do not appear to be lethal but the loss of fluid and electrolytes do (Geraci *et al.*, 1985). Thus, acute shock secondary to the extreme fluid loss will present the most life-threatening challenge.

The more acute symptomatic effects occurring in the gastrointestinal system, even after doses as low as 2–5 Gy, may quickly incapacitate the exposed astronaut. This incapacitation will no doubt be exacerbated by two other factors: (1) astronauts are usually in negative fluid balance for the first 6 weeks in weightlessness and (2) emesis induced by space sickness and emesis induced by radiation may share a common pathogenesis. A synergy between motion sickness and radiation-induced emesis has been demonstrated in preliminary experiments by H. Borison (personal communication). Both the onset and severity of nausea and vomiting are dose related to a considerable degree, and they may be expected to occur within

the first few hours postexposure. Obviously, these effects would interfere promptly with individual and crew performances. Thus it is extremely important to the accomplishment of missions in space to prevent these attacks, attenuate them, or delay their onset. Regrettably, little is known of the mechanisms of postirradiation gastrointestinal dysfunction.

1. Radiation-Induced Gastroenteritis during the Prodromal Period

The role of the prodromal effects of ionizing radiation in producing performance decrement in personnel is not clearly established, and the mechanism by which nausea and vomiting are produced by irradiation is also not clear. There are indications that vomiting may be triggered by irradiation of either the head or the torso, that the mechanisms by which these two types of vomiting are produced are different, and that neutrons and photons differ in their ability to cause vomiting after irradiation of the head or the trunk (Grant *et al.*, 1979; Middleton and Young, 1975). No prodromal symptom dose–response data exist for the particulate radiation encountered in space.

Vomiting is a complex, multilevel physiological act that requires the relaxation of esophageal and stomach smooth muscles and the concomitant contraction of skeletal muscles of the abdomen, thorax, and diaphragm. This response can be modified by drugs whose site of action is the chemoreceptor trigger zone (CTZ) in the lateral segment of the area postrema and the vomiting center found near the fasciculus solitarius (Browne and Sparks, 1961). Vomiting can be initiated by humoral stimuli to the CTZ, while the vomiting zone receives neural stimuli (autonomic) from the GI tract, vestibular apparatus, and possibly the CTZ. The precise etiology of this response has not been elucidated, but complex interactions participate in radioemesis (Grallo *et al.*, 1979). Studies performed at the USAF School of Aerospace Medicine (Cooper and Mattson, 1979) showed the efficacy of chlorpromazine, promethazine, cimetidine, and thiethylperazine in preventing radioemesis in canines. They found the emesis dose for 50% (ED_{50}) in the dog to be 170 ± 38.5 cGy cobalt-60 radiation. The ED_{50} dose was doubled when several of the agents were administered.

The primary disadvantage of many of the antiemetics is their neurological side effects. Wood *et al.* (1984) studied the performance of several antiemetics, using a computerized "pursuit meter" (evaluating manual dexterity and reactions) as a test device. Scopolamine produced no performance decrement (PD), whereas proficiency was reduced with promethazine. The PD from promethazine could be ablated with *d*-amphetamine, although the occurrence of drowsiness was unchanged.

Domperidone is a peripheral dopamine antagonist that has demon-

strated efficacy in preventing vomiting secondary to a variety of situations: postoperative, chemotherapeutic, pediatric, migraine, and hemodialytic (Reyntjens, 1981). Recent studies have demonstrated the prevention of radioemesis in 90% of dogs exposed to 800 rads total-body cobalt-60 (Dubois *et al.*, 1981). These studies have been extended to subhuman primates after irradiation, where the drug was ineffective. This points out the importance of using drugs with demonstrated efficacy in humans whenever possible. More recently, the central dopamine antagonist metoclopropamide has demonstrated significant antiemetic efficacy postirradiation in subhuman primates (Dubois *et al.*, 1984).

It is now recognized that histamine, which is released secondary to irradiation, plays a major role in the systemic manifestations of radiation injury (Doyle and Strike, 1975; Turns *et al.*, 1971; Mickley *et al.*, 1982). For example, histamine induces the secretion of gastric acid, which is not blocked by conventional histamine antagonists. Research in recent years has produced evidence of at least two types of receptors for histamine. They are the sites affected by conventional "antihistamine" drugs, now designated "H_1" receptors, and those in the gastric mucosa, "H_2" receptors. Several new drugs block the H_2 receptors of histamine and could therefore inhibit the gastric secretion that normally ensues from histamine released in the irradiated person. What is not known is whether the blocking of H_2 receptors will decrease radiation-induced nausea and vomiting (Chapman and Young, 1968). The H_2 blockers (cimetidine, ranitidine) are effective orally, and their use in a space environment is feasible.

In relation to cancer chemotherapy, it has been found that marijuana provides protection from vomiting, and appears to be better than other antinausea drugs. Although performance and cognitive impairment may preclude the use of marijuana, the mechanism of its antiemetic properties merits further study (Montgomery, 1978).

Evidence exists that prostaglandin inhibition of gastric secretion is not related to interference with the H_2 receptor (Wollen *et al.*, 1974). Thus, the possibility of agonist or synergistic effects of these newer compounds needs to be evaluated, especially in conjunction with H_2 antagonists. In addition to increases in histamine and prostaglandins postirradiation, marked increase in β-endorphins, decrease in electrical activity, decrease in gastric emptying, and reduced output of gastric acid are all postirradiation sequelae (Danquechin-Dorval *et al.*, 1984a; Laporte *et al.*, 1984). Whether these changes are paraphenomena or are responsible for the prodrome is the subject of intense investigation.

Recent studies showing a radiation-induced decrease in the integrity of intestinal-cell tight junctions suggest that agents which increase the integrity of these junctions may also be useful in alleviating radiation-

induced diarrhea (Porvaznik, 1979; Erilij and Martinez-Palomo, 1978; Bentzel and Hainau, 1979). It should also be noted that hypersecretion into the intestinal lumen associated with diarrhea may itself trigger nausea and vomiting (Rubin and Hopkins, 1984). Part of this diarrheal response postirradiation is secretory in nature occurring because normally absorptive epithelial cells become secretory (P. Gunter-Smith, personal communication). In addition, several studies (Jackson and Entenman, 1959; Sullivan, 1962) have shown that bile salts exacerbate diarrhea associated with radiation enteritis. Berk and Seay (1972) have suggested that the diarrhea may be related to radiation injury of the terminal ileum; such damage results in failure to reabsorb bile salts. This suggestion is quite reasonable as bile salts increase both colonic motility and water secretion when they are not 90% removed in the terminal ileum (Hofman, 1967). Related to this, Berk and Seay (1972) also showed that cholestyramine could reduce the mortality in radiation enteritis in experimental animals. Cholestyramine, a quaternary nitrogen anion-exchange resin that irreversibly binds bile salts, has been used to control choleraic-like diarrhea associated with several disease states (Thompson, 1971). Hevsinkveld *et al.*, (1978) extended these observation in humans suffering refractory radiation-induced diarrhea after high-dose pelvic irradiation.

Also of potential importance is the role of other luminal contents in the pathogenesis of radiation enteritis. Mulholland *et al.* (1983) have evaluated the empty intestine, the intestine containing pancreatic secretion, and the intestine containing bile salts and all other normal luminal contents. Using quantitative histochemical techniques, these investigators showed that injury occurred progressively, with the least injury in the empty bowel, next least in the bowel containing pancreatic secretions, then the bowel containing bile and other luminal constituents except pancreatic secretions, and finally the greatest injury in the bowel containing all normal constituents. Of the individual constituents, bile salt was the most potent augmentor of injury.

Mennies *et al.* (1975) observed that acetylsalicylate decreased radiation-induced enteritis, while prostaglandins produced diarrhea. Using a lethal abdominal irradiation model in the female Sprague–Dawley rat, (J. P. Delaney personal communication) found that intraperitoneally injected indomethacin (a prostaglandin synthetase inhibitor) converted a 100% lethal abdominal radiation dose to a 6% lethal dose. A dose of 4 mg/kg of indomethacin resulted in increase in survival, and the intestine, when histochemically scored, showed much less radiation injury. These observations need to be extended and confirmed; but if validated, this intervention combined with cholestyramine may offer a real advance in the treatment of radiation enteritis. Confounding these data is the obser-

vation by Hanson (1984) that certain prostaglandins protect intestinal stem cells from the cell-killing properties of ionizing radiation. Recent experiments by Geraci *et al.* (1985) suggest that the most important factor influencing GI syndrome lethality in neutron-irradiated rats is not the accumulation of bile salts but rather the loss of fluids and electrolytes into the bowel lumen.

It is apparent that the successful treatment of the irradiated person will require a combination of treatment regimens. With high doses of γ- or X-radiation (Maisin *et al.*, 1971; Quastler, 1956) and considerably lower doses of neutron irradiation (Bond, 1964; Geraci *et al.*, 1975; Otto and Pfeiffer, 1972), the electrolyte loss and bacterial toxemia associated with the gastrointestinal system appear to have greater consequences than does damage to various other organ systems such as the hematopoietic system. Bacterial toxemia resulting from radiation-induced breakdown in the integrity of the intestinal mucosa may contribute to the lethality. Studies at the cellular level have revealed a decrease in the structural integrity of the tight junctional complex in mice with doses as low as 200 cGy whole-body γ-radiation (Porvaznik, 1979). In addition, very recent *(in vivo)* studies indicate histopathological damage of the supralethally irradiated canine intestinal mucosa at 2 hr postirradiation in the presence of increased submucosal blood flow and absence of ischemia (Cockerham *et al.*, 1984). These studies implicate a rapid effect of radiation on the intestinal integrity, most likely mediated either by a humoral agent or by indirect damage secondary to ischemia.

D. Microvascular and Central Nervous Systems

Radiation exposures greatly in excess of those causing the gastrointestinal syndrome cause increases in vascular permeability (Fanger and Lushbaugh, 1967). This results in extensive extravasation of intravascular fluids and in inability to maintain blood pressure and tissue perfusion, despite volume replacement and the use of pressor drugs. Severe nausea, vomiting, and explosive diarrhea occur within minutes to several hours after irradiation. Malaise, weakness, ataxia, and seizures may also occur. Death resulting from subsequent intractable shock will ensue within hours to several days.

Many tasks to be performed by astronauts require stamina, involving demanding physical and cognitive skills. Data from animal studies and from radiation accidents involving humans have shown that the maintenance of cardiovascular function is of prime importance in determining postirradiation performance and survival. Even minimal decreases in car-

diovascular function may result in substandard cognitive performance and thus, in space, have the potential for severe consequences. Factors that may be responsible for derangements in cardiovascular function include direct vascular tissue damage, effects of vasoactive substances, and disruption in tissue metabolism. Postirradiation cardiovascular sequelae manifest themselves as a radiation shock syndrome, which in many ways is similar to other types of cardiovascular shock (hemorrhagic, endotoxic, and traumatic). In addition to direct tissue damage, these forms of circulatory shock have been shown to depend on the release of vasoactive substances (e.g., neurotensin, histamine, endogenous opiate peptides, and prostaglandins) and disruption in tissue metabolism. Although pharmacological intervention has been shown to reduce radiation-induced cardiovascular dysfunction, elimination of the sequelae and elucidation of the mechanisms have not been accomplished.

Since it was first recognized that histamine is released postirradiation and plays a significant role in the systemic manifestation of radiation injuries (Doyle *et al.*, 1971; Doyle and Strike, 1975, 1977; Carpenter, 1979), many pathophysiological responses associated with high-dose irradiation have been found to be mediated, at least in part, by histamine; these include early transient incapacitation (ETI), performance decrement (PD), hypotension, and gastrointestinal dysfunction (GID) (Doyle *et al.*, 1974; Doyle and Strike, 1975). Moreover, histamine antagonists, although they do not prevent these responses, can attenuate some of the effects of radiation (Doyle *et al.*, 1973). Second- and third-generation antihistamines need to be rigorously studied postirradiation.

Cardiovascular deconditioning during spaceflight is a well-described physiological response to weightlessness (Levy and Talbot, 1983). The cardiovascular instability that occurs immediately after landing results from resumption of the upright posture which causes orthostatic hypotension, tachycardia, decreased pulse pressure, presyncope, diminished exercise capacity, and impaired locomotion (Sandler, 1980). Of more concern for a potentially irradiated astronaut is the cephalic translocation of blood and fluid, resulting in vascular congestion in the head and neck, and the reduction in total blood volume (Levy and Talbot, 1983). It is postulated that as much as 2 liters of fluid shifts into the compliant pulmonary, cardiac, and systemic venous systems. This has several important sequelae: the increased right atrial pressure results in a marked diuresis, and the cephalic fluid redistribution causes increased transcapillary pressure gradients and probably increased cerebrospinal fluid pressure (Epstein, 1978).

In a series of elegant experiments, Casarett and colleagues (Eddy and Casarett, 1966; Casarett and Eddy, 1970; Kurohara and Casarett, 1972;

Eassa and Casarett, 1973; Ullrich and Casarett, 1977; Ballelos and Casarett, in press) showed that ionizing radiation induced hyperfibrinolytic activity and microvascular damage and increased endothelial permeability in several types of tissues including lung, heart, skin, skeletal muscle, intestine, kidney, liver, pancreas, and spleen. Because of the variety of tissues affected, it is reasonable to presume that the central nervous system (CNS) would have behaved similarly. Impairment of microcirculation secondary to radiation, when coupled with the cephalic redistribution of body fluid in weightlessness, may seriously compromise organ function. It is easy to speculate that these microvascular changes resulting from high doses of radiation may produce altered judgment, disorientation, and reduced physical capability, all of which are critical for space operation.

Casarett and colleagues (Eassa and Casarett, 1973; Ballelos and Casarett, in press) found that ε-amino-*n*-caproic acid (EACA) given in doses of 300 mg/kg in several species reversed the acute and delayed CNS effects. Specifically, a single administration of EACA (IV, IP, or per os) shortly before or after exposure to ionizing radiation precluded or diminished both the fibrinolytic effects of radiation and the early and delayed increases in endothelial permeability, fluid extravasation, and inflammation. Although this type of therapy would not be expected to alter late mortality, it may allow the exposed crew member to remain competent to save lives or recover the vehicle.

Early transient incapacitation (ETI) is the complete cessation of performance during the first 30 min after radiation exposure. Performance decrement (PD) is a reduction in performance ability observed at any time after irradiation. The etiology of ETI/PD has long been correlated with the hypotensive response after high-dose radiation (Carpenter, 1979). Until recently, it was not clear whether there is a concomitant decrease in regional cerebral blood flow (RCBF). Recent experiments (Cockerham *et al.*, 1984; Doyle *et al.*, 1984) in the subhuman primate showed significant decreases in RCBF in the supraoptic nucleus of the hypothalamus and postcentral gyrus of the cerebral cortex, as measured by the hydrogen polarograph method. These investigators have also shown a loss of RCBF autoregulation postirradiation. The precise mediators of these postirradiation changes are unclear; however, significant postirradiation changes in prostaglandin E_2, thromboxane B_2, histamine, and β-endorphins have been observed (Cockerham *et al.*, 1984; Doyle *et al.*, 1984; Steel and Catravas, 1982; Donlon *et al.*, 1983). The mast-cell histamine-release inhibitor disodium chromoglycate has been shown to inhibit histamine release, but it was unable to mitigate the motor PD in rats after high-dose radiation exposures (Hampton *et al.*, 1983).

E. High-LET Radiobiology

The radiobiology of high-LET irradiation differs significantly from low-LET irradiation, as described earlier. Sinclair (1983) recently reviewed RBEs for cytogenetic effects, mutations, transformation of cultured mammalian cells, tumor induction, and life shortening after neutron exposure. He noted that low-LET effects are smaller when the dose is protracted by a decreased dose rate or fractionation. This is not true for neutrons, where the RBE increases for a number of end points with decreasing dose rate (Sinclair, 1983). In fact, for some end points, the RBE at protracted dose rates is between 30 and 50 (Sinclair, 1983). Much of what is currently known of high-LET radiobiology has been obtained from neutron studies. By examining these data, some of the specific differences between high-LET and low-LET radiobiology will become apparent. There are also some direct reasons for briefly discussing data involving neutrons: (1) neutrons may be in the astronaut's environment from nuclear power sources or artificial events, (2) recoil neutrons from high-energy particles interact with spacecraft shielding, (3) for neutron exposure, a large fraction of the energy deposited in tissue derives from "knock-on" protons, and (4) high-energy protons, such as those accelerated by the inner belt, produce neutrons upon interaction with atmospheric gases.

The important differences in the biophysical action of neutrons compared to low-LET irradiation have been comprehensively reviewed elsewhere (Kellerer and Rossi, 1972). Likewise, the cellular radiobiological characteristics of neutron irradiation have been introduced above. Acute effects of any of the space radiations will have to be dealt with if the dose is high, and although the radiations may have different potencies the interventions will be the same. It is when we consider late effects (e.g., carcinogenesis, teratogenesis, cataractogenesis, and life shortening) that there is a significant quantitative difference between low- and high-LET radiations. The increasing RBE recently seen with decreasing dose rates of neutrons warns us to carefully evaluate protracted exposures of HZE particles.

The RBE of neutrons has been a hotly contested scientific question (Hall, 1978; Radford, 1980). For example, several investigators (Rossi, 1980; Fabrikant, 1980; Radford, 1980) have written disclaimers on the subject of RBE to the conclusions of the BEIR III report (NRC, 1980). More importantly, since the T65 human dose estimates at Hiroshima and Nagasaki have recently been questioned (Marshall, 1981), a greater reliance must now be placed on experimental animal results.

As early as 1939, when the Lawrence cyclotron at Berkeley, California,

became available for medical use, neutron therapy was used in the treatment of cancer (Stone and Larkin, 1942; Stone *et al.*, 1940; Stone, 1948). During a 5-year period, 226 patients were treated. This study concluded that although fast neutrons could eradicate cancer, the late effects on normal tissue were more severe than expected. When Stone and Larkin's results (1942) were evaluated, the data indicated that the California patients had been overexposed with respect to certain radiobiological factors unknown at the time.

Radiobiological experiments using the Berkeley cyclotron (Axelrod *et al.*, 1941) showed neutrons to be more effective than X rays by a factor as great as 11 for end points such as leukopenia and tumor growth. Broerse and colleagues (1968) showed that the RBE of fast neutrons increases with decreasing neutron energy, a fact confirmed by Carsten and colleagues (1976), using six different monoenergetic neutron beams and two fission spectra. Carsten *et al.* (1976) found that the RBE for monoenergetic fast neutrons for marrow stem-cell depression did not vary appreciably over the energy range of 0.43 to 1.8 MeV. For 5.7- and 13.4-MeV neutrons, however, a drop in RBE was noted. The existence of energy dependence is quite important, as there may be a broad spectrum of neutron energies encountered in the spacecraft environment either from solar proton conversion or from emissions from power reactors.

1. Mortality Studies of Animals after Neutron Exposures

The RBE values of neutrons generally observed in mortality studies are lower than those in experiments involving the inactivation of single cells. Of 20 studies cited in a paper by Otto and Pfeiffer (1972), the RBE values vary from 1.05 to 7.0; in 13 of these studies, RBE values are below 2.00. The discrepancies among the reported values may be explained by variations in neutron energy; differences and uncertainties in neutron dosimetry; differences in animal strain, sex, and age; differences in animal maintenance and exposure conditions; and differences in type, energy, and dose rate of the reference radiation.

The RBEs of fission neutrons for intestinal death or hematopoietic death for guinea pig, rabbit, sheep, and goat have been obtained (Carsten *et al.*, 1976; Gordon, 1975; Otto and Pfeiffer, 1972; Batchelor *et al.*, 1966; Edmondson and Batchelor, 1971). Species variations are considerable, with the larger animals having the lower RBE values, which may be related to the change in the neutron spectrum and the neutron-to-γ ratio with depth dose. On several occasions, the neutron-irradiated animals tended to die earlier than those irradiated with X rays or gamma rays, and the average survival time after neutron irradiation increased with neutron en-

ergy (Earle *et al.*, 1971). However, these are not consistent findings (Broerse *et al.*, 1978). Taking into account the self-shielding factors for neutrons and X rays in goat, an RBE value of 3 was calculated for damage of hematological tissue (Edmondson and Batchelor, 1971). Broerse *et al.* (1978) found an RBE of approximately 2 for occurrence of the bone marrow syndrome in rhesus monkeys, by comparing X rays and fission neutrons with a mean energy of 1 MeV.

The late effects of high-LET irradiation was also the subject of a long-term study conducted in conjunction with George Washington University (Alderson *et al.*, 1979; Bradley *et al.*, 1979), a study that evaluated the comparison of cobalt-60 irradiation with 15-MeV neutrons. The initial group of animals, used in a variety of studies, yielded a wealth of information on the late effects of 15-MeV neutrons on lung, heart, brain, spinal cord, and liver (Bradley *et al.*, 1978, 1979; Zook *et al.*, 1980; Conklin *et al.*, 1982; Bradley and Zook, 1979; Rogers and Bradley, 1977). Some of the more salient conclusions of these studies are as follows: (1) When the dome of the liver was in the hemithorax radiation port, hepatic necrosis caused a high mortality among the neutron-irradiated dogs. (2) Neutron-irradiated dogs showed significant cardiovascular effects, including intimal fibrosis, medial thickening and calcification, disruption and duplication of the elastic lamina, and formation of atheromatous plaque. (3) Microvascular derangements were seen in skeletal muscle, pulmonary parenchyma (the largest vascular bed), and the CNS. Other changes included hemorrhage, necrosis, fibrosis, and vascular damage. All of these changes were significantly worse in the neutron-irradiated dogs. Regardless of the methodology of computing RBE in the lung, the values obtained were always consistently between 4 and 6. There was also a high incidence of cancer in the 15-MeV irradiated animals, with very short latency periods and significant late tissue effects of neutrons, implying that misrepair may be important for these exposures.

2. *Behavior, Performance, and Central Nervous System Function*

Since man has evolved in a low-radiation environment he should have a low neurobiological and behavioral tolerance to ionizing radiation. In fact, the nervous system (described as radioresistant) has more recently been found to be quite susceptible to functional alterations produced by even low doses of radiation. The opening and closing of neuronal sodium and potassium channels is the basis of all nervous function. After doses of 1 Gy or more of high-energy electrons, one of the basic processes of neuroexcitiation, sodium ion flux, is significantly disrupted (Wixon and Hunt, 1983). The necessary increases of sodium ions into neurons are

reduced by radiation in a dose-dependent manner, suggesting that there are fewer sodium channels remaining functional. Similarly, synaptic transmission involving the neurotransmitters acetylcholine and dopamine are significantly altered by ionizing radiation exposure (Davydov, 1961; Hunt *et al.*, 1979).

The brain concentrations of the cyclic nucleotides cAMP and cGMP, which are important as "second messengers" in neurotransmission, were also found to be transiently altered following exposure to high-energy electrons (Hunt and Dalton, 1980). The endorphin system, which serves many functions including a neuromodulator function, can be disrupted by intermediate doses of radiation (Mickley *et al.*, 1983). In addition to functional changes, neuronal death occurs even after relatively low therapeutic doses of ionizing radiation (Nakagaki *et al.*, 1976). In fact, the brain is a quite sensitive biological detector of small changes in radiation dose (Marks and Wong, 1985). Additionally, the blood–brain barrier, which acts as a natural defense against potentially neurotoxic insults to the brain, is altered after exposure to ionizing radiation. This change in permeability of the blood–brain barrier can last as long as 9 days following exposure to 20 Gy of 300-kV X rays (Storm *et al.*, 1985) and has also been reported for low dosage x-irradiation (Brownson *et al.*, 1963) and γ photons (Griffin *et al.*, 1977). Several nervous system functions are altered by ionizing radiation exposure. The neuronal changes produced by the radiations found in space are largely uninvestigated.

Radiation-induced changes in nervous system function will produce a corresponding variety of behavioral alterations. A sufficiently large dose of electron radiation can completely eliminate an animal's capacity to perform physically demanding tasks (Mickely, 1980). This deficit can be observed soon after exposure and may be transient (Franz, 1985). Lower doses of radiation will produce less severe decrements in performance, but the PDs will persist for longer periods of time (Kimeldorf *et al.*, 1963). These findings in experimental animals may relate to the malaise and weakness reported after human irradiations (Furchgott, 1963).

There is some evidence that some of these decrements in performance are mediated by factors other than physical capacity. Irradiated animals will, for example, continue to work on a task if they are sufficiently motivated to do so (Mickley and Teitelbaum, 1978). At the same time they may frequently fail to perform an identical task motivated by different rewards (Burghardt and Hunt, 1985). Performance on less physically demanding tasks is also altered by exposure to a variety of ionizing radiations (Bruner *et al.*, 1975). Radiogenic decrements in performance have been observed in animals doing a discrimination task requiring button pushing.

Self-maintenance behaviors are less likely to be observed after exposure to ionizing radiation (Kimeldorf and Hunt, 1965). Experimental animals often reduce their eating and drinking (Mickley and Stevens, 1986). "Psychological" changes may also be associated with these basic behavioral deficits. Chimpanzees, for example, seem to be less curious after irradiation, showing reduced spontaneous activity and investigation of novel objects (Davis, 1965).

Exposure to ionizing radiation may also limit the basic capacity of individuals to sense their environment. Ionizing radiation is visible, especially in the dark-adapted eye (Lipetz, 1955). This artificial stimulation may be responsible for the deceased sensitivity of the eye after irradiation (Kimeldorf and Hunt, 1965). In addition, there are decrements in visual acuity observed in irradiated monkeys (Graham *et al.*, 1971). The auditory system may also be sensitive to radiation exposure. In this regard loss of acoustic sensitivity has been reported in human patients who have received therapeutic irradiation of the ear (Borsanyi, 1962). Similarly, deficits in attention to salient stimuli have also been reported. While irradiated monkeys continued to attend to stimuli easily within their forward field of view, they became more self-directed and were less likely to respond to peripherally occurring events (Brown and McDowell, 1962).

To date, high-LET studies involving performance decrement and behavioral incapacitation have been performed solely with neutron radiation. Studies using the miniature pig or primates have addressed both fission-spectrum and high-energy neutrons. In one case, the relative effectiveness of a fission-spectrum neutron field was compared to that of a γ field in producing performance decrement in the miniature pig after whole-body irradiation (George *et al.*, 1971). The incident neutron-to-γ ratio for the neutron field was approximately 10, and the neutron-to-γ ratio for the γ photon field was 0.08. The median effective dose for producing early performance decrement in both these fields was determined for the miniature pig performing a shuttle-box avoidance task. Comparison of the median effective doses for the miniature pig in these two fields indicates an RBE of 0.23 for the neutron field. The same experimental configuration was used to evaluate the relative effectiveness of fission-spectrum neutrons in producing early transient incapacitation in the monkey performing the visual discrimination task. For this study, the relative effectiveness for the neutron field was calculated to be 0.68 for primates irradiated with whole-body radiations (Young, 1977).

In an effort to evaluate the effectiveness of high-energy neutrons in producing behavioral incapacitation, a study was conducted in which primates performed the visual discrimination task after one of the following head-only irradiations: a neutron beam from the Naval Research Labo-

ratory 15-MeV cyclotron or a bremsstrahlung beam from the AFRRI linear accelerator, matched for dose rate and distribution of depth dose. Although the size of the available cyclotron beam prevented replication of the whole-body exposure given to the fission-spectrum animals, it produced an RBE of 0.56, which was very similar to the RBE for incapacitation (Young and Middleton, 1975). In the study of high-energy neutron effectiveness, survival and emesis data were also taken for each of the primates irradiated in either the neutron or the photon field.

These data highlight the complexity of the radiation effects and the importance of specifying end points when referring to the relative biological effectiveness of neutrons. Although the neutron field was less effective in incapacitating animals, it was found to be more effective in producing lethality in the same animals. The RBE for mortality in this study was calculated to be 1.34 (Young and Middleton, 1975). Likewise, the photon field, which was more effective in incapacitating visual discrimination performance, was less effective in producing emesis. This finding has been replicated in two species with two different behavioral tasks for both whole-body and head-only irradiations, strongly suggesting that neutrons are less effective than photons in producing behavioral incapacitation.

Further evidence to support this point can be obtained from the extensive dose–response studies with primates performing a visual discrimination task. These dose–response studies have been completed for mixed-spectrum radiation fields having neutron-to-γ ratios of 0.4 and 3.0, respectively. The median effective dose to produce incapacitation in the 0.4 field was approximately 1700 cGy (Young and Middleton, 1974). The median effective dose required to produce incapacitation in primates performing the same behavioral task in the 3.0 field was approximately 2800 cGy (Young and Middleton, 1975). Again, these observations contrast with those concerning survival after irradiation. A dose-for-dose comparison of the neutron-rich and γ-rich fields indicates that the neutron-irradiated animals survive for significantly shorter periods of time after irradiation. In addition, recent data on the rat suggest that the effectiveness of neutrons and of γ photons for producing performance decrement may not be equal. Apparently, assays for neural damage that depend on damaging large regions of the cortex show less effect from densely ionizing radiations. However, it will be the discrete function involving a single neural pathway or nucleus that will test for the "microlesion." An experimental paradigm has yet to be examined for these presumed effects.

It is now well established that the CNS/behavior system is profoundly affected by exposure to ionizing radiation. Recognition of this sensitivity should lead to appropriate precautions and a research agenda in preparation for human performance requirements in a space environment.

3. Tumor Induction

The Harderian gland tumor system developed by Fry (1975) has been quite useful for evaluating carcinogenesis after HZE irradiation. This system has the advantages that the tumor incidence is low and that the latency period can be reduced by pituitary isografts. Using this system to evaluate Janus and Fermi neutrons as well as helium, carbon, neon, argon, iron ions, and cobalt-60 γ rays, Fry *et al.* (1983, 1985) chose as the end point tumor incidence at 600 days of age. The dose for 30% incidence of tumors from iron-56 nuclei was about 15 cGy, whereas the dose for cobalt-60 was 360 cGy. Other ion beams yield intermediate dose values that fill in between these limits; however, this still reveals a potential for carcinogenesis that is 25 times greater than that for cobalt-60 irradiation. Very recent studies by Alpen and Fry (1985) at acute doses of less than 10 cGy of HZE particles show an RBE as high as 100. Of considerable interest is the significantly increased RBE ($\sim$50) of α particles at these low acute doses using the Harderian gland tumor system. This last observation is important because of the potentially large percentage of α particles in solar radiation. If these ions show increased carcinogenic potential with more protracted exposures, significant countermeasures will need to be developed for spaceflight of long duration.

In a comprehensive study of female rhesus monkeys, Wood *et al.* (1983) noted a significant incidence of endometriosis among the proton-irradiated animals. Three of 23 (13%) control animals developed tumors, and 52 of 128 (41%) proton-irradiated animals developed tumors. A comprehensive report of these data (Yochmowitz *et al.*, 1985) on the chronic mortality of 31 controls (20 males, 11 females) and 217 survivors (124 males, 93 females) has been reported over a 17-year period. Single acute proton exposures were made with beams of 32, 55, 138, 400, or 2300 MeV. Doses were from 25 to 800 cGy, and dose rates ranged from 12.5 to 100 cGy/min. Protons with energies above 138 MeV were totally penetrating, and the dose distribution was relatively homogeneous. The most salient observations from monkeys chronically irradiated with protons include (1) the development of endometriosis in females and neoplasms in males and (2) the development of endometriosis at relatively low proton energies (32 MeV) and doses (25–113 cGy), which may be a limiting factor for female astronauts on extended missions. McClure *et al.* (1971) have suggested that the radiation may alter the immunological response of the host, promoting the proliferation of endometrial tissue. Regardless, it could represent a radiation hazard to female astronauts.

Leith *et al.* (1983) reported a comprehensive review of normal-tissue studies with HZE particles. They noted a large range of RBE values for

normal-tissue responses to single-dose HZE exposures. For multifraction cell-death data in skin, jejunal crypt cells, and spinal cord, the RBE values varied from 1 in the jejunum to 10 in the spinal cord. Clearly, the study of the effects of HZE irradiation of normal tissue is still in its infancy.

4. Genetic and Developmental Abnormalities

Low-level radiation exposure can cause genetic effects through mutations or chromosomal aberrations. While these changes are insignificant in population genetics, they may be profound for the individual. In his evaluation of the potential genetic risk from exposure to fission-spectrum neutrons, Grahn (1983) noted an RBE of 20–40. For chronic exposures, the RBE may be as much as 50–120. HZE genetic-risk studies may have significant implications for spaceflight (Goldstein, 1980) especially among NASA female astronauts. While rigorous flight policy can minimize the chance of a developing conceptus being irradiated, certainly the effects of HZE and proton irradiation on development must be ascertained.

5. Nonstochastic Effects

HZE particles interact with matter and lose energy in a way that can be described with the Bethe–Bloch equation. Because of the tremendous energies of these particles, 10 g/cm^2 of aluminum may decrease the number of HZE particles to only 25% of their incident fluence (Curtis and Wilkinson, 1968). In an EVA sortie, an astronaut will be protected by spacesuit shielding, currently less than 0.2 g/cm^2. In the future, stiff suits may shield at 1 cm^2. Both are almost transparent to HZE particles. These HZE particles have LETs greater than 100 keV/μm along the particle track. Further, Magee and Chatterjee (1977) demonstrated a 10-μm penumbra of high-energy secondary electrons (delta rays) circumferentially around the particle track, resulting in large accompanying local doses of low-LET radiation. The particle track of very high LET radiation surrounded by a cylindrical shell of high-dose low-LET radiation has resulted in new radiobiological phenomenon, the microlesion. Todd (1983) has reviewed the nature of these microlesions and suggested that at least 200 keV/μm along the track is necessary for their production. He notes that the penumbra of δ rays may represent from 25 to several hundred cGy. Furthermore, the threshold for a particular biological effect will vary from organ to organ; consequently, the microlesion may not be an all-or-none phenomenon.

High-altitude balloon experiments conducted over 30 years ago resulted in the first potentially identifiable HZE lesions. During the conduct of those studies, Chase (1954) observed depigmented hairs in the fur of rodents recovering from these flights. Subsequent studies (Chase *et al.*, 1963;

Tobias and Grigor'yev, 1975) showed that a single nitrogen ion track could inactivate all melanocytes at the base of a hair follicle.

Tobias (1952) predicted that light flashes would be seen by dark-adapted individuals when HZE particles passed through their eyes and activated the retinal photoreceptors. Astronauts on Apollo missions 11 through 17 reported seeing light flashes outside the magnetosphere when their eyes were dark-adapted (Pinsky *et al.*, 1974). Fazio *et al.* (1970) proposed that Cerenkov radiation may have been responsible for the light flashes, whereas Tobias and colleagues (Tobias *et al.*, 1970) implicated an ionization mechanism. Madey and McNulty (1972) calculated that at least two coincident Cerenkov photons must be absorbed by rhodopsin molecules in a small area of the retina and concluded that these theoretical data predicted the observed phenomenon. In an extension of their work, the same authors (McNulty and Madey, 1972) showed that nonrelativistic particles (no Cerenkov radiation) can cause the visual sensations by virtual-quanta interactions with the retina in the same way that ordinary light photons interact. To confirm these predictions, McNulty *et al.* (1978) exposed their own eyes to carbon ions with and without Cerenkov radiation. They reported that large light flashes occurred only with ion velocities sufficient to produce Cerenkov radiation. These investigators concluded that the space light-flash phenomenon is primarily a Cerenkov radiation phenomenon.

The foregoing discussion would be only an interesting observation if it did not have implications for significant events that must be occurring not only in the cornea, vitreous, and fovea centralis but also in the central nervous system. The eye has always represented a window into the body to observe significant structures, especially the microcirculation.

Bonney and colleagues (1977) reported posterior capsular cataracts 10 months after exposure to oxygen ions. Cox and colleagues (1983) followed these experiments with several animal models, different nuclear species, and different-aged animals within each group, and had disturbing observations. Dose fractionation with HZE particles resulted in no tissue sparing, compared to photon irradiations. There was an age-related difference in cataract formation, with the young developing a greater number of early cataracts than did the older animals. Surprisingly, the older animals developed late cataracts at a much greater rate than did the young animals, ultimately experiencing more severe cataracts in greater numbers. The full implications of these observations are still not clear, and the studies must be continued. J. Lett (personal communication) has reported some recent work in this area.

Poorly documented Soviet reports about decreased visual acuity after spaceflight has prompted many additional visual studies. Philpott and col-

leagues (Philpott *et al.*, 1978, 1980), in collaboration with Soviet investigators, evaluated the retinas of rats taken aboard two Soviet flights. They observed significant retinal changes from neon and argon nuclei (possible secondaries from the spacecraft itself). Among the changes observed were increased capillary permeability, channel production (microlesions), abnormal DNA, and necrotic cells. In the second series of experiments, the control animals experienced weightlessness, acceleration, and other environmental conditions, confirming that the observed changes were due only to cosmic-ray exposure (Philpott *et al.*, 1978). Kraft and colleagues (1979) performed a study using 10, 100, and 1000 cGy (surface) of neon ions to confirm the effects observed by Philpott at 1000 cGy. They noted defects for doses above 10 cGy. In an experiment by Nelson and Tobias (1983), scanning electron micrographs were made of rat corneas that had been irradiated with heavy ions. The micrographs showed microlesions in the plasma membrane of the corneal surface, with the lesion numbers correlating linearly with particle fluences. Theoretical calculations of heavy tracks from etched plastics, emulsions, and bubble chambers led these investigators to conclude that particle tracks occurred in biological tissues and that one HZE particle produced each microlesion. The authors further concluded that HZE particle traversal of biological tissue caused complex microscopic deposition of high-energy and low-energy events. Furthermore, they suggested that the macroscopic concept of dose may be meaningless for HZE particles.

Just as these lesions can be produced within the retina, similar damage may be produced in neural tissue throughout the CNS. For example, Kraft and colleagues (1979) noted a dose-dependent increase in necrotic cerebral neurons in pocket mice 3 weeks after exposure to neon ions. Injured neuroglial cells were also observed after the irradiation. These authors concluded that only exposures less than 10 cGy delivered over a protracted time are likely to completely spare the brain or retina of an astronaut. In recent experiments in rodents, however, high-energy electrons at doses in the tens of centigrays caused changes in the animal's ability to navigate a maze (P. J. McNulty, personal communication). Thus, the potential of anomalous phenomena cannot be excluded when the particle fluence increases by several orders of magnitude. Furthermore, it may be prudent to think of constellations of cells (such as the fovea centralis, pineal, or pituitary nuclei) as critical targets, especially if HZE particle fluence increases.

Tobias (1985) has suggested that 10–20% of human cerebral cortical pyramidal cells may be hit by HZE particles in a spaceflight of 1-year duration. The implications of this injury may be very serious, and its existence has been confirmed. Miguel *et al.* (1976), studying HZE effects

on the *Drosophila* brain, found that ^{40}Ar particles impinging on the brains of *Drosophila melanogaster* did inactivate the neurons. Whether these neural lesions related to the thermophysical domain of the microlesion core or the area of free-radical chemistry or both, many significant issues must be resolved in this area of research.

IV. Physiological Adaptation to Space

For over 20 years now man has flown in space. During that time, it became clear that microgravity is the primary physiological challenge to which man in low-Earth orbit must adjust. Soviet and U.S. astronauts have adapted well to the space environment, functioning effectively for periods of 3–6 months. Despite this adaptability, significant physiological derangements may adversely interact with any significant radiation exposure. Some of the physiological changes noted, in addition to those previously discussed, can be categorized as hematological, hemodynamic, those involving demineralization or calcium resorption, and motion sickness.

A. Hematological Changes

Changes in red cell morphology, combined with a loss of the red blood cell mass and a decrease in plasma volume, have accompanied all U.S. and Soviet flights (Mengel, 1977). The decrease in red cell components reaches its nadir at 60 days and then appears to stabilize. Attempts to discover the etiology of these changes have not been fruitful. In 1973, a 59-day ground-based experiment was performed to parallel the Skylab mission. The environmental conditions were as identical to the actual flight as possible. Only those Skylab astronauts in space showed a changed hemogram (Dietlein, 1977). The decreased red cell mass, like other anemic states, may be the result of either increased destruction or decreased production. The weight of the evidence currently supports a suppression of red cell production (Mengel, 1977).

Spaceflight also alters the humoral and cellular immune systems. Changes have been noted in β_2-macroglobulin, IgA, IgG, IgM, α_2-glycoprotein, and C3 and C4 complement factors (Cogoli, 1981; Kimzey, 1977). The most significant changes took place during the 175-day Soviet spaceflight, when a significant decrease in immunoglobulin levels occurred (Yegorov, 1981). In addition, changes in the cellular immune system have been observed through the *in vitro* response of lymphocytes to mitogenic challenge (Cogoli, 1981). During the Russian Solyut-6 orbital program, five space missions lasted from 96 to 185 days. Immunological studies

during these flights showed decreased cytotoxic (killer) T cells, decreased helper (effector) T cells, and no change in suppressor T cells (Yegorov, 1981). The responsiveness of lymphocytes to the mitogen phytohemagglutinin (PHA) was markedly depressed on the day of recovery of Skylab mission astronauts. Despite the brief duration of STS-4, the lymphocytes of crew members of all these flights showed a decreased response to the PHA (Taylor and Dardano, 1983). The fact that both components of the immune system are decreased is cause for concern, in view of the profound immunosuppression that accompanies paralethal radiation exposures.

Another subject of immunological concern is the change in endogenous microflora. Soviet astronauts developed changes in flora of the skin, mucosa, and intestine. These changes included (1) increased resistance to antibiotics and (2) development of pathogenic properties, especially gram-negative organisms (Vorobyov *et al.*, 1983). If these changes are physiologically significant, it may be true that radiation injuries in space will be exacerbated.

B. Hemodynamic Changes

One of the most profound physiological changes that occurs during spaceflight is in body fluids and electrolytes. Microgravity neutralizes the normal hydrostatic pressure gradients throughout the body, resulting in a cephalic migration of 1.5–2 liters of fluid (Leach, 1979). This redistribution of interstitial and intravascular fluid is interpreted by atrial stretch receptors as an increase in total blood volume (Leach *et al.*, 1983; Vorobyov *et al.*, 1983). This sets in motion a cascade of events to restore homeostasis, involving reflex peripheral vasodilation, decreased renin–angiotensin–aldosterone activation, decreased antidiuretic hormone, increased natriuresis, and diminished thirst (Blomqvist, 1983). The net result is rapid diuresis, kaliuresis, and natriuresis with a concomitant weight loss. The fluid shifts result in increases in transcapillary pressure in the upper body and a decrease in the lower extremities (Alviolz *et al.*, 1979). In addition, there are facial edema, headache, nasal congestion, and decreased leg girth. The exact mechanism of this adaptive response is still unclear; however, cardiovascular function is maintained in space.

Multiple observations suggest that physical training during spaceflight may prevent deconditioning. A systematic and rigorous evaluation of aerobic and anaerobic types of exercise has not been made. Of serious concern before we embark on prolonged spaceflight is the pathological change seen in the myocardium of Soviet cosmonauts. These histological changes must be rigorously verified in appropriate animal models.

Return to normal gravity is accompanied by orthostatic hypotension

TABLE II

ARTERIAL, CAPILLARY, AND VENOUS BLOOD PRESSURES IN UPRIGHT AND 5° HEAD-DOWN TILTED HUMAN[a]

Pressure	Head	Heart	Feet	Head	Heart	Feet
Arterial	60	100	220	80	80	70
Capillary	20	30	2	32	30	20
Venous	−5	2	90	10	7	15

[a] From Hargens (1983).

as well as altered regional blood flow to the lungs. These adaptive changes are the results of cephalad fluid shifts, with concomitant reflexes resulting in fluid movements, altered cardiopulmonary capacity, and altered dynamics. During the Skylab missions, the cardiovascular deconditioning stabilized after 4–6 weeks (Hargens, 1983). Many of the derangements are related to the fluid shifts previously described and are summarized in Table II. Hargens (1983), modeling the effect of weightlessness by placing subjects in a head-down tilt of 5°, measured these volume shifts in a series of experiments (results illustrated in Fig. 13). Here, the roughly 400 ml of fluid lost from the lower legs during the first 4 hr of tilting was shown to be shifted cephalad via increased venous blood volume (Hargens, 1983). This central fluid shift causes increased central venous pressure, pulmonary artery pressure, and stroke volume (Leach, 1979). Increased pressure stimulates atrial stretch receptors, which in turn inhibit the secretion of arginine vasopression, resulting in a loss of urine potassium, sodium, and volume (Dietlein, 1977). Regardless of the mechanism, orthostatic intolerance, which is present during reentry and postflight, is not completely corrected by volume replacement (Gauer and Henry, 1976).

C. Mineral and Bone Loss

Microgravity reduces the mechanical stress on the body and decreases the physical effort required to perform tasks or to maintain posture. This has resulted in profound alterations in bone and mineral metabolism during prolonged spaceflight. Bone mineral changes have been studied by both U.S. and Soviet investigators. A 3-month mission may result in a 4–8% decrease in bone mineral density (Yegorov, 1981; Blomqvist *et al.*, 1980). The bone loss correlates very well with the severity of the negative calcium and phosphorus balance. Urinary calcium increases to a plateau at about

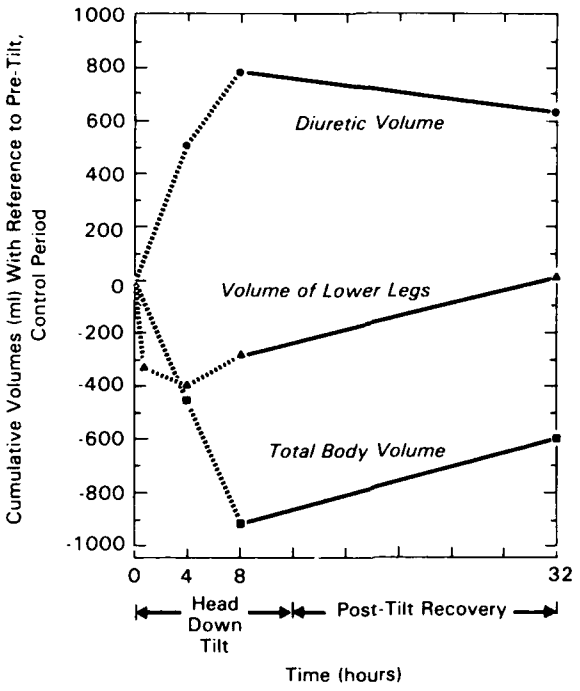

FIG. 13. Net cumulative volumes of various body fluid parameters during and after head-down tilt. (After Hargens, 1983.)

30 days in flight, whereas fecal calcium excretion continues to increase for the flight duration (Blomqvist *et al.*, 1980). Of significant concern is the fact that continued calcium loss may result in clinically manifested osteoporosis after 4–8 months in space, with consequent risk of fracture on return to normal gravity (Rambaut and Johnston, 1979). The fecal and urinary calcium losses during spaceflight are graphically shown in Fig. 14. The precise mechanism of these changes is not well characterized, but it is related to weight bearing, muscular activity, hormonal influences, mineral loss, and nitrogen loss.

Dietlein and colleagues (1983) have pointed out four major concerns: (1) the time required for bone loss to plateau, (2) the possibility of irreversible trabecular bone loss, (3) the nephrotoxicity of released calcium and phosphate, and (4) the risk of impact loading and torsional fractures. Another very real concern is the increased protein catabolism and muscle wasting seen in prolonged spaceflight. Not only might this limit effective astronaut performance but it may also have serious implications for healing of a traumatic injury, especially if associated with radiation exposure.

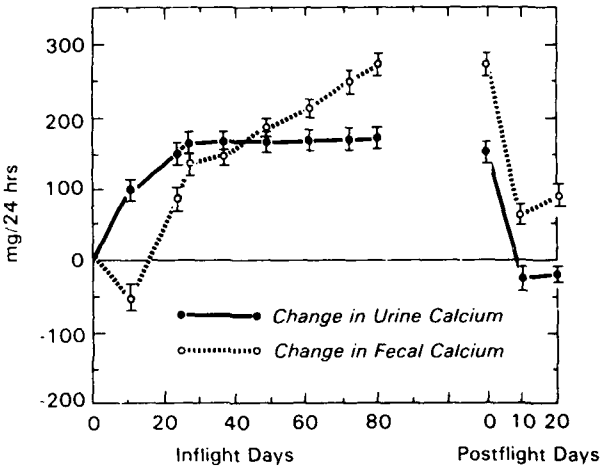

FIG. 14. Change in urine and fecal calcium as a function of Skylab flight duration. (From Rambaut and Johnston, 1979.)

D. Space Motion Sickness

The neurovestibular system provides information about gravity and inertia so that the body can maintain its equilibrium. The body is primarily dependent on the semicircular canals and the otolithic organ to provide the necessary sensory input for equilibrium (J. P. McNulty, personal communication). During the first few days in space, a number of vestibular side effects occur, which result in postural illusions, sensations of rotation, nystagmus, dizziness, vertigo, nausea, and vomiting (Mills and Harding, 1983). Although the etiology of the response is unknown, it is believed to be the result of a mismatch between the otolith information and the semicircular canal information. It is doubtful that the cephalic redistribution of fluid has a direct effect (Graybiel *et al.*, 1977; Graybiel, 1980). Of significant concern are preliminary experiments showing that exposure to ionizing radiation increases the sensitivity of animals to motion sickness (H. Borison, personal communication).

V. Enhancement of Radiation Syndromes

In developing a strategy for radiation protection for astronauts, it is important to take a very broad view of protection rather than one narrow and conventional. This means that any approach which decreases the risk or effects of radiation exposure, whether acute or late somatic effects, should be considered radioprotective. Using this definition, it is obvious

that we do not want to increase an astronaut's intrinsic sensitivity to radiation. Intrinsic radiosensitivity could inadvertently be increased in a spacecraft or spacesuit by use of radiosensitizing drugs (electron-affinic compounds), supernormal ambient oxygen or hyperbaric exposure, hyperthermia, or exposure to radiosensitizing toxic fumes. A large number of radiation-sensitizing drugs are known (Workman, 1980). A prototype drug is metronidazole, which is an antihelmenthic agent; like its analog misonidazole, it has marked radiosensitizing properties. Metronidazole is extensively used in many disease states such as intestinal amebiasis, intestinal giardiasis, anaerobic infections, vaginitis, amebic liver abscess, and other rarer conditions (Rubinstein and Federman, 1985). Amebiasis is endemic in the southwestern United States and the Middle East, giardiasis is endemic in northern Europe. For prolonged space missions (3 months or longer), careful thought should be given to any proposed therapeutic drugs that may be administered in space. Analysis should be made of the risks and benefits to crew members from their use.

Several hereditary diseases are characterized by a marked increase in radiosensitivity. The inheritance patterns include autosomal dominant (AD), autosomal recessive (AR), X-linked recessive (XR), and X-linked dominant (XD). Genetic diseases that have radiosensitivity similar to ataxia telangiectasia include retinoblastoma (AD), Huntington's disease (AD), neurofibromatosis (AD), tuberous schlerosis (AD), nevoid basal cell carcinoma (AD), Fanconi's anemia (AR), Bloom's syndrome (AR), Chediak–Higashi syndrome (AR), Wiskott–Aldrich (XR), agammaglobulinemia (XR), dyskeratosis congenita (XR), and incontentia pigmenti (XD) (Weichselbaum and Little, 1983). Astronauts who have relatives with these diseases might be screened by testing fibroblast specimens to determine intrinsic radiosensitivity. In the future, it may even be prudent for NASA to determine individual radiosensitivity of astronauts for specific types of missions and for responses to radiation emergencies.

Hyperthermia has been well characterized as a radiosensitizing agent. Over the past 10 years, tremendous interest has been rekindled in the use of hyperthermia and radiation for tumor therapy, resulting in a significant body of data (Dewey *et al.*, 1977). These data are important because of the possible radiosensitizing effects of (1) hyperthermia secondary to physical exertion and/or the wearing of an environmental suit during extravehicular activity (EVA), and (2) possible exposure to microwaves capable of thermal effects. *In vitro* and *in vivo* experiments show increasing cell kill with increasing temperatures. Because the time of exposure to heat and the level of physical exertion are closely related to elevated core temperature, they should be considered if an astronaut must work in a known radiation environment. Advantage may be taken of the research

program sponsored by the U.S. Army Institute of Environmental Research, whose mission is investigating the adverse effects of elevated core body temperatures and subsequent performance degradation. This research program has resulted in the design of several prototype human cooling garments. Any physical or chemical agent that increases radiosensitivity will need to be carefully reviewed in order to define its impact on performance decrement and survival.

VI. Mitigation of Radiation Syndromes

A. Chemical Radioprotection

The first animal experiment that stimulated widespread interest in developing radioprotective drugs for humans was performed by Patt *et al.* (1949). Large doses of cysteine were given intravenously 5 min before a near-lethal dose of X rays. Of the pretreated rats, 85% survived, but only 10% of the nontreated rats survived. It was immediately recognized that development of a radioprotectant drug for humans could have significant implications. Since that time, a tremendous amount of research has been conducted on the development of potential radioprotective drugs. The Walter Reed Army Institute of Research alone was instrumental in developing over 4400 candidate radioprotective compounds (Davidson *et al.*, 1980). For application to the space program, radioprotectant drugs should meet several criteria. Ideally, a radioprotective drug should be effective when administered orally, provide protection over extended periods of time, have no side effects, be stable, and not be abusable. Many of the early radioprotective drugs, analogs of cystine and cysteamine, fell far short of those ideals. They were protective only at paratoxic doses, their protection was of limited duration and limited potency, and they were ineffective orally. However, through extensive developmental research and analysis of structure–function relationships, newer radioprotectors have been developed that more closely approach these requirements.

1. Radioprotection by WR-2721

The leading candidate of the radioprotective compounds developed thus far is a phosphorothioate designated as WR-2721. This compound has protected mice, dogs, and rhesus monkeys from X- or γ-radiation. Using photon radiation, Yuhas (1970) demonstrated a dose reduction factor (DRF) of 2.7 against 30-day mortality in C57BL/6J mice. This is the highest DRF reliably reported for lethality, with a single treatment as the end point. Further, WR-2721 showed modest protection against neutron ra-

diation in mice (Davidson *et al.*, 1980). Also, WR-2721 has been better tolerated than other compounds at radioprotective doses.

It is important to recognize that the protective effect depends on end point. Yuhas and Storer (1969) evaluated the DRF for a series of compounds with end points of hematopoietic death ($LD_{50/30}$), gastrointestinal ($LD_{50/5}$) death, and immediate or CNS death ($LD_{50/0}$). The DRF for WR-2721 varies from 0.49 for immediate death to 2.7 for hematopoietic death.

The primary disadvantages to WR-2721 are that it requires parenteral administration, has substantial side effects, and does not cross the blood–brain barrier (Yuhas, 1970). In addition, the large doses of WR-2721 that are needed to protect large animals after whole-body low-LET radiation may not be sufficient to protect them against high-LET irradiation. It should also be possible to use a combination of agents to provide a better therapeutic index, or to provide better stability of WR-2721 in order to reduce its toxicity.

The mechanism of action of WR-2721 is still open to question. While some believe that direct free-radical scavenging is paramount, others consider factors such as vasomotor action, hydrogen donation, mixed disulfide formation, decreased intracellular oxygen tension, or alteration of radiation repair processes to be important. WR-2721 has been found to induce changes in tissue lysosomal enzymes, cyclic nucleotides, and prostaglandin mediators that are closely involved with tissue injury (Riklis *et al.*, in press; Trocha and Catravas, 1982). WR-2721 suppresses radiation-induced prostaglandin excretion in rats and attenuates the increased urinary volume associated with radiation injury (Donlon *et al.*, 1983). A more detailed study of the effects of WR-2721 on prostaglandin metabolism is being carried out because of the importance of prostaglandins and related arachidonic acid metabolites as modulators of various types of inflammatory and immune responses. The effects of WR-2721 on urinary histamine excretion after irradiation are also being investigated.

Protection or stimulation of the immune system is an important aspect of holistic radioprotection. Srinivasan and Weiss (1984) have shown radioprotection of cell-mediated immunity in irradiated mice by measuring *in vivo* changes in delayed-type hypersensitivity. WR-2721 administered shortly before irradiation was found to be very effective in preventing radiation-induced immunosuppression as measured by this assay. WR-2721 was effective to a lesser extent when administered even 2 days before irradiation, suggesting interaction of the drug with immune competent cells. Although it is known that WR-2721 has a strong protective effect for bone marrow stem cells, a more comprehensive and comparative study is needed on the protection of lymphohematopoietic tissues.

The presently available radioprotective drugs are also associated with

some disadvantages. For example, the drugs neither eliminate nor alleviate prodromal symptoms (nausea, vomiting, etc.). WR-2721 is very unstable in the acid medium of gastric secretions and undergoes rapid breakdown. Research is in progress to microencapsulate WR-2721 and other similar compounds in the form of microspheres made with acid-stable lipid matrix, permitting release of the active form in the alkaline environment of the intestine (D. E. Davidson, personal communication). Recent clinical trials of WR-2721 have revealed significant acute toxicity of the parenterally administered drug. In patients treated with WR-2721, 44 of 71 had nausea or vomiting, 18 were somnolent, and 11 experienced hypotension (Glick *et al.*, 1982; Kligerman *et al.*, 1981). Perhaps even more disconcerting is the observation of a significant WR-2721-mediated parathyroid hormone (PTH) inhibition with hypocalcemia and calciuria (Glover *et al.*, 1983). Mean levels of serum calcium decreased from 9.33 to 7.62 mg/dl, while ionized calcium decreased from 0.98 to 0.80 mmol/liter. These studies were precipitated when a patient in the first clinical trials developed mild carpopedal spasm and distal parathesia. These effects, superimposed on the well-documented hypocalcemia seen in prolonged spaceflight, require careful consideration before the use of these drugs.

The recent phase I clinical trials of WR-2721 have provided important data about its pharmacology and toxicity. In patients receiving WR-2721, it was observed that the venous oxygen tension (PvO_2) was increased. In 20 patients treated with WR-2721 (430–910 mg/m^2 at a rate of 15 mg/m^2/min), the mean PvO_2 rose from a baseline of 34.0 ± 1354 torr to a value of 54.60 ± 12.47 torr (p .001) (Glover *et al.*, 1983a). Glover and colleagues postulated that the changes may have been secondary to increased affinity of hemoglobin to oxygen, microcirculatory shunting, and decreased tissue requirements for oxygen. They further suggested that WR-2721 may afford protection by decreasing oxygen consumption (especially in granulocytes and delivery to normal tissues) and increasing intracellular sulfhydryls. These same researchers also observed that patients receiving WR-2721 developed distal parasthesia and mild carpal pedal spasm, suggestive of hypocalcemia (Glover *et al.*, 1983a, b). They also found that infusion of WR-2721 was followed within 2–5 hr by a significant decrease in serum calcium (total and ionized), magnesium, and PTH.

In a review of the toxicities of WR-2721, Kligerman and colleagues (1983) noted that the dose-limiting toxicity is persistent hypotension (greater than 20 torr systolic), occurring in 7% of the patients for single-dose infusions. Other toxicities include vomiting, somnolence, sneezing, and hypocalcemia. In the multiple-dose studies, allergic reactions were the most severe, including fever, rash, and hypotension. Patient self-withdrawal occurred because of persistent vomiting after WR-2721 infusion.

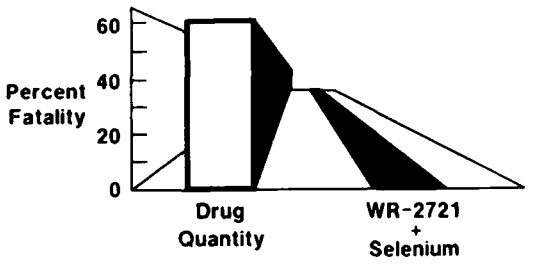

FIG. 15. Effect of selenium (1.6 mg/kg) pretreatment on acute toxicity obtained with WR-2721 (800 mg/kg) (Weiss *et al.*, 1986).

Despite the foregoing comments about the current pharmacological efforts addressing these complications, there is reason for optimism. Many of the side effects are attenuated by decreasing the infusion rate. It is therefore hoped that the oral preparation will have minimal toxicity. Recent studies by Weiss *et al.* (1986) show that coadministration of selenium with WR-2721 does two things: it decreases the toxicity of the thiol (Fig. 15), and it increases the efficacy of the drug (Fig. 16). In addition, the latest generation antihistamines are potent but have few intrinsic side effects. Thus, they may be administered with WR-2721 or a derivative to control aminothiol toxicity and to increase the efficacy of WR-2721 in mice (M. Donlon, unpublished results).

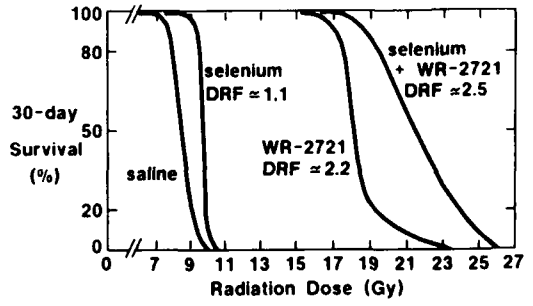

FIG. 16. Effect of selenium pretreatment on radioprotection by WR-2721 (Weiss *et al.*, 1986).

B. Other Potential Radioprotectants and Combined Treatments

Other drugs related to WR-2721, such as mercaptoethylamine (MEA) and aminoethylisothiourea (AET), are being investigated in model systems. Studies have shown synergistically increased survival of irradiated animals that had been administered a combination of MEA and AET, with non-additive toxicity (Maisin *et al.*, 1977). The radioprotective properties and mechanisms of action of various immunomodulators or biological response modifiers are also being investigated, and they show promise. Special emphasis is being given to the use of combinations of traditional radioprotectors and immunostimulants to reduce the known toxicity and side effects of WR-2721. Studies (Jeng *et al.*, 1982) have shown that azimexon, a cyanoaziridine compound, stimulates granulocyte–macrophage and monocyte–macrophage progenitor cells, which may play a role in radioprotection. Azimexon has been proposed as a radioprotector that can be given after radiation exposure.

Several immunomodulating agents (e.g., glucan, *C. parvum*, BCG) have been shown to enhance hematopoiesis and reticuloendothelial functions when administered to normal rodents. The particulate form of glucan was shown to profoundly enhance hemopoietic recovery when administered either before or after sublethal doses of γ-radiation (Patchen *et al.*, 1984). In addition, glucan has been shown to significantly increase survival when administered before lethal doses of γ-radiation (Bicker *et al.*, 1979; Patchen and MacVittie, 1983). A major disadvantage of particulate glucan was that it activated complement, but that disadvantage was recently overcome by the availability of soluble glucan (Patchen *et al.*, 1984). The soluble form is particularly noteworthy in that it provides some protection even when given 24 hr postirradiation (Patchen *et al.*, 1984).

Endotoxins (ETs) isolated from bacterial cell walls are well-established immunostimulants that increase survival postirradiation. Ainsworth and colleagues (1970) showed increased survival in mice (DRF 1.23) and dogs (DRF 1.4). When ET and AET were coadministered to mice, survival was further increased (DRF 2.26). Of particular interest is the fact that ET is effective when given after irradiation (Vignuelle and Baum, 1982). One of the factors that limit the use of ET is its toxicity at therapeutic doses. Recent studies of radioprotection using detoxified ET are encouraging (Bertok, 1980; Snyder *et al.*, 1986). More recently, detoxified ET (lipid A) has been combined with WR-2721 with increased radioprotection (Fuchs *et al.*, 1986).

Studies on the effect of thymic peptides (which modulate immune re-

sponses) on postirradiation survival and cellular immunity are being undertaken by Neta *et al.* (1985), with promising results. Studies of levamisole, another immunostimulant, have emphasized the interrelationship of antioxidant activity, radioprotection, , and immunoprotection (Dobbs *et al.*, 1981). Sodium diethyldithiocarbamate is an immunomodulator with both radioprotective and radiosensitizing effects. Current studies indicate that it protects cell-mediated immunity, as measured by changes in delayed-type hypersensitivity, and increases the survival of irradiated mice (Weiss *et al.*, 1983). The biochemical properties of these drugs are being compared to those of WR-2721, including the effects on circulating and cellular factors that either alter the immune response or involve physiological processes important in postirradiation survival. More recently, the monokine interleukin-1 has shown significant protection when administered postirradiation (Neta *et al.*, 1985).

Newer drugs that affect the cyclooxygenase and lipoxygenase pathways of arachidonic acid metabolism and also drugs that affect cellular nucleotides are being studied for their effects on postirradiation survival and cell-mediated immunity. A simplified model of radioprotection by various agents involving the induction of interferon has been proposed (Steel *et al.*, 1982), and the role of interferon on hematopoietic stem-cell stimulation and radioprotection has been studied (Lvovsky, 1981; Hale and McCarthy, 1983).

Dietary constituents may play a protective role against the effects of radiation. It appeared that an experimental elemental diet was associated with both an enhanced cellular proliferation in the blood-forming tissues and a better response to antigen stimulation (Srinivasan *et al.*, 1982). When rats were exposed to doses of cobalt-60 γ-irradiation, 1 of 16 rats fed the usual food pellets survived the radiation; the mean survival time was 9 days. In contrast, 11 of 15 rats survived after having been fed an elemental diet for 1 week before irradiation, and the mean survival time was 59 days. Beginning the diet after irradiation offered no protection.

Vitamin E has been shown to be an integral part of the mammalian antioxidant defense system, protecting against various oxidative stresses, including chemicals, drugs, and ionizing radiation. Recent work (Srinivasan *et al.*, 1982) has shown that mice fed several times the minimal dietary level of vitamin E had improved survival postirradiation. Irradiated mice treated with increased vitamin E had an improved immune response and increased levels of endogenous radioprotective enzymes. Selenium is an integral part of the selenium-dependent glutathione peroxidase enzyme complex in many mammalian organisms, which helps remove damaging peroxides from the organism. Animals maintained on a diet containing selenium in trace amounts have shown increased glutathione peroxidase

activity (K. Kumar, personal communication). Current studies have shown that mice allowed water *ad libitum* with increased trace amounts of selenium had improved postirradiation survival. Mice treated with increased selenium and vitamin E had a better survival and weight gain than did groups on either treatment alone (A. Jacobs, personal communication). Preliminary studies indicate that part of this protective effect may be due to increased tissue levels of glutathione peroxidase activity in the irradiated mice treated with selenium and vitamin E. Further studies will be conducted using other treatments of vitamins and trace elements, with the aim of providing nontoxic physiological protection.

Several other therapeutic modalities may be used after irradiation to increase survival. The correction of immunological deficiences is one approach. Replacement of immunoglobulins or opsonic proteins is feasible, and has recently been demonstrated experimentally. The microbial clearance process can also be facilitated by the nonspecific enhancement of cells involved in immunological defense. For example, macrophage stimulation by glucan or muramyl dipeptide or enhancement of T-cell differentiation by substances such as thymosin are practical prophylactic measures that are being evaluated in humans, with immunosuppression secondary to radiation therapy for advanced lung tumors (Schuloff *et al.*, 1985).

Active or passive specific immunoprotection has been demonstrated in immunosuppressed mice by Walker *et al.* (1984). This approach of immunized hosts to maintain immunity after radiation must be pursued. If active vaccination appears practical, based on antibody titers, the protective immunity against major opportunistic pathogens such as *Pseudomonas aeruginosa* (which emerges in the intestinal microflora during protracted spaceflight) can be tested by use of various vaccine candidates. Passive immunization via monoclonal antibodies, demonstrated in burns, should be studied postirradiation.

During active mixed infections, the selection of an appropriate antibiotic regimen can be critical to the success of treatment. Antibiotics can be directed against specific pathogens to demonstrate their importance in infection and to increase bacterial killing. The synergistic effects of some antibiotic combinations as well as some antibiotics and biological response modifiers have been noted (Neta *et al.*, 1985). Possible beneficial combinations must be evaluated *in vivo*. Certain antiinflammatory substances, such as prostaglandin or endorphin inhibitors, may also prove to have synergistic beneficial effects with antibiotics. The efficacy of prophylactic systemic or oral antibiotics should also be studied for their impact on existing microbial populations and for their protective value.

Future prospects suggest potentially exciting and innovative ap-

proaches to radio protection. This could be accomplished by augmentation of cellular DNA repair capacity by specifically enhancing the production of DNA repair enzymes. Sarasin (1985) has reported evidence of the presence of DNA damage-inducible enzymes that increase radioresistance. In prokaryotes, the molecular details of the SOS system have been described. At the rate molecular biology is progressing, we envision a day when a molecule can be administered to derepress the genes that code for DNA repair enzymes, resulting in maximum resistance to irradiation.

C. Physical Radioprotectors

The design of NASA projects has always been concerned with radiation shielding. Any material that attenuates photon or particulate radiation provides some protection for crew members. Partial shielding of the body, especially marrow-dense areas, can significantly enhance survival. Experiments using photon irradiations have shown a nearly 3-fold increase in the $LD_{50/30}$ with appropriately designed shields (Schick *et al.*, 1981). Studies by Soviet investigators (Rozgovoror, 1975) show that shielding various body parts from 1-MeV neutrons and 120-MeV protons increased radioresistance. This protection was not as much as for photon irradiations alone. Careful consideration should be given to protection of the pelvis and abdomen for missions that may involve prolonged exposure to radiation (such as an SPE, rescue of a crew member, working with a reactor, or working in a contaminated area). Maneuvering the spacecraft can also provide significant shielding from anisotropic radiation exposures.

For geosynchronous orbit space stations or for interplanetary flight, consideration must be given to a storm shelter in the event of an SPE. Studies of laminated shields have already received considerable attention (Seltzer, 1980). Because of secondary radiations from HZE particles interacting with any laminated shield, a many radiation transport and shielding studies are required. The weight penalty to be paid is a significant consideration. The shelter volume required to provide storm-shelter protection for each crew member dramatically affects the total weight of the shelter. For example a volume of 50 or 150 ft^3 per occupant will result in storm-shelter weight for a crew of 10 of 25,000 and 45,000 lbs, respectively (Rossi and Stauber, 1977). It is essential to continue efforts to understand HZE transport (Wilson, 1983), HZE fragmentation (Townsend *et al.*, 1984), and HZE propagation in the atmosphere (Wilson and Townsend, 1986) so we can design spacecraft that minimize the total radiobiological insult to crew members.

The oxygen effect has been well characterized and results in significant

differences in biological response, especially with low-LET irradiation. Consideration should be given to hypobaric environments in a space-station storm cellar during a solar flare. Rats breathing 5% oxygen instead of 20% increased their radioresistance 2-fold (Dowdy *et al.*, 1950; Lindrop and Rothbalt, 1960). It may be that sedation, monitored hypoxia, slight hypothermia, and some radioprotection can yield significant protection for short periods of time. In addition, *hyperoxic* environments must be avoided during a solar flare.

D. Bone Marrow Rescue

Bone marrow transplantation offers the only hope of survival for radiation casualties whose stem cells have been destroyed. Bone marrow transplantation has shown considerable promise in the treatment of aplastic anemia and refractory acute leukemia. Aplastic anemia patients receiving bone marrow transplantation from human leukocyte antigen (HLA)-compatible donors show a 30-month survival of 57%, as opposed to a 25% survival in nontransplanted patients (Thomas, 1975). Graft failure (20–40%) is usually secondary to patient presensitization and graft rejection. These patients have usually received numerous transfusions, which sensitize them to foreign HLA antigens (Santos *et al.*, 1979). A variety of protocols have been developed to permit the engraftment of the presensitized patient. The most significant complication of bone marrow transplantation is graft-versus-host disease (GVHD). The acute form of this disease is thought to be mediated by T lymphocytes that are present in donor cells during engraftment. The occurrence of GVHD is a major obstacle to successful bone marrow transplantation between nonrelated HLA recipients. The major requirements for successful transplantation are HLA compatibility and lack of presensitization (Storb, 1979). Very recent studies show that in nontransfused aplastic anemia patients with HLA-identical family donors, 80% of the patients will be long-term survivors (Storb *et al.*, 1983). This is not a problem using autologous grafts.

A radiation casualty who had received 600 cGy of whole-body γ-irradiation was successfully treated with bone marrow transplantation from his identical twin brother (Thoma and Wald, 1968). At radiation doses above 500 cGy, nearly all bone marrow cells will be destroyed. Autologous bone marrow transplants (ABMT) are uniformly successful because there is no GVHD disease. The concept of an ABMT is not a new one, although it is only recently that these have proven clinically useful. Cavins and colleagues (1960) demonstrated that supralethally irradiated canines (1200 roentgens) could be saved with ABMT. The marrow cells were frozen in

10% dimethylsulfoxide at −80°C for 10–30 days before exposure of the animals. Twelve of the 16 canines were long-term survivors. In a similar study, the researchers infused 2–20 × 10^9 frozen autologous leukocytes (Cavins *et al.*, 1964). Three of 9 dogs had a full recovery but the other dogs infused with less than 9 × 10^9 cells died after some marrow regeneration. It was concluded that the peripheral blood contains stem cells that are capable of resuscitating the marrow postirradiation.

With the success of BMT in multiple species, the momentum began to build for allogenic grafting. Storb and colleagues (1969) showed that allogeneic bone marrow stem cells (BMSC) could be frozen for 40 days and then successfully reinfused. By 1978, BMSC had been frozen for 5 months without loss of function when reinfused into canines (Gorin *et al.*, 1978). Within 1 year, reports appeared that detailed the procedures for the cryopreservation of human BMSC for ABMT (Wells *et al.*, 1979; Graze *et al.*, 1979). Since then, numerous reports have been published that establish therapeutic indications and also procedures for the collection (aspiration or peripheral), storage, and pre- and postfreezing washing procedures (Herve, 1984).

Several authors have reported the long-term storage of BMSC. Parker *et al.* (1981) stored aspirated human BMSC for 42 months with no loss of function from the cryopreservation. Scheiwe and colleagues (1981) reported on the performance of 400 cryopreserved units of peripheral BMSC. This group summarized the advantages of peripheral BMSC as follows: (1) BMSC can be combined with immunotherapy, (2) repeated cell separation is atraumatic, (3) no anesthetic is required, (4) cryopreservation is simpler, and (5) there is decreased risk of contamination. To date, cryopreserved peripheral BMSC have been reinfused in 40 lethally irradiated patients after the BMSC remained in storage for 3–12 months and, in one case, for 4 years. Because astronauts are such a select group and are difficult to replace, it may be prudent to harvest marrow from each crew member. For prolonged missions with little hope of short-term rescue, shielded frozen marrow could be carried with the crew for extreme emergency exposures. Another consideration is the preservation of individual bone marrow for use in the case of a space radiation-induced neoplasm, particularly leukemia, where the best results are obtained with combination total-body irradiation, chemotherapy, and bone marrow transplantation.

The mass storage of autologous bone marrow cells is feasible for any planned prolonged spaceflight. The extent to which the administration of immunostimulants will affect radiation-induced immunosuppression is unknown, and it is not known if this treatment decreases the incidence of late effects.

VII. Summary

Stassinopoulos (1975) has shown that for a 5-year period during solar maximum, the solar flare predictive model (SOLPRO) predicts four anomalously large solar flares with 89% confidence. When the solar flare hazard is added to the other radiation hazards in space, radiation poses a formidable challenge to providing a safe permanent presence in space. From this article it is clear that there are many unknown questions about space radiation, particularly involving HZE particles and the interaction of other space stressors with radiation. Despite the challenge, we are optimistic that the problems can be solved. NASA has achieved an extraordinary record of radiation safety during the first 25 years of spaceflight. During the next 25 years in space, the radiobiological challenge will be significantly greater, but so will the rewards. There are many tools that can be applied with current and future technologies. It is our opinion that the problems will be solved, and that they require only the commitment to solve them. We recommend the following research and development programs.

A. Warning and Avoidance

The most effective radiation reduction technique is obviously avoidance. This requires a dynamic and rapid early warning capability. The system must be able to provide real-time measurements and predictions. The system must be accurate and reliable to avoid the costs (economic and personal) of aborting missions when no significant radiation hazard exists, and must also be reliable enough to prohibit orbiting when there is a significant hazard.

B. Shielding

Shielding studies for both spacecraft and individuals must be conducted. Radiation transport codes must be developed to describe incident and scattered particle fluences as well as the respective contributions to dose. Evaluations are needed of the hazards of the secondary radiation and of the laminated shielding and storm-shelter designs. An additional requirement is evaluation of the hazard from activation of the spacecraft itself during its lifetime, which is usually expected to be at least 10 years.

C. Exposure Criteria

A current standard for exposure to space radiations must be developed. The National Council on Radiation Protection is reviewing the 1970 standards and should provide new standards soon. During this effort, the Council has confronted many uncertainties in the data that should be transformed into research requirements. Among these are biological dose-rate responses to particulate irradiation, especially HZE particles. Do HZE particles represent a long-term hazard that is different from photons and neutrons? Many of these requirements are well characterized in the 1980 Proposed Federal Research Agenda (Vinograd, 1980).

D. Acute Effects

A number of techniques could protect crew members from the acute effects of space radiations. Among these are shielding (shelters, partial body), medical antishock trousers, antiemetics, dietary adjuvants, and circulatory support. Some of these protection modalities are available now, and others could be available in the near term.

E. Short-Term Effects

In the event of a significant exposure to radiation in which crew members could not be returned rapidly to Earth for treatment, a number of treatment modalities may be used. In the event of a protracted (hours or days) high-dose exposure of several hundred centigrays, chemical radioprotectors may still be lifesaving. Immunoglobulin replacement (i.e., IgG), biological response modifiers (i.e., glucan), and broad-spectrum antibiotics may be protective. The capability also exists to provide autologous bone marrow transplantation from shielded supplies for missions of long duration.

F. Industrial Accidents and Combined Effects

Even though construction in space will be performed in microgravity the mass of structures will be unchanged. Consequently, structural components will develop significant inertia, which will inevitably lead to periodic construction accidents. Provisions for care and resuscitation must be provided in the space environment for geosynchronous missions and beyond. Combined injuries (radiation plus trauma) were well described in Hiroshima and Nagasaki as well as in early animal studies (Alpen and Sheline, 1952; Brookes *et al.*, 1952; Schildt and Thoren, 1968). More re-

cently this area has received significant attention (Conklin *et al.*, 1983; Walker *et al.*, 1984). The scope of this article does not permit review of this area; however, most of the combined-injury research related purely to space-related insults has been done by the Russians (Calvin and Gazenko, 1975; Langham, 1967; Aceto *et al.*, 1974).

G. Long-Term Effects

Many more quantitative data are required in order to understand the long-term effects (life shortening, mutations, cataracts, microlesions, cancer, etc.) of space radiation. Of all the facets of space radioprotection, this is the most important, in our opinion. Novel ways of decreasing these hazards must be aggressively pursued. The use of new chemical radioprotectants for long-term radioprotection requires a reorientation of our thinking and the development of oral, nontoxic, and effective agents that can be chronically administered if necessary. If these things are done (and we believe they can be), then man is on the threshold of establishing a permanent, productive, presence in space.

ACKNOWLEDGMENTS

We wish to thank Mrs. Betty Markovich and Mrs. Sheila Pizzuti for their tireless efforts in producing this manuscript. We are also indebted to Ms. J. A. Van Deusen, Dr. R. I. Walker, Dr. R. J. M. Fry, Dr. E. Blakely, Dr. L. Giambarresi, and Dr. W. Blakely for their critical review and helpful suggestions. Finally, we want to thank Mr. Mike Flynn who, in addition to being chief research technician, always seems to be able to find the most obscure references.

REFERENCES

Aceto, H., Leith, J., and Baker, J. (1974). *In* "Space Radiation Biology and Related Topics", (C. A. Tobias and P. Todd, eds.), pp. 354–434. Academic Press, New York.

Afzal, J. M., Tenforde, T. S., and Curtis, S. B. (1985). *Abst. Radiat. Res. Soc. Mtg.*, Los Angeles, California.

Ainsworth, E. J., Fry, R. J. M., Brennan, P. C., Stearner, S. P., and Williamson, F. S. (1976). *In* "Biological and Environmental Effects of Low Level Radiation," Vol. 1, pp. 77–92. International Atomic Energy Agency, Vienna.

Ainsworth, E. J., Mahlmann, L. J., Prioleau, J. C., and Howard, J. (1984). *Abst. 32nd Annu. Mtg. Radiat. Res. Soc.*, Orlando, Florida, March 25–29, 1984, 1-F8, p. 105.

Alderson, P. O., Bradley, E. W., Mendenhall, K. G., Vieras, F., Siegel, B. A., Sloan, G. E., and Rogers, C. L. (1979). *Radiology* **130**, 425–433.

Alpen, E. L., and Powers-Risius, P. (1981). *Radiat. Res.* **88**, 132–143.

Alpen, E. L., and Sheline, G. E. (1952). *Ann. Surg.* **140**, 113–118.

Alviolz, L., Biglieri, E. G., Boughaday, W., Raisz, L. G., Reichlin, S., and Vogel, J. (1979). Space Science Board, National Research Council-National Academy of Sciences, Washington, D.C.

Ashikawa, J. K., Sondhaus, C. A., Tobias, C. A., Greenfield, A. G., and Paschkea, V. (1964). *In* "Proceedings of Symposium on Biological Effects of Neutron and Proton Irradiations," Vol. 1, p. 240. International Atomic Energy Agency, Vienna.

Auxier, J. A., Cheka, J. S., Haywood, F. F., Jones, T. D., and Thorngale, J. H. (1966). *Health Phys.* **12,** 425–429.

Axelrod, D., Aebersold, P. C., and Lawrence, J. H. (1941). *Proc. Soc. Exp. Biol. Med.* **48,** 251.

Ballelos, E. E., and Casarett, G. W. (1981). *Radiat. Res.* **87,** 505.

Barendsen, G. W., Koot, C. J., van Kersen, G. R., Bewley, D. K., Field, S. B., and Parnell, L. J. (1966). *Int. J. Radiat. Biol.* **10,** 317–327.

Batchelor, A. L., Horne, A. W., Husle, E. V., and Stuart, C. E. (1966). *Int. J. Radiat. Biol.* **11,** 583.

Benton, E. V., and Henke, R. P. (1983). *Adv. Space Res.* **3**(8), 171–185.

Bentzel, C. J., and Hainau, B. (1979). *In* "Mechanisms of Intestinal Secretion" (H. Binder, ed.), pp. 275–286. Alan R. Liss, Inc., New York.

Bergonie, J., and Tribondeau, L. (1968). *In* "Clinical Radiation Pathology" (P. Rubin and B. W. Casarett, eds.), p. 29. Saunders, Philadelphia, Pennsylvania.

Berk, R. N., and Seay, D. G. (1972). *Radiology* **104,** 153–156.

Bertok, L. (1980). *Persp. Biol. Med.* **24,** 61–66.

Bichsel, H. (1968). *In* "Radiation Dosimetry" (F. H. Attix and W. C. Roesch, eds.), Vol. 1, pp. 157–228. Academic Press, New York.

Bicker, U., Friedberg, K. D., Hebold, B., and Mengel, K. (1979). *Experientia* **35,** 1361–1363.

Biogden, R. N., *et al.* (1974). *Drugs* **7,** 164.

Blakely, E. A., Tobias, C. A., Yang, T. C. H., Smith, K. C., and Lyman, J. T. (1979). *Radiat. Res.* **80,** 122–160.

Blakely, E. A., Ngo, F. Q. H., Curtis, S. B., and Tobias, C. A. (1984). *In* "Advances in Radiation Biology" (*J. T. Lett, ed.), Vol. 11, pp. 295–389. Academic Press, New York.*

Blakely, E. A., Chang, P. Y., and Lommel, L. (1985). *Radiat. Res., Suppl.* **8** 144–157.

Blomqvist, C. G. (1983). *Med. Sci. Sports Exerc.* **15**(5), 428–431.

Blomqvist, C. G., Nixon, J. V., Johnson, R. L., Jr., and Mitchell, J. H. (1980). *Acta Astronaut.* **7,** 543–553.

Bond, V. P. (1964). *In* "Proceedings of Symposium on Biological Effects of Neutron and Proton Irradiation," Vol. 2, pp. 365–377. International Atomic Energy Agency, Vienna.

Bonney, C. H., Hunter, D. M., Conley, G. E., and Hardy, K. A. (1977). *Aviat. Space Environ. Med.* **48**(8), 731–733.

Borek, C., and Hall, E. J. (1984). *In* "Epidemiology and Biological Significance" (J. D. Boice, Jr., and J. F. Fraumenir, Jr., eds.), pp. 291–302. Raven, New York.

Borek, C., and Sachs, L. (1966). *Nature (London)* **210,** 276–278.

Borek, C., and Sachs, L. (1967). *Proc. Natl. Acad. Sci. U.S.A.* **57,** 1522–1527.

Borek, C., and Sachs, L. (1968). *Proc. Natl. Acad. Sci. U.S.A.* **59,** 83–85.

Borsanyi, S. J. (1962). *Southern Med. J.* **55,** 740–743.

Bradley, T. R., and Hodgson, G. S. (1979). *Blood* **54,** 1446–1450.

Bradley, E. W., Alderson, P. O., Deye, J. A., Mendenhall, K. G., Fisher, M. P., Vieras, F., and Rogers, C. C. (1979). *Int. J. Radiat. Oncol. Biol. Phys.* **5,** 197–207.

Bradley, E. W., Alderson, P. O., McWhorter, R. E., Vieras, F., Olmsted, W. W., Fisher, M. P., and Rogers, C. C. (1981b). *Int. J. Radiat. Oncol. Biol. Phys.* **7,** 1055–1064.

Bradley, E. W., Zook, B. C., Casarett, G. W., and Rogers, C. C. (1981a). *Int. J. Radiat. Oncol. Biol. Phys.* **7,** 1103–1108.

Broerse, J. J., Barendsen, G. W., and van Kersen, G. R. (1968). *Int. J. Radiat. Biol.* **13,** 559–572.

Broerse, J. J., Knaan, S., van Bekkum, D. W., Hollander, C. F., Nooteboom, A. L., and van Zwieten, M. J. (1978). *In* "Late Biological Effects of Ionizing Radiation," Vol. 2, pp. 13–27. International Atomic Energy Agency, Vienna.

Broerse, J. J., van Bekkum, D. W., Hollander, C. F., and David, J. A. (1978). *Int. J. Radiat. Biol.* 253–264.

Brown, W. L., and McDowell, A. A. (1962). *In* "Response of the Nervous System to Ionizing Radiation," pp. 729–746. Academic Press, New York.

Browne, D. C., and Sparks, R. (1961). *Southern Med. J.* **54,** 953–961.

Brownson, R. H., Suter, D. B., and Diller, D. A. (1963). *Neurology* **13,** 181–191.

Bruner, A., Bogo, V., and Jones, R. K. (1975). *Radiat. Res.* **63,** 83–96.

Burghardt, W. F., and Hunt, W. A. (1985). *Radiat. Res.* **103,** 149–157.

Calvin, E. M., and Gazenko, O. G. (eds.) (1975). "Foundations of Space Biology and Medicine," NASA, U.S. Govt. Printing Office, Washington, D.C.

Carpenter, D. O. (1979). Scientific Report SR79-1, Armed Forces Radiobiology Research Institute, Bethesda, Maryland.

Carsten, A. L., Bond, V. P., and Thompson, K. (1976). *Int. J. Radiat. Biol.* **29,** 65–70.

Casarett, G. W. (1976). *Cancer* **37**(2), 1002–1010.

Casarett, G. W., and Eddy, H. A. (1970). *In* "Time and Dose Relationships in Radiation Biology as Applied to Radiotherapy" (V. P. Bond, H. D. Suit, and V. Marcial, eds.), National Cancer Institute, Atomic Energy Commission Conference, Vol. BNL 50203 (C-57), pp. 181–185. Brookhaven National Laboratory, New York.

Cavins, J. A., Kaskvra, S., Thomas, E. D., and Ferrebee, J. N. (1960). *Blood* **20**(6), 730–734.

Cavins, J. A., Scheer, S. C., Thomas, E. D., and Ferrebee, J. W. (1964). *Blood* **23**(1), 38–42.

Chapman, P. H., and Young, R. J. (1968). *Radiat. Res.* **35,** 78–85.

Chase, H. B. (1954). *J. Aviat. Med.* **25,** 389–391.

Chase, H. B., Straite, W. E., and Arsenault, C. (1963). *Ann. N.Y. Acad. Sci.* **100**(1), 390–398.

Cockerham, L. G., Doyle, T. F., and Hampton, J. D. (1984). *23rd Annu. Mtg. Soc. Toxicol. 12–16 March 1984.* Atlanta, Georgia.

Cockerham, L. G., Doyle, T. F., Trumbo, R. B., and Nold, J. B. (1984). *Int. J. Radiat. Biol.* **45**(1), 65–72.

Cogoli, A. (1981). *Acta Astronaut.* **8,** 995–1002.

Conard, R. A., Cronkite, E. P., Brecher, G., and Strome, C. P. A. (1956). *J. Appl. Physiol.* **9,** 227.

Conklin, J. J., Bradley, E. W., Eng, R. R., *et al.* (1982). *J. Nucl. Med.* **23,** 86.

Conklin, J. J., Walker, R. I., and Hirsch, E. F. (1983). *Surg. Gyn. Obs.* **156,** 809–829.

Cooper, J. R., and Mattson, J. L. (1979). *Am. J. Vet. Res.* **40,** 1057–1061.

Cox, A. B., Ainsworth, E. J., Jose, J. G., Lee, A. C., and Lett, J. T. (1983). *Adv. Space Res.* **3**(8), 211–219.

Cronkite, E. P. (1982). "Proceedings of a Symposium by National Council of Radiation Protection and Measurements. The Control of Exposure of the Public to Ionizing Radiation in the Event of Accident or Attack," pp. 46–57.

Curtis, S. (1974). *In* "Space Radiation Biology and Related Topics" (C. A. Tobias and P. A. Todd, eds.), pp. 21–99. Academic Press, New York.

Curtis, S. B., and Wilkinson, M. (1968). *Natl. Aeronaut. Space Admin. Rept.*, NASA CR-1037. U.S. Govt. Printing Office, Washington, D.C.

Dalrymple, G. F. (1965). Technical Report TR-65-5B. USAF School of Aerospace Medicine.

Danquechin-Dorval, E., Mueller, G. P., Eng, R. R., Durakovic, A., Conklin, J. J., and Dubois, A. (1985). *Gastroenterology* **89**(2), 374–380.

Danquechin-Dorval, E., Muller, G. P., Eng, R. R., Durakovic, A., Conklin, J. J., and Dubois, A. (1984b). *Mtg. Am. Gastroenterol. Assoc. May 20–23, 1983*. New Orleans, Louisiana.

Davidson, D. E., Grenan, M. M., and Sweeney, T. R. (1980). *In* "Radiation Sensitizers—Their Use In the Management of Cancer" (L. W. Brady, ed.), pp. 309–320. Masson, New York.

Davis, R. T. The Radiation Syndrome. (1965). *In* "Behavior of Nonhuman Primates" Vol. 2, pp. 495–524. Academic Press, New York.

Davydov, B. I. (1961). *Radiobiologiya* **1**, 550–554.

Dewey, W. C., Hopwood, L. E., Sapareto, S. A., and Gerwek, L. E. (1977). *Radiology* **123**, 463–474.

Dietlein, L. F., Rambaut, P. C., and Nicogossian, A. (1983). *Aviat. Space Environ. Med.* **54**, S6–8.

Dobbs, C. R., Weiss, J. F., Kumar, K. S., and Chirigos, M. A. (1981). *In* "Oxygen and Oxy-Radicals in Chemistry and Biology" (M. A. J. Rodgers and E. L. Powers, eds.), pp. 622–624. Academic Press, New York.

Donlon, M., Steel, L., Helgeson, E. A., Shipp, A., and Catravas, G. N. (1983). *In* "Radioprotectors and Anticarcinogens" (O. F. Nygaard and M. G. Simic, eds.), p. 43. Academic Press, New York.

Dowdy, A. H., Benet, L. R., and Chastain, S. M. (1950). *Radiology* **35**, 879.

Doyle, T. F., and Strike, T. A. (1975). Scientific Report SR75-17, Armed Forces Radiobiology Research Institute, Bethesda, Maryland.

Doyle, T. F., and Strike, T. A. (1977). *Experientia* **33**, 1047–1049.

Doyle, T. F., Turns, J. E., and Strike, T. A. (1971). *Aerospace Med.* **42**, 400–403.

Doyle, T. F., Curran, C. R., and Turns, J. E. (1973). Scientific Report SR73-9, Armed Forces Radibiology Research Institute, Bethesda, Maryland.

Doyle, T. F., Curran, C. R., and Turns, J. E. (1974). *Proc. Soc. Exp. Biol. Med.* **145**, 1018–1024.

Doyle, T. F., Cockerham, L. G., and Hampton, J. D. (1984). *9th Annu. Mtg. Soc. Armed Forces Med. Lab. Sci. March 7–11, 1984*. Washington, D.C.

Dubois, A., Jacobus, J., Grissom, M. *et al.* (1981). *1st Int. Symp. Brain–Gut Axis, June, 1981*. Rome.

Dubois, A., Dorval, E. D., O'Connel, L., Durakovic, A., and Conklin, J. J. (1984). *Am. Gastroenterol. Assoc. Annu. Mtg. May 20–23, 1984*.

Durand, R. E., and Olive, P. L. (1976). *Int. J. Radiat. Biol.* **30**, 583–592.

Earle, J. D., Ainsworth, E. J., and Leong, G. E. (1971). *Radiat. Res.* **45**, 487–498.

Eassa, E. H. M., and Casarett, G. W. (1973). *Radiobiology* **106**, 679–688.

Eddy, H. A., and Casarett, G. W. (1966). *In* "Excepta Medica Monographs on Nuclear Medicine and Biology No. 1, Gastrointestinal Radiation Injury," pp. 385–395. Richland, Washington.

Edmondson, P. W., and Batchelor, A. L. (1971). *Int. J. Radiat. Biol.* **20**, 269–290.

Elkind, M. M., Han, A., and Volz, K. W. (1963). *J. Natl. Cancer Inst.* **30**, 705–721.

Epstein, M. (1978). *Physiol. Rev.* **58**, 529–581.

Erilj, D., and Martinez-Palomo, A. (1978). *In* "Membrane Transport in Biology" (G. Giebish, D. C. Tosteton, and H. H. Ussing, eds.), Vol. 3, pp. 27–53. Springer-Verlag, Berlin.

Fabrikant, J. I. (1980). *Radiat. Res.* **84**, 361–368.

Fanger, A., and Lushbaugh, C. C. (1967). *Arch. Pathol.* **83**, 446–460.

Fazio, G. G., Jelly, J. V., and Charman, W. N. (1970). *Nature (London)* **228**, 260.

Feher, I., and Gidali, J. V. (1980). *Cell Tissue Kinet.* **13**, 415–424.

Feldman, E. J., and Isenberg, H. (1976). *N. Engl. J. Med.* **295**, 1178.

Fowler, J. F., Morgan, R. L., Wood, C. A. P., *et al.* (1963). *Br. J. Radiol.* **36**, 77.

Frankenberg-Schwager, M., Frankenberg, D., and Harbich, R. (1984). *Br. J. Cancer* **49,** Supp. VI, 167–175.

Franz, C. G. (1985). *Radiat. Res.* **101,** 434–441.

Fry, R. J. M. (1975). *In* "Particle Radiation Therapy" (V. P. Smith, ed.), pp. 303–330. Amer. Coll. Radiol., Philadelphia, Pennsylvania.

Fry, R. J. M., Powers-Risiuns, P., Alpen, E. L., Ainsworth, E. J., and Ullrich, R. L. (1983). *Adv. Space. Res.* **3(8),** 241–248.

Fry, R. J. M., Powers-Risius, P., Alpen, E. A., and Ainsworth, E. J. (1985). *Radiat. Res. Suppl.* **8,** S188–S195.

Fuchs, P., Snyder, S., and Walden, T. (1986). *Radiat. Res. Soc. Mtg.* Los Vegas, Nevada.

Furchgott, E. (1963). *Psychol. Bull.* **60,** 157–199.

Garenko, O. G., Zeman, A. M., and Yegorov, A. D. (1981). *Proc. 32nd Congr. Int. Astronaut. Fed. September 6–12, 1981,* NASA NDB 2747. Rome.

Gauer, O. H., and Henry, J. P. (1976). *In* "International Review of Physiology" (A. C. Gryton and A. W. Conley, eds.), Cardiovascular Physiology, Vol. 9, pp. 145–190. University Park Press, Baltimore, Maryland.

Geard, C. R. (1980). *Radiat. Res.* **83,** 696–709.

Geard, C. R. (1985). *Radiat. Res.* **104** Suppl. 8, S112–S121.

George, R. E., Chaput, R. L., Verrelli, D. M., *et al.* (1971). Scientific Report SR71-2. Armed Forces Radiobiology Research Institute, Bethesda, Maryland.

Geraci, J. P., Jackson, K. L., Christensen, G. H., Thrower, P. D., and Fox, M. S. (1975). *Radiology* **115,** 459–463.

Geraci, J. P., Jackson, K. L., and Mariano, M. C. (1985). *Radiat. Res.* **101,** 442–450.

Glick, J. H., Glover, D. J., Weiler, C., Blumberg, A., Nelson, D., Yuhas, J. M., and Kligerman, M. (1982). *Int. J. Radiol. Oncol. Biol. Phys.* **8,** 575–580.

Glover, D., Goldfarb, S., and Glick, J. A. (1984b). *Int. J. Radiat. Oncol. Biol. Phys.* **10,** 4–19.

Glover, D., Negendank, W., Delivoria, M., and Glick, J. A. (1984a). *In* "Chemical Modifiers of Cancer Treatment," pp. 4–18. Banff, Canada.

Glover, D., Riley, L., Carmichael, K., Spar, B., Glick, J., Kligerman, M. M., Agus, Z. S., Slatopolsky, E., Attie, M., and Goldfarb, S. (1983). *N. Engl. J. Med.* **309,** 1137–1141.

Goldstein, L. S. (1980). Report LBL 11220. Lawrence Berkeley Laboratory, Berkeley, California.

Gordon, M. Y. (1975). *Int. J. Radiat. Biol.* **28,** 285–290.

Gorin, N. C., Herzig, G., Bull, M. I., and Grow, R. G., Jr. (1978). *Blood* **51**(2), 257–265.

Graham, E. S., Farrer, D. N., Carsten, A. L., and Roizin, L. (1971) *Radiat. Res.* **54,** 373–383.

Grahn, D. (1983). *Adv. Space Res.* **3**(8), 161–170.

Grahn, D. (1984). Space Radiation Effects Workshop, January 17, 1984. USAF Geophysics Lab, Massachusetts.

Gralla, E. J., Sabo, J. P., Hayden, D. W., *et al.* (1979). *Radiat. Res.* **78,** 286–295.

Grant, G. A., Cairnie, A. B., Harding, R. K., *et al.* (1979). DREO Report No. 817, October. Defense Research Establishment, Ottawa.

Graybiel, A. (1980). *Aviat. Space Environ. Med.* **51,** 814–822.

Graybiel, A., Miller, E. F., and Homick, J. L. (1977). *In* "Biomedical Results from Skylab" (R. S. Johnson and L. F. Dietlein, eds.), NASA SP 377, U.S. Govt. Printing Office, Washington, D.C.

Graze, P. R., Wells, J. R., Ho, W., Gale, R. P., and Cline, M. J. (1979). *Transplantation* **27**(2), 142–145.

Griffin, T. W., Rasey, J. F., and Bleyer, W. A. (1977). *Cancer* **40,** 1109–1111.

Guichard, M., Tenforde, T., Curtis, S., and Malaise, E. P. (1982). *Radiology* **142,** 219–226.
Hale, M. L., and McCarthy, K. F. (1983). *In* "Radioprotectors and Anticarcinogens" (O. F. Nygaard and M. G. Simic, eds.), p. 61. Academic Press, New York.
Hall, E. J. (1978). p. 214. Harper & Row, Hagerstown, Maryland.
Hall, E. J. (1982). *Int. J. Radiat. Oncol. Biol. Phys.* **8,** 2137–2146.
Hampton, J. D., Bogo, V., and Cockerham, L. G. (1983). *68th Annu. Mtg. Fed. Am. Soc. Exp. Biol. April 1–6, 1983.* St. Louis, Missouri.
Hanson, W. (1984). *Proc. Mtg. Radiat. Res. Soc., March, 1983.* Orlando, Florida.
Hardy, A., Beever, R., and Atwell, W. (1983). *Proc. Space Radiat. Effects Workshop, November 16–18, 1983.* Houston, Texas.
Hargens, A. R. (1983). *Med. Sci. Sports. Exerc.* **15**(5), 421–427.
Hempelmann, L. H., Lisco, H., and Hoffman, J. G. (1952). *Ann. Int. Med.* **36,** 279.
Hendry, J. H., Potten, C. S., and Roberts, N. P. (1983). *Radiat. Res.* **96,** 100–112.
Herve, P. (1984). *Pathol. Biol.* **32,** 5–8.
Hevsinkveld, R. S., Manning, M. R., and Aritazabol, S. A. (1978). *Int. J. Radiat. Oncol. Biol. Phys.* **4,** 687–690.
Hill, C. K., Buonaguro, F. M., Myers, C. P., Han, A., and Elkind, M. M. (1982). *Nature (London)* **298,** 67–69.
Hofman, A. F. (1967). *Gastroenterology* **52,** 752–757.
Hunt, W. A., and Dalton, T. K. (1980) *Radiat. Res.* **83,** 210–215.
Hunt, W. A., Dalton, T. K., and Darden, J. H. (1979). *Radiat. Res.* **80,** 556–562.
Iliakis, G. (1980). *Radiat. Res.* **83,** 537.
Jackson, K. L., and Entenman, C. (1959). *Radiat. Res.* **10,** 67–69.
Jeng, J. C., McCarthy, K. F., Chirigos, M. A., and Weiss, J. F. (1982). *Experientia* **38,** 132–133.
Kellerer, A. M., and Rossi, H. H. (1972). *Curr. Top. Radiat. Res. Qtrly.* **8,** 85–158.
Keng, P. C., Bergtold, D. S., and Lett, J. T. (1983). *Int. J. Radiat. Biol.* **43,** 219–229.
Kerr, G. D. (1982). *In* "Proceedings of the Fourth Symposium on Neutron Dosimetry, Munich-Neuhenberg" (G. Berger and H. G. Ebert, eds.), Vol. 1, pp. 501–514. Luxembourg.
Kiefer, J. (1984). *Br. J. Cancer* **49,** Suppl. 6, 151–155.
Kimeldorf, D. J., and Hunt, E. L. (1965). "Ionizing Radiation: Neural Function and Behavior." Academic Press, New York.
Kimeldorf, D. J., Jones, D. C., and Castanera, T. J. (1963). *Am. J. Physiol.* 174, 331–335.
Kimzey, S. L. (1977). *In* "Biomedical Results from Skylab" (R. S. Johnston and L. F. Dzetlein, eds.), NASA 377. U.S. Govt. Printing Office, Washington, D.C.
Kligerman, M. M., Blumberg, A. L., Glick, J. H., Nelson, D. F., Glover, D., Yuhas, I. M., Amak, H. I., and Goodman, R. L. (1981). *Cancer Clin. Trials* **9,** 469–474.
Kligerman, M. K., Glover, D. J., Turrisi, A. T., Coia, L. R., Simone, C., and Glick, J. H. (1983). *Int. J. Radiat. Oncol. Biol. Phys.* **10,** 6–24.
Kraft, L. M., Kelly, M. A., Johnson, J. E., Benton, E. V., Henke, R. P., Cassou, R., Haymaker, W., Philpott, D. E., Vogel, F. S., and Zeman, W. (1979). *Int. J. Radiat. Biol.* **35**(1), 33–61.
Kraft, G., Kramer, M., Meister, H., Miltenburger, H. G., Roots, R., and Wulf, H. (1983). *In* "Proceedings of the Eighth Symposium on Microdosimetry" (H. Booz and H. G. Ebert, eds.), pp. 743–753. Commission of the European Communities, Luxembourg.
Kurohara, S. S., and Casarett, G. W. (1972). *Radiat. Res.* **52,** 263–290.
Langham, W. H. (ed.) (1965). National Academy Press, Washington, D.C.
Langham, W. H. (ed.) (1967). "Radiobiological Factors in Manned Space Flight." National Academy of Sciences–National Research Council, Washington, D.C.
Laporte, J. L., O'Connell, Durakovic, A., Sjogren, R., Conklin, J. J., and Dubois, A. (1984). *Gastroenterology* **86,** 1152.

Leach, C. S. (1979). *Acta Astronaut.* **8,** 968–977.
Leith, J. T., Ainsworth, E. J., and Alpen, E. L. (1983). *Adv. Radiat. Biol.* **10,** 191–236.
Levy, M. N., and Talbot, J. M. (1983). *Physiologist* **26**(5), 297–303.
Liebow, A. A., Warren, S., and DeCoursey, E. (1949). *Am. J. Pathol.* **25,** 853–1029.
Lin, R. P., and Anderson, K. A. (1966). *J. Geophys. Res.* **71**(7), 1927–1935.
Lindrop, P. J., and Rothbalt, J. (1960). *Nature (London)* **185,** 593.
Lipetz, L. E. (1955). *Br. J. Ophthalmol.* **39,** 557–598.
Little, J. B. (1968). *N. Engl. J. Med.* **278,** 369.
Little, J. B., Nagasawa, H., and Kennedy, A. R. (1979). *Radiat. Res.* **79,** 241–255.
Loftus, J. P. (1983). Space Radiation Effects Workshop, November 16–18, 1983. Houston, Texas.
Loewe, W. E., and Mendelsohn, E. (1981). *Health Phys.* **41,** 663–666.
Lucke-Huhle, C., Blakely, E. A., Chang, P. Y., and Tobias, C. A. (1979). *Radiat. Res.* **79,** 97–112.
Lucke-Huhle, C., Hieber, L., and Beck-Bornholdt, H. P. (1984). *Radiat. Res.* **100,** 576–584.
Lundquist, C. A. (Ed.) (1979). "Skylab's Astronomy and Space Sciences," NASA SP 404. U.S. Govt. Printing Office, Washington, D.C.
Lushbaugh, C. C. (1982). "Proceedings of a Symposium by National Council of Radiation Protection and Measurements. The Control of Exposure of the Public to Ionizing Radiation in the Event of Accident or Attack," pp. 46–57.
Lvovsky, E. A. (1981). *Int. J. Radiat. Oncol. Biol. Phys.* **7,** 1290–1291 (Abstract).
Madey, R., and McNulty, P. J. (1972). *Proc. Natl. Symp. Natural Manmade Radiat. Space,* 767–772.
Magee, J. C., and Chatterjee, A. (1977). Report LBL-5610, p. 149. Lawrence Berkeley Laboratory, Berkeley, California.
Maisin, J., Maisin, J. R., and Dunjii, A. (1971). *In* "Pathology of Irradiation" (C. C. Berdjis, ed.), pp. 296–344. Williams & Wilkins, Baltimore, Maryland.
Maisin, J. R., Mattelin, G., and Lambiet-Collier, M. (1977). *Radiat. Res.* **71,** 119–131.
Marks, J. E., and Wong, J. (1985). *Prog. Exp. Tumor Res.* **29,** 210–218.
Marshall, E. (1981). *Science* **212,** 900–903.
McClure, H. M., Ridley, J. H., and Graham, C. E. (1971). *J. Med. Assoc. Georgia* **60,** 11–13.
McNulty, P. J., and Madey, R. (1972). *Proc. Natl. Symp. Natural Manmade Radiat. Space,* 767–772.
McNulty, P. J., Pease, V. P., and Bond, V. P. (1978). *Science* **201,** 341–343.
Mengel, C. E. (1977). *In* "Biomedical Results from Skylab" (R. S. Johnson and L. F. Dietlein, eds.), NASA SP 337. U.S. Govt. Printing Office, Washington, D.C.
Mennies, A. T., Dalley, V. M., Dinneen, L. C., and Collier, H. O. J. (1975). *Lancet* **22,** 942–943.
Mickley, G. A. (1980). *Radiat. Res.* **81,** 48–75.
Mickley, G. A., and Stevens, K. A. (1986). *Aviat. Space Environ. Med.* **57,** 250–255.
Mickley, G. A., and Teitelbaum, H. (1978). *Aviat. Space Environ. Med.* **49,** 868–873.
Mickley, G. A., Teitelbaum, H., Parker, G. A., Vieras, F., Dennison, B. A., and Bonney, C. H. (1982). *Aviat. Space Environ. Med.* **53,** 633–638.
Mickley, G. A., Stevens, K. E., White, G. A., and Gibbs, G. L. (1983). *Science* **220,** 1185–1187.
Middleton, G. R., and Young, R. W. (1975). *Aviat. Space Environ. Med.* **46,** 170–172.
Miguel, J. Herman, M. M., Benton, E. V., and Welch, G. (1976). *Int. J. Radiat. Biol.* **29,** 101–124.
Miller, C. P., Hammond, C. W., and Tompkins, M. (1950). *Science* **111,** 540–541.

Mills, F. J., and Harding, R. M. (1983). *Br. Med. J.* 287, 478–482.
Mole, R. H. (1984). *Br. J. Radiol.* **57,** 355–359.
Montgomery, B. J. (1978). *JAMA, J. Am. Med. Assoc.* **240,** 1469–1470.
Mortimer, R., Brustad, T., and Cormack, D. V. (1965). *Radiat. Res.* **28,** 465–482.
Mulholland, M. W., Levitt, S. H., Song, C. W., Potish, R. A., and Delaney, J. P. (1983). *Int. J. Radiat. Oncol. Biol. Phys.* **4,** 687–690.
Nagasawa, H., Robertson, J. B., and Little, J. B. (1982). *Environ. Mutagenesis* **4,** 377–378.
Nakagaki, H. Brunhart, G., Kemper, T. L., and Caveness, W. F. (1976). *J. Neurosurg.* **44,** 3–11.
Nathan, M. A., and Craig, D. J. (1972). *Radiat. Res.* **50,** 543–555.
National Research Council, Committee on the Biological Effects of Ionizing Radiation. (1980). National Academy Press, Washington, D.C.
Nelson, B. M., and Andrews, G. A. (1976). "Advances in Radiation Biology" (J. T. Lett and H. Adler, eds.), Vol. 6, pp. 325–338. Academic Press, New York.
Nelson, A. C., and Tobias, C. A. (1983). *Adv. Space Res.* **3**(8), 195–209.
Neta, R., Walker, R. I., and Brook, I. (1985). *Fed. Am. Soc. Exp. Biol.* 44, 471.
Ngo, F. Q. H. (1980). *In* "Biological and Medical Research with Accelerated Heavy Ions at the Bevelac 1977–1980." (M. C. Pirruccello and C. A. Tobias, eds.), pp. 89–102. Univ. of California, Berkeley, California.
Ngo, F. Q. H., Blakely, E. A., and Tobias, C. A. (1981). *Radiat. Res.* **87,** 59–78.
NRC. (1980). "The Effects on Population of Exposure to Low Levels of Ionizing Radiation" (BEIR III). Nuclear Regulatory Commission, Washington, D.C.
Otto, F. J., and Pfeiffer, U. (1972). *Radiat. Res.* **50,** 125–135.
Ohno, T., Nishimura, T., Nakano, K., and Kameko, I. (1984). *Int. J. Radiat. Biol.* **45,** 21–26.
Parker, L. M., Bender, N., Gelman, R., Richman, C. M., Weiner, R. S., and Yankee, R. A. (1981). *Transplantation* **31**(6), 454–457.
Patchen, M. L., and MacVittie, T. J. (1983). *Immunopharmacology* **5,** 303–313.
Patchen, M. L., DiLuzio, N. R., Jacques, P., and MacVittie, T. J. (1984). *J. Biol. Resp. Modif.* **3,** 627–633.
Patt, H., *et al.* (1949). *Science* **110,** 213.
Peterson, E. L. (1983). *IEEE Trans. Nucl. Sci.* **NS-30**:2, 1638.
Philpott, D. E., Corbett, R., Turnbill, C., Harrison, G., Leafer, D., Black, S., Sapp, W., Klein, G., and Savik, L. F. (1978). *Aviat. Space Environ. Med.* **49**(1), 19–28.
Philpott, D. E., Corbett, R., Turnbill, C., Black, S., Dayhoff, D., McCourty, R. L., Harrison, G., and Savick, L. (1980). *Aviat. Space Environ. Med.* **51**(6), 556–562.
Pinsky, L. S., Osborne, W. Z., Bailey, J. V., Benson, R. E., and Thompson, L. F. (1974). *Science* **183,** 957–959.
Porvaznik, M. (1979). *Brain Res.* **78,** 233–250.
Porvaznik, M., Walker, R. I., and Gilmore, J. D. (1979). *Scanning Electron Microscopy* **3**(15), 15–22.
Potten, C. S., and Hendry, J. H. (1983). *In* "Stem Cells: Their Identification and Characterization" (C. S. Potten, ed.), pp. 155–199. Churchill Livingston, London.
Potten, C. S., Chadwick, C., Injiri, K., Tsubouchi, S., and Hanson, W. R. (1984). *Int. J. Cell Cloning* **2,** 126–140.
Quastler, H. (1956). *Radiat. Res.* **4,** 302–303.
Radford (1980). *In* "Radiation Carcinogenesis: Epidemiology and Biological Significance on Progress in Cancer Research and Therapy" (J. D. Boice and J. F. Fraumeni, eds.). Raven, New York.
Rambaut, P. C., and Johnston, R. S. (1979). *Acta Astronaut.* **6,** 1113–1122.

Reetz, A., Jr. (ed.) (1965). *Natl. Aeronaut. Space Admin.* Rep., NASA SP-71. U.S. Govt. Printing Office, Washington, D.C.

Reyntjens, A. J. (1981). *R. Soc. Med. Int. Congr. Symp. Ser.*, No. 36, pp. 97–108. Academic Press, London.

Riklis, E., Hagan, M. P., Freschi, J. E., and Catravas, G. N. *Int. J. Radiat. Oncol. Biol. Phys.* (In press).

Roberts, A., Nezamins, J. F., Lancaster, C., Hanchir, A. J., and Klepper, M. S. (1976). *Prostaglandins* **11**, 809–828.

Robertson, J. B., Williams, J. R., Schmidt, R. A., Little, J. B., Flynn, D. F., and Suit, H. D. (1975). *Cancer* **35**, 1664–1677.

Robertson, J. B., Koehler, A., George, J., and Little, J. B. (1983). *Radiat. Res.* **96**, 261–274.

Robertson, J. B., Werdeman, P. A., McNulty, P. J., and Koehler, A. M. (1984). *32nd Annu. Radiat. Res. Soc. Mtg., March 25–29, 1984*, p. 67. Orlando, Florida.

Rogers, C. C., and Bradley, E. W. (1977). *Abstr., Ann. Mtg. Soc. Radiat. Res.*, 147.

Roots, R. J., Yang, T. C., Craise, L., Blakely, E. A., and Tobias, C. A. (1979). *Radiat. Res.* **78**, 38–49.

Rossi, H. H. (1959). *Radiat. Res.* **10**, 522.

Rossi, H. H. (1980). *Radiat. Res.* **84**, 395–406.

Rossi, M. L., and Stauber, M. C. (1977). *Nucl. Sci. H. S.* **24.6**, 2248–2251.

Rozgovoror, B. L. (1975). *In* "Foundations of Space Biology and Medicine" (M. Calvin and O. G. Gazenko, eds.), Vol. 2, pp. 267–287. National Aeronautic and Space Administration, Washington, D.C.

Rubin, R. H., and Hopkins, C. C. (1984). *In* "Scientific American Medicine" (E. Rubinstein, ed.), Vol. 2, p., Vol. 2, pp. 1–34. Scientific American Inc., New York.

Rubinstein, E., and Federman, D. D. (eds.) (1985). "Scientific American Medicine." Scientific American Inc., New York.

Sandler, H. (1980). *In* "Heats and Heart Like Organs" (G. H. Bourne, ed.), Vol. 2. Academic Press, New York.

Santos, G. W., Elfenbein, G. J., and Tutschka, P. T. (1979). *Transplant. Proc.* **11**, 182.

Sarasin, A., Bourre, F., Benoit, A., Daya-Grosjean, L., Gentil, A. (1985). *Int. J. Radiat. Biol.* **47**(5), 479–488.

Sasaki, H. (1984). *Radiat. Res.* **99**, 311–324.

Schaefer, H. J. (1968). *Aerospace Med.* **39**(3), 271–276.

Scheiwe, M. W., Pvszta-Markos, Z. S., Essers, U., Seelis, R., Rav, G., and Korber, C. (1981). *Cryobiology* **18**, 344–356.

Schick, P., Messerschmidt, O., and Sailor, J. (1981). *Proc. 1981 Workshop Res. Study Group Assessment Ionizing Radiat. Injury Nucl. Warfare, NATO*, H1–7. Paris.

Schildt, B., and Thoren, L. (eds.) (1968). "Combined Injuries and Shock." Forsvaret Forsk ningsanstalt, Stockholm.

Schimmerling, W., and Curtis, S. B. (eds.) (1979). National Technical Information Service Report, CONF-7809164. National Technical Information Service, Springfield, Virginia.

Schopfer, F. Schnerder, E., Rose, S., Kiefer, J., Kraft, G., and Liesen, H. (1984). *Int. J. Radiat. Biol.* **46**, 305–316.

Schuloff, R. S., Lloyd, M. J., Cleary, P. A., Palaszynski, S. R., Mai, D. A., Cox, J. W., Jr., Alabaster, O., and Goldman, A. L. (1985). *J. Biol. Resp. Modif.* **4**, 147–158.

Seltzer, S. M. (1980). NBS Technical Note 1116, pp. 1–69. National Bureau of Standards, Washington, D.C.

Sheline, G. E., Philips, T. L., Field, S. B., Brennan, J. T., and Raventos, A. (1971). *Am. J. Roentgen.* **31**, 111.

Shellabarger, C. J., Brown, R. D., Rao, A. R., Shanley, J. P., Bond, V. P., Kellerer, A. M., Rossi, H. H., Goodman, L. J., and Mills, R. E. (1974). *In* "Biological Effects of Neutron Radiation," pp. 391–400. International Atomic Energy Agency, Vienna.

Shellabarger, C. J., Chmelevsky, D., and Kellerer, A. M. (1980). *J. Nat. Cancer Inst.* **64**, 821–833.

Shellabarger, C. J., Chmelevsky, D., Kellerer, A. M., Stone, J. P., and Holtzman, S. *J. Natl. Cancer Inst.* (In press).

Sinclair, W. K. (1983). *In* "Proceedings of the Eighth Symposium on Microdosimetry" (J. Booz and H. G. Ebert, eds.), pp. 1–39. Commission of the European Communities, Luxembourg.

Smith, H. H. (1967). *Radiat. Res.* (Suppl.) **7**, 190–195.

Snyder, S. L., Walden, T. L., Patchen, M. L., MacVittie, T. J., and Fuchs, P. (1986). *Radiat. Res.* **107**, 107–114.

Srinivasan, V., and Weiss, J. F. (1982). *Radiat. Res.* **91**, 399.

Srinivasan, V., and Weiss, J. (1984). *Radiat. Res.* **98**, 438–444.

Srinivasan, V., and Weiss, J. F. *Radiat. Res.* (In press).

Srinivasan, V., Jacobs, A. J., Simpson, S. A., and Weiss, J. F. (1982). *Proc. 1st Int. Conf. Modulation Mediation Cancer Vitamins.*

Stauber, N. C., Rossi, M. L., and Stassinopoulus, E. G. (1983). "AAS Proceedings: Space Safety and Rescue," Vol. 1982/1983.

Stassinopoulos, E. G. (1975). NSSDC75-11, April. National Space Sciences Data Center, Greenbelt, Maryland.

Stassinopoulos, E. G. (1979). *In* "Workshop on the Radiation Environment of the Satellite Power System (SPS)," pp. 184–216 (Rept. CONF-7809164). National Technical Information Service, Springfield, Virginia.

Stassinopoulos, E. G., and King, J. H. (1974). *IEEE Trans. Aerospace Elec. Sys.* **AES-10**, No. 4.

Steel, L. K., and Catravas, G. N. (1982). *Int. J. Radiat. Res.* **42**, 517–530.

Steel, L. K., Weiss, J. F., and Catravas, G. N. (1982). *Int. J. Immunopharmacol.* **4**, 298.

Stone, R. S. (1948). *Am. J. Roentgen.* **59**, 771.

Stone, R. S., and Larkin, J. C. (1942). *Radiology* **39**, 608.

Stone, R. S., Lawrence, H. H., and Abersold, P. C. (1940). *Radiology* **35**, 322.

Stoner, J. B., Haris, P. S., Furchner, J. E., and Langham, W. H. (1957). *Radiat. Res.* **6**, 188.

Storb, R. (1979). *Transplant. Proc.* **11**, 196.

Storb, R., Epstein, R. B., LeBlond, R. F., Rudolph, R. H., and Thomas, E. D. (1969). *Blood* **33**(6), 918–923.

Storb, R., Prentice, R. L., Sullivan, K. M., Shulman, H. M., Deeg, J., Doney, K. C., *et al.* (1983). *Ann. Intern. Med.* **98**, 461–466.

Storer, J. B., and Ullrich, R. L. (1983). *Radiat. Res.* **96**, 334–347.

Storm, A. J., Van Der Kogel, A. J., and Nooter, K. (1985). *Eur. J. Cancer Clin. Oncol.* **6**, 759–764.

Sullivan, M. F. (1962). *Nature (London)* **195**, 1217–1218.

Taylor, G. R., and Dardano, J. R. (1983). *Aviat. Space Environ. Med. Suppl.* **54**(12), 555–559.

Teague, M. J., and Stassinopoulos, E. G. (1972). NASA/GSFC Report X-601-72-48, December, 1972.

Thoma, G. E., and Wald, N. (1968). *J. Occup. Med.* **1**, 421.

Thomas, E. D. (1975) *N. Engl. J. Med.* **292**, 832–985.

Thompson, W. G. (1971). *Can. Med. Assoc. J.* **104**, 305–309.

Thomson, J. F., Williamson, F. S., Grahn, D., and Ainsworth, E. J. (1981). *Radiat. Res.* **86,** 559–572.
Thomson, J. F., Williamson, F. S., and Grahn, D. (1985). *Radiat. Res.* **103,** 77–88.
Tobias, C. A. (1952). *J. Aviat. Med.* **23,** 345–372.
Tobias, C. A. (1985). *Radiat. Res.* **103,** 1–33.
Tobias, C. A., and Grigor'yev, Y. G. (1975). (M. Calvin and O. G. Gazenko, eds.) *In* "Foundations of Space Biology and Medicine" (E. M. Calvin and O. G. Gazenko, eds.), Vol. 2, pp. 473–531. NASA, U.S. Govt. Printing Office, Washington, D.C.
Tobias, C. A., and Todd, P. (1974). "Space Radiation Biology and Related Topics." Academic Press, New York and London.
Tobias, C. A., Anger, H. O., and Lawrence, J. H. (1952). *Am. J. Roentgenol. Rad. Therm. Nucl. Med.* **63,** 1–27.
Tobias, C. A., Budinger, T. F., and Lyman, J. T. (1970). Report UCRL-19868. University of California, Lawrence Laboratory, California.
Tobias, C. A., Blakely, E. A., Alpen, E. L., Cistro, J. R., Ainsworth, E. J., Curtis, S. B., Ngo, F. Q., Rodriguez, A., Roots, R. J., Tenforde, T., and Young, T. C. (1982). *Int. J. Rad. Oncol. Biol. Phys.* **8,** 2109–2120.
Todd, P. (1983). *Adv. Space Res.* **3**(8), 187–194.
Tomson, J. F., Williamson, F. S., and Grahn, D. (1985). *Radiat. Res.* **103,** 77–88.
Tori, G., and Gasbarrini, G. (1963). *Radiol. Clin.* **32,** 47–56.
Townsend, L. W., and Wilson, J. W. (1986). *Radiat. Res.* **106,** 283–287.
Townsend, L. W., Wilson, J. W., Norbury, J. W., and Bidasariz, H. B. (1984). *NASA Tech. Pap.*, 2305.
Trocha, P. J., and Catravas, G. N. (1982). *Int. J. Radiat. Oncol. Biol. Phys.* **8,** 543–546.
Turbyfill, C. L., Roudon, R. M., Young, R. W., *et al.* (1972). AFRRI SR72-3. Armed Forces Radiobiology Research Institute, Bethesda, Maryland.
Turns, J. E., Doyle, T. F., and Curran, C. R. (1971). AFRRI SR71-16. Armed Forces Radiobiology Research Institute, Bethesda, Maryland.
Ullrich, R. L. (1984). *Radiat. Res.* **97,** 587–597.
Ullrich, R. L., and Casarett, G. W. (1977). *Radiat. Res.* **72,** 107–121.
United Nations Scientific Committee on Effects of Atomic Radiation. (1977). "Sources and Effects of Ionizing Radiation: 1977 Report to the General Assembly with Annexes." United Nations, New York.
Van Bekkum, D. W., and De Vries, M. J. (1967). Logos Press/Book/Academic Press, London, New York.
Van Zweiten, M. J., Broerse, J. J., and Hollander, C. F. (1982). *In* "Proceedings of Seminar on Neutron Carcinogenesis," pp. 117–134. Commission of the European Communities, Luxembourg.
Vignuelle, R., and Baum, S. J. (1982). *Exp. Hemat.* **10**(Suppl. 12), 249–262.
Vinograd, S. P. (1980). "Proceedings of Proposed Federal Research Agenda," pp. 433–466. Interagency Radiation Research Committee, Washington, D.C.
Vogel, H. H., and Dickerson, H. W. (1982). *In* "Neutron Carcinogenesis" (J. J. Broerse and G. B. Gerber, eds.), pp. 135–154. Commission of the European Communities (Radiation Protection), Luxembourg.
Vorobyov, E. I., Garenko, O. G., Genin, A. M., and Egorov, A. D. (1983). *Aviat. Space Environ. Med. (Suppl.)* **54**(12), 531–540.
Walker, R. I., and Porvaznik, M. (1978). *Infect. Immun.* **21,** 655–658.
Walker, R. I., and Porvaznik, M. (1983). *In* "Immunologic Consequences of Thermal and Traumatic Injury" (J. Ninneman, ed.), pp. 1–16.

Walker, R. I., Myhal, M. L. (1985). *In* "Pathophysiology of Combined Injury and Trauma" R. I. Walker, D. F. Gruber, T. J. MacVittie, and J. J. Conklin, eds.), pp. 183–192. Univ. Park Press, Baltimore, Maryland.

Walker, R. I., Brook, I., and MacVittie, T. J. (1984). *Mtg. Am. Soc. Microbiol., March 5–9.* St. Louis, Missouri.

Walker, R. I., Brook, I., Costerton, J. W., MacVittie, T. J., and Myhal, M. L. (1985). *Radiat. Res.* **104.** 346–357.

Wefel, J. P. (1978). *In* "Workshop on the Radiation Environment of the Satellite Power System" (W. Schimmerling and S. B. Curtis, eds.), pp. 117–183. Lawrence Berkeley Laboratory, Berkeley, California.

Weichselbaum, R. R., and Little, J. B. (1983). *In* "Radioprotectors and Anticarcinogens" (O. F. Nygaard and M. G. Simic, eds.), pp. 607–614. Academic Press, New York.

Weiss, J., Jacobs, A. J., and Rankin, W. A. (1983). "Proceedings of the 7th International Congress of Radiation Research" (J. J. Broerse, G. W. Barendsen, H. B. Kal, and A. J. van der Kogel, eds.), pp. C1–37. Nijhoff, Amsterdam.

Weiss, J. Hoover, R. L., and Kumar, K. S. (1986). *34th Annu. Mtg. Radiat. Res. Soc.* (Abstract).

Wells, J. R., Sullivan, A., and Cline, M. J. (1979). *Cryobiology* **16,** 201–210.

Wheeler, K. T., Norton, K. L., Deen, D. F., and Lieth, J. T. (1980). *Int. J. Radiat. Biol.* **37,** 225–229.

Wixon, H. N., and Hunt, W. A. (1983) *Science* **220,** 1073–1074.

Wilson, J. W. (1978). *In* "Workshop on the Radiation Environment of the Satellite Power System" (W. Schimmerling and S. B. Curtis, eds.), pp. 33–116. Lawrence Berkeley Laboratory, Berkeley, California.

Wilson, J. W. (1983). *NASA Tech. Pap.*, 2178.

Wilson, J. W., Townsend, L. W., and Bada, F. F. (1986). *Radiat. Res.* **109,** 173–183.

Wollen, A. *et al. (1974). Clin. Res.* **23,** *260A.*

Wood, D. H., Yochmowitz, M. G., Salmon, Y. C., Eason, R. L., and Bosler, R. A. (1983). *Aviat. Space Environ. Med.* **54**(8), 714–718.

Wood, C. D., Manno, J. E., Manno, B. R., Redetsk, H. M., Wood, M., and Vkovirs, W. A. (1984). *Aviat. Space Environ. Med.* **55**(2), 113–116.

Workman, P. (1980). *Cancer Clin. Trials* **3,** 237–251.

Wulf, H., Kraft-Weyather, H. G., Blakely, E. A., Tobias, C. A., and Kraft, G. L. (1985). *Radiat. Res.* **109,** S122–S134.

Yang, T. C., and Tobias, C. A. (1984). *Adv. Space Res.* **4**(10), 239–245.

Yegorov, A. D. (1981). Academy of Sciences USS, Ministry of Health, Moscow, 1980, NASA TM-76450, January, 1981.

Yochmowitz, M. G., Wood, D. H., and Salmon, Y. L. (1985). *Radiat. Res.* **102,** 14–34.

Young, R. W. (1977). Annual Research Report ARR-11, Armed Forces Radiobiology Research Institute, Bethesda, Maryland.

Young, R. W., and Middleton, G. R. (1974). *In* "Annual Research Report ARR-8." Armed Forces Radiobiology Research Institute, Bethesda, Maryland.

Young, R. W., and Middleton, G. R. (1975). *In* "Annual Research Report ARR-9." Armed Forces Radiobiology Research Institute, Bethesda, Maryland.

Yuhas, J. M. (1970). *Radiat. Res.* **44,** 621–628.

Yuhas, J. M., and Storer, J. B. (1969). *Int. J. Radiat. Biol.* **15,** 233.

Zook, B. C., Bradley, E. W., Casarett, G. W., and Roger, C. C. (1980). *Radiat. Res.* **84,** 562–578.

RADIATION RESEARCH 112, 508–516 (1987)

Quantification of Gut Injury with Diamine Oxidase Activity: Development of a Fission Neutron RBE and Measurements with Combined Injury in Mouse Models[1]

ROBERT M. DEBELL, G. DAVID LEDNEY, AND STEPHEN L. SNYDER

Armed Forces Radiobiology Research Institute, Bethesda, Maryland 20814

DEBELL, R. M., LEDNEY, G. D., AND SNYDER, S. L. Quantification of Gut Injury with Diamine Oxidase Activity: Development of a Fission Neutron RBE and Measurements with Combined Injury in Mouse Models. *Radiat. Res.* **112**, 508–516 (1987).

Plasma and small intestine diamine oxidase (DAO) activities were measured on Days 2, 4, and 6 following irradiation of mice with a range of doses of fission neutrons and ^{60}Co. With increasing doses of radiation, plasma DAO activity increased on Day 2 and intestinal DAO activity decreased on Day 4; moreover, the approximate relative biological effectiveness values for these changes in activity were 5.81 for plasma DAO activity on Day 2 and 3.88 for intestinal DAO activity on Day 4. On Day 6 relatively high levels of radiation caused DAO activity in the small intestine to remain depressed whereas low levels resulted in recovery with activities at or near controls. In animals with combined injury (radiation plus 30% surface burn or wound), changes in DAO activity in the intestine were similar to those with radiation alone; plasma DAO activity, in contrast to radiation alone, did not show an increase at the 2-day mark. These dose-dependent relationships should provide a basis for using DAO as a potential indicator of biological damage from radiation exposure within the lethal range.

INTRODUCTION

The second step in the polyamine catabolic pathway results in the conversion of putrescine to γ-aminobutyraldehyde by means of the enzyme diamine oxidase or DAO (EC 1.4.3.6). The activity of this enzyme has been correlated with a variety of clinical conditions in man either induced as with heparin administration (*1, 2*) and cancer chemotherapy (*3*) or naturally occurring such as appendicitis (*4*), renal failure, (*5*), oncogenesis (*6, 7*), and intestinal ischemia (*8*). Because it has been suggested that DAO is implicated in the regulatory processes which govern cell proliferation and growth (*9*), it is important to understand the effects of radiation damage on DAO activity, especially with regard to the fact that DAO occurs in high concentrations in

[1] Supported by the Armed Forces Radiobiology Research Institute, Defense Nuclear Agency, under work unit 4420-B3129. Views presented in this paper are those of the authors; no endorsement by the Defense Nuclear Agency has been given or should be inferred. Research was conducted according to the principles enunciated in the "Guide for the Care and Use of Laboratory Animals" prepared by the Institute of Laboratory Animal Resources, National Research Council.

0033-7587/87 $3.00

the microvilli of the small intestine (*10*), a target almost as radiosensitive as bone marrow (*11*).

In a dose-dependent manner radiation causes damage to the mucosa of the small intestine characterized by loss and denudation of villi and diminished crypt cell mitosis. These effects eventually lead to "intestinal radiation death" (*11–13*).

It has been reported that the intestinal integrity of rats can be correlated with DAO activity in both the intestine and plasma (*14*), and increases in damage to the intestine using hyperosmolar sodium sulfate or 1-β-D-arabinofuranosylcytosine, a chemotherapeutic agent, cause proportional decreases in DAO activity (*3, 14*). The relationship between whole-body electron irradiation and DAO activity in the rat ileum and plasma was described recently (*15*). As the radiation dose increased from 5 to 12 Gy, both plasma and ileal DAO activity, as percentage of control, decreased to a minimum 3 days following radiation challenge.

Knowledge of the effects of radiation on DAO activity in both the small intestine and plasma is expanded in this investigation to include dose-dependent relationships using fission neutron and ^{60}Co irradiation of a mouse model. Because the modification to the DAO assay to improve the sensitivity of plasma measurements, a positive correlation is shown for the first time between plasma DAO activity and exposure dose 2 days postirradiation. Because of the importance of accurately estimating radiation dose in combined injury in the event of nuclear accidents or detonations (*11, 16, 17*), changes in DAO activities are measured in animals subjected to both burn or wound and radiation trauma.

MATERIALS AND METHODS

Animals. Female B6D2F1/J mice (Jackson Laboratories, Bar Harbor, ME) 12 to 20 weeks old were quarantined for 2 weeks and used only if routine tests of samples for *Pseudomonas* species and histologic lesions of common murine diseases were negative. Methoxyflurane anesthesia was given to all mice prior to treatment involving wound or burn trauma or euthanized via intracardiac exsanguination. Wounding was accomplished by removal of a 2.5 × 3.8 cm section of dorsal skin fold and underlying panniculus carnosus muscle with a steel punch immersed in 70% alcohol before each animal was injured. Burning was performed on a 2.5 × 3.8 cm shaved dorsal surface area by a 12-s ignition of 100% alcohol. All experimental mice, including controls, were given 0.5 ml of 0.9% NaCl fluid therapy ip and placed in microisolator cages. Either type of injury was approximately 30% body surface area and was performed immediately following radiation exposure.

Radiation. The techniques and dosimetry of exposing mice to AFRRI-TRIGA reactor produced fission neutrons (fn) and the AFRRI 5,18 PBq ^{60}Co source were described previously (*18*). For neutron irradiation, mice rotating at 1.5 rpm in aluminum restraining tubes received midline tissue doses of fn total body at 0.4 Gy/min. A neutron to γ ratio of approximately 25:1 was achieved by irradiating the mice through a 6-in. lead reactor shield and maintaining the exposure array of mice in a 2-in. lead cave. For γ irradiation mice in Plexiglas restrainers received midline tissue doses at 0.4 Gy/min from bilaterally positioned ^{60}Co elements.

Tissue extracts. Plasma was prepared by removal of approximately 1 ml of blood via intracardiac puncture and expelling this into a 1.5 ml vial containing 0.02 ml of sodium heparin, 1000 units/ml. Samples were mixed well and centrifuged at 10,500*g* for 15 min at 4°C. Supernatant fractions were saved at −20°C until use.

The small intestine of each animal was dissected free of associated tissue and cut into five or six segments. The contents of each was extruded gently with a blunt instrument, and the intestine wet weight was determined. Each intestine was rinsed with an excess of cold Sorensen's phosphate buffer, pH 7.4, and stored at −20°C in 9.0 ml of buffer.

To prepare the enzyme extract, the intestines in the buffer were homogenized using a Polytron mechanical homogenizer (Brinkman Instruments, Westbury, NY) at high speed for two 30-s intervals. Each tube was cooled on ice for at least 5 min between runs. These homogenates were centrifuged at 17,000*g* for 20 min at 4°C, and supernatant fractions were tested for DAO activity.

Enzyme assays. DAO activity was measured by the [^{3}H]putrescine method of Okuyama and Kobayashi (*19*) as modified by Kusche *et al.* (*20*). For intestine samples, 0.1 ml of enzyme preparation was mixed with 0.1 ml of 1.0 m*M* putrescine (10^4 dpm/m*M*) and placed in a 37°C water bath for 30 min. Reactions were terminated with 0.2 ml of 0.04 m*M* aqueous aminoguanidine. Plasma samples were assayed similarly except the substrate was 0.1 m*M* putrescine (10^5 dpm/m*M*), and the incubation period was 60 min. Two milliliters of scintillant (PPO-POPOP in toluene) was added to each reaction tube and vortexed vigorously for 10 s. After 15 min 1 ml of the upper phase was added to 8 ml of scintillant for counting. The potential for dynamic changes in DAO activity in plasma and intestines postirradiation necessitated kinetic studies to establish optimal substrate concentrations and periods of incubation. The conditions used here insured measured activities were a function of first-order kinetics to compare DAO activity at various doses of ionizing radiation.

Protein assays were performed with the Bio-Rad dye reagent. Bovine plasma γ-globulin and albumin were standards for intestine and plasma samples, respectively.

RESULTS

Time course changes of DAO activity. Pilot studies were performed to determine which specific days following radiation exposure resulted in peak changes in DAO activity. Measurements of DAO activities were taken on Days 2, 4, and 6 following irradiation in both the small intestine and plasma from groups of three to five mice exposed to 0 to 7 Gy fn or 0 to 16.1 Gy ^{60}Co (Fig. 1). Dose-dependent changes in DAO activity were prominent on Day 2 in the plasma and Day 4 in the intestine. Above 3 Gy fn or 11.5 Gy ^{60}Co, there were decreases in intestinal activities on Day 4 to approximately 75% of either controls or low radiation doses. DAO activity on Day 6 remained depressed with 5 Gy fn or 16.1 Gy ^{60}Co but returned to normal with doses of 3 Gy fn or 11.5 Gy ^{60}Co.

DAO dose response and RBE values. Figures 2A and 2B show the relationships between radiation dose and DAO activity as percentage of control in the small intestine at Day 4 and the plasma at Day 2, respectively. The trend of diminishing intestinal DAO activity with an increasing dose of radiation was consistent, regardless of the radiation quality. The plasma dose relationships on Day 2 were linear below 5 Gy fn or above 6.9 Gy ^{60}Co. The RBE was determined to be 3.88 in the small intestine where the DAO activity was 50% of control. Because the plasma DAO response increased as the radiation dose was higher, an RBE of 5.81 was calculated at the midpoint (179% of control) of the fn curve between 100 and 259% of control. Although RBE values change with radiation dose, these RBEs and the appearance of the curves in Figs. 2A and 2B suggest that DAO increasing in the blood at Day 2 following exposure involves a more sensitive mechanism to the differences in radiation quality than that in the small intestine.

Inspection of the plot of plasma DAO activity with time (Figs. 1C and 1D) indicated a trend of diminishing DAO activity in the plasma on Day 4 with increasing radiation doses. These changes could be correlated with the dose–response relationships observed on Day 4 with DAO activities measured in the small intestine (Figs. 3A and 3B). This result suggests the rate of decrease between the relative plasma DAO activities on Days 2 and 4 following exposure correlates with the radiation exposure doses.

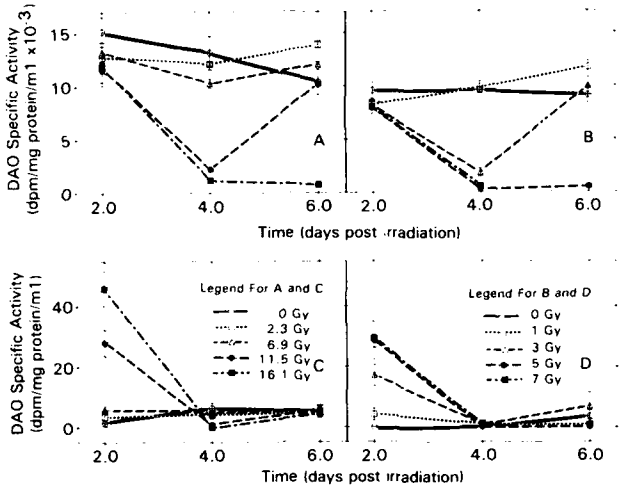

FIG. 1. Effect of radiation on the time course of DAO activity. Panels A and B show intestinal DAO activity with ^{60}Co and fission neutron radiation, respectively. Panels C and D show plasma DAO activity with ^{60}Co and fission neutron radiation, respectively. Values for dpms were corrected for background before calculation of DAO activity. For comparison the relative biological effectiveness (RBE) of 2.3 was used. Maximum change was observed on Day 2 for plasma and Day 4 for intestinal measurements of DAO. For Day 6 values at 16.1 Gy ^{60}Co, one animal survived; at 7 Gy fn, none survived. All other points represent the mean of three to five animals with bars for standard errors. A one-way analysis of variance demonstrated mean values for controls in each panel were statistically equal at a level of significance greater than 0.05.

Combined injury and DAO activity. A separate study was undertaken to determine if these same relationships were maintained in combined injured animal models. Six groups of mice (controls, burned, wounded, irradiated, irradiated and wounded, irradiated and burned) were used, and irradiated animals were exposed to 11.5 Gy ^{60}Co. This dose was selected for two reasons: changes in DAO activity varied most at this dose during the 6 days postirradiation, and previous studies in this laboratory suggested combined injury complications are most severe at relatively high exposure doses.

Intestinal DAO activities of burned and wounded animals did not differ from controls, and values for combined injured animals were similar to those only irradiated (Figs. 4A and 4B). Essentially identical experiments except performed with 3 Gy fn gave similar results (data not shown). Plasma DAO activities for both the wounded and burned groups were similar to that for the control mice; however, there were only slight elevations of DAO activity on Day 2 of the irradiated and wounded or irradiated and burned mice in comparison to the group subjected to radiation alone (Figs. 4C and 4D).

DISCUSSION

Diamine oxidase has shown potential as a clinical marker for a variety of medical problems, especially in cases with a loss of intestinal integrity (*1–8*). Damage to the

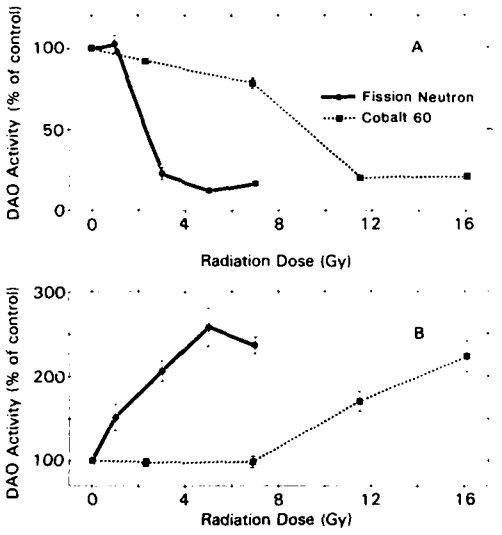

FIG. 2. Small intestine (A) and plasma (B) DAO activity with radiation dose. Dose-dependent changes occurred on Day 4 for the small intestine and on Day 2 for plasma. The $LD_{50/30}$ (50% mortality in 30 days) was determined empirically to be 9.65 Gy ^{60}Co; moreover, the RBE was calculated at 2.46. The approximate RBE values for the above curves were calculated at 50% activity for A and 179% activity for B; these were 3.88 and 5.81, respectively.

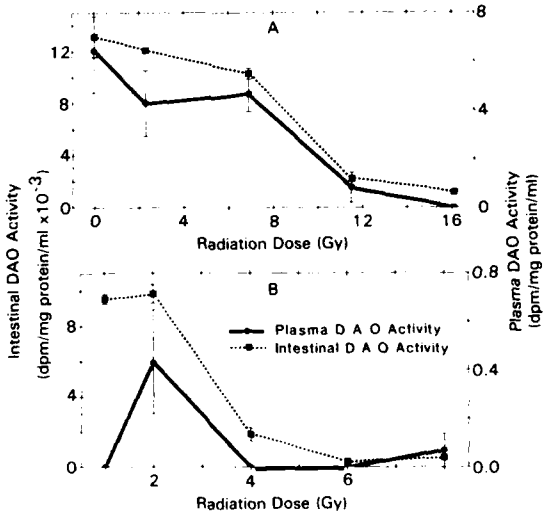

FIG. 3. Comparison of plasma and small intestine DAO activities. Four days post-^{60}Co(A) and fission neutron (B) irradiation. Plasma DAO activity is much less than that measurable in the small intestine. The DAO activities on Day 4 postirradiation challenge were scaled to demonstrate the similarities in the trends of activities found in the plasma and small intestine. Vertical bars indicate standard errors.

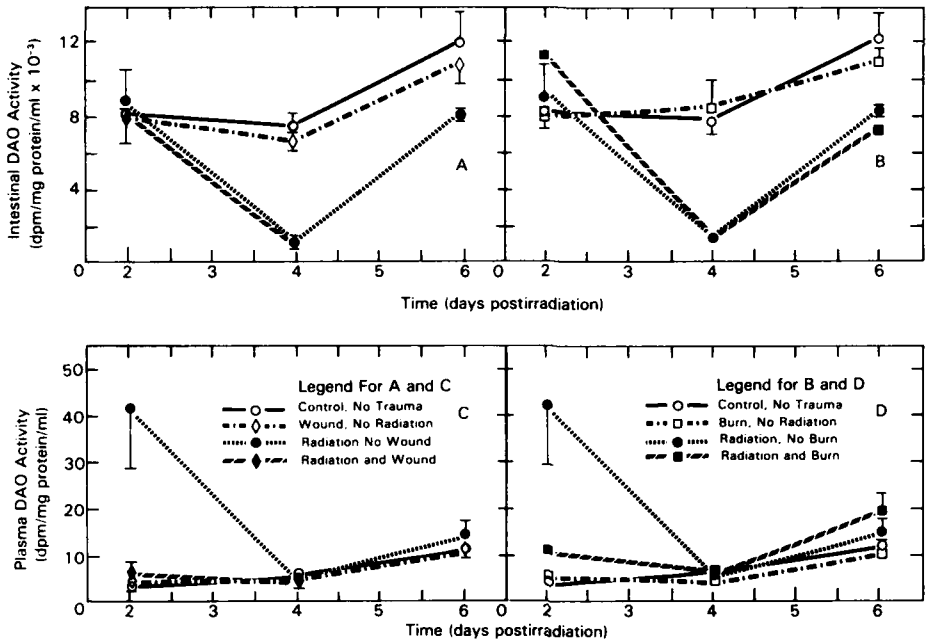

FIG. 4. Time course of DAO activities with combined injury. Burn or wound trauma affected approximately 30% of body surface area. Intestinal DAO activity was not changed markedly with combined injury as compared with radiation alone. The effect of combined injury on the plasma DAO activity at Day 2 was observed as a significant decrease, almost to control levels, as compared to the effect of radiation alone. Vertical bars represent standard errors. A one-way analysis demonstrated mean values for controls in each panel were statistically equal at a level of significance greater than 0.05.

intestine has been widely documented to be a serious and likely effect of whole-body irradiation (*11–13*). These considerations suggest the possibility that the activity of DAO would provide an important criterion for quantifying biological damage resulting from radiation exposure.

It should be noted that, with whole-body exposures at high radiation doses, failure of both the intestinal mucosa and the myelocytic renewal system contribute to lethality. At lower radiation doses loss of bone marrow function may predominate, but gastrointestinal disturbances exist as evidenced by a reappearance of obvious symptoms during severe illness with bone marrow syndrome (*21*). Significant gastrointestinal deterioration from radiation contributing to lethality within 30 days should occur at doses $\geq$5 Gy fn or $\geq$11.5 Gy ^{60}Co where the mean times of death at these doses were determined in this laboratory to be 6.3 and 12 days, respectively.

This study showed that DAO activity was altered significantly in both the small intestine and plasma with sublethal and lethal levels of radiation exposure, and the observed changes were dose dependent. Although DAO activity was approximately 1000-fold less in the plasma than the intestine, the sensitivity of the assay permitted statistically accurate correlations between whole-body radiation exposure and plasma DAO activity. Measuring temporal changes in circulating levels of DAO should con-

tribute much to improving the accuracy of determining radiation exposures. The importance of this is substantiated by the observations where increases in plasma DAO activity on Day 2 followed by decreases in both intestinal and plasma activities on Day 4 resulted from relatively high levels of exposure. When intestinal levels remained depressed until Day 6, exposure doses were within the range of lethal radiation (i.e., radiation dose greater than the $LD_{100/30}$) where no surviving animals would be expected within 30 days. Although the use of DAO as a "precise dosimeter" of radiation exposure would be premature, changes in DAO activity following whole-body irradiation could be used with other symptoms to assess clinical damage from radiation exposure.

Day 2 levels of DAO activity in the small intestine appeared normal whereas those in the plasma were elevated. If increased plasma levels resulted from a loss of DAO in the small intestine, elevated plasma levels would be expected to follow the loss of intestinal DAO activity on Day 4, not precede these on Day 4. Also, the RBE value of 5.81 for plasma DAO activity on Day 2 was substantially higher than 3.88, the RBE for changes in intestinal DAO on Day 2. If increases in circulating DAO on Day 2 resulted directly from the loss of intestinal DAO activity on Day 4, it is likely that the RBE values would be similar. These findings suggest that the plasma DAO response on Day 2 did not necessarily result from the intestinal damage alone. Because almost all organs contain DAO, the alternatives would be that changes in plasma DAO on Day 2 result from damage to the circulatory system or from a general response involving cellular damage to almost all tissues. Since plasma DAO activity has been shown to be a potentially effective marker of human intestinal damage (*4, 7*), the observations in this study confirm that this should be useful for radiation damage as well, with the provision that changes in plasma DAO activity with time and with combined injury are fully explained.

The high probabilities of combined injury in a nuclear disaster or radiation accident (*11, 16, 17*) require that intense efforts be directed to understand the effects of this syndrome. Although both nonlethal radiation doses and burn or wound trauma alone did not show marked changes in normal levels of DAO activity in the plasma and intestine, correlations between the dose of radiation and DAO activities were complicated by combined injury. The drop in plasma DAO activity between Days 2 and 4 following radiation challenge in animals only irradiated was eliminated when a surface burn or wound was present. The 30% surface burn or wound, however, may be above a particular threshold to obtain the increase in DAO activity observed with radiation alone. This is suggested because the activity was slightly higher on Day 2 in burned and irradiated animals compared to those wounded and irradiated. (We have observed that combined injury which incorporates wound trauma is usually more lethal than that with comparable burn trauma.) Another possible explanation may be that the wound or burn injury causes the release of an inhibitor of DAO or a protease which destroys the circulating enzyme. Although preliminary studies have suggested this is not true, a third possibility is that the time course of the DAO elevation is advanced to a point before the 2-day mark in combined injured animals. Studies are underway to explain the cause of the attenuated DAO activity with combined injury.

DAO activity measured with varying degrees of combined injury and different radiation qualities and doses will be a subject for future studies. The relationships between DAO activity, especially with regard to plasma levels, in both irradiated and combined injured animal models should prove useful in the management of radiation-induced biological damage.

ACKNOWLEDGMENTS

The authors express their appreciation for the technical assistance of David Funckes and Parkson Lin.

RECEIVED: March 13, 1987; REVISED: August 4, 1987

REFERENCES

1. S. B. BAYLIN, M. A. BEAVEN, R. M. KRAUSS, and H. R. KEISER, Response of plasma histaminase activity to small doses of heparin in normal subjects and patients with hyperlipoproteinemia. *J. Clin. Invest.* **52,** 1985–1993 (1973).
2. O. DAHLBACK, R. HANSSON, G. TIBBLING, and N. TRYDING, The effect of heparin on diamine oxidase and lipoprotein lipase in human lymph and blood plasma. *Scand. J. Clin. Lab. Invest.* **21,** 17–25 (1968).
3. G. D. LUK, W. P. VAUGHAN, P. J. BURKE, and S. B. BAYLIN, Diamine oxidase as a plasma marker of rat intestinal mucosal injury and regeneration after administration of 1-β-D-arabinofurnaosylcytosine. *Cancer Res.* **41,** 2334–2337 (1981).
4. R. MENNINGEN, M. GUNTHER, N. BONNINGHOFF, C. D. STAHLKNECHT, I. KUBITZA, and J. KUSCHE, Diamine oxidase as a marker of intestinal integrity in acute appendicitis. *Agents Actions* **18,** 38–40 (1986).
5. D. GIARNIERI, M. T. COSTA, V. GIARNIERI, and B. MONDOVI, Diamine oxidase content in urine of patients with renal failure. *Agents Actions* **16,** 249–251 (1985).
6. S. B. BAYLIN, M. D. ABELOFF, K. C. WIEMAN, J. W. TOMFORD, and D. S. ETTINGER, Elevated histaminase (diamine oxidase) activity in small-cell carcinoma of the lung. *N. Engl. J. Med.* **293,** 1286–1290 (1975).
7. J. KUSCHE, T. BIEGANSKI, R. HESTERBERG, C. D. STAHLKNECHT, K. D. FEUBNER, I. STAHLENBERG, and W. LORENZ, The influence of carcinoma growth and diamine oxidase activity in human gastrointestinal tract. *Agents Actions* **10,** 110–113 (1980).
8. J. KUSCHE, W. LORENZ, and R. HESTERBERG, The relevance of the diamine oxidase–histamine system for shock development following intestinal ischemia. In *Animal Models for Intestinal Disease* (C. J. Pfeiffer, Ed.), pp. 256–280. CRC Press, Boca Raton, FL, 1985.
9. O. HEBY, Role of polyamines in the control of cell proliferation and differentiation. *Differentiation* **19,** 1–20 (1981).
10. K. M. M. SHAKIR, S. MARGOLIS, and S. BAYLIN, Localization of histaminase (diamine oxidase) in rat small intestinal mucosa: Site of release by heparin. *Biochem. Pharmacol.* **26,** 2343–2347 (1977).
11. J. J. CONKLIN, R. I. WALKER, and E. F. HIRSCH, Current concepts in the management of radiation injuries and associated trauma. *Surgery* **156,** 809–829 (1983).
12. R. A. CONRAD, Some effects of ionizing radiation on the physiology of the gastrointestinal tract: A review. *Radiat. Res.* **5,** 167–188 (1956).
13. H. QUASTLER, The nature of intestinal radiation death. *Radiat. Res.* **4,** 303–320 (1956).
14. G. D. LUK, T. M. BAYLISS, and S. B. BAYLIN, Diamine oxidase (histaminase). A circulating marker for rat intestinal mucosal maturation and integrity. *J. Clin. Invest.* **66,** 66–70 (1981).
15. M. J. ELY, J. M. SPEICHER, G. N. CATRAVAS, and S. L. SNYDER, Radiation effects on diamine oxidase activities in intestine and plasma of the rat. *Radiat. Res.* **103,** 158–162 (1985).
16. J. J. CONKLIN, T. J. MACVITTIE, and R. I. WALKER, Pathophysiology of combined injury and trauma. In *The Pathophysiology of Combined Injury and Trauma* (R. I. Walker, D. F. Gruber, T. J. MacVittie, and J. J. Conklin, Eds.), pp. 3–10. University Park Press, Baltimore, MD, 1985.

17. O. MESSERSCHMIDT, Results of animal experiments as a basis for recommendations on therapy of combined injuries. In *The Pathophysiology of Combined Injury and Trauma* (R. I. Walker, D. F. Gruber, T. J. MacVittie, and J. J. Conklin, Eds.), pp. 11–18. University Park Press, Baltimore, MD, 1985.

18. D. A. STEWART, G. D. LEDNEY, W. H. BAKER, E. G. DAXON, and P. A. SHEEHY, Bone marrow transplantation of mice exposed to a modified fission neutron (N/G 30:1) field. *Radiat. Res.* **92,** 268–279 (1982).

19. T. OKUYAMA and Y. KOBAYASHI, Determination of diamine oxidase activity by liquid scintillation counting. *Arch. Biochem. Biophys.* **95,** 242–250 (1961).

20. J. KUSCHE, H. RICHTER, R. HESTERBERG, J. SCHMIDT, and W. LORENZ, Comparison of the ^{14}C-putrescine assay with the NADH test for the determination of diamine oxidase: Description of a standard procedure with a high precision and improved accuracy. *Agents Actions* **3,** 148–156 (1973).

21. V. P. BOND, T. M. FLEIDNER, and J. O. ARCHAMBEAU. *Mammalian Radiation Lethality,* pp. 159–275. Academic Press, New York, 1965.

Journal of Leukocyte Biology 42:181–187 (1987)

Rat Monocytes in a Model of Combined Injury Express the OX8 Antigen

W. Kaffenberger, D.F. Gruber, and T.J. MacVittie

Department of Experimental Hematology, Armed Forces Radiobiology Research Institute, Bethesda, Maryland

We have analyzed peripheral blood mononuclear cell preparations from a rat model of combined injury (CI) [whole-body irradiation (500 cGy ^{60}Co) followed by a thermal injury (20% body surface area, dorsal, scald burn)] for the expression of OX8 antigens. Ficoll-separated mononuclear fractions were labeled with monoclonal antibodies MRC OX8, MRC OX19, W3/13 HLK, or W3/25 for flow cytometric analysis. Combined-injury trauma resulted in decreased mononuclear cells to 6% of normal. This effect was due to the rapid decrease in radiosensitive lymphocytes from 83% to 10%. The relative numbers of monocytes increased from a normal 13% to 70% at day 4 after CI. Labeling of cells with OX8 after CI shifted to a population which was significantly larger in volume than normal lymphocytes. At the same time the mean fluorescence intensity of OX8-positive cells was considerably reduced. With the use of a F(ab) fragment of OX8 as a probe, these results could be partially explained as unspecific binding of the whole molecule of OX8 to Fc receptors expressed by activated monocytes. But double-labeling and cell-sorting experiments also revealed the expression of OX8 antigens by a subset of OX8 + / OX19 – monocytes after CI.

Key words: rat monoclonal antibody, MRC OX8, monocytes, flow cytometry

INTRODUCTION

Immunologic dysfunction(s) may ultimately be responsible for the life-threatening circumstances that follow a singular incidence of trauma such as burn or radiation. However, little is known of the immunologic dysfunction(s) that arises after combined-injury trauma. A rat model was selected for the investigation of combined-injury (CI) trauma because several aspects of its immune response to thermal trauma and radiation have been previously investigated [6, 8, 9]. Because of the pivotal role of T-suppressor cells in the down-regulation of immunocompetence, it was our purpose to study the population dynamics of the nonhelper T-lymphocytes following CI. The application of monoclonal antibodies (mcAB) in flow cytometry has proved to be very useful in the identification and quantification of cell surface receptors and cell population subtypes. The mcAB probe MRC OX8 was selected to examine the nonhelper T-lymphocyte population because it purportedly labels only those cells possessing epitopes peculiar to cytotoxic/suppressor T-lymphocytes [3, 5] and a subset of large granular lymphocytes that previously have been identified as natural killer (NK) cells [4, 10, 13]. Before this report, monocytes have not been reported to express the MRC OX8 surface epitope. In this paper, we will present evidence that in our model of combined injury rat monocytes express the OX8 antigen.

MATERIALS AND METHODS

Animals

Sprague-Dawley male rats (Charles River Breeding Laboratory, Wilmington, MA) were maintained in quarantine for 2 weeks until they proved free of *Pseudomonas* spp. All animals were maintained on a 12 h light/12h dark cycle; Wayne Lab-Blox and acidified water (pH 2.5) were available ad libitum. Experiments were initiated when rats were 8–10 wk of age (250–300 g).

Combined Injury (CI)

A sublethal, bilateral, total-body radiation dose of 500 cGy as a mid-line tissue dose was delivered by ^{60}Co sources at a dose rate of 40 cGy/min. Probit calculated analysis of mortalities indicated an LD50/30 of 832 cGy

Received September 26, 1986; accepted February 4, 1987.

Reprint requests: T.J. MacVittie, Department of Experimental Hematology, Armed Forces Radiobiology Research Institute, Bethesda, MD 20814-5145.

with confidence limits of 818 and 845 cGy, respectively. Within 1–2 h of irradiation, rats anesthetized by Nembutal [(0.1 ml/100 g body weight) Abbot Laboratories, North Chicago, IL] received a dorsal thermal injury. Hair was shaved from the back and the area was depilated with a hair remover (Nair, Carter Products, New York, NY). Rats were placed on a plastic template containing an opening that exposed 20% of the body surface area, as calculated by Meeh's formula [7]. The thermal injury was produced by immersing the shaved back of the animal through the template into 96°C water for 10 s. Histological examinations verified the burn to be of full thickness over the entire area. Immediately after thermal trauma, 5 ml of sterile, lactated Ringer's solution was administered intraperitoneally.

TABLE 1. Reactivity of Monoclonal Antibodies as Relevant to This Study

mcAB	Cell types labeled	References
MRC OX8	Suppressor/cytotoxic T-lymphocytes	[3–5]
	large granular lymphocytes	[10,13]
W3/13 HLK	Pan T-cell marker	[12]
MRC OX19	Pan T-cell marker	[5]
W3/25	Helper T-lymphocytes, monocytes	[1,3]
MRC OX42	Subset of monocytoid cells	[11]

Cell Preparation

Rats were anesthetized with Halothane (Halocarbon Laboratories, Inc., Hackensack, NJ) and exsanguinated by cardiac puncture at various times up to 28 days after CI. Heparinized (20 units/ml; Lypho-Med., Inc., Chicago, IL) whole blood was incubated with an equal volume of 3% gelatin (Knox Gelatin, Inc., Englewood Cliffs, NJ) in Hanks' balanced salt solution (HBSS) without Ca^{2+} and Mg^{2+} at 37°C for 30 min. The leukocyte-enriched supernatant was removed and overlayered on Ficoll-Hypague gradients (*Lymphocyte Separation Medium*, LSM; Litton Bionetics, Inc., Kensington, MD) and centrifuged at 400g for 30 min at room temperature. The interface layers were aspirated off and washed (300g, 10 min, 4°C) in HBSS. Contaminating RBC were removed by NH_4Cl substituted isotonic lysing. Viability determinations were made by trypan blue or propidium iodide exclusion. Cellular viabilities were routinely ~95%. Total mononuclear cell counts of the interfaces were determined by Coulter counter (Model ZBI, Coulter Electronics, Inc., Hialeah, FL). Cells were resuspended in PBS (pH 7.3) at a concentration of up to 4×10^7 nucleated cells/ml, and cytospin smears for morphologic cell differential examinations were prepared. Histologic characteristics used routinely to discriminate for monocytes included cytoplasmic/nuclear staining, size, shape, and ratio, and appearance of the plasma membrane.

Labeling of Cells

The cell suspensions (100 μl) were placed into individual wells of a 96-well Linbro microtitration plate (Flow Laboratories, Inc., McLean, VA) containing up to 50 μl mouse antirat monoclonal antibodies (mcAB) in saturating concentrations. The monoclonal antibodies used in this study (MRC OX8, MRC OX19, W3/13 HLK, and W3/25) were purchased as affinity-purified supernatant, or as ascites fluid (Pel-Freez Biologicals, Rogers, AR). The biotin-labeled F(ab) fragment of MRC OX8 and MRC OX42 were kind gifts of Dr. Ken McCarthy, AFRRI, and Dr. Philip Carter, North Carolina State University, Raleigh, NC, respectively. The reactivity of these mcAB is summarized in Table 1.

Following a 1-h incubation at 4°C, cells were washed (300g, 5 min, 4°C) in PBS containing 10% heat-inactivated fetal bovine serum (PBS-10% FBS). Cells were then indirectly labeled for 30 min at 4°C using affinity-purified FITC-labeled anti-mouse IgG (Fc fragment specific) (*Pel-Freez Biologicals*, Rogers, AR). Biotin-coupled MRC OX8 (F[ab] fragment) was labeled with avidin-phycoerythrin conjugate (Becton-Dickinson Monoclonal Center, Inc., Mountain View, CA). Cells were washed (300g, 5 min) and resuspended in PBS-2% FBS for flow cytometric analysis. Control assays were cells incubated with the second antibody or the avidin-phycoerythrin conjugate only.

Flow Cytometry

Dual parameter (green or red fluorescence versus cell volume) measurements using 3-decades logarithmic amplifiers were performed using a FACS ANALYZER (Becton-Dickinson, Mountain View, CA) in conjunction with a CONSORT 30 data analysis system. Normally 10^4 cells/sample were analyzed on a multichannel analyzer (256 channels) and stored in list mode. After gating out small-volume material (unlysed RBC and cellular debris), percentages of positive cells were calculated by plotting the fluorescence histograms of the samples. Threshold levels were established from the fluorescence histograms of the control cells, which were incubated with the secondary antibody only. At such thresholds, no more than 1% of the total events were above the cut-off channel. In experimental histograms, the percentages of positive events above threshold were calculated. Cell-sorting experiments were performed using a Becton-Dickinson FACS II cell sorter.

RESULTS

Changes of Mononuclear Cell Populations in Interfaces of Ficoll-Hypaque Gradients After CI

As depicted in Figure 1, the total cellularity as recovered from the interface of LSM-gradients of peripheral blood decreased to approximately 6% of normal (N) during the first day post-treatment. Total cell counts returned to near normal levels by day 14 and remained at normal levels throughout the 28-day observation time. Cytospin differentials revealed that the initial decrease in total interface cellularity was due primarily to the disappearance of radiosensitive lymphocytes, which normally contributed to 83% of the cell counts in the interfaces (Table 2). Lymphocyte counts remained reduced (40% of N) through day 28 post-trauma (Fig. 1). Monocyte percentages increased from 13% (normal) to 70% by day 4 after CI, and remained elevated (45%–60%) through day 28 post-CI. Between days 1 and 28, abnormally high proportions of neutrophils (13%–73%, usually 4%; see Table 2) were also recovered from the interfaces.

Flow Cytometric Analysis of Mononuclear Cells

In control rats, 86% of the total peripheral blood lymphocytes were determined to be T-lymphocytes as calculated by the cumulative percentages of OX8+ and W3/25+ labeling (Fig. 2, and Table 2) and by labeling with the mcAB W3/13 (Table 2). However, throughout the observation time after CI, the cumulative percentages of OX8+ and W3/25+ cells considerably exceeded the percentages of labeling with OX19 (data not shown) as well as the percentages of morphologically recognizable lymphocytes in the cell preparations, with the exception of day 17 post-treatment (Fig. 2). The initial decrease of cumulative labeling of T-lymphocytes on day 1 post-CI was primarily due to the decrease in labeling with W3/25, whereas labeling with OX8 was only slightly reduced and remained at that level (about 70% of N) through day 28. Between days 1 and 11, when using complete OX8 as a probe, the percentage of OX8+ cells equalled or exceeded identifiable percentages of lymphocytes. However, the F(ab) fragment of OX8 consistently labeled a considerably smaller proportion of cells (40%) during the second week post-CI but similar proportions of cells

TABLE 2. Labeling of Peripheral Blood Mononuclear Cells of Control Rats With T-Cell Monoclonal Antibodies[a]

mcAB	% Labeling ± SEM
MRC OX8	27.81 ± 0.57
W3/25	43.73 ± 1.89
W3/13 HLK	68.64 ± 2.48

[a]Typically, mononuclear cell preparations of control rats consisted of 83% lymphocytes, 13% monocytes, and 4% neutrophils.

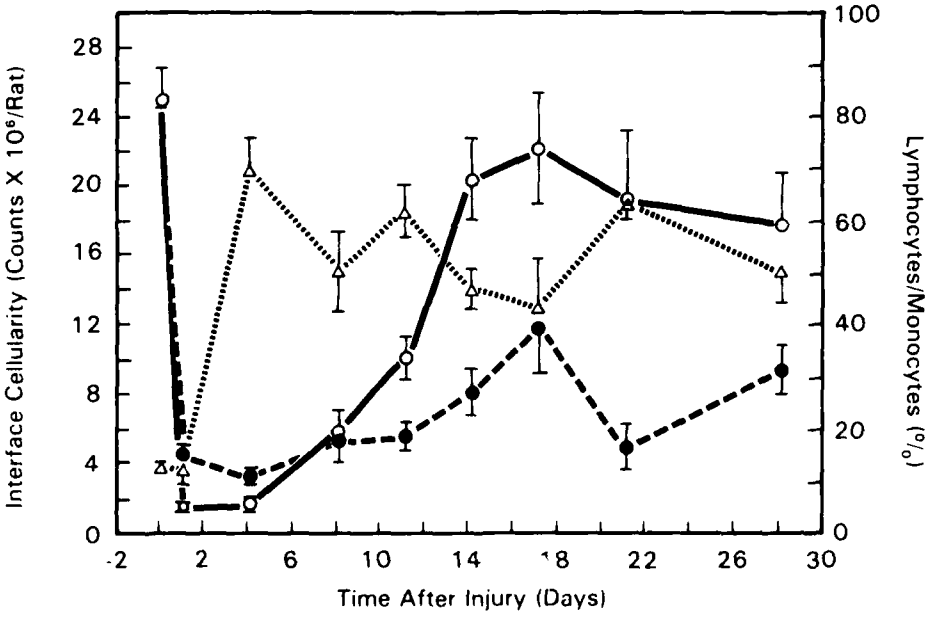

Fig. 1. Total cell counts as recovered from interfaces of LSM-gradients (○), and percentages of lymphocytes (●) and monocytes (△) in samples as a function of time after combined injury. Each data point in figures represents means (+/− SEM) of 4 to 14 experimental animals.

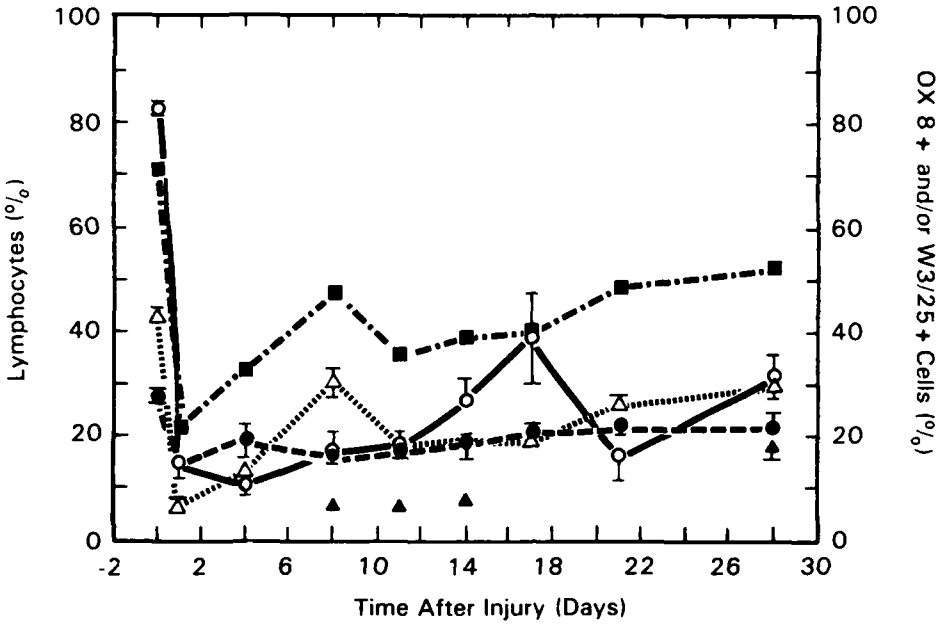

Fig. 2. Percent lymphocytes (○) in cell preparations and labeling of cells with *monoclonal antibodies* MRC OX8 (●) *or* W3/25 (△), *percentages of OX8-positive plus* W3/25-positive cells (■) as function of time after CI. Percentages of labeling with F(ab) fragment of OX8 (▲) are depicted for days 7, 11, 14, and 28 post-CI only.

at 28 days post-CI. Because we were aware of the potential of labeling monocytes with the mcAB W3/25 [1], our experiments focused on the examination of monocytes for the expression of OX8 antigen.

OX8+ cells from control rats demonstrated high mean fluorescence intensities, which distinctly separated them from OX8− cells (Fig. 3A). The majority of OX8+ cells exhibited small-volume signals, in a range similar to that of OX19+ cells (data not shown). During the second and third week post-CI, OX8+ cells demonstrated reduced mean fluorescence intensity and were no longer clearly distinguishable from OX8− cells. Positive cells were attached instead as a "shoulder" to the OX8− population (Fig. 3B). The loss of mean fluorescence intensity of OX8+ cells occurred simultaneously with the shift of OX8+ labeling to a population of cells that differed in the cell volume. The dominant cell volume, during this period of time post-CI, was larger than that of normal lymphocytes. Both positive and negative cells existed within that same cell volume distribution. Figure 4 summarizes the changes of the mean fluorescence intensities and the mean cell volumes of OX8+ cells over 28 days post-CI. It shows extraordinarily high mean volumes of OX8+ cells during the second week post-treatment when blood differentials exhibited a high percentage of monocytoid cells (Fig. 1). To test further the monocytic expression of OX8 antigens after CI, double-labeling experiments were conducted with the F(ab) fragment of OX8 and OX19. The OX8+/OX19+ and the OX8+/OX19− cell populations were sorted. The first population (OX8+/OX19+) was determined by histological examination, primarily lymphoid (data not shown). By the same morphological criteria, the OX8+/OX19− population appeared to consist of approximately 75% monocytes (Fig. 5) and 25% large granular lymphocytes. The OX8+/OX19− population composed 3%–4% of the total mononuclear cell population. Double-labeling experiments with the F(ab) fragment of OX8 and OX42 after CI revealed the same percentage of double- positive cells as was found for OX8+/OX19− cells above. No OX8+/OX42+ cells were observed in mononuclear cells of normal rats.

DISCUSSION

This paper presents, for the first time, evidence in a rat model of combined injury that peripheral blood monocytes express the OX8 cell surface antigen. The OX8 antigen has been previously considered to be a characteristic epitope of the W3/25 negative cytotoxic/suppressor T-lymphocyte subpopulation [3, 5] as well as large gran-

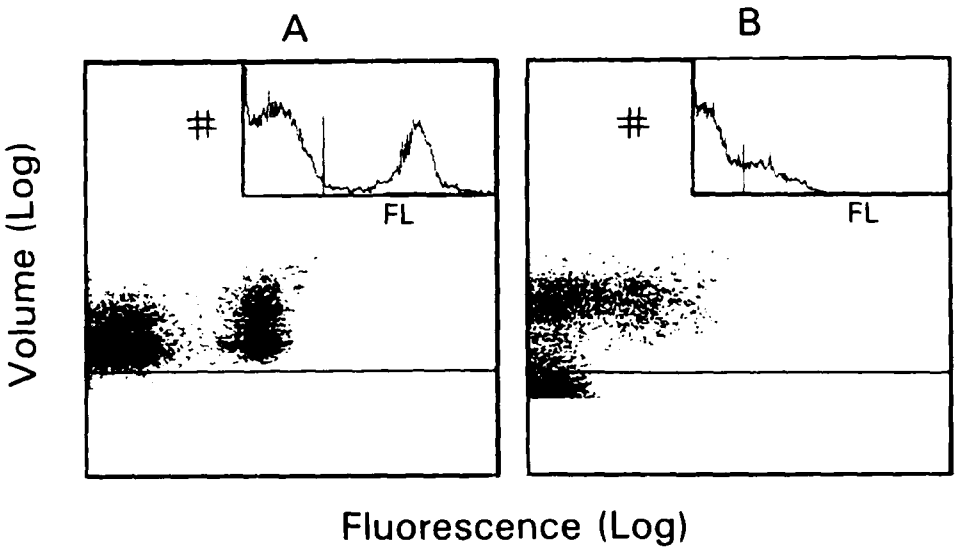

Fig. 3. Fluorescence versus volume cytograms (logarithmic scales) with fluorescence histograms (insert) after labeling of control cells (A) and cells from day 11 post-CI (B) with monoclonal antibody OX8. A volume gate was set to exclude unlysed RBC from statistics.

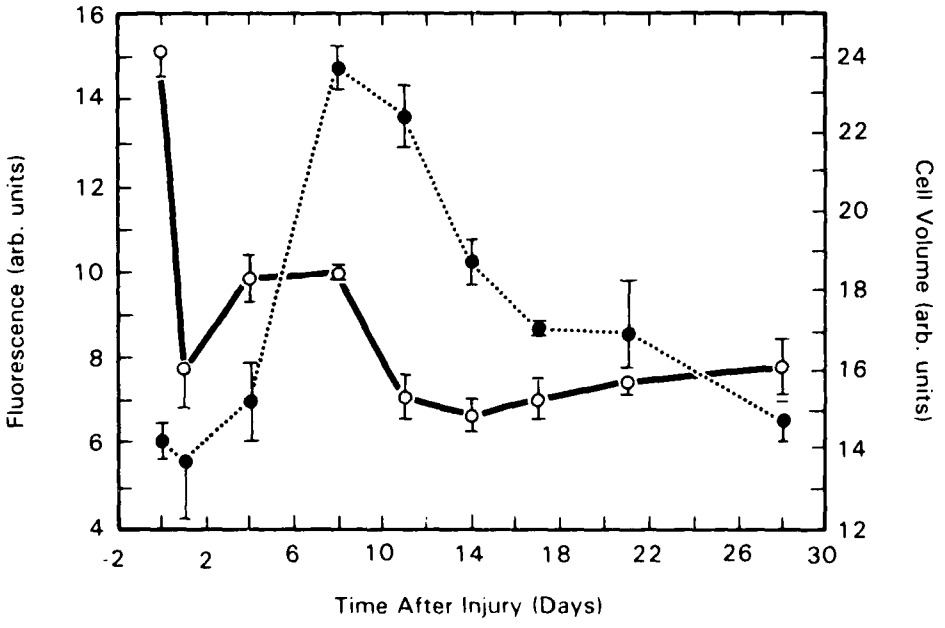

Fig. 4. Changes in mean fluorescence intensities ( ) and relative mean cell volumes (●) of OX8-positive cells as a function of time after CI.

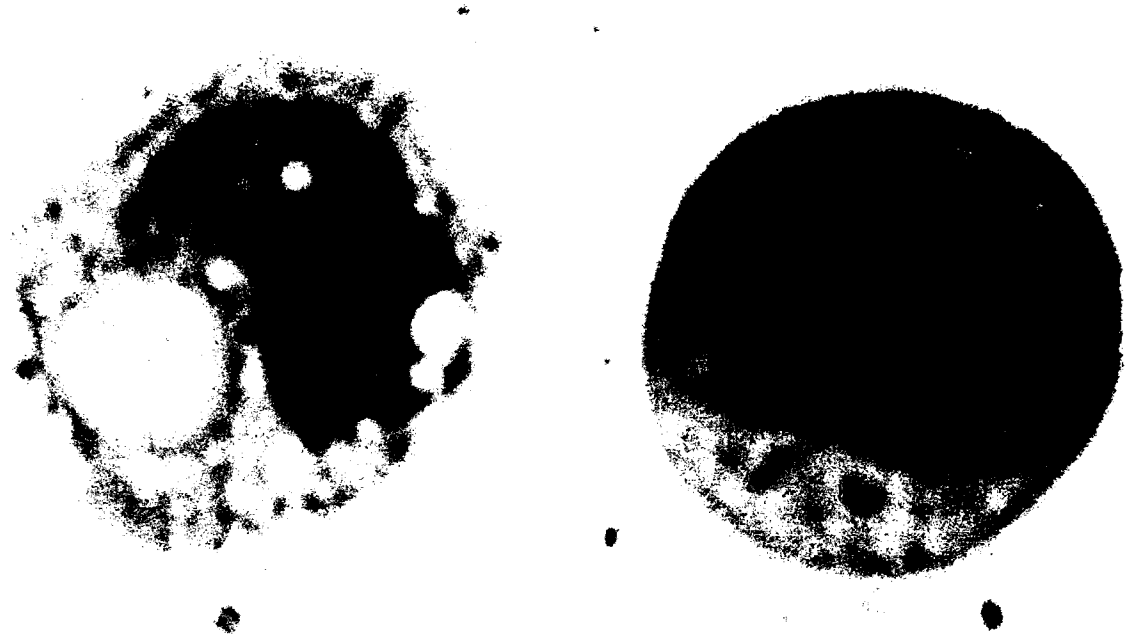

a b

Fig. 5. Sorted OX8-positive/OX19-negative cells (day 10 post-CI). a: Monocyte with an engulfed RBC. b: Large granular lymphocyte. Magnifications are ×4,760 and ×5,880, respectively.

ular lymphocytes previously identified as natural killer cells [4, 10, 13].

When the "whole OX8 antibody" was used (instead of the F[ab] fragment), nonspecific labeling of monocytes via Fc receptors accounted for more than half of the amount of positive labeling of mononuclear cells during the first 11 days post-treatment. Partially as a result of that, the positive labeling of cells with OX8 equalled or exceeded the percentages of morphologically/histologically identifiable lymphocytes. During the first 11 days, monocytes appeared highly activated and contained many cytoplasmic vacuoles. It has been reported in the literature that activated monocytes express elevated numbers of Fc receptor-binding sites [2]. However, the binding density of OX8 to Fc receptors on monocytes is considerably lower than the specific binding of mcAB to OX8 antigens on lymphocytes. Thus, the mean fluorescence intensity of all OX8-positive cells (lymphocytes plus monocytes) decreased post-CI.

Nonspecific labeling of monocytes with the "whole molecule OX8" antibody was also demonstrated when the mean cell volumes of these OX8-positive cells were compared to volumes of cells labeled with the F(ab) fragment. Except for day 28 post-CI, when no difference was detected, mean cell volumes of OX8-F(ab)-fragment-positive cells were always lower than those of cells that were labeled with the "whole OX8 molecule."

However, the identification of monocytes as the major component of a sorted OX8-positive/OX19-negative population where the F(ab) fragment of OX8 had been used to avoid nonspecific labeling, strongly indicated the expression of the OX8 epitope on rat peripheral blood monocytes after combined injury. No monocytes have been found among the OX8-positive cells of nontreated animals.

Evidence of monocytes' possessing OX8 receptors was also noted in further double-labeling experiments. In mononuclear cell preparations from control rats, no dou-

AD-A194 461 AFRRI (ARMED FORCES RADIOBIOLOGY RESEARCH INSTITUTE) 2/3
REPORTS OCTOBER NOVEMBER AND DECEMBER 1987(U) ARMED
FORCES RADIOBIOLOGY RESEARCH INST BETHESDA MD MAR 88

UNCLASSIFIED F/G 22/1 NL

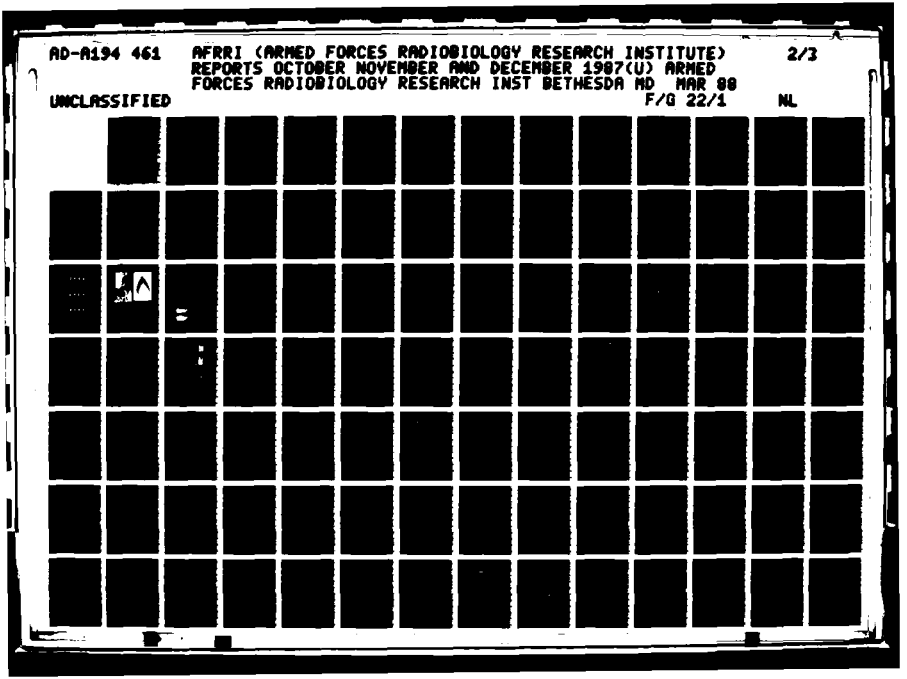

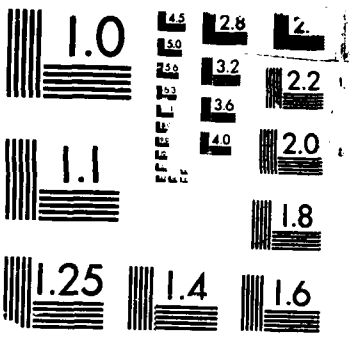

MICROCOPY RESOLUTION TEST CHART

BUREAU OF STANDARDS-1963-A

ble-labeling of cells with the F(ab) fragment of OX8 and OX42 was found. However, a small percentage (4%) of double-positive cells was detected in rats 8 days post-CI. The mcAB OX42 labels subsets of macrophages and monocytes and not B- or T lymphocytes [11]. In summary, data suggest that rat peripheral blood monocytes express OX8 antigens after combined injury. Therefore, future OX8 data should be correlated carefully with morphological and/or cytochemical characteristics of the positive cells.

ACKNOWLEDGMENTS

We thank Mr. T.A. Davis and J.H. Darden for skillful technical help and Mrs. G.G. Contreras and Junith Van Deusen for excellent secretarial and editorial assistance.

Supported by the Armed Forces Radiobiology Research Institute, Defense Nuclear Agency, under work unit 00130. Views presented in this paper are those of the authors; no endorsement by the Defense Nuclear Agency has been given or should be inferred. Research was conducted according to the principles enunciated in the "Guide for the Care and Use of Laboratory Animals," prepared by the Institute of Laboratory Animal Resources, National Research Council.

REFERENCES

1. Barclay, A.N. The localization of populations of lymphocytes defined by monoclonal antibodies in rat lymphoid tissue. Immunology 42, 593, 1981.
2. Bianco, C., Griffin, F.M., and Silverstein, S.C. Studies of the macrophage complement receptor. Alteration of receptor function upon macrophage activation. J. Exp. Med. 141, 1278, 1975.
3. Brideau, R.J., Carter, P.B., McMaster, W.R., Mason, D.W., and Williams, A.F. Two subsets of rat T lymphocytes defined with monoclonal antibodies. Eur. J. Immunol. 10,609, 1980.
4. Cantrell, D.A., Robins, R.A., Brooks, C.G., and Baldwin, R.W. Phenotype of rat natural killer cells defined by monoclonal antibodies marking rat lymphocyte subsets. Immunology 45,97, 1982.
5. Dallman, M.J., Mason, D.W., and Webb, M. The roles of host and donor cells in the rejection of skin allografts by T cell-deprived rats injected with syngeneic T cells. Eur. J. Immunol. 12, 511, 1982.
6. Duque, R.E., Phan, S.H., Hudson, J.L., Till, G.O., and Ward, P.A. Functional defects in phagocytic cells following thermal injury. Application of flow cytometric analysis. Am. J. Pathol. 118,116, 1985.
7. Glasser, O. (Ed). Medical Physics, Vol. I. Chicago: Year Book Publishers, Inc. p. 1493, 1955.
8. Hale, M.L., and McCarthy, K.F. Effect of sublethal ionizing radiation on rat Peyer's patch lymphocytes. Radiat. Res. 99,151, 1984.
9. McManus, A.T. Examination of neutrophil function in a rat model of decreased host resistance following burn trauma. Rev. Infect. Dis. 5(Suppl.),S898, 1983.
10. Reynolds, C.W., Sharrow, S.O., Ortaldo, J.R., and Herberman, R.B. Natural killer activity in the rat. II. Analysis of surface antigens on LGL by flow cytometry. J. Immunol. 127,2204, 1981.
11. Robinson, A.P., White, T.M., and Mason, D.W. Macrophage heterogeneity in the rat as delineated by monoclonal antibodies MRC OX-41 and MRC OX-42, the latter recognizing complement receptor type 3. Immunology 57,239, 1986.
12. Williams, A.F., Galfre, G., and Milstein, C. Analysis of cell surfaces by xenogenic myeloma-hybrid antibodies: Differentiation antigens of rat lymphocytes. Cell 12,663, 1977.
13. Woda, B.A., McFadden, M.L., Welsh, R.M., and Bain, K.M. Separation and isolation of rat natural killer (NK) cells from T cells with monoclonal antibodies. J. Immunol. 132,2183, 1984.

Life Sciences, Vol. 42, pp. 555-563 Pergamon Journals
Printed in the U.S.A.

INVOLVEMENT OF HISTAMINE H1 AND H2 RECEPTORS IN HYPOTHERMIA INDUCED BY IONIZING RADIATION IN GUINEA PIGS

Sathasiva B. Kandasamy and Walter A. Hunt

Behavioral Sciences Department
Armed Forces Radiobiology Research Institute
Bethesda, Maryland 20814-5145

(Received in final form November 30, 1987)

Summary

Radiation-induced hypothermia was examined in guinea pigs. Exposure to the head alone or whole-body irradiation induced hypothermia, whereas exposure of the body alone produced a small insignificant response. Systemic injection of disodium cromoglycate (a mast cell stabilizer) and cimetidine (H2-receptor antagonist) had no effect on radiation-induced hypothermia, whereas systemic and central administration of mepyramine (H1-receptor antagonist) or central administration of disodium cromoglycate or cimetidine attenuated it, indicating the involvement of central histamine through both H1 and H2 receptors in this response. Serotonin is not involved, since the serotonin antagonist methysergide had no effect on radiation-induced hypothermia. These results indicate that central histaminergic systems may be involved in radiation-induced hypothermia.

Changes in body temperature can be observed after radiation exposure (1), an effect that depends on the species being used. For example, radiation induces hyperthermia in cats, rabbits (2) and humans (3), a biphasic response in monkeys (a fall followed by a rise (4)), and a dual effect in rats (low and high doses produce hyper- and hypothermia, respectively (5)). Preliminary experiments in our laboratory have demonstrated that, unlike other species, radiation induces only hypothermia in guinea pigs (6). Therefore, guinea pigs may serve as a useful animal model to study the hypothermic effect of ionizing radiation without the confounding influence of fever as seen with most species studied.

The purpose of the present study was to characterize the actions of radiation on body temperature in guinea pigs (a) by determining the effect of variable doses of radiation on body temperature, (b) by determining whether radiation is acting on the brain or the periphery, and (c) by then elucidating the mechanisms underlying the effect. The mechanisms explored related to systems mediated by histamine or serotonin, since these agents induce hypothermia when injected centrally in several species (7,8).

Methods

Drugs used: Serotonin creatinine sulfate (Sigma Chemical Co., St. Louis, MO); mepyramine maleate (Mallinckrodt Inc., St. Louis, MO); methysergide maleate

0024-3205/88 $3.00 + .00

(Sandoz Pharmaceuticals, E. Hanover, NJ); 2-methylhistamine dihydrochloride, 4-methylhistamine dihydrochloride and cimetidine (Smith Kline and French Laboratory, Philadelphia, PA); disodium cromoglycate (Fisons Corporation, Bedford, MA); ketamine hydrochloride (Parke-Davis, Detroit, MI); xylazine (Hayer-Lockhart, Shawnee, KS); acepromazine (Ayerst Laboratories, NY). 2-Methylhistamine, 4-methylhistamine, mepyramine, serotonin, and disodium cromoglycate were dissolved in sterile, nonpyrogenic saline. Methysergide was dissolved in 10% dimethylsulfoxide and pyrogen-free distilled water. Cimetidine was dissolved in 0.1 ml of 1 N HCl and diluted to the final volume with saline.

Radiation exposure: Male guinea pigs weighing 200-300 g were placed in clear plastic containers for approximately 5 min before irradiation or sham exposure. The animals were then exposed bilaterally to 1- to 100-Gy doses of gamma photons using a Co-60 source. The dose rate was 5 Gy/min for doses of 1 and 3 Gy and at a rate of 10 Gy/min for higher doses. Shielding of the head (head and neck exposed) or body (thorax to pelvis exposed) was accomplished using lead bricks. The animals were placed in a plastic restraining tube that was in turn enclosed in a cave made of lead bricks to a minimum thickness of 10 cm. The bricks were drilled to accept the part of the tube containing either the head or the body of the rat. During the irradiation, the rats were observed with a remote video monitor to verify that the animals did not shift position within the tube. Dosimetry was performed using paired 50-ml ion chambers. Delivered dose was expressed as a ratio of the dose measured in a tissue-equivalent plastic phantom enclosed in a restraining tube to that measured in air.

Central administration of drugs: Guinea pigs were anesthetized with 1 ml/kg, I.M., of a mixture of ketamine (50 mg/kg), xylazine (5 mg/kg), and acepromazine (1 mg/kg), and were placed in a stereotaxic apparatus (David Kopf Instruments, Tujunga, CA). A single cannula was inserted into the lateral ventricle according to coordinates derived from the atlas of Luparello et al. (9): 2 mm lateral to the midline and 0.5 mm rostral to the bregma. The cannula was lowered until cerebrospinal fluid rose in the cannula. Dental acrylic was used to secure the cannula. At least 1 wk was allowed for recovery before animals were used for experiments. Injections/radiation were done at the same time of day (0900) to avoid diurnal variation in temperature. The antagonists (disodium cromoglycate, mepyramine, cimetidine, and methysergide) were given 30 min before the administration of the radiation/agonists (Histamine agonists 2-methylhistamine and 4-methylhistamine, or serotonin). The volume of intracerebroventricular (i.c.v) injections was always 10 μl. After the end of the experiment, injections sites were verified histologically.

Measurement of body temperature: All experiments were performed at an environmental temperature of 22 $\pm$ 1° C. The animals were placed in cages 1 hr before the beginning of the experiments and body temperature was measured every 15 min over a period of 2 hr with thermistor probes inserted approximately 6 cm into the rectum and connected to a datalogger (Minitrend 205). After each experiment, all animals were euthanized immediately with an overdose of carbon dioxide.

Statistics: Statistical evaluations were undertaken using Student's t-test with a significance of $P < 0.05$.

Results

Exposure to 1 to 100 Gy of gamma radiation induced hypothermia in a dose-dependent manner (Fig. 1). The onset of hypothermia was rapid and reached its maximum extent within 15 min. Doses above 100 Gy, for example 150 Gy, produced convulsions in some guinea pigs (3 of 6). On the basis of these results

a 10-Gy dose of radiation was used to determine the site of action of the radiation, i.e. whether it acts on the brain or the periphery. As can be seen in Fig. 2, hypothermia induced by a 10-Gy dose of gamma radiation occurred only after whole-body or head-only exposure, not when the head was shielded. Since whole-body exposure resulted in the same effect as head-only exposure, subsequent studies used only whole-body exposure to ionizing radiation.

Experiments were then undertaken to determine what mechanisms may underlie radiation-induced changes in body temperature by comparing to radiation the effects of drugs with known actions and by determining whether antagonists to these drugs could block the effects of radiation. Since histamine, stored in mast cells throughout the body (10), is released by exposure to ionizing radiation (11), its possible role in the thermoregulatory effects of radiation was examined. Disodium cromoglycate is known to be a potent inhibitor of the immunological release of chemical mediators secreted from mast cells (12) and has been established as an effective therapy in human asthma. Disodium cromoglycate (1-10 mg/kg, i.p.) produced neither a significant change in temperature in control animals nor an attenuation of hypothermia induced by 10 Gy of radiation (data not shown). But, centrally administered disodium cromoglycate (10-50 μg, i.c.v.), attenuated radiation-induced hypothermia (Fig. 3). In control animals, disodium cromoglycate produced a slight but insignificant fall in temperature (Fig. 3).

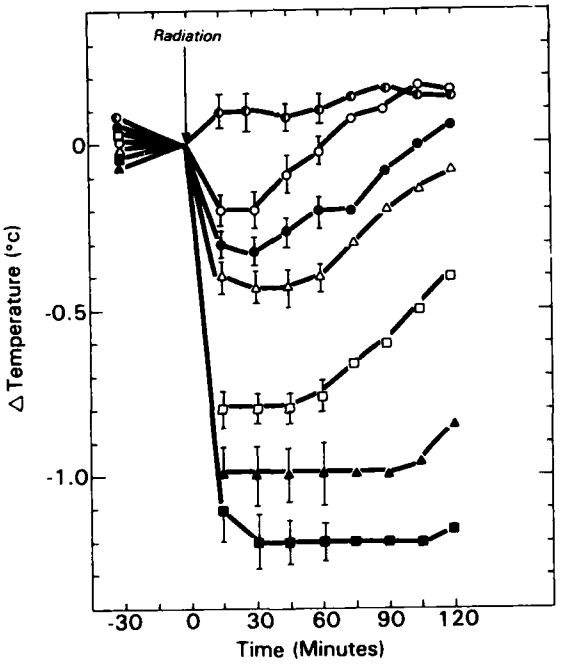

FIG. 1

Changes in rectal temperature of guinea pigs exposed to variable doses of ionizing radiation: Sham radiation (●), 1 Gy (○), 3 Gy (●), 5 Gy (△), 10 Gy (□), 50 Gy (▲), 100 Gy (■). Each point represents the mean ± SE of six observations except (●) and (□) which represent 16 observations. Zero on the abscissa represents body temperature at the time of irradiation

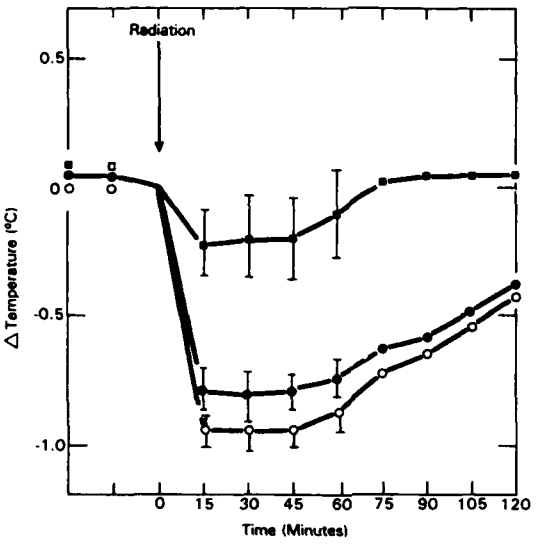

FIG. 2

Effect of 10 Gy of ionizing radiation on body only (■), whole body (●), and head only (⊘). Each point represents the mean ± SE of 6 observation except (●) which represents 8 observations. Zero on the abscissa represents body temperature at the time of irradiation.

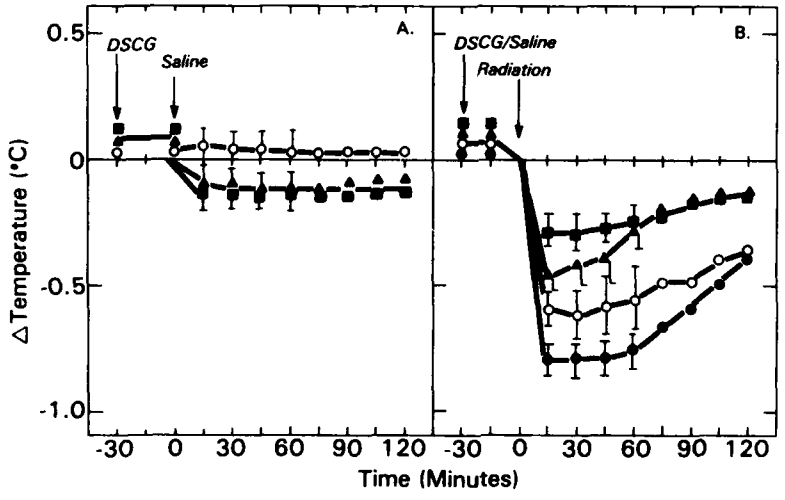

FIG. 3

Effect of i.c.v. disodium cromoglycate on hypothermia induced by ionizing radiation: (A) disodium cromoglycate (DSCG) 10 μg (○), 30 μg (▲) and 50 μg (■), (B) 10 Gy of ionizing radiation alone (●) and in the presence of DSCG 10 μg (○), 30 μg (▲) and 50 μg (■). Each point represents mean ± SE of 5 observations. Zero on abscissa represents temperature at the time of second injection (A) or irradiation (B).

To differentiate between actions on H1 and H2 receptors, agonists and antagonists specific for these receptors were used. Mepyramine (1-10 mg/kg, i.p. or 10-30 μg, i.c.v.), an H1 antagonist and cimetidine (10-30 μg, i.c.v.) an H2 antagonist, both of which were previously found to antagonize hypothermia induced by histamine in guinea pigs (13,14), significantly antagonized in a dose-dependent manner hypothermia induced by exposure to a 10-Gy dose of radiation (Table 1; Fig. 4 and 5). Systemic injection of cimetidine 1-10 mg/kg, i.p. did not antagonize radiation-induced hypothermia (data not shown). In addition, mepyramine injected systemically or centrally antagonized hypothermia induced by 2-methylhistamine (10 μg, i.c.v.), an H1 agonist, but did not antagonize the hypothermia induced by 4-methylhistamine (50 μg, i.c.v.), an H2 agonist (13,14). Likewise, cimetidine, only when administered centrally, significantly attenuated the hypothermia induced by 4-methylhistamine but not that produced by 2-methylhistamine (10 μg, i.c.v.) (13,14).

TABLE 1

EFFECT OF INTRAPERITONEAL ADMINISTRATION OF MEPYRAMINE ON RADIATION-INDUCED HYPOTHERMIA

TREATMENT	MEAN Δ TEMP (°C ± SE)
Radiation (10 Gy)	-0.9 ± 0.20 (N=8)
Mepyramine (1 mg/kg) + Radiation	-0.7 ± 0.25 (N=5)
Mepyramine (3 mg/kg) + Radiation	-0.4 ± 0.20 (N=5)*
Mepyramine (10 mg/kg) + Radiation	-0.2 ± 0.25 (N=5)*

* Significantly different from radiation alone; $p < 0.05$, N = number of animals.

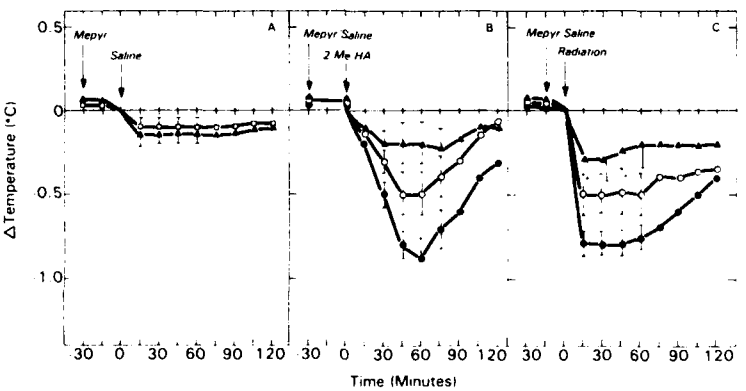

FIG. 4

Effect of i.c.v. mepyramine on hypothermia induced by 2-methylhistamine and ionizing radiation: (A) mepyramine (MEPYR) 10 μg (□) and 30 μg (▲), (B) of 2-methylhistamine (2-me-HA) alone 10 μg (●) and in the presence of MEPYR 10 μg (○) and 30 μg (▲), (C) 10 Gy of ionizing radiation alone (●) and in the presence of MEPYR 10 μg (○) and 30 μg (▲). Each point represents mean ± SE of 5 observations. Zero on abscissa represents temperature at the time of second injection (A and B) or irradiation (C).

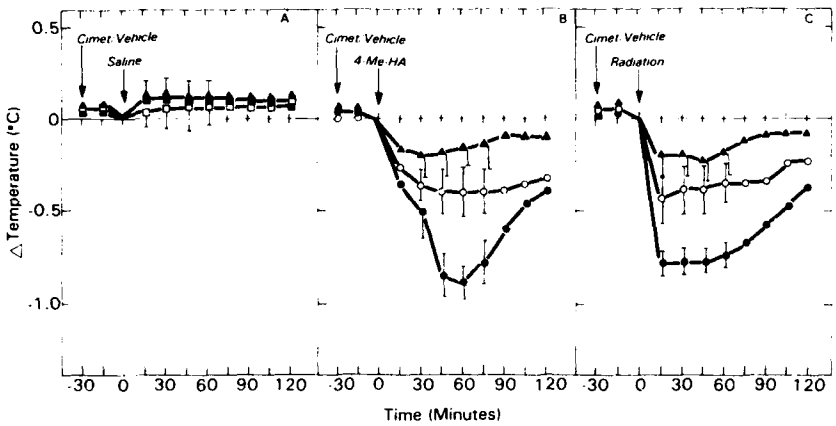

FIG. 5

Effect of i.c.v. cimetidine on hypothermia induced by 4-methylhistamine and ionizing radiation: (A) Cimetidine (Cimet) 10 μg (■), 30 μg (▲) and vehicle (■), (B) 4-methylhistamine (4-me-HA) alone 50 μg (●) and in the presence of cimetidine (Cimet) 10 μg (○) and 30 μg (▲), (C) 10 Gy of ionizing radiation alone (●) and in the presence of cimetidine (Cimet) 10 μg (○) and 30 μg (▲). Each point represents mean ± SE of 5 observations. Zero on abscissa represents temperature at the time of second injection (A and B) or irradiation (C).

Since mepyramine and cimetidine are equally potent in blocking radiation-induced hypothermia in this study, combinations of half of the doses of each drug were administered to determine whether the effects of drugs are additive or supra-additive in antagonizing radiation-induced hypothermia. Combinations of 5 μg or 15 μg (i.c.v) of each drug produced only additive effects (Table 2).

TABLE 2

EFFECT OF INTRAVENTRICULAR ADMINISTRATION OF MEPYRAMINE OR CIMETIDINE OR COMBINATIONS ON RADIATION-INDUCED HYPOTHERMIA

TREATMENT	MEAN Δ TEMP (°C ± SE)
Radiation (10 Gy)	-1.0 ± 0.10 (N=6)
Mepyramine (10 μg) + Radiation	-0.5 ± 0.15 (N=5)*
Cimetidine (10 μg) + Radiation	-0.4 ± 0.20 (N=5)*
Mepyramine (5 μg) + Cimetidine (5 μg) + Radiation	-0.3 ± 0.20 (N=5)*
Mepyramine (30 μg) + Radiation	-0.3 ± 0.22 (N=5)*
Cimetidine (30 μg) + Radiation	-0.3 ± 0.15 (N=5)*
Mepyramine (15 μg) + Cimetidine (15 μg) + Radiation	-0.1 ± 0.20 (N=5)*

*Significantly different from radiation alone; $p < 0.05$, N=number of animals.

Serotonin has been shown to be involved in thermoregulation (15). It induces hypothermia in guinea pigs, rats, mice, rabbits, and goats, but hyperthermia in cats and primates (8). Serotonin-induced hypothermia (30 μg, i.c.v.) can be blocked by pretreatment with methysergide, a serotonin antagonist (data not shown). However, methysergide (10-30 μg, i.c.v., N=5) had no effect on radiation-induced hypothermia.

Discussion

Exposure to ionizing radiation in guinea pigs induced only hypothermia, in contrast to the results obtained with other species (2-5). This effect appears to be mediated by the central release of histamine, since body-only exposure to ionizing radiation had no effect on temperature and peripherally released histamine would not cross the blood brain barrier. In addition, mepyramine, which crosses the blood brain barrier, effectively attenuated radiation-hypothermia when injected systemically and centrally, whereas cimetidine and disodium cromoglycate, which do not penetrate the blood-brain barrier, were effective only when centrally administered, again indicating the involvement of central histamine in the production of hypothermia.

Histamine has also been implicated in other actions of ionizing radiation including hypotension, reductions in cerebral blood flow, and performance decrements (16). Furthermore, circulating blood histamine concentrations have been reported to be elevated in humans undergoing radiation therapy (17), as well as canine and primate plasma histamine levels (11,18,19) following radiation exposure and decreases in tissue histamine levels in rats (20). All these observations suggest that exposure to ionizing radiation releases histamine.

Histamine is present in high concentrations in the hypothalamus (21,22) and is localized in nerve terminals (23), suggesting that it may act as a central neurotransmitter. Also, ascending histamine tracts are found in the median forebrain bundle (24); histidine decarboxylase, the enzyme that converts histidine to histamine, is localized in different regions of the brain (25); histamine activates adenylate cyclase in the brain (26); and brain histamine turnover is increased by stress (27). Administration of histidine systemically or histamine centrally evokes hypothermia due to both H1- and H2-receptor activation (28). These neurochemical and pharmacological studies suggest that histamine may be a neurotransmitter involved in many physiological functions including thermoregulation and could underlie radiation-induced hypothermia.

Histamine is stored in mast cells throughout the body (10), including the brain, where mast cells are particularly numerous in the hypothalamus (29), which contains the highest concentration of histamine in the brain (30,31). Also, the hypothalamus is one of the most important areas in the brain responsible for thermoregulation (32). In our experiment, the mast cell stabilizer disodium cromoglycate administered centrally attenuated radiation-induced hypothermia indicating the role of central histamine in this response. However, Carmichael et al. (33) have recently demonstrated that disodium cromoglycate may act in some other mode rather than as mast cell stabilizer. The action may be as an electron scavenger.

The hypothermic effect of variable doses of radiation seems to involve an action of histamine on both H1 and H2 receptors. Previously (13,14), central administration of 2-methylhistamine (a relatively specific H1-receptor agonist) and 4-methylhistamine (a relatively specific H2-receptor agonist) caused hypothermia in guinea pigs that was selectively attenuated by the H1- and H2-receptor antagonists mepyramine and cimetidine, respectively. Similar results have already

been reported in rabbits (35). In the present experiments, both mepyramine and cimetidine specifically attenuated the hypothermia induced by 2-methylhistamine and 4-methylhistamine, respectively, and also antagonized radiation-induced hypothermia, indicating the involvement of both histaminergic H1 and H2 receptors. The combination of half of each dose of mepyramine and cimetidine resulted in additive effects in antagonizing radiation-induced hypothermia.

Central injection of serotonin in guinea pigs induced hypothermia and was specifically antagonized by the serotonin antagonist, methysergide (13). However, serotonin was not involved in radiation-induced hypothermia, since methysergide did not antagonize the hypothermia.

The present results indicate that in guinea pigs ionizing radiation induces hypothermia and that central histaminergic H1 and H2 receptors, but not serotonin receptors, may underlie this response.

Acknowledgments

This research was supported by the Armed Forces Radiobiology Research Institute, Defense Nuclear Agency, under work unit B4157. Views presented in this paper are those of the authors; no endorsement by the Defense Nuclear Agency has been given or should be inferred. Research was conducted according to the principles enunciated in the 'Guide for the Care and Use of Laboratory Animal Resources, National Research Council.'

References

1. D.J. KIMELDORF and E.L. HUNT, Ionizing Radiation: Neural Function and Behavior, pp. 125, Academic Press, New York (1965).
2. T.S. VENINGA, Radiat. Res. 48 358-367 (1971).
3. H. FANGER and C.C. LUSHBAUGH, Arch. Pathol. 83 446-460 (1967).
4. W.L. MCFARLAND and J.A. WILLIS, Armed Forces Radiobiology Research Institute Scientific Report, SR74-7, Bethesda, Maryland (1974).
5. S.B. KANDASAMY, W.A. HUNT, and G.A. MICKLEY, Radiat. Res. in press (1987).
6. S.B. KANDASAMY, W.A. HUNT, and G.A. MICKLEY, Toxicologist 7 1014 (1987).
7. W.G. CLARK and J.M. LIPTON, Neurosci. Biobehav. Rev. 9 479-552 (1985).
8. W.G. CLARK and J.M. LIPTON, Neurosci. Biobehav. Rev. 10 153-220 (1986).
9. T.J. LUPARELLO, M. STEIN, and C.D. PARK, J. Comp. Neurol. 122 201-218 (1964).
10. D.D. METCALF, M. KALINER, and M.A. DONLON, CRC Critical Reviews in Immunology. M.Z. Atassi, Ed., pp. 23-74, CRC Press, Boca Raton, FL (1981).
11. T.F. DOYLE, and T.A. STRIKE, Experientia 33 1047-1048 (1977).
12. A. GOTH, Medical Pharmacology, Eleventh Edition, C. V. Mosby Co., St. Louis (1984).
13. S.B. KANDASAMY and B.A. WILLIAMS, Neuropharmacol. 23 49-53 (1984).
14. P.N. KAUL, S.B. KANDASAMY, and W.G. KIRLIN, Environment, Drugs, and Thermoregulation. P. Lomax and E. Schönbaum, Eds., pp. 55-57. Karger, Basel (1982).
15. W. FELDBERG and R.D. MYERS, J. Physiol. 173 226-237 (1964).
16. T.F. DOYLE, J.E. TURNS, and T.A. STRIKE, Aerospace Med. 42 400-403 (1971).
17. E.C. LASSER and K.W. STENSTROM, Amer. J. Roentgenol. 72 985-988 (1954).

18. L.G. COCKERHAM, T.F. DOYLE, M.A. DONLON, and E.A. HELGESON, Aviat. Space Environ. Med. 55 1041-1045 (1984).
19. L.G. COCKERHAM, T.F. DOYLE, M.A. DONLON, and C. GOSSETT-HAGERMAN, Fundament. Appl. Toxicol. 5 597-604 (1985).
20. V.D. EISEN and C.M. WILSON, J. Physiol. 136 122-130 (1957).
21. H.M. ADAM and H.K. HYE, Brit. J. Pharmacol. 28 137-152 (1957).
22. J.F. LIPINSKI, H. SCHAUMBURG, and R.J. BALDESSARINI, Brain Res. 52 403-408 (1973).
23. S.H. SNYDER and K.M. TAYLOR, Perspectives in Neuropharmacology, S.H. Snyder, Ed., pp. 43-73, Oxford University Press, New York (1972).
24. J.C. SCHWARTZ, Ann. Rev. Toxicol. 17 325-339 (1977).
25. M. BAUDRY, M.P. MARTRES, and J.C. SCHWARTZ, J. Neurochem. 21 1301-1309 (1973).
26. M. BAUDRY, M.P. MARTRES, and J.C. SCHWARTZ, Nature 253 362-364 (1975).
27. K.M. TAYLOR and S.H. SNYDER, Science 172 1037-1039 (1971).
28. P. LOMAX and M.D. Green, Body Temperature: Regulation, Drug Effects and Therapeutic Implications, P. Lomax and E. Schonbaum, Ed., pp. 289-304, Dekker, New York (1979).
29. L. EDVINSSON, J. CERVOS-NAVARRO, L. LARSSON, C.H. OWMAN, and A.L. RONNBERG, Neurol. 27 878-883 (1977).
30. P.M. GROSS, J. Cereb. Blood Flow Metabol. 2 3-23 (1982).
31. K.M. TAYLOR, E. GFELLER, and S.H. SNYDER, Brain Res. 41 171-179 (1972).
32. W. FELDBERG and R.D. MYERS, J. Physiol. 177 239-245 (1965).
33. A.J. CARMICHAEL, C.M. ARROYO, and L.G. COCKERHAM, Toxicologist 7 111 (1987).
34. K.K. TANGRI, G. PALIT, N. MISRA, and K.P. BHARGAVA, Thermoregulatory Mechanisms and Their Therapeutic Implications, B. Cox, P. Lomax, A. S. Milton, and E. Schönbaum, pp. 224-228. Karger, Basel (1979).

Locomotor Behavior in Mice Following Exposure to Fission-Neutron Irradiation and Trauma

MICHAEL R. LANDAUER, M.S., Ph.D.,
G. DAVID LEDNEY, M.S., Ph.D., and
HIRSCH D. DAVIS, B.A., M.S.

Departments of Behavioral Sciences and Experimental Hematology, Armed Forces Radiobiology Research Institute, Bethesda, Maryland

LANDAUER MR, LEDNEY GD, DAVIS HD. *Locomotor behavior in mice following exposure to fission-neutron irradiation and trauma.* Aviat. Space Environ. Med. 1987; 58:1205–10.

Locomotor activity, body weights, and food and water consumption were monitored in female mice for 35 d following a sublethal wound (W), burn (B), exposure to 3 Gray fission neutron radiation (R), or combination of these injuries: radiation-wound (RW) and radiation-burn (RB). Activity in groups W and RW was depressed immediately after injury, with recovery to control levels after 5 and 14 d, respectively. Mice that received radiation alone showed a biphasic response with decrements in activity on days 0–4 and 9–11. Groups B and RB exhibited depressed activity levels that differed significantly from control levels until day 17. Food intake was reduced for about 6 d in groups R, W, RW, and RB. Body weights decreased for 4 d in groups R, W, RW, and RB, but returned to control levels by the end of the experiment. Animals in group B did not show significant reduction in food intake or body weight. Water consumption was reduced for 5–6 d in groups R and RB and was increased in groups W, RW, and B. The data suggest that behavioral responses to fission-neutron radiation are exacerbated by tissue trauma.

COMBINED INJURY, including wounds, thermal burns, and radiation exposure, is a primary concern in military medicine as well as in clinical practice (6). The increasing use of radiation devices and radioisotopes in industry and medicine requires the transportation of potentially hazardous substances on public highways. If an accident occurs, casualties are likely to be the result of combined-injury trauma. The explosion of the Soviet nuclear reactor in Chernobyl in April 1986 further exemplifies the need to study the effects of radiation in association with tissue trauma (22).

Sublethal levels of total-body irradiation have been shown to act synergistically with thermal injuries and wound trauma, resulting in death. Messerschmidt *et al.* (24) reported that 30% of mice receiving a contact burn or 510 rads of radiation died. However, when the injuries were combined, the mortality rose to 90%. Similarly, a dose of radiation that resulted in 26% mortality rose to 90% when combined with open skin wounds (23).

The pathophysiology of combined injury is currently being addressed (11,34). Although the physiological and immunological effects of combined injury have been investigated, the recovery of behavioral function following these events has not been explored. It is important to understand the time course for recovery of behavioral parameters, as well as the resumption of normal food and water consumption, so that appropriate treatment can be undertaken.

This study examines the effects of burn and wound injuries in mice, alone and in combination with a dose of 3 Gy fission neutrons, on the locomotor performance, body weight, and food and water intake over a 35-d period. Locomotor activity was selected as the behavioral parameter to be investigated because it is readily quantifiable and has been demonstrated to be affected by exposure to ionizing radiation (12,13,15).

MATERIALS AND METHODS

Subjects

Sixty-six adult female B6D2F1 mice (Jackson Labs., Bar Harbor, ME) weighing 22–30 grams, were housed under a 12:12 hr light-dark cycle with lights on at 0700. Immediately following arrival, animals were quarantined for 2 weeks to ensure that they were free of *Pseudomonas* sp and showed

This manuscript was received for review in September 1986. The revised manuscript was accepted for publication in January 1987.

Address reprint requests to Michael R. Landauer, Ph.D., who is a Research Scientist in the Behavioral Sciences Department (BHS) at the Armed Forces Radiobiology Research Institute, Bethesda, Maryland 20814-5145.

no serologic evidence or histologic lesions of any common murine diseases. Mice were maintained in groups of 2–4 in clear plastic cages (30 × 20 × 12 cm) according to treatment. They were provided with a Wayne Rodent Blox diet and acidified water (pH = 2.5) to control opportunistic infections (21).

Treatment Groups

Animals were randomly assigned to six treatment groups for the examination of behavioral effects of radiation, burn, and wound traumas. These consisted of 1) Control (C), N = 12; 2) Radiation (R), N = 10; 3) Wound (W), N = 10; 4) Radiation plus Wound (RW), N = 12; 5) Burn (B), N = 9; and 6) Radiation plus Burn (RB), N = 13. All animals including the control group were shaved on the dorsal surface, exposed to radiation or sham irradiation, anesthetized with methoxyfluorane, administered the appropriate trauma, given an injection of 0.5 ml physiological saline as fluid therapy, and placed into sanitized cages.

Radiation: The techniques and dosimetry of exposing mice to fission neutrons (fN) produced by the AFRRI TRIGA reactor were previously described (30). Mice were given 3 Gray [1 Gray (Gy) = 100 rad] mid-line tissue doses of fN total body at a dose rate of 0.4 $Gy \cdot min^{-1}$. Mice were individually exposed in aluminum restraining tubes that rotated 1.5 RPM. A neutron-to-gamma ratio of 20:1 was achieved by irradiating the mice through a 15.2 cm lead reactor shield and maintaining the exposure array of mice in a 5.1 cm lead cave. All mice were habituated to the restraining tubes for 1 $h \cdot d^{-1}$ for 3 d prior to being irradiated. Animals in groups R, RW, and RB were irradiated. Animals in groups C, W, and B were transported to the radiation source but not irradiated. Within 1 h after irradiation or sham exposure, animals were anesthetized and administered the appropriate trauma.

Wound: Wounds were made by removal of a 2.5 × 3.8 cm section of the dorsal skin fold and underlying panniculus carnosus muscle with a steel punch while animals were anesthetized with methoxyfluorane (20). This wound represented about 30% of the body-surface area. The punch was immersed in 70% ethanol before each animal was injured. The wounds were left open to the environment and were not treated.

Burn: Burning was performed on mice anesthetized with methoxyfluorane by igniting a 2.5 × 3.8 cm shaved area of the dorsal surface with 100% ethanol for 12 s (31). The burn covered about 30% of the body-surface area.

Controls: Control animals were anesthetized and handled in a manner similar to the other treatment groups. They received a sham exposure in the AFRRI TRIGA reactor.

Behavioral Testing

Apparatus: Locomotor behavior was automatically recorded by a computerized Digiscan Animal Activity Monitor (Omnitech Electronics, Columbus, OH, Model RXYZCM-16) which included an acrylic activity arena (40.6 × 40.6 × 30.5 cm) and an array of infrared horizontal and vertical sensors spaced 2.5 cm apart. The horizontal and vertical sensors were positioned 1.3 and 6.4 cm above the floor of the cage, respectively. Two 20.3 × 20.3 cm acrylic cages were placed diagonally into the activity arena in order to monitor the motor activity of two individual mice. Locomotor parameters were analyzed by a Digiscan Analyser (Omnitech, Model DCM) which in turn stored the data onto an IBM-PC computer with disk drive. Both horizontal and vertical activity were recorded.

Procedure: Animals were habituated to the test apparatus, 30 $min \cdot d^{-1}$, for 3 d prior to administration of radiation or trauma. On the day before treatment, baseline levels of activity were recorded (day −1). Mice were tested individually 3–9 h following treatment (day 0) and on days 1–7, 9, 11, 14, 17, 20, 25, 30, and 35. Each test session was 30 min in duration and was performed during the light portion of the light-dark cycle. The apparatus was cleaned with a 50% alcohol solution and allowed to air dry after each trial. Body weights were recorded immediately before testing. Food and water consumption for each cage were measured for the 24-h period before each test day. The amounts consumed were determined by daily weighing of the food hoppers and water bottles.

Statistical Analysis

All parameters were subjected to a two-way analysis of variance with repeated measures (BMDP Statistical Software, Los Angeles, CA) to determine the effects of treatments over days. Post-hoc comparisons were made using the Neuman-Keuls' test (37).

RESULTS

For the purpose of clarification, the results of the wound and burn groups are presented separately and are expressed as the percent difference from the control group. The control group is always considered to be 100% of the response and is represented by a solid line. The means ± the standard error (S.E.M.) of all the parameters of the control group are presented in Table I. Wound and burn data are presented as separate panels in the same figure. The control group and

TABLE I. MEANS ± S.E.M. OF THE CONTROL GROUP FOR VERTICAL ACTIVITY COUNTS, BODY WEIGHT (g), FOOD (g) AND WATER (ml) CONSUMPTION AS A FUNCTION OF EXPERIMENTAL DAY. THESE VALUES WERE USED TO COMPUTE THE CONTROL LINES THAT APPEAR IN FIG. 1–4.

Day[a]	Activity[b,c]	Body wt[c]	Food[d]	Water[d]
0	160 ± 13	24.1 ± 0.3	3.4 ± 0.2	4.2 ± 0.3
1	186 ± 21	24.2 ± 0.3	3.4 ± 0.4	4.3 ± 0.3
2	175 ± 23	24.4 ± 0.4	3.5 ± 0.2	5.1 ± 0.4
3	134 ± 21	24.7 ± 0.4	3.9 ± 0.1	6.0 ± 0.6
4	179 ± 24	25.0 ± 0.4	4.3 ± 0.3	5.8 ± 0.4
5	166 ± 22	25.3 ± 0.5	4.5 ± 0.6	4.3 ± 0.3
6	155 ± 22	25.2 ± 0.5	4.1 ± 0.2	4.0 ± 0.1
7	139 ± 25	25.0 ± 0.5	3.4 ± 0.1	4.1 ± 0.3
9	192 ± 26	25.0 ± 0.4	4.0 ± 0.1	4.6 ± 0.6
11	172 ± 26	25.0 ± 0.4	3.3 ± 0.4	4.2 ± 0.3
14	115 ± 23	25.0 ± 0.4	4.2 ± 0.5	4.3 ± 0.3
17	142 ± 29	25.8 ± 0.5	3.2 ± 0.2	3.8 ± 0.2
20	139 ± 28	25.7 ± 0.5	3.2 ± 0.3	4.5 ± 0.5
25	162 ± 24	25.7 ± 0.5	3.3 ± 0.1	3.8 ± 0.3
30	131 ± 24	25.1 ± 0.3	3.3 ± 0.2	4.3 ± 0.5
35	121 ± 20	25.4 ± 0.4	3.2 ± 0.2	4.4 ± 0.6

[a] Day 0 = Day radiation or injury was given to treatment groups.
[b] Activity was monitored for 30 min.
[c] N = 10.
[d] Based on the amount consumed per mouse per cage. Animals housed 2–4 per cage (N = 4 cages).

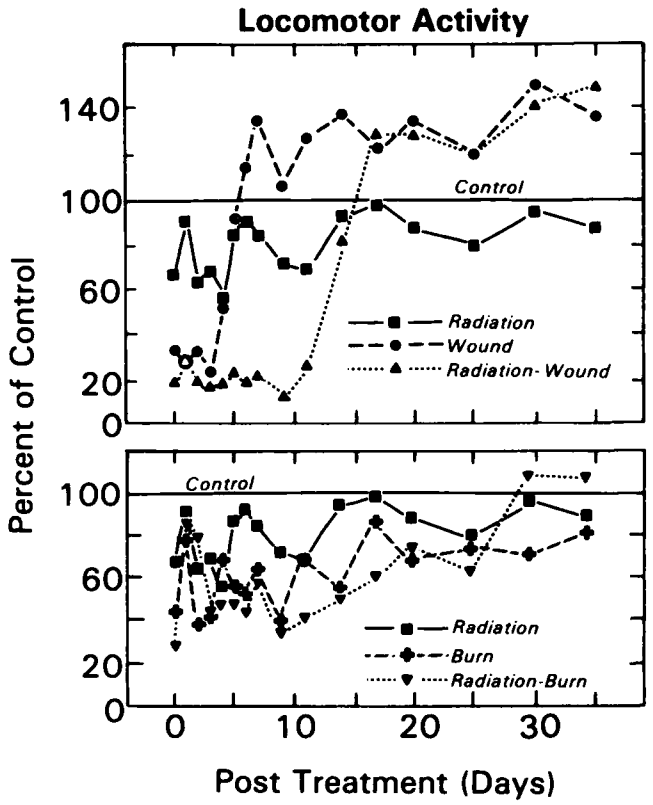

Fig. 1. (Top panel) Changes in vertical activity after exposure to 3 Gy fission neutrons (N = 10), a 30% skin wound (N = 10), or a combination of these effects (N = 11). Data are presented as percentage of control group (N = 12). Activity was monitored for 30 min on each test day. (Bottom panel) Changes in vertical activity as a function of 3 Gy radiation (N = 10), a 30% thermal burn (N = 9) or a combination of these injuries (N = 13). Radiation and control groups were reproduced from top panel.

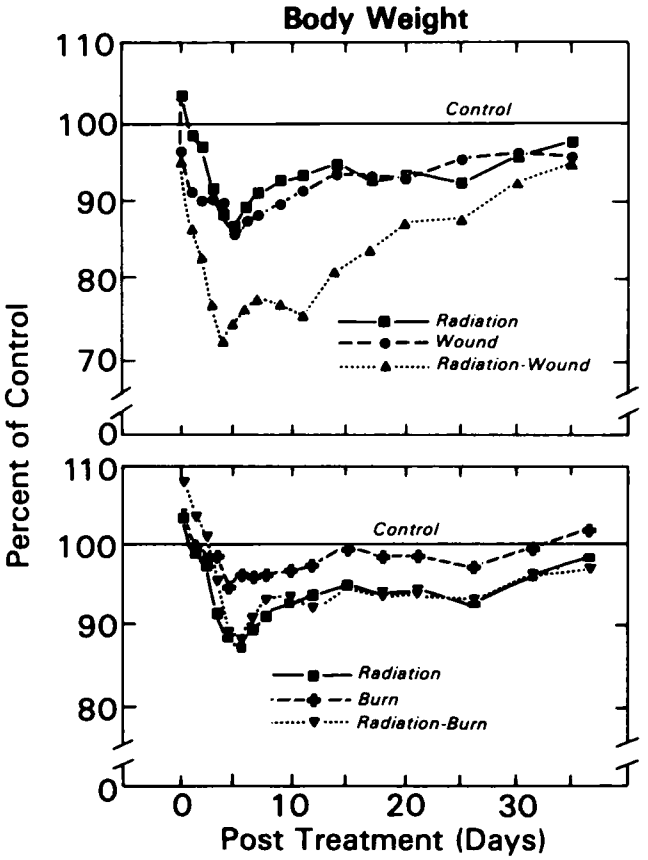

Fig. 2. (Top panel) Body weights of animals that received 3 Gy fission neutrons (N = 10), a 30% skin wound (N = 10), or a combination of these treatments (N = 11). Data are presented as percent of control group (N = 12). (Bottom panel) Alterations in body weights of groups that received radiation and/or burns: 3 Gy fission-neutron radiation (N = 10), a 30% burn (N = 9), or a combination of radiation and burn (N = 13). Radiation and control groups were reproduced from top panel.

radiation-only group have been reproduced in both burn and wound illustrations in order to assist in comparing the two types of injuries. Because horizontal activity and vertical activity were highly correlated, the results of only the vertical activity are presented.

Analysis of variance indicated that, for all treatments combined, there was a significant treatment by day effect for vertical activity ($F = 9.51$, $df = 80/944$, $p < 0.0001$), body weight ($F = 12.52$, $df = 80/944$, $p < 0.0001$), food intake ($F = 4.05$, $df = 25/77$, $p < 0.0001$), and water consumption ($F = 6.87$, $df = 25/77$, $p < 0.0001$). One animal in group RW died 13 d after treatment, and its data were deleted from the analysis.

Wound: Vertical activity in the wound-group (W) was depressed on days 0–4 and recovered completely to control levels by day 5. Animals that received both radiation and wounds (RW) did not recover activity levels until day 14. Mice that received radiation alone (R) showed a biphasic decrement in locomotor behavior with depressed activity on days 0–4 and again on days 9–11. Animals in this group showed complete recovery by day 14 (Fig. 1).

Beginning on day 2, body weights of groups R, W, and RW were significantly depressed from control values. Animals in groups R and W showed complete recovery of body weights by day 30, while group RW did not recover until day 35 (Fig. 2). Food intake for group W was depressed on days 1–4, while groups that received radiation (R and RW) exhibited decreased consumption levels on days 1–5 (Fig. 3). Water consumption in group R was depressed on days 1–6, with complete recovery by day 7. Animals in group W showed increased levels of water consumption until returning to control values by day 11. Group RW exhibited a biphasic effect with an initial increase in water consumption levels on days 1–2, and a return to control levels on days 3–4. The second period of increased intake on days 5–8 was followed by a return to normal by day 9 (Fig. 4).

Burn: Both groups R and RB showed depressed activity levels on day 1, recovered on day 2, and then remained below control values until day 17. Animals in the burn groups (B and RB) showed lower levels of activity than did group R (Fig. 1).

Body weights of R and RB were significantly depressed from control values beginning on day 3 and did not return to normal until day 30. Animals in group B did not show any significant loss in body weight throughout the experi-

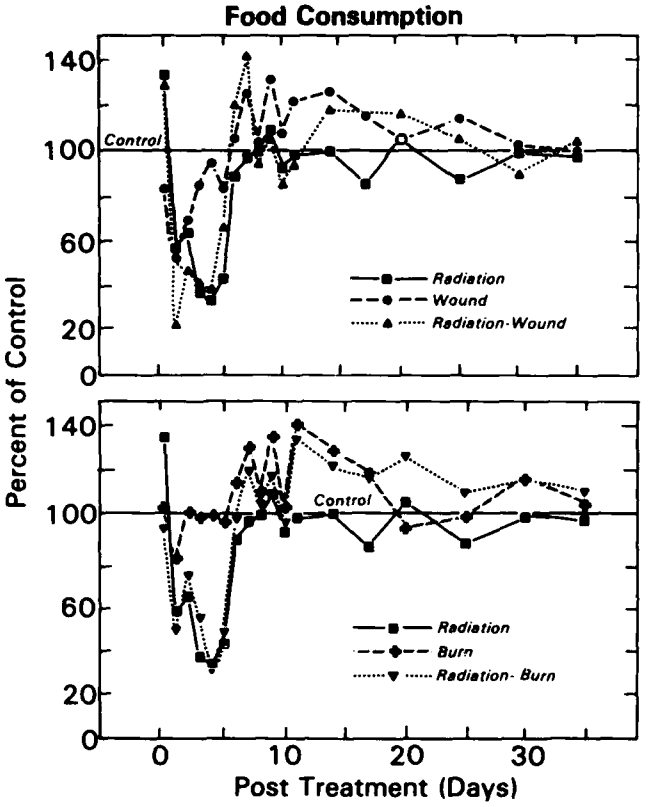

Fig. 3. (Top panel) Food consumption of groups of mice that received 3 Gy fission-neutron radiation or wounds. Since animals were housed 2–4 per cage, food consumption is based on average consumed per animal per cage. Radiation only (N = 3 cages), wound only (N = 4), radiation plus wound (N = 4). Data are presented as percentage of control group (N = 4). (Bottom panel) Changes in food consumption as a function of 3 Gy fission-neutron radiation (N = 3 cages), a 30% burn (N = 3) or a combination of these injuries (N = 4). Radiation and control groups were reproduced from top panel.

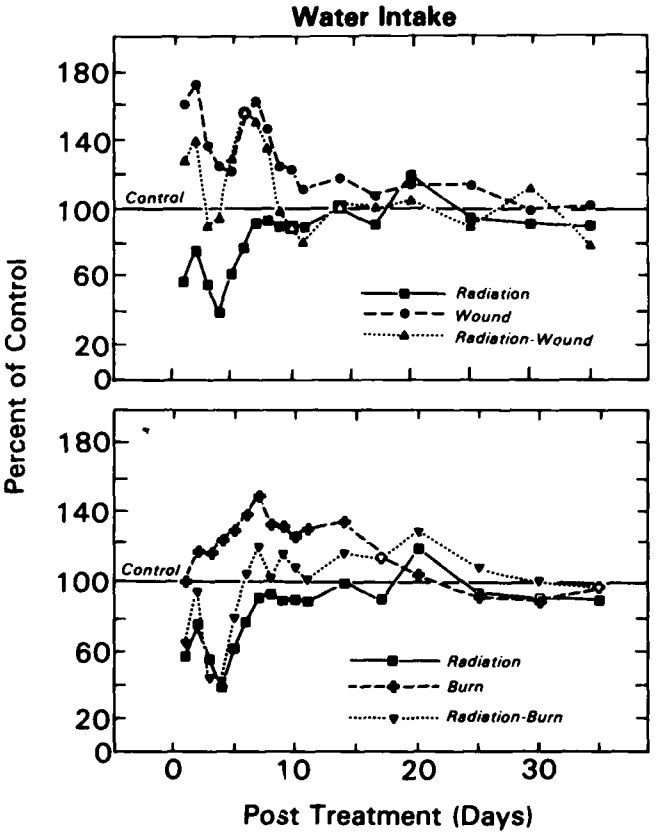

Fig. 4. (Top panel) Alterations in fluid consumption of groups of mice that received 3 Gy fission-neutron radiation or wounds. Water intake is based on average amount consumed per mouse per cage. Radiation only (N = 3 cages), a 30% wound (N = 4) or radiation plus wound (N = 4). Results were expressed as percent of control group (N = 4). (Bottom panel) Alterations in water consumption in groups of mice that received 3 Gy fission-neutrons (N = 3 cages), a 30% burn (N = 3), or a combination of these injuries (N = 4). Radiation and control groups were reproduced from top panel.

ment (Fig. 2). Food intake was suppressed for groups R and RB on days 1–6, but in general remained above control levels on days 7–35 (Fig. 3). Groups R and RB showed similar patterns of water intake, with depressed levels on days 1–5 and recovery by day 6. On days 7–20, water intake in group RB remained above control levels. Mice in group B showed increased levels of water intake on days 1–17 and returned to control values by day 20 (Fig. 4).

DISCUSSION

The results of this study point to significant alterations in locomotor activity as well as in body weight and food and water consumption produced by 3 Gy modified fission neutrons alone and in combination with wound and burn trauma. The data indicate that the effects of combined injury on the parameters recorded in this study are a function of the radiation insult and the additional type of trauma associated with it. In general, a wound injury potentiated the deleterious effects of radiation, while a burn injury did not.

A possible explanation of our findings may be that irradiation interferes with the healing process. It was recently reported that wound closure, eschar formation and loss, and healing occurred about 14 d following a 30% wound. Animals receiving 3 Gy radiation plus wound were not fully healed until 30 d following the injury (18). Similarly, Messerschmidt (24) determined that healing times lengthen by as much as 50% when combined injury included wounding and 5.19 Gy irradiation. Radiation has previously been reported to retard wound healing by resulting in a decrease in the activity of fibroblasts, and obliterative endoarteritis (28,32). Mice receiving a 30% burn healed in approximately 25 d, while animals that were irradiated and burned healed in 30–40 d (18).

The results of the present study agree with previous studies exploring locomotor activity in rats. Jones *et al.* (13) reported that male rats showed a significant depression in activity for the first 4 d following exposure to 400 rads x-irradiation. This was followed by a period of recovery and a second depression in activity on days 13–17. In the present experiment, female mice exposed to 300 rads fission-neutron showed significant depression in activity on days 0–4, a return to control levels of activity on days 5–7, and a second depression in activity on days 9–11 with recovery by

day 14. Similar biphasic depressions have been reported in rats following 648 rads x-irradiation (3) and mice exposed to 700 rads gamma radiation (15).

The initial decrease in activity observed during the first 4 d following irradiation has been largely associated with the degree of gastrointestinal dysfunction (3). During this period of depressed activity, gastric retention (33), changes in propulsive motility (7), diarrhea (10), anorexia (29, present study), and a reduction in body weight (29) have been reported to occur. The second depression of activity appears to be correlated with radiation-induced hematopoietic injury characterized by anemia, leukopenia, and changes in proliferative cell quantities (19). The association with hematopoietic injury was further demonstrated when rats treated with a suspension of homologous bone marrow no longer exhibited decreases in activity (12).

The decrement in locomotor activity observed in the animals in this study may be mediated by prostaglandins. Ledney *et al.* (18) reported increases in prostaglandin E2 in wounded, burned, and irradiated mice that received combined injuries at times similar to those that resulted in decreases in locomotor performance. Prostaglandins have previously been reported to depress locomotor activity (2,16) and to be activators of pain at peripheral sites (14).

The effects of radiation on body weight and food and water intake observed in the present study are similar to the effects reported by other investigators. The rapid, transient decrease in food consumption (9,29) and body weight (4,5) has previously been reported for rodents and is believed to be due to the disturbances in gastrointestinal function. Mice in the radiation-only group (R) also showed a temporary decrease in water consumption that lasted 6 d. This hypodipsic effect has also been reported in rats (1,9,26), although others have found increases in water consumption following irradiation (27).

Water loss is a serious problem in clinical burn trauma (8), and the open skin areas resulting from wounding or burning the test animals may have led to a loss of body water through evaporation. This was compensated for by an increase in fluid consumption in animals that received burns or wounds. RB animals first showed a brief period of decreased fluid intake, similar to that of the R group. However, more water was consumed by mice that received wounds (W and RW) than by animals that received burns (B and RB). It is speculated that this difference is attributable to the "open" nature of wounds compared to the "closed" nature of the injury resulting from burn trauma. Messerschmidt (25) also reported increased fluid intake in wounded mice.

The observations reported here may be due to the effects of endotoxin. Irradiated mice exhibit reduced food and water intake, concomitant loss of body weight, and lethargy which are mimicked in endotoxin-challenged animals (17). Mice exposed to radiation have detectable levels of endotoxin in their tissues (35), possibly derived from the endotoxin pool in the intestinal tract. Disruption of intestinal epithelial cell integrity (36) may account for the passage of endotoxin into the bloodstream and the resulting deleterious effects observed in this study.

These findings demonstrate that irradiation delays the healing process of both burn and wound injuries. By day 35 postirradiation, however, animals did return to control levels of locomotor activity, body weight, and food and water consumption.

ACKNOWLEDGMENTS

We thank William Jackson for statistical analysis and Marion Golightly, Darrell Grant, Donna Maier, and Junith Van Deusen for assistance in the preparation of the manuscript. This work was supported by the Armed Forces Radiobiology Research Institute, Defense Nuclear Agency, under Work Units B3129-4420 and B4160-4320.

Portions of this paper were presented at the 34th Annual Meeting of the Radiation Research Society, Las Vegas, NV, April 1986.

Research was conducted according to the principles enunciated in the 1985 "Guide for the Care and Use of Laboratory Animals" prepared by the Institute of Laboratory Animal Resources, National Research Council.

The views presented in this paper are those of the authors. No endorsement by the Defense Nuclear Agency has been given or should be inferred.

REFERENCES

1. Afifi AK, Osborne JW, Mitchell CL. Changes in neurosecretory material, water intake, and urine output in x-irradiated rats. Radiat. Res. 1964; 23:1–12.
2. Chiu EK, Richardson JS. Behavioral and neurochemical aspects of prostaglandin in brain function. Gen. Pharmacol. 1985; 16:163–75.
3. Castanera TJ, Jones DC, Kimeldorf DJ. The effect of x-irradiation on the diffuse activity performance in rats, guinea pigs and hamsters. Br. J. Radiol. 1959; 32:386–9.
4. Chapman WH. The weight and mortality response of male and female mice in the lethal x-ray dose range. Radiat. Res. 1955; 2:502–11.
5. Chapman WH, Jerome EA. An analysis of the effects of total-body x-irradiation on the body weight of Swiss mice. II. Body weight changes of male mice as a biological dosimeter. Radiat. Res. 1956; 4:519–31.
6. Conklin JJ, MacVittie TJ, Walker RI. Pathophysiology of combined injury and trauma: an overview. In: Walker RI, Gruber DF, MacVittie TJ, Conklin JJ, eds. The pathophysiology of combined injury and trauma: radiation, burn and trauma. Baltimore: University Park Press, 1985:3–10.
7. Conard RA. Effect of x-irradiation on intestinal motility of the rat. Am. J. Physiol. 1951; 165:375–85.
8. Davies JWL. Physiological responses to burning injury. New York: Academic Press, 1982.
9. Garcia J, Kimeldorf DJ, Hunt EL, Davies BP. Food and water consumption of rats during exposure to gamma radiation. Radiat. Res. 1956; 5:79–87.
10. Geraci JP, Jackson KL, Marino MS. The intestinal radiation syndrome: sepsis and endotoxin. Radiat. Res. 1985; 101:442–50.
11. Gruber DF, Walker RI, MacVittie TJ, Conklin JJ, eds. The pathophysiology of combined injury trauma: management of infectious complications in mass casualty situations. Orlando, FL: Academic Press, 1987.
12. Jones DC, Kimeldorf DJ, Castanera TJ, Rubadeau DO, Osborn GK. Effect of bone marrow therapy on volitional activity of whole-body x-irradiated rats. Am. J. Physiol. 1957; 189:21–31.
13. Jones DC, Kimeldorf DJ, Rubadeau DO, Osborn GK, Castanera TJ. Effect of x-irradiation on performance of volitional activity by the adult male rat. Am. J. Physiol. 1954; 177:243–50.
14. Juan H. Prostaglandins as modulators of pain. Gen. Pharmacol. 1978; 9:403–9.
15. Landauer MR, Davis HD, Dominitz JA, Pierce SJ. Effects of acute gamma radiation exposure on locomotor activity in Swiss-Webster mice. Toxicologist 1987; 7:253.
16. Landauer MR, Walden TL, Davis HD, Dominitz JA. Alterations in locomotor activity induced by radioprotective doses of 16,16-dimethyl prostaglandin E2. In: Walden TL, Hughes HN, eds. Prostaglandin and lipid metabolism in radiation injury. New York: Plenum Press.
17. Ledney GD. Diet and water consumption and body weight of germfree mice following whole body x-irradiation. Radiat. Res. 1964; 22:207–8.

18. Ledney GD, Steel LK, Exum ED, Gelston HM Jr. Pathophysiologic responses in mice after neutron irradiation combined with burn or wound trauma. Paper presented at the 2nd International Symposium on the Pathophysiology of Combined Injury. Wintergreen, VA. Feb. 1985.
19. Ledney GD, Stewart DA, Exum ED, Sheehy PA. Skin wound enhanced survival and myelocytoporesis in mice after whole body irradiation. Acta. Radiologica Oncol. 1981; 20:29–38.
20. Ledney GD, Stewart DA, Gruber DF, Gelston HM Jr, Exum ED. Hematopoietic colony-forming cells from mice after wound trauma. J. Surg. Res. 1985; 38:55–65.
21. McPherson, CW. Reduction of *Pseudomonas aeruginosa* and coliform bacteria in mouse drinking water following treatment with hydrochloric acid or chlorine. Lab. Anim. Care; 1963; 13:737–44.
22. Marshall E. Reactor explodes amid Soviet silence. Science 1986; 232:814–5.
23. Messerschmidt OE. Strahlenbelastung und offene Hautwunde. Arch. Klin. Exp. Dermatol. 1966; 227:329–35.
24. Messerschmidt OE, Birkenmay E, Bomes H. Radiation sickness combined with burns. Int'l Atomic Energy Ass'n Science Manual-119/34, 1970: 173–9.
25. Messerschmidt OE. Results of animal experiments as a basis for recommendation on therapy of combined injuries. In: Walker RI, Gruber DF, MacVittie TJ, Conklin JJ. eds. The pathophysiology of combined injury and trauma: Radiation, burn and trauma. Baltimore: University Park Press, 1985:11–8.
26. Mickley GA, Stevens KE. Stimulation of brain muscarinic acetylcholine receptors acutely reverses radiogenic hypodipsia. Aviat. Space Environ. Med. 1986; 57:250–5.
27. Nims IF, Sutton E. Weight changes and water consumption of rats exposed to whole-body x-irradiation. Am. J. Physiol. 1952; 171:17–21.
28. Odling-Smee GW. Tissue repair and wound healing. In: Odling-Smee W, Crockard A, eds. Trauma care. New York: Academic Press, 1981:53–74.
29. Smith DE, Tyree EB. Influence of x-irradiation upon body weight and food consumption of the rat. Am. J. Physiol. 1954; 177:251–60.
30. Stewart DA, Ledney GD, Baker WH, Daxon EG, Sheehy PA. Bone marrow transplantation of mice exposed to a modified fission neutron (N/G 30:1) field. Radiat. Res. 1982; 92:268–79.
31. Stieritz DD, Bondi A, McDermott D, Michaels EB. A burned mouse model to evaluate anti-*Pseudomonas* activity of topical agents. J. Antimicrobial. Chem. 1982; 9:133–40.
32. Stromberg WR, Woodward KT, Mahin DT, Donati RM. Combined surgical and radiation injury: the effect of timing of wounding and whole body gamma irradiation on 30 day mortality and rate of wound contracture in the rodent. Ann. Surg. 1968; 167:18–22.
33. Swift MN, Taketa ST, Bond VP. Delayed gastric emptying in rats after whole and partial body x-irradiation. Am. J. Physiol. 1955; 182:479–86.
34. Walker RI, Gruber DF, MacVittie TJ, Conklin JJ. The pathophysiology of combined injury and trauma: radiation, burn and trauma. Baltimore: University Park Press, 1985.
35. Walker RI, Ledney GD, Galley CB. Aseptic endotoxemia in radiation injury and graft vs. host disease. Radiat. Res. 1975; 62:242–9.
36. Walker RI, Porvaznik M. Association of bacteria and endotoxin with posttrauma events. In: Ninnemann JJ, ed. Traumatic injury: infection and other immunologic sequelae. Baltimore: University Park Press, 1983:1–15.
37. Winer BJ. Statistical principles in experimental design. New York: McGraw-Hill, 1971.

From: PROSTAGLANDIN AND LIPID METABOLISM
IN RADIATION INJURY
Edited by Thomas L. Walden, Jr. and Haywood N. Hughes
(Plenum Publishing Corporation, 1987)

ALTERATIONS IN LOCOMOTOR ACTIVITY INDUCED BY RADIOPROTECTIVE DOSES OF 16,16-DIMETHYL PROSTAGLANDIN E_2

M. R. Landauer[1], T. L. Walden[2], H. D. Davis[1], and J. A. Dominitz[1]

[1]Behavioral Sciences Department
[2]Radiation Biochemistry Department
Armed Forces Radiobiology Research Institute
Bethesda, Maryland 20814-5145

ABSTRACT

16,16-Dimethyl prostaglandin E_2 ($DiPGE_2$) is an effective radioprotectant when administered before irradiation. A notable side effect of this compound is sedation. In separate experiments, we investigated the dose-response determinations of the time course of locomotor activity and 30-day survival after 10 Gy gamma irradiation (LD_{100}). Adult male CD2F1 mice were injected subcutaneously with vehicle or $DiPGE_2$ in doses ranging from 0.01 to 40 μg/mouse. A dose of 0.01 μg did not result in alterations in locomotor behavior or enhance survival. Doses greater than 1 μg produced ataxia and enhanced radiation survival in a dose-dependent fashion. Full recovery of locomotor activity did not occur until 6 and 30 hr after injection for the 10 μg and 40-μg groups, respectively. Radioprotection was observed when $DiPGE_2$ was administered preirradiation but not postirradiation. Doses of 1 and 10 μg were maximally effective as a radioprotectant if injected 5 min prior to irradiation (80%-90% survival). A dose of 40 μg resulted in 100% survival when injected 5-30 min before irradiation. Therefore, increasing doses of $DiPGE_2$ resulted in enhanced effectiveness as a radioprotectant. However, the doses that were the most radioprotective were also the most debilitating to the animal.

INTRODUCTION

The ideal radioprotective agent is one that maintains both high efficacy and mental alertness. An agent having both of these characteristics would be useful in the event of a radiation accident. Compounds providing a high degree of radioprotection but temporarily impairing mental alertness may still prove to be beneficial in radiotherapy. 16,16-Dimethyl prostaglandin E_2 ($DiPGE_2$) has been shown to be effective in enhancing the radiation survival of hematopoietic and intestinal stem cells *in vivo* (1) and also for whole-animal survival (2). Although

the mechanism(s) for the radioprotection is unknown, the induction of hypoxia through prostaglandin-mediated vascular changes remains a viable hypothesis. Radioprotective doses of $DiPGE_2$ result in significant increases in the hematocrit (2) and a concomitant reduction in the respiration rate (T. Walden, unpublished).

Exogenously administered prostaglandins, including those of the E series, have been demonstrated to produce sedative or tranquilizing effects in a variety of species (3-8). A decrease in gross locomotor movements has been observed following the administration of radioprotective doses of $DiPGE_2$, but the magnitude and duration of the response have yet to be quantified (2). Sedative effects might limit the usefulness of $DiPGE_2$ as a radioprotectant. We have examined the reduction in locomotor activity induced by $DiPGE_2$ over a dose range associated with radioprotection. In this paper we report that the doses that result in the greatest disruption of locomotor activity are the doses that offer the most radioprotection.

METHODS

Subjects

CD2F1 male mice, 3-5 months of age and obtained from Harlan Sprague-Dawley (Indianapolis, IN), served as subjects. They were housed under a 12-hour light-dark cycle. Immediately following arrival, animals were quarantined for 2 weeks to ensure that they were free from *Pseudomonas* and other common murine diseases, based on serological and histological examination. Mice were maintained in groups of 9-10 in clear plastic cages with filter tops, and were provided with Wayne Rodent Blox diet and acidified water (pH 2.5) ad libitum.

Drug

$DiPGE_2$ was obtained from the UpJohn Co. (Kalamazoo, MI). The drug was dissolved in a solution containing 4% ethanol in saline (0.9%). The mice received a single 100-μl subcutaneous injection in the skin at the back of the neck.

Locomotor Activity

Locomotor behavior was measured using a computerized Animal Activity Monitor (Model RXYZCM-16, Omnitech Electronics, Columbus, OH), which recorded horizontal activity (ambulation) by means of infrared photodetectors. Animals received subcutaneous injections of the vehicle or 0.01, 0.1, 1.0, 10.0, or 40.0 μg/mouse $DiPGE_2$ ($N = 9$/group) and were placed immediately into the test apparatus. Locomotor activity was monitored at 1-min intervals for the first 60 min to determine the latency of onset of the drug. Thereafter, activity was recorded at 1-hour intervals for the next 5 hours and again from hours 25 to 30 postinjection. After that time, all groups had returned to control values. All testing took place during the dark portion of the light-dark cycle.

Radioprotection

Additional mice were bilaterally irradiated with 10 Gy cobalt-60 radiation at a dose rate of 1 Gy/min, as previously described (9). Prior to irradiation, mice were injected subcutaneously with doses of vehicle or 0.1, 1.0, 10.0, or 40.0 μg/mouse DiPGE$_2$. The drug was administered at 5, 20, 30, or 60 min before irradiation. Separate groups of mice received these same doses postirradiation. Control animals received vehicle alone. Ten mice were used for each dose at each time point. Irradiated animals were monitored for the fraction surviving 30 days postirradiation.

Statistical Analysis

A one-way analysis of variance with repeated measures was performed on the locomotor activity data. Post hoc comparisons were made using Dunnett's test. Significant differences in percent 30-day survival were determined by using the method of Fleiss to compare proportions (10).

RESULTS

16,16-Dimethyl prostaglandin E$_2$ produced a dose-dependent decrease in locomotor activity. Analysis of variance indicated that the effect of dose on locomotor activity was significant over time ($F = 8.36$, $df = 44/440$, $p < .0001$). A dose of 0.01 μg did not significantly alter locomotor activity from control values. For doses between 0.1 and 40 μg/mouse, the latency to onset of the drug occurred within 2-3 min. Only those animals receiving a dose of 0.1 μg fully recovered during the first hour following injection (Figure 1). Increasing the concentration of the DiPGE$_2$ treatment extended the duration of the locomotor decrement (Figure 2). A dose of 1.0 μg resulted in full recovery of locomotor function by 2 hours postinjection, whereas mice administered doses of 10 and 40 μg did not return to control levels until 6 and 30 hours, respectively.

The time intervals for radioprotective activity of DiPGE$_2$ at concentrations tested for locomotor activity are shown in Table 1. The 40-μg dose provided the greatest level of radioprotection. At this dose, 100% survival from 10 Gy radiation was observed when DiPGE$_2$ was administered during the first 30 min before irradiation. Eighty percent of the animals survived when this dose was administered at 60 min preirradiation. When injected 5 and 20 min preirradiation, doses of 1 and 10 μg, respectively, were not significantly different from the 40-μg dose. However, at 30 and 60 min prior to irradiation, a dose of 40 μg was significantly more effective than doses of 0.1-10 μg DiPGE$_2$. Pretreatment with doses of less than 1 μg DiPGE$_2$ or administration of doses of 0.1-40 μg postirradiation did not yield any radioprotection. DiPGE$_2$ did not affect the rate of radiation-induced mortality. Radiation-induced deaths in both vehicle- and DiPGE$_2$-treated mice occurred between 9 and 14 days postirradiation. None of the vehicle-treated animals survived the 10-Gy radiation dose.

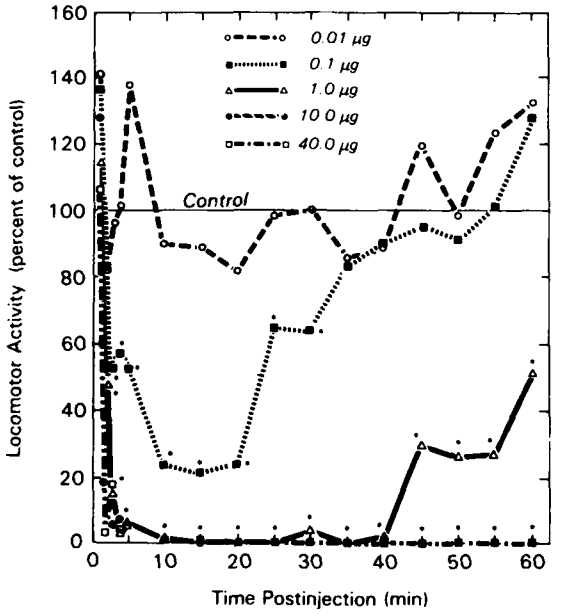

Fig. 1. Time course of $DiPGE_2$ as a function of dose on locomotor activity (ambulation) during first 60 min after injection. $DiPGE_2$ administered subcutaneously immediately before testing. Data are expressed as percent of vehicle control group (N = 9/group). *Significantly ($p < 0.01$) different from vehicle control group.

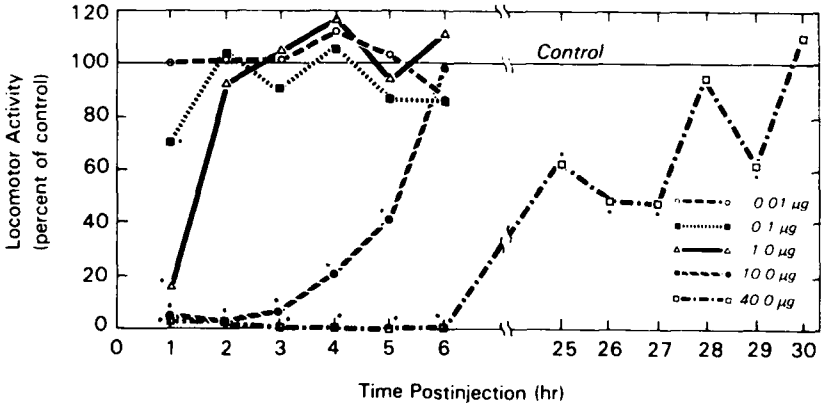

Fig. 2. Duration of action of effects of $DiPGE_2$ on locomotor behavior. Locomotor activity (ambulation) is expressed as percent of control group (N = 9/group). *Significantly ($p < 0.01$) different from vehicle control group.

Table 1. Effect of Dose and Time of PGE$_2$ on Percent 30-day Survival

	Min Preirradiation				Min Postirradiation			
Dose[1]	5	20	30	60	5	10	20	60
0.1	0	0	0[3]	0[3]	0	0	0	0
1.0	80[2]	60[2]	10[3]	0[3]	0	0	0	0
10.0	90[2]	70[2]	20[3]	10[3]	0	0	0	0
40.0	100[2]	100[2]	100	80	0	0	0	0

[1]Dose in μg/mouse subcutaneously (N = 10/group). All mice received 10 Gy gamma radiation at a dose rate of 1 Gy/min.

[2]These groups did not differ from each other and are significantly ($p < 0.05$) different from 0.1-μg group.

[3]These groups did not differ from each other and are significantly different ($p < 0.05$) from 40-μg group.

DISCUSSION

Radioprotective doses of DiPGE$_2$ (1-40 μg/mouse) resulted in rapid reduction of locomotor activity. Almost total cessation of ambulation occurred within 2 min after subcutaneous administration. The duration of the loss of activity was dose-dependent over a range of 0.1 to 40 μg. Activity recovered within 35 min following a dose of 0.1 μg, but remained depressed for up to 30 hours after the administration of 40 μg DiPGE$_2$. A dose of 0.01 μg did not disrupt locomotor activity. Prostaglandins of the E series administered to rodents have previously been shown to result in reduction of spontaneous locomotor activity (4,6-8), although the present study is the first to detail these effects for DiPGE$_2$.

Increasing the dose of DiPGE$_2$ enhanced the radioprotection but also extended the duration of the disruption of locomotor activity. A similar relationship between radioprotective efficacy and locomotor performance decrement in mice has been reported for other radioprotective compounds (11-13). The duration of the radioprotective activity of DiPGE$_2$ was much shorter than the disruptive effects on locomotor activity. For example, a dose of 10 μg resulted in 90% survival if injected 5 min preirradiation but only 10% survival wben administered 60 min before 10 Gy radiation. However, locomotor activity was significantly depressed from 2 min following injection, with total recovery delayed until 6 hours after drug administration. The differences in the duration of the radioprotective and behavioral effects may indicate that two separate processes are involved.

No significant difference was seen in the radioprotection induced by 1, 10, or 40 μg of DiPGE$_2$/mouse when administered 5 to 20 min prior to 10 Gy cobalt-60 radiation. However, at a higher dose of radiation (14.75 Gy), 40 μg DiPGE$_2$ has been shown to have greater radioprotective efficacy than a 10-μg dose (2).

The rapid onset of the reduction in locomotor activity may reflect a direct effect of $DiPGE_2$ on the central nervous system. Prostaglandins are capable of passing the blood-brain barrier (14), and have been shown to stimulate or modify neuronal activity (15-17) and disrupt behavior (3-8). Indirect effects on the central nervous system may result from a decrease in cerebral blood flow following the administration of $DiPGE_2$. PGE_2-induced sedation is believed to occur through this mechanism (4). Forty μg of $DiPGE_2$/mouse has been shown to increase the hematocrit from 61% to 71% within 10 min postadministration (2), and the cardiovascular response may also play a role in the suppression of activity.

The extended duration of depressed locomotor activity produced by radioprotective doses of $DiPGE_2$ may prevent the use of this compound as a general radioprotectant, particularly in those situations where operator activity must be maintained. The radioprotectant and the behavioral effects of $DiPGE_2$ appear to be the result of different mechanisms. Therefore, it may be possible to eliminate the deleterious behavioral side effects without the loss of radioprotective efficacy.

ACKNOWLEDGMENTS

We thank Dr. Douglas Morton of The UpJohn Company for very kindly supplying the prostaglandin used in this investigation. This research was supported by the Armed Forces Radiobiology Research Institute, Defense Nuclear Agency, under Research Work Units 4320-B4160 and 4230-B2152. The views presented in this paper are those of the authors; no endorsement by the Defense Nuclear Agency has been given or should be inferred. Research was conducted according to the principles enunciated in the "Guide for the Care and Use of Laboratory Animals" prepared by the Institute of Animal Laboratory Resources, National Research Council.

REFERENCES

1. Hanson, W. R., and Ainsworth, E. J. 16,16-Dimethyl prostaglandin E_2 induces radioprotection in murine intestinal and hematopoietic stem cells. Radiat. Res. 103: 196-203, 1985.
2. Walden, T. L., Jr., Patchen, M., and Snyder, S. L. 16,16-dimethyl prostaglandin E_2 increases survival in mice following irradiation. Radiat. Res. 109: 440-448, 1987.
3. Desiraju, T. Effect of intraventricularly administered prostaglandin E1 on the electrical activity of cerebral cortex and behavior in the unanesthetized monkey. Prostaglandins 3: 859-870, 1973.
4. Gilmore, D. P., and Shakh, A. A. The effect of prostaglandin E_2 in inducing sedation in the rat. Prostaglandins 2: 143-151, 1972.
5. Horton, E. W. Actions of prostaglandins E_1, E_2, and E_3 on the central nervous system. Brit. J. Pharmacol. 22: 189-192, 1964.

6. Weiner, M., and Olson, J. W. Comparative behavioral effects of dibutyryl cyclic AMP and prostaglandin E_1 in mice. Prostaglandins 9: 927-943, 1975.
7. Chiu, E. K. Y., and Richardson, J. S. Behavioral and neurochemical aspects of prostaglandins in brain function. Gen. Pharmac. 16: 163-175, 1985.
8. Potts, W. J., East, P. F., and Mueller, R. A. Behavioral effects. In: "The Prostaglandins," Vol. 2. P. W. Ramwell, ed. Plenum Press, New York, 1974, pp. 157-173.
9. Snyder, S. L., Walden, T. L., Jr., MacVittie, T. J., Patchen, M. L., and Fuchs, P. Radioprotective properties of detoxified lipid A from *Salmonella minnesota* R595. Radiat. Res. 107: 107-114, 1986.
10. Fleiss, J. L. "Statistical Methods for Rates and Proportions." John Wiley, New York, 1981, pp. 138-143.
11. Landauer, M. R., Davis, H. D., Dominitz, J. D., and Weiss, J. F. Dose and time relationships of the radioprotector WR-2721 on locomotor activity in mice. Pharmacol. Biochem. Behav. 27: 573-576, 1987.
12. Landauer, M. R., Davis, H. D., Dominitz, J. D., and Weiss, J. F. Comparative behavioral toxicity of four sulfhydryl radioprotective compounds in mice. WR-2721, cysteamine, diethyldithiocarbamate, and N-acetylcysteamine. Parmac. Ther., in press.
13. Landauer, M. R., Davis, H. D., Dominitz, J. D., and Weiss, J. F. Long-term effects of radioprotector WR-2721 on locomotor activity and body weight of mice following exposure to ionizing radiation. Toxicology, in press.
14. Bito, L. Z., Davson, H., and Hollingsworth, J. R. Facilitated transport of prostaglandins across the blood-cerebrospinal fluid and blood-brain barriers. J. Physiol. 253: 273-285, 1976.
15. Bergstrom, S., Farnebo, L. O., and Fuxe, K. Effect of prostaglandin E_2 on central and peripheral catecholamine neurons. Eur. J. Pharmacol. 21: 362-368, 1973.
16. Hayaishi, O. Prostaglandin D_2: A neuromodulator. In: "Advances in Prostaglandin, Thromboxane, and Leukotriene Research," Vol. 12. B. Samuelsson, R. Paoletti, and P. Ramwell, eds. Raven Press, New York, 1983, pp. 333-337.
17. Wolfe, L. S. Eicosanoids: Prostaglandins, thromboxanes, leukotrienes, and other derivatives of carbon-20 unsaturated fatty acids. J. Neurochem. 38: 1-14, 1982.

Brain Research, 424 (1987) 239–248
Elsevier

BRE 12989

Fetal hypothalamic brain grafts reduce the obesity produced by ventromedial hypothalamic lesions*,**

G. Andrew Mickley[1], Herman Teitelbaum[2] and Paul J. Reier[3]

[1]*Experimental Psychology Division, Behavioral Sciences Department (BHS), The Armed Forces Radiobiology Research Institute (AFRRI), Bethesda, MD 20814-5145 (U.S.A.);* [2]*Division of Research Grants, National Institutes of Health, Bethesda, MD 20892 (U.S.A.) and* [3]*Departments of Neurological Surgery and Neuroscience, University of Florida, College of Medicine, Gainesville, FL 32610 (U.S.A.)*

(Accepted 31 March 1987)

Key words: Transplant; Neural graft; Obesity; Ventromedial hypothalamus; Lesion; Hyperphagia; Feeding; Consummatory behavior

Bilateral destruction of the rat ventromedial hypothalamus (VMH) produces a syndrome characterized by hyperphagia and obesity. In the present study we examined whether grafts of fetal hypothalamus could reverse the effects of this lesion. Three groups of adult rats received bilateral electrolytic lesions of the VMH. The first group of animals was then implanted with embryonic day 14–16 hypothalamic tissue by stereotaxic injection into the lesion sites. The second series of animals received comparable-sized grafts from a variety of non-hypothalamic regions of the fetal CNS. The third group experienced similar VMH lesions but did not receive any tissue grafts. After surgery, body weight and food consumption were recorded daily for up to 8 weeks. These measures were compared with similar ones obtained from non-operated rats. Hyperphagia and obesity were consistently observed in all of the lesioned animals not bearing transplants. An initial period of weight gain was also observed in animals receiving hypothalamic grafts, but the duration of the 'dynamic' phase of this syndrome was reduced. Consequently, these graft recipients exhibited significantly less weight gain. This depressed weight gain, however, did not coincide with a statistically significant decrease in hyperphagia. Transplantation of non-hypothalamic tissue also caused an attenuation of the VMH-lesion effect but this was more modest than that induced by homotopic grafts.

The results of this experiment show that homotopic transplants can alter the dynamics of weight gain induced by bilateral VMH lesions. However, lesion-induced hyperphagia was not completely reversed in these grafted animals. The fact that other regions can exert a similar effect, though of lesser magnitude, suggests that a more general property of fetal CNS tissue may be involved.

INTRODUCTION

An extensive literature has developed over the last several years which establishes that embryonic neural tissue can be successfully transplanted into the CNS of adult hosts. Such grafts typically exhibit growth, long-term survival and some degree of organotypic differentiation. Furthermore, some of the neuroanatomical connections established by neural grafts have been shown to be physiologically appropriate and anatomically similar to those observed in normal brain tissue. Many laboratories have also reported that fetal neural tissue can compensate for a variety of motor, cognitive and neuroendocrine deficits (for reviews see refs. 5, 6, 33).

The hypothalamus represents one area of the brain that has been the focus of a number of transplantation studies. For example, grafting of preoptic tissue from male rat neonates into the preoptic area of female littermates has led to increased masculine and feminine sexual behavior in the recipients during adulthood[2]. Similarly, mating and pregnancy can be

* Research was conducted according to the guidelines presented in the "Guide for the Care and Use of Laboratory Animals" prepared by the Institute of Laboratory Animal Resources, National Research Council. Views presented in this paper are those of the authors. No endorsement by AFRRI or DNA has been given or should be inferred.

** A portion of this paper was presented at the 15th Annual meeting of The Society for Neuroscience, Dallas, TX, 1985.

Correspondence: G. A. Mickley, Experimental Psychology Division, Behavioral Sciences Department (BHS), The Armed Forces Radiobiology Research Institute (AFRRI), Bethesda, MD 20814-5145, U.S.A.

established in genetically hypogonadal mice following transplantation of cells from the developing preoptic area[15]. In addition, transplantation of vasopressin-containing neurons from the hypothalamic neurosecretory system of normal fetal donors in the Brattleboro rat has been reported to alleviate symptoms of diabetes insipidus[14].

The role of the hypothalamus in the control of appetite and satiety is well known. Bilateral lesions of the ventromedial hypothalamus (VMH) have been shown to produce hyperphagia and obesity[7,8,19,40], as well as metabolic dysfunctions[23]. Still in question, however, are the neurochemical and neuroanatomical substrates of appetite and weight gain[16,23,24,37]. Neural grafting techniques have the potential to be used as an effective research tool to characterize these underlying mechanisms. The present experiments reflect a first step towards this end. Here we determine whether embryonic hypothalamic tissue can ameliorate the obesity and hyperphagia observed after bilateral VMH lesions.

MATERIALS AND METHODS

Subjects. Female Sprague–Dawley rats (200–275 g) were obtained from Charles River (Raleigh, NC) and maintained on an ad-lib food and water schedule. They were housed in a room, maintained at 21 °C, in which the lights came on at 06.00 and were turned off at 18.00 h. Animals had access to food in two forms: (1) Wayne Rodent Blox (pellets), Continental Grain, Chicago, IL, and (2) powder derived from crushing Wayne Rodent Blox. The food pellets were suspended in a tray over the animal's head while the powder was placed in a supported round dish on the bedding of the cage floor.

Surgery. Rats were injected with atropine sulfate (0.4 mg/kg, i.p.) and then anesthetized with sodium pentobarbital (50 mg/kg, i.p.). In each brain hemisphere an 18 gauge guide cannula was stereotaxically directed toward the VMH[26] using the following coordinates: AP = −2.0 mm behind Bregma; Lateral = ± 0.8 mm; Depth = 5.5 mm from skull surface. A nichrome electrode was placed through this guide cannula. The shaft of the electrode (0.2 mm diameter) was insulated except for 0.5 mm of the tip. The electrode extended 4.0 mm beyond the end of the guide cannula, thus, positioning its tip in the VMH at a depth of 9.5 mm. A lesion was produced by passing current (1.5 mA) through the electrode for 15 s. Immediately following this procedure we inserted a blunt-tipped 20-gauge injection needle into the cannula guide and directed it 4.0 mm beyond the tip of the established cannula. Embryonic CNS tissue was then slowly injected into the lesion site.

Experimental groups. Experimental animals (n = 11) received VMH lesions and hypothalamic grafts. Some control rats (n = 8) received VMH lesions and then brain tissues from non-homologous CNS areas, including cerebral cortex, tegmentum, cerebellum, hippocampus and spinal cord. Other control subjects (n = 12) received VMH lesions but no grafts. Additional rats (n = 12), with neither lesions nor grafts, provided normal maturational growth data. Fetal VMH tissue was obtained from the ventral half of the mid-region of the hypothalamus. These implants thus included portions of other closely adjacent hypothalamic nuclei but excluded anterior and posterior hypothalamic regions.

Fetal tissue preparation and injection. Fetal donor CNS tissue was dissected from E14–16 day embryos. Each embryo was removed as needed while the mother was maintained under deep anesthesia. Following exposure of the brain and spinal cord of the fetuses, these tissues were removed and transferred to sterile tissue culture medium (Dulbecco's Modified Eagle Medium, Whittaker M.A. Bioproducts, Walkersville, MD). The meninges and dorsal root ganglia were removed and specific regions of the CNS were dissected as previously described in Stenevi et al.[39]. Donor tissues were cut into approximately 0.3-mm cubes before 2 or 3 of the pieces were suspended in tissue culture medium and injected into each side of the host brain. The total injection volume was 2.0–5.0 μl.

Data collection and statistical analyses. Animals were weighed on the day of surgery (day 1) and then daily for 54 days. Food consumption (both pellets and powder) was also monitored on the same basis.

A Repeated Measures Analyses of Variance (RMANOVA) was used to compare the body weights of the 4 groups of animals over the course of the experiment[10,42]. Data from subjects with non-homologous control fetal CNS transplants were similar and, therefore, combined for purposes of statistical analyses. We converted the data to logarithms to

meet the assumptions of homogeneity of variance required by the RMANOVA. This analysis of weight revealed statistically significant differences between the treatment groups ($F = 13.6$, $df = 3$, $P < 0.001$). Not surprisingly, there were also significant increases in weight over time ($F = 336.59$, $df = 53$, $P < 0.001$). The Treatment × Time interaction was also statistically significant ($F = 21.84$, $df = 159$, $P < 0.001$). This interaction effect prompted us to further analyze treatment group weight differences through the use of One-Way Analyses of Variance on the following days of the experiment: 1–20, 25, 30, 35, 40, 45, 50 and 54. As outlined below, this analysis resulted in statistically significant F scores (ranging from 3.39 to 21.42, $df = 39$) yielding P values from 0.0273 to < 0.001. Newman–Keuls statistics[42] were used to make group comparisons after statistical significance was determined via each One-Way ANOVA. Throughout these analyses we set the alpha = 0.05. We performed a second RMANOVA[10] to compare the cumulative food consumed by the animals in the 4 treatment groups over 5 overlapping blocks of time: postsurgical days 5–15, 6–25, 6–35, 6–45, and 6–54. The data underwent logarithmic conversion in order to meet the assumptions of homogeneity of variance required by the RMANOVA. The RMANOVA revealed a significant difference between the food consumed by the animals in the surgical treatment groups ($F = 9.95$, $df = 3$, $P = 0.0001$) and a significant time effect ($F = 3772.59$, $df = 4$, $P < 0.0001$). However, there was no significant interaction between time and treatment groups ($F = 1.74$, $df = 12$, $P = 0.1469$). t-Tests (reported below) were subsequently used to discern individual group differences.

Histology. At the end of the experiment subjects were anesthetized with 60 mg/kg sodium pentobarbital (i.p.) and then perfused intracardially with physiological saline followed by 10% buffered formalin. The brains were sliced and stained with Thionin or Toluidine blue. Each series of brain sections was then reviewed by two independent observers who were unaware of the experimental conditions and other data associated with each case. Reviewer agreement regarding lesion placement and size, as well as the presence of viable neuronal grafts, were two of the criteria that had to be met for a case to be included in the data analyses. Subjects with transplants that were completely located outside of the hypothalamus were excluded. Three rats with unusually large grafts were also eliminated from the data pool since very large grafts were also shown to produce lesion-like phenomena[9]. Fig. 1 illustrates representative brain lesions of the subjects retained in the experimental and control groups. Fig. 2 shows 3 of the hypothalamic grafts.

In order to differentiate graft and host brain tissue at the time of histological inspection, some of the fetal tissues were labeled with [methyl-^{3}H]thymidine (spec. act. 50–80 Ci/mM, New England Nuclear, Boston, MA) prior to transplantation. This entailed injecting (i.p.) the dam with 5 μCi thymidine/g of b. wt. at each of the following times: (1) the afternoon of embryonic day 12, (2) the morning and afternoon of embryonic day 13, and (3) the morning of embryonic day 14. At the end of the experiment, this brain tissue was cryostat-sectioned or embedded in plastic and processed for autoradiographic visualization of thymidine-labeled nuclei as previously described[43].

RESULTS

The results may be briefly described by noting that hypothalamic brain grafts reduced the obesity observed after bilateral lesions of the VMH (Fig. 3). Non-homologous CNS grafts did not reliably reduce the weight gains of lesioned rats. Despite a tendency for these hypothalamus recipients to consume less food than the rats with VMH lesions alone this was not a statistically significant phenomenon (Fig. 5).

Descriptions of VMH lesions and graft cytology. Similar VMH lesions were produced in all of the experimental and control animals included in this study (see Fig. 1). Destruction of the VMH was virtually complete in all cases with any sparing (if it occurred) representing approximately 10% of the nucleus. The lesions sometimes encroached slightly into the anterior hypothalamus and, in their most posterior extent, into the lateral and dorsomedial nuclei of the hypothalamus. General cytological examination of all of the grafts indicated that they were extensively differentiated and well-vascularized. Although efforts were made to restrict placement of fetal tissue to the original lesion sites (Fig. 2A), there were many instances in which transplants were found in the third ventricle (Fig. 2C) or positioned slightly dorsal to the

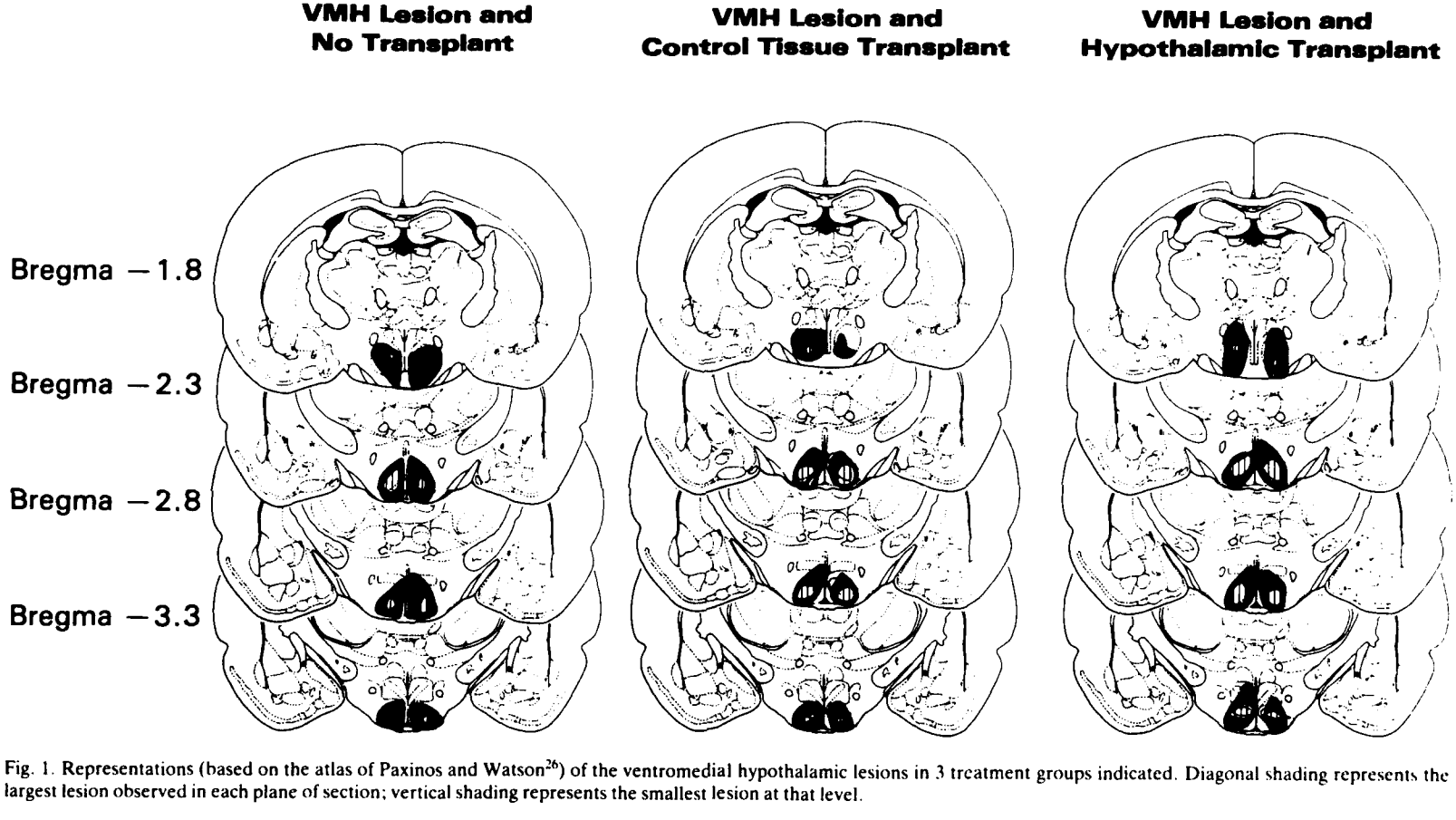

Fig. 1. Representations (based on the atlas of Paxinos and Watson[26]) of the ventromedial hypothalamic lesions in 3 treatment groups indicated. Diagonal shading represents the largest lesion observed in each plane of section; vertical shading represents the smallest lesion at that level.

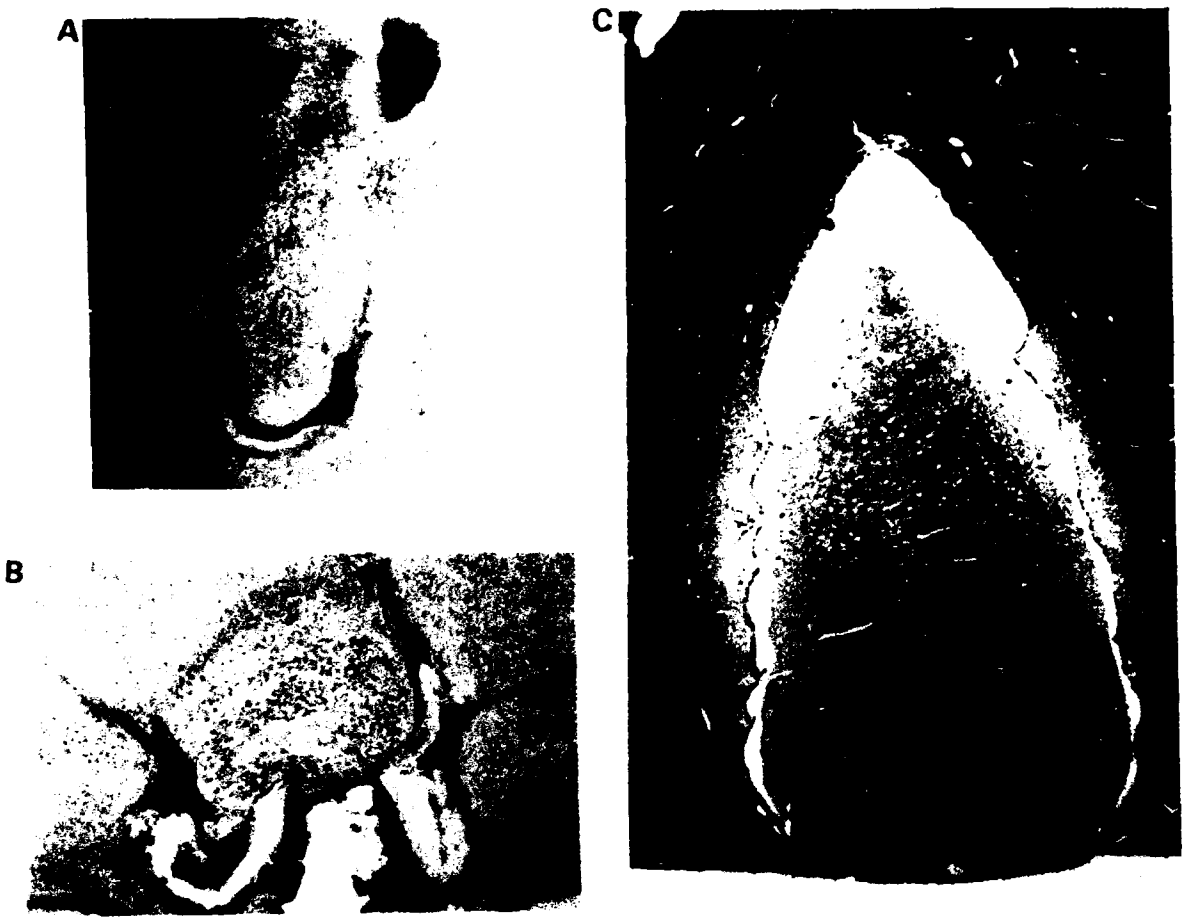

Fig. 2. Representative hypothalamic grafts in host brain. A: a graft inhabiting a lesion site. B: a hypothalamic transplant in, as well as dorsal to, the lesion. C: a graft in the third ventricle.

VMH with a portion of the graft extending ventrally into the lesion site (Fig. 2B).

Examination of the extent to which host and graft neuropils were fused indicated that, while close apposition was frequently observed, integration of these neural matrices was only partially achieved. For example, implants in the third ventricle were often separated from the host hypothalamus by the ependymal lining. However, as described elsewhere[29,30,32,34] there were many cases in which denuding of the ependyma had occurred at which points host and graft tissues fused without an intervening cellular partition (Fig. 2C). Those grafts, which were embedded within the parenchyma of the host hypothalamus, also exhibited partial integration of the host neuropil, although many regions of the donor tissues periphery were separated from the host brain by scarring or cystic cavities (Fig. 2A,B).

VMH lesion effects. At the time of surgery, and for the first 10 days thereafter, the weights of all the animals were not statistically distinguishable. The similarity of the slopes of these growth curves is consistent with our observation of comparable brain damage in each of the experimental groups. However, from day 11 through the end of the analysis (day 54) the subjects with only bilateral VMH lesions exhibited a statistically significant increase in weight over that observed in non-lesioned control subjects (see Fig. 3).

Weight gain following transplantation of homotopic fetal tissue. Grafts of fetal hypothalamus reduced the obesity observed after bilateral VMH lesions (Fig. 4).

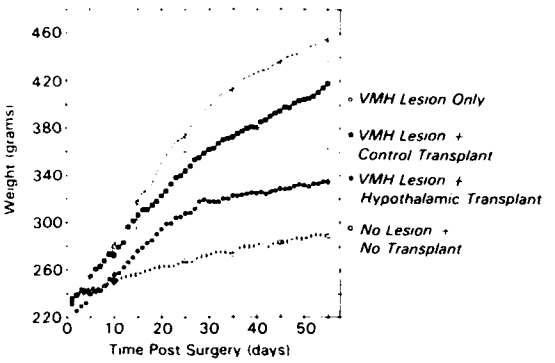

Fig. 3. Daily average postsurgical weights of rats in particular treatment groups. Embryonic hypothalamic grafts reduced the obesity observed after bilateral VMH lesions. Non-homologous grafts were less effective in this regard. Vertical bars represent S.E.M.

The one-way ANOVAs conducted on specific days postlesion revealed a reduction in the duration of the 'dynamic phase' of weight gain in these graft recipients. The first indication of change in the pattern of weight gain, as compared with rats having VMH lesions only, was observed between 6–10 days after surgery (Fig. 3). The first statistically significant difference between these two groups, however, was not established until two weeks after lesion and transplantation. At this time the weights of homotopic graft recipients were not statistically distinguishable from those of normal rats.

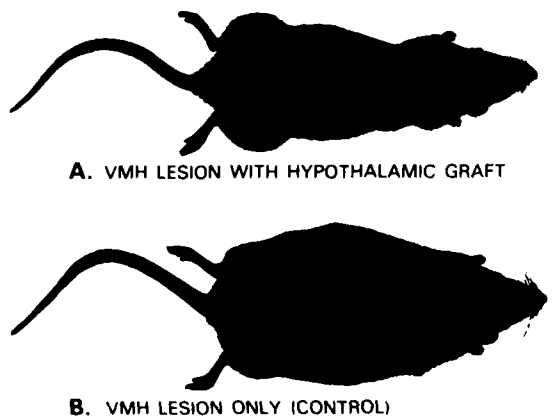

Fig. 4. Silhouettes of rats with either VMH lesions and confirmed hypothalamic grafts (A) or, bilateral VMH lesions alone (B) (Control).

By 25 days after surgery a plateauing in weight gain was seen in these hypothalamic transplant recipients. In contrast, the rate of weight increase in the lesioned rats without grafts was relatively unchanged at this time and continued to accelerate at approximately the same level throughout the duration of this study. Thus, at the times analyzed from 25 to 54 days postlesion, animals with homotopic grafts were significantly lighter (showing only an 8% increase in weight) than control rats with VMH lesions alone (showing a 22% increase). By 54 days, rats with only VMH lesions weighed 57% more than normal rats. On the other hand, animals with hypothalamic grafts weighed 26% less than the non-transplanted lesioned group and only 16% more than intact animals. Although mean body weights of these graft recipients were significantly greater than those of intact animals over the period from 25 to 50 days, these weights ultimately became so normalized that by 54 days they could not be statistically distinguished from those of normal rats.

Some animals with fetal hypothalamus transplants exhibited a particularly dramatic effect in that the attenuation in the 'dynamic' phase of weight increase was followed by an actual reduction in weight. This phenomenon was not observed in any of our animals with VMH lesions only.

With regard to these observations, it is important to note that none of these transplant recipients exhibited any signs of malaise or other deficits to which a change in the pattern of weight gain could be attributed. A few of the graft recipients that had shown a particularly dramatic early reduction in weight gain were autopsied and underwent histological review. No obvious pathological features were noted in any organ system and white blood cell counts measured at time of sacrifice were within normal ranges.

Effects of heterotopic CNS grafts on weight gain. Rats with bilateral VMH lesions and grafts of non-hypothalamic CNS tissue showed a rate of weight increase which practically parallelled that of homologous graft recipients until 14 days after surgery. At that time, a statistically significant difference in absolute weight was seen between hypothalamic and non-homologous transplant recipients. This difference persisted for the remainder of the study. Accordingly, the former group continued to show a progressive increase in weight, whereas the homologous trans-

plant recipients began to exhibit a decline in weight gain.

Although hypothalamic tissues seemed to exert a more pronounced effect on the weight gain following bilateral VMH lesions, comparison of VMH-lesion-only animals with those lesioned rats having transplants of non-hypothalamic CNS tissue, suggested that non-homologous tissue may also have some influence over this syndrome. Thus, by 14 days postsurgery, the rate of weight gain was greater in the rats with only VMH lesions. Despite these differences, however, the weights of animals with non-hypothalamus grafts could not be differentiated statistically from those animals with VMH lesions alone on many of the postsurgical days analyzed (days 25–45).

Analysis of food consumption. Rats with VMH lesions consumed significantly more food than did normal subjects ($t = 5.288$, $df = 21$, $P < 0.0001$) (Fig. 5). However, implantation of heterotopic neural grafts did not reduce this hyperphagia, and these transplanted control animals ate significantly more than normal non-lesioned rats ($t = 4.729$, $df = 17$, $P = 0.0002$). Although hypothalamic grafts produced a reduction in the lesion-induced hyperphagia, this was not a statistically reliable effect ($t = 1.449$, $df = 21$, $P = 0.1622$). The amount of food consumed by VMH-lesioned animals implanted with homotopic tissue was comparable to that eaten by lesioned rats with heterotopic grafts. Further, the animals with VMH lesions and hypothalamic transplants consumed significantly more food than normal control rats ($t = 3.473$, $df = 20$, $P = 0.0024$).

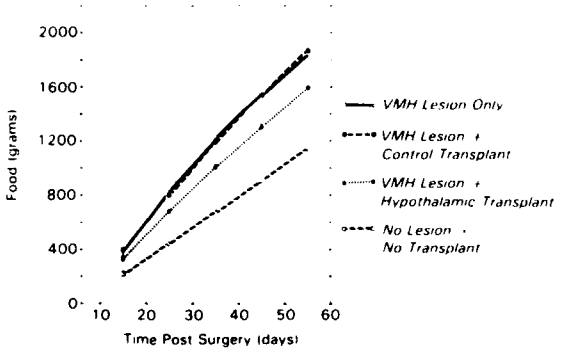

Fig. 5. Average cumulative total food consumed by rats in each treatment group. VMH lesions produced a hyperphagia that was not significantly attenuated by embryonic brain grafts. Vertical bars indicate S.E.M.

DISCUSSION

The results of this study demonstrate that the transplantation of embryonic hypothalamic tissue (containing in part the presumptive VMH) into the hypothalamus of the adult rat can significantly reduce the degree of weight gain caused by bilateral destruction of the VMH. Critical to the interpretation of these observations is the reproducibility of lesions within the 3 groups of operated animals. In this regard, independent review of the various specimens indicated uniformity in terms of lesion location, bilateral symmetry and general rostral-caudal and medial-lateral extent. In addition, the data demonstrated a rather consistent initial increase in body weight in all 3 of the VMH lesion groups regardless of whether or not a transplant was present. Furthermore, all of the operated animals exhibited hyperphagia which is a hallmark feature of this syndrome[40]. Based upon these lines of evidence, it appears that destruction of the VMH was achieved to a comparable degree in all of the experimental groups and that the diminished degree of weight gain in recipients of fetal hypothalamic tissue was not merely coincident with partial sparing of the host VMH.

Although fetal hypothalamic grafts reduced the obesity associated with bilateral VMH lesions, they did not significantly alter the hyperphagia induced by this damage. A trend, however, was seen toward a reduction in food intake. In this regard, some debate exists (for reviews, see refs. 23, 24) whether VMH-lesion-induced obesity is the result of a central regulatory dysfunction manifested by hyperphagia or the consequence of an independent primary metabolic disturbance (i.e. independent of hyperphagia). For instance, some investigators[17,18] have shown that VMH-lesioned rats become fatter and heavier than sham-operated controls even when fed comparable amounts of food. This finding may be due to lipogenesis-inducing meal patterns in the VMH-lesioned rats[28,35]. Future studies should address these issues more directly by using an experimental design similar to the one described here but incorporating, in addition to measurements of food consumption, data related to blood insulin levels, basal metabolic rates, types of food preferred and body fat.

Irrespective, however, of which component of the VMH lesion syndrome is being influenced by fetal

hypothalamic tissue, it is reasonable to speculate that the action of the graft may be exerted by its release of an active amine or peptide into the host CSF or adjacent brain tissue. A variety of neurotransmitters and neuromodulators are thought to be involved in the regulation of appetite and satiety[20,37]. This putative mechanism would be similar to that which has been suggested to occur in other transplantation models (e.g. refs. 12, 14, 27) and is consistent with previous demonstrations that symptoms of brain damage may be reversed by treatments affecting neurochemistry[21].

It is also possible that the reduced VMH lesion effect seen in fetal hypothalamic tissue recipients was due to the development of afferent and efferent synapses with the host brain (e.g. refs. 3, 11, 31). Many of the brain structures believed to mediate feeding behavior (e.g. the paraventricular and lateral nucleus of the hypothalamus) are in close proximity to the transplantation sites in this study[1,4,13,16]. Future immunocytochemical analyses may provide more insight into the cellular populations of our hypothalamic grafts and their axonal interactions with the host brain.

Non-hypothalamic grafts were less effective in reducing VMH lesion-induced hyperphagia than were transplants of homologous tissues. Despite the fact that some initial reduction in absolute body weight gain was observd in the hosts of heterotopic tissue grafts (Fig. 4), the rate of gain in these animals (especially after 30 days postsurgery) was comparable to that seen in lesioned animals without grafts. These data suggest that the reduced hyperphagia produced by hypothalamic grafts may be mediated by specific attributes of that tissue. Non-specific factors such as transplant-induced increases in intracranial pressure or irritation may be less important in this phenomenon.

On the other hand, during the interval of postsurgical days 15–25 the rates of weight increase observed in recipients of hypothalamic and heterotopic transplants were comparable. This raises the question of whether the effect of fetal hypothalamus seen in this study may be due to a common property of embryonic CNS tissue which is longer lasting or augmented in the hypothalamus. Functional recovery has also been observed with heterotopic fetal tissues in other brain lesions models[38]. Kesslak et al.[22] have shown that astrocytes previously grown in tissue culture and subsequently grafted into the ablated frontal cortex of adult rats can abolish the learning deficit on a reinforced alternation task. These results were interpreted to mean that astroglia may produce tropic factors to promote reactive synaptogenesis and may also be capable of preserving some of the host neuropil that would otherwise degenerate. More recently, Smith et al.[36] have reported that implants of embryonic glia can reduce some of the pathology associated with CNS injury. Although this discussion of astrocytes is offered purely as a matter of illustration, it is not inconceivable that glial cells in the fetal hypothalamus differ in some functional ways from those present elsewhere in the CNS thereby accounting for the more substantial long-range effects of homotopic versus heterotopic grafts. The more prolonged effects of fetal homotopic grafts may also be related to the later development of neuronal interactions.

The greater benefits provided by homologous tissue grafts are similar to other data such as those described by Labbe et al.[25] who showed that the cognitive deficits in spatial alternation learning following bilateral destruction of the medial forebrain cortex can be reduced in rats with transplants of frontal cortical tissue. This disorder, however, is not altered by grafts of fetal cerebellum. Similarly, neonatal striatal grafts prevent the lethal aphagia and adipsia produced by kainic acid lesions of the striatum, whereas tissue from other CNS sites appears to be ineffective[41].

These data are in agreement with a growing literature suggesting that neural grafts can reverse behavioral and physiological disorders caused by CNS damage. Our finding that fetal hypothalamic transplants attenuate the obesity produced by bilateral VMH lesions, extends this literature. Furthermore, the model system provided here may be useful to those interested in further specifying the physiological and behavioral mechanisms of hunger, satiety and obesity.

ACKNOWLEDGEMENTS

The authors wish to thank the following individuals for their expert assistance: Dr. Cathie Alderks, Mr. Paul Brenner, Mr. Bernard Dennison, Dr. Leland Ferguson, Mr. Thomas Nemeth, Ms. Diane Pickle,

and Ms. Becky Wade. We appreciate the help of Mr. William Jackson who advised us on statistics. These experiments were carried out under Defense Nuclear Agency Work Unit B4163.

REFERENCES

1 Aravich, P.F. and Beltt, B.M., Perifornical fiber system mediates VMH electrically-induced suppression of feeding, *Physiol. Behav.*, 29 (1982) 195–200.

2 Arendash, G.W. and Gorski, R.A., Enhancement of sexual behavior in female rats by neonatal transplantation of brain tissue from males, *Science*, 217 (1982) 1276–1278.

3 Arendash, G.W. and Gorski, R.A., Brain tissue transplantation and reproductive function. Implications for the sexual differentiation of the brain. In J.R. Sladek and D.M. Gash (Eds.), *Neural Transplants — Development and Function*, Plenum, New York, 1984, pp. 223–241.

4 Bernardis, L.L., Ventromedial and dorsomedial hypothalamic syndromes in the weanling rats: Is the 'center' concept really outmoded?, *Brain Res. Bull.*, 14 (1985) 537–549.

5 Björklund, A. and Stenevi, U., Intracerebral neural implants: neuronal replacement and reconstruction of damaged circuitries, *Annu. Rev. Neurosci.*, 7 (1984) 279–308.

6 Björklund, A. and Stenevi, U. (Eds.), *Neural Grafting in the Mammalian CNS*, Elsevier, Amsterdam, 1985.

7 Brobeck, J.R., Tepperman, J. and Long, C.N.H., Experimental hypothalamic hyperphagia in the albino rat, *Yale J. Biol. Med.*, 15 (1943) 831–853.

8 Brobeck, J.R., Mechanism of the development of obesity in animals with hypothalamic lesions, *Physiol. Rev.*, 26 (1946) 541–559.

9 Deckel, A.W. and Robinson, R.G., Transplantation of different volumes of fetal striatum: effects on locomotion and monoamine biochemistry, *Soc. Neurosci. Abstr.*, 12 (1986) 1479.

10 Dowdy, S.D. and Wearden, S., *Statistics for Research*, John Wiley, New York, 1983, pp. 267–271.

11 Fray, P.J., Dunnett, S.B., Iversen, S.D., Björklund, A. and Stenevi, U., Nigral transplants reinnervating the dopamine-depleted neostriatum can sustain intracranial self-stimulation, *Science*, 219 (1983) 416–419.

12 Freed, W.J., Morishisa, J.M., Spoor, E., Hoffer, B.J., Olson, L., Seiger, A. and Wyatt, R.J., Transplanted adrenal chromaffin cells in the rat brain reduce lesion-induced rotational behavior, *Nature (London)*, 292 (1981) 351–352.

13 Friedman, M.I. and Stricker, E.M., The physiological psychology of hunger: a physiological perspective, *Psychol. Rev.*, 83 (1976) 409–431.

14 Gash, D., Sladek, J.R. and Sladek, C.D., Functional development of grafted vasopressin neurons, *Science*, 210 (1980) 1367–1369.

15 Gibson, M.J., Krieger, D.T., Charlton, H.M., Zimmerman, E.A., Silverman, A.-J. and Perlow, M.J., Mating and pregnancy can occur in genetically hypogonadal mice with preoptic area brain grafts, *Science*, 225 (1984) 949–951.

16 Grossman, S.P., Contemporary problems concerning our understanding of brain mechanisms that regulate food intake and body weight. In A.J. Stunkard and E. Stellar (Eds.), *Eating and Its Disorders*, Raven, New York, 1984, pp. 5–13.

17 Han, P.W., Energy metabolism of tube-fed hypophysectomized rats bearing hypothalamic lesions, *Am. J. Physiol.*, 215 (1968) 1343–1350.

18 Han, P.W. and Frohman, L.A., Hyperinsulinemia in tube-fed hypophysectomized rats bearing hypothalamic lesions, *Am. J. Physiol.*, 219 (1970) 1632–1636.

19 Hetherington, A.W. and Ranson, S.W., Hypothalamic lesions and adiposity in the rat, *Anat. Rec.*, 78 (1940) 149–172.

20 Hoebel, B.G., Neurotransmitters in the control of feeding and its rewards: monoamines, opiates, and brain-gut peptides. In A.J. Stunkard and E. Stellar (Eds.), *Eating and Its Disorders*, Raven, New York, 1984, pp. 15–35.

21 Honma, S. and Honma, K., SCN independent rhythms in the circadian domain appeared in rats treated with methamphetamine, *Proceedings of the U.S.–Japan Conference on Biological Rhythms*, Honolulu, HI, July 30–August 2, 1986.

22 Kesslak, J.P., Nieto-Sampedro, M., Globus, J. and Cotman, C.W., Transplants of purified astrocytes promote behavioral recovery after frontal cortex ablation, *Exp. Neurol.*, 92 (1986) 377–390.

23 King, B.M. and Frohman, L.A., The role of vagally-mediated hyperinsulinemia in hypothalamic obesity, *Neurosci. Biobehav. Rev.*, 6 (1982) 205–214.

24 King, B.M., Smith, R.L. and Frohman, L.A., Hyperinsulinemia in rats with ventromedial hypothalamic lesions: role of hyperphagia, *Behav. Neurosci.*, 98 (1984) 152–155.

25 Labbe, R., Firl, A., Mufson, E.J. and Stein, D.G., Fetal brain transplants: reduction of cognitive deficits in rats with frontal cortex lesions, *Science*, 221 (1983) 470–472.

26 Paxinos, G. and Watson, C., *The Rat Brain in Stereotaxic Coordinates*, Academic, New York, 1982, Figs. 18–21.

27 Perlow, M.J., Freed, W.J., Hoffer, B.J., Seiger, A., Olson, L. and Wyatt, R.J., Brain grafts reduce motor abnormalities produced by destruction of the nigrostriatal dopamine system, *Science*, 204 (1979) 643–647.

28 Putten, L.M. van, van Bekkum, D.W. and Querido, A., Influence of hypothalamic lesions producing hyperphagia, and of feeding regimens on carcass composition in the rat, *Metabolism*, 4 (1955) 68–74.

29 Reier, P.J., Perlow, M.J. and Guth, L., Development of embryonic spinal cord transplants in the rat, *Dev. Brain Res.*, 10 (1983) 201–219.

30 Reier, P.J., Bregman, B.S. and Wujek, J.R., Intraspinal transplantation of embryonic spinal cord tissue in neonatal and adult rats, *J. Comp. Neurol.*, 247 (1986) 275–296.

31 Rogers, J., Hoffman, G.E., Zornetzer, S.F. and Vale, W.W., Hypothalamic grafts and neuroendocrine cascade theories of aging. Immunocytochemical viability of preoptic hypothalamic transplants from fetal to reproductively senescent female rats. In J.R. Sladek and D.M. Gash (Eds.), *Neural Transplants — Development and Function*, Plenum, New York, 1984, pp. 205–222.

32 Scott, D.E. and Sherman, D.M., Neuronal and neurovascular integration following transplantation of the fetal hypothalamus into the third cerebral ventricle of adult Brattleboro rats, *Brain Res. Bull.*, 12 (1984) 453–467.

33 Sladek, J.R. and Gash, D.M., *Neural Transplants — Devel-*

opment and Function, Plenum, New York, 1984.
34 Sladek, J.R. and Gash, D.M., Morphological and functional properties of transplanted vasopressin neurons. In J.R. Sladek and D.M. Gash (Eds.), *Neural Transplants — Development and Function*, Plenum, New York, 1984, pp. 243–282.
35 Slattery, J.M. and Potter, R.M., Hyperphagia: a necessary precondition to obesity?, *Appetite*, 6 (1985) 133–142.
36 Smith, G.M., Miller, R.H. and Silver, J., Changing role of forebrain astrocytes during development, regenerative failure, and induced regeneration upon transplantation, *J. Comp. Neurol.*, 251 (1986) 23–43.
37 Stricker, E.M., Brain neurochemistry and the control of food intake. In E. Satinoff and P. Teitelbaum (Eds.), *Handbook of Behavioral Neurobiology, Vol. 6, Motivation*, Plenum, New York, 1983, pp. 329–366.
38 Stein, D.G., Labbe, R., Attella, M.J. and Rakowsky, H.A., Fetal brain tissue transplants reduce visual deficits in adult rats with bilateral lesions of the occipital cortex, *Behav. Neural Biol.*, 44 (1985) 266–277.
39 Stenevi, U., Kromer, L.F., Gage, F.H. and Björklund, A., Solid neural grafts in intracerebral transplantation cavities. In A. Björklund and U. Stenevi (Eds.), *Neural Grafting in the Mammallian CNS*, Elsevier, Amsterdam, 1985, pp. 41–49.
40 Teitelbaum, P., Sensory control of hypothalamic hyperphagia, *J. Comp. Physiol. Psychol.*, 48 (1955) 156–163.
41 Tulipan, N., Huang, S., Whetsell, W.O. and Allen, G.S., Neonatal striatal grafts prevent lethal syndrome produced by bilateral intrastriatal injection of kainic acid, *Brain Research*, 277 (1986) 163–167.
42 Winer, B.J., *Statistical Principles in Experimental Design*, McGraw-Hill, New York, 1971, pp. 149–257, 514–599.
43 Williams, M.A., *Autoradiography and Immunocytochemistry*, North-Holland, Amsterdam, 1977, pp. 77–155.

Exp. Hematol. 14:904–911 (1986)

Experimental Hematology

The Rhesus Monkey: a Primate Model for Hemopoietic Stem Cell Studies

Rod L. Monroy, Thomas J. MacVittie, John H. Darden, Gretchen N. Schwartz, and Myra L. Patchen
Department of Experimental Hematology, Armed Forces Radiobiology Research Institute, Bethesda, Maryland, USA
(Received 3 September 1985; in revised form 22 April 1986; accepted 30 April 1986)

Abstract. Two heterogeneous cell populations (CP 1–7 and CP 8–10) were separated from rhesus monkey bone marrow using counterflow centrifugation–elutriation (CCE). These two cell populations were distinct with respect to morphological composition, expression of cell surface antigens, hemopoietic progenitor cell activity, and concentration of hemopoietic stem cells (HSC). The hemopoietic progenitor cell activity and HSC were concentrated in CP 8–10. In autologous transplantation studies, CP 8–10 reconstituted the lymphohemopoietic system of lethally irradiated monkeys in a manner similar to that of monkeys transplanted with unfractionated bone marrow cells. CP 1–7 was lymphocyte rich and depleted of progenitor cell activity. Transplantation of CP 1–7 led to eventual lymphohemopoietic reconstitution of irradiated monkeys; however, complete engraftment was delayed by as much as 14 days compared to either the transplantation of CP 8–10 or to unfractionated bone marrow. Thus, a presence of the HSC in the lymphocyte-rich progenitor-cell-depleted population can be detected in the rhesus model.

Key words: Counterflow centrifugation–elutriation (CCE) — Hemopoietic stem cell (HSC) — Rhesus monkey — Hemopoietic progenitor cells

A variety of hemopoietic studies have been pursued in nonhuman primates in an attempt to find a valuable nonhuman model. Several hemopoietic cell-separation techniques have been applied to the bone marrow of the rhesus monkey (*Macaca mulatta*), and results have been compared to those obtained using human bone marrow. Moore et al. [1] used two albumin gradient-density centrifugation steps to obtain a cell population enriched in progenitor cells for granulocyte–macrophage (CFU-c). Rhesus and human bone marrow CFU-c were isolated and enriched in the same light-density region of the gradient. In a further study using albumin gradient centrifugation, the enriched CFU-c fraction from rhesus monkey was evaluated in allogeneic bone marrow transplantations in order to prevent graft-versus-host disease [2]. The transplantation of this bone marrow fraction, however, resulted in a low proportion of bone marrow engraftment.

Another method of bone marrow separation in both nonhuman primates and humans used the lectin, soybean agglutinin, in which the nonagglutinated (or negative) fraction in both species was shown to be enriched in CFU-c activity [3]. The nonagglutinated human marrow fraction was evaluated successfully in clinical allogeneic bone marrow transplantations [4]. A correlation suggests that the hemopoietic stem cell (HSC) would also be found in the nonagglutinated marrow fraction of primates; in fact, a preliminary report supports these findings [5].

Jemionek et al. [6] separated human and rhesus monkey bone marrow using counterflow centrifugation–elutriation (CCE) equipped with a continuous albumin gradient. The elutriation activity profiles for the granulocyte–macrophage colony-forming cell (GM-CFC) was shown to be similar for both rhesus monkey and human bone marrows. Additional studies using CCE separated human bone marrow cells into a population enriched in myeloid progenitor cell activity [7, 8]. This enriched myeloid progenitor cell population showed a similarity to the enriched GM-CFC marrow cells separated from rhesus monkey and human marrow by Jemionek et al. [6]. Based on these reports, there appears to be a relationship between the elutriation position of both rhesus monkey and human marrow GM-CFC activity.

Although bone marrow cell separation techniques and isolated progenitor cell activities in nonhuman primates and humans have been compared, an extension of this comparison to include func-

The views presented in this paper are those of the authors; no endorsement by the Defense Nuclear Agency has been given or should be inferred.

Address reprint requests to: Dr. R.L. Monroy, Department of Experimental Hematology, Armed Forces Radiobiology Research Institute, Bethesda, MD 20814-5145, USA.

tional hemopoeitic reconstitution in vivo has not been reported. The studies presented in this paper use the rhesus monkey to study HSC physiology in the hope that information obtained from this model might be extrapolated to the human. The objective was to use CCE to rapidly separate various bone marrow cell populations. The separated cell populations were identified morphologically, evaluated against antihuman monoclonal antibodies, and cultured in vitro for progenitor cell activity. In addition, the pluripotent HSC content of these cell populations was assayed by testing for their ability to reconstitute the lymphohemopoeitic systems in an autologous bone marrow transplantation model.

Materials and methods

Monkeys

Normal male rhesus monkeys, *Macaca mulatta*, weighing 6–9 kg and born and raised in the USA, were used. All technical manipulations of the animals were performed with the monkeys under anesthesia (ketamine, 10 mg/kg, i.m.). Monkeys undergoing bone marrow aspirations or used as plateletpheresis donors were further anesthetized with Biotal (4% sodium thiamylal, 10 mg/kg; Bioceutic Labs, St. Joseph, Missouri). All monkeys were under the care and supervision of the veterinary staff, and research was conducted according to the principles enunciated in the "Guide for the Care and Use of Laboratory Animals," prepared by the Institute of Laboratory Animal Resources, National Research Council.

Bone marrow aspirations

Both iliac crest areas were shaved and prepared aseptically, and marrow was collected from the posterior horn of the iliac crest with multiple aspirations, using an 18-gauge Rosenthal needle (Becton-Dickinson, Mountain View, California) and a 10-cm^3 syringe with preservative-free heparin (500 U). Enough bone marrow was aspirated to yield between 300 and 600 × 10^6 cells. Aspirated bone marrow was washed twice with Hanks' balanced salt solution minus calcium and magnesium (HBSS−), resuspended to twice the original volume with HBSS−, and then centrifuged (400 *g* for 30 min) over a layer of lymphocyte separation medium (Litton Bionetics, Rockville, Maryland). All cells above the red blood cell pellet were recovered, washed twice with HBSS−, and resuspended in 40 ml of elutriation medium. This sample was identified as the *pre* sample. Bone marrow cells used in in vitro studies were also obtained by flushing cells from rib sections obtained from healthy donors killed for organ procurement (Flow Labs, McLean, Virginia).

Counterflow centrifugation–elutriation (CCE)

The study was divided into two phases. The first involved determining the elutriation position of specific cell populations and in vitro culture activities of the hemopoietic progenitor cells. The second phase used an abbreviated elutriation procedure to separate the marrow into two cell populations.

CCE was performed as described by Jemionek et al. [17] with the following modifications: The initial parameters for the run were a centrifuge speed of 2000 rpm, a temperature of 18°C, and a flow rate of 7.5 ml/min. Marrow *pre* sample cells were first allowed to enter the chamber, and then were separated by increasing the flow rate in a sequence defined by the curve in Figure 1. A total of 16 40-ml fractions were collected. After the 14th fraction, the centrifuge was turned off while the flow rate was held constant. The cells from each fraction were collected by centrifugation. Fractions 15 and 16 were pooled as the rotor-off fraction.

In the second phase of the CCE studies, the elutriation run was abbreviated. The flow rates for the first eight fractions were the same as in phase 1; then the centrifuge was turned off at fraction 9, collecting through fraction 10. Fractions were centrifuged, cells resuspended, and fractions 1–7 and 8–10 were pooled, respectively.

Cellular analysis

Cell counts were determined using Coulter Counter model ZBI. Cytospin cell preparations were made for each elutriation bone marrow fraction and stained with Wright–Giemsa solution; 500 cell-count bone marrow differentials were made on each fraction. Hematology reports on peripheral blood samples were accomplished using Coulter Counter model S Plus II. Differentials were made on the peripheral blood smears.

Antigenic determinations

Monoclonal antibody analysis. Fluorescein conjugates of Leu 2a (suppressor/cytotoxic), Leu 3a/b (helper/inducer), and HLA-DR (Becton-Dickinson) were used for analyses of peripheral blood and bone marrow cells. Procedures used for cellular preparations and monoclonal labeling have been described by Hale and McCarthy [9]. Analyses of the samples were performed on either the FACS analyzer or on the FACS II system.

Sheep red blood cell E-rosette analysis. The preparation of neuraminidase-treated sheep red blood cells (S-RBC) and the procedure for E-rosette analysis were as described by Weiner et al. [10]. After the cold incubation, the cell pellet was gently disrupted, and positive cell counts were made using a hemocytometer. The criterion for an E-rosette-positive cell was that it have four or more S-RBC attached to it.

In vitro culture progenitor cell analysis

GM-CFC and CFU-MK culture techniques. The double-layer, soft agar culture technique was used to assay for both GM-CFC and CFU-MK (megakaryocyte progenitors) [11]. Colony-stimulating activity (CSA) was added to the lower agar layer. The source of CSA for GM-CFC was giant-cell-tumor-conditioned medium (GCTCM) (Gibco, Grand Island, New York) used at 10% (vol/vol). CFU-MK expression required GCTCM (7% vol/vol) plus human spleen-conditioned medium (HUSCM) (7% vol/vol) and normal human plasma (5% vol/vol). HUSCM was prepared using the technique described in Ref. [12]. Cultures were incubated at 37°C in an atmosphere of humidified air containing 5% CO_2. GM-CFC-derived colonies (>50 cells) were counted on day 10 of culture. CFU-MK cultures were incubated for 10–12 days. After this, the upper agar layer was fixed and dried. CFU-MK colonies (>50 cells) were enumerated after staining with Wright-Giemsa solution.

CFU-e, BFU-e, and CFU-mix culture techniques. Erythroid burst-forming units (BFU-e), erythroid colony-forming units (CFU-e), and mixed cell colony-forming units (CFU-mix) were determined using a plasma clot culture system described in detail by Weinberg et al. [13] Bone marrow cells (5×10^5 cells/ml) were plated as 0.1-ml clots for CFU-e and BFU-e. Cells ($2.5–5.0 \times 10^5$ cells/ml) were plated as 0.4-ml clots for CFU-mix. Anemic sheep *plasma, step III erythropoietin* (Connaught Labs), was added to culture media for CFU-e (0.5 U/ml), BFU-e (2.0 U/ml) and CFU-mix (1.0 U/ml). Lymphocyte-conditioned medium, 5% (vol/vol), was added to the culture media for CFU-mix. Lymphocyte-conditioned medium was prepared as described by Ash et al. [14], except that a pool of three rhesus monkey peripheral blood mononuclear cells was used as the lymphocyte source. Plasma-clot cultures were harvested on day 4 for CFU-e, on days 8–9 for BFU-e, and on days 11–14 for CFU-mix. Clots were fixed, stained, and evaluated as described previously [14–16].

Transplantation

Monkeys, recipients of autologous bone marrow transplantation, had their bone marrow removed and recovered from anesthesia before being irradiated. They were placed in a Plexiglas chair for irradiation, and exposed bilaterally, using two equivalent cobalt-60 sources. A midline tissue dose of 9.0 Gy was delivered at a dose rate of 0.1 Gy/min. Bone marrow cells were transfused intravenously through the saphenous vein within 1–2 h after irradiation exposure.

Preliminary peripheral blood samples used to establish a hematological baseline were drawn from the monkeys over a two-week period prior to irradiation. Mean irradiation control values were determined and represented 100% levels. The mean of the preirradiation peripheral blood granulocyte levels for all experimental animals was 4.12×10^6/ml ± 0.43. After irradiation and transplantation, the animals were clinically evaluated; hematological parameters were monitored, fluids administered as clinically warranted, and antibiotic treatment (gentamycin sulfate [3 mg/kg/day, i.m.]) was administered prophylactically (beginning on day 5 and continuing until the granulocyte count was maintained above 1000/mm³). Platelet concentrates irradiated with 50.0 Gy cobalt-60 were administered on days 8, 11, 14, and 17. Recovery and a sustained level of the peripheral blood granulocytes and platelets were used to indicate engraftment of the transplanted bone marrow cells.

Results

Recovery of nucleated bone marrow cells

The initial objective of the phase 1 studies was to establish a rapid and reproducible physical separation technique for separating cell populations containing hemopoietic progenitor cells (GM-CFC, CFU-e, CFU-MK). Nucleated bone marrow cells, $300–600 \times 10^6$, were separated over 16 fractions, using CCE, in less than 60 min, with a cell recovery of 86.3% and a viability greater than 98%. The nucleated cell recovery profile (Fig. 1) obtained by eluting the cells from the chamber with increasing flow rates was shown to be reproducible, with only 5%–10% of the nucleated cells being recovered in any

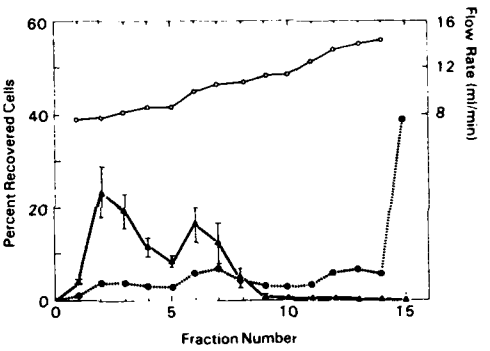

Fig. 1. Cellular elutriation characteristics of aspirated rhesus monkey bone marrow. A graphic presentation of flow rate (O) schedule used per fraction. Recovery of nucleated cells (●) per fraction expressed as percentage of total number of nucleated cells recovered. Recovery of lymphocytes (▲) per fraction expressed as percentage of total number of lymphocytes recovered.

of the fractions until fraction 15. Fraction 15 had the highest concentration of cells, and it represented the chamber contents when the rotor was turned off. In several experiments (data not shown), elutriation was continued through 20 fractions and a final flow rate of 20 ml/min, but the nucleated-cell profile was still relatively unremarkable. Thus, the existing 16-fraction procedure was followed. Morphological identification of cells in each fraction resolved the characteristic elutriation position of specific bone marrow cells. For example, lymphocytes were separated into a biphasic elutriation profile with peak cell concentrations at fractions 2 and 6 (Fig. 1). Other morphologically identifiable bone marrow cells (e.g., normoblasts, myelocytes, monocytes) also had characteristic and reproducible elutriation positions.

Recovery profiles of hemopoietic progenitor cells

Analysis of each fraction for hemopoietic progenitor cell activities (GM-CFC, CFU-e, and CFU-MK) resulted in the total-activity-recovered profiles depicted in Figure 2. The first elutriation fraction that contained any progenitor cell activity (GM-CFC and CFU-MK) was fraction 5. GM-CFC activity was recovered in every fraction after fraction 5, but in any one fraction, with the exception of fraction 15, only 1%–8% of the total activity was contributed. Fraction 15 contained 43.4% of the recovered GM-CFC activity. The CFU-MK elutriation profile was similar to that of GM-CFC, except that more of the activity (58%) was found in fraction 15. Almost all of the CFU-e activity was confined to fraction 15.

The results of the phase 1 studies led to the fol-

Table 1. Expression of cell surface antigens on rhesus monkey peripheral blood mononuclear cells and bone marrow cells

Sample	(*n*)	Leu 2A[a]	Leu 3 A/B	HLA-DR	S-RBC[b]
PB[c]	(11)	34.6 ± 2.6	33.5 ± 1.7	8.7 ± 0.9	74.6 ± 9.0
Pre	(7)	11.1 ± 3.0	11.7 ± 3.7	7.9 ± 1.3	11.7 ± 1.7
CP 1–7	(7)	18.7 ± 3.6	19.5 ± 4.5	7.8 ± 2.4	51.8 ± 4.7
CP 8–10	(7)	1.7 ± 0.5	1.9 ± 0.7	7.0 ± 2.4	2.9 ± 0.8

[a] The mean ± SEM are listed, expressed as the percentage of total population evaluated. All marrow cell data are based on aspirated marrow.

[b] E-rosette receptor with neuraminidase-treated sheep red blood cells.

[c] Peripheral blood mononuclear cells.

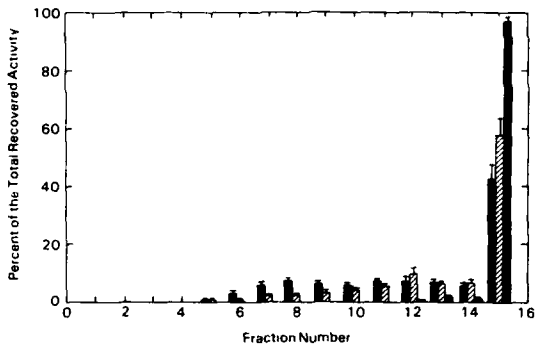

Fig. 2. Elutriation characteristics of progenitor cell activities. Recovery of progenitor cell activities (GM-CFC, ■; CFU-MK, ▨; and CFU-E, ▧) per fraction expressed as percentage of total progenitor cell activity recovered.

lowing observations: (a) more than 99% of the lymphocytes were elutriated by fraction 10, (b) the progenitor cell activity was not observed until fraction 5, and (c) specific, morphologically identifiable cell types were elutriated in a characteristic and reproducible manner. At this point, a decision was made (based on the above observations) to separate the fractioned bone marrow into two cell populations. The first cell population was enriched by lymphocytes and contained a small percentage of the progenitor cell activity. This cell population was composed of fractions 1–7 (CP 1–7). It contained 94.4% of the recovered lymphocytes, 32.9% of the recovered bone marrow cells, and only 9.9% of the recovered GM-CFC activity. The second population was composed of fractions 8–15 (CP 8–10). It contained 67.9% of the recovered bone marrow cells, 90.1% of the recovered GM-CFC activity, 96% of the recovered CFU-MK activity, all of the CFU-e activity, and only 5.6% of the recovered lymphocytes.

Phase 2: Characterization of CP 1–7 and CP 8–10

Morphology. Phase 2 studies focused on the characterization of the two populations identified in phase 1. The cellular composition of CP 1–7 contained predominantly lymphocytes (75.2%), with a smaller number of normoblasts (14.8%), monocytes (5.0%), and only a few myeloid cells (band and segmented forms). CP 1–7 did not contain blast forms of any cell lineage and no mitotic cells were observed. In contrast, CP 8–10 was predominantly composed of mature myeloid cells (69.5% band and segmented forms). The other major cell types in this cell population were normoblasts (10.6%), lymphocytes (7.8%), and monocytes (4.8%). In addition, CP 8–10 contained blast forms of all cell lineages, as well as mitotic cells.

Cell surface antigens. Cell surface antigens of cells from the peripheral blood, *pre* bone marrow, CP 1–7, and CP 8–10 bone marrow fractions are compared in Table 1. Comparisons of the cells of the *pre* marrow with those of the peripheral blood showed that approximately one-third fewer E-rosette-, Leu 2a-, and Leu 3a/b-positive cells existed in the bone marrow. By contrast, the levels of HLA-DR-positive cells in the bone marrow and in the peripheral blood were approximately equal. Comparison of the separated bone marrow cell populations, CP 1–7 and CP 8–10, showed that the cell surface antigens characteristic of lymphocytes (S-RBC E-rosette, helper–inducer, and suppressor–cytotoxic) were concentrated in CP 1–7. This was consistent with the morphological composition of CP 1–7. The HLA-positive cells were distributed equally in both populations.

Hemopoietic progenitor cell activities. Hemopoietic progenitor cell activities of CP 1–7 and CP 8–10 are presented in Table 2. The two populations exhibit quite different activities, with almost all of the hemopoietic progenitor cell activity recovered in CP 8–10. BFU-e, CFU-e, and CFU-mix activities were enriched in CP 8–10, recovering 207.5%, 128.2%, and 125.9% of the *pre* activities, respectively. The

Table 2. Progenitor cell activity recovered in isolated bone marrow populations[a]

Sample	GM-CFC (n = 8)	CFU-e (n = 9)	BFU-e (n = 6)	CFU-mix (n = 4)
Pre	100.0	100.0	100.0	100.0
CP 1-7	5.6 ± 2.5	1.7 ± 1.2	0.2 ± 0.2	3.6 ± 3.1
CP 8–10	90.3 ± 15.8	128.2 ± 56.0	207.5 ± 49.9	125.9 ± 45.2

[a] Mean ± SEM are expressed as the percentage of total preactivity recovered.

GM-CFC activity, although not enriched in CP 8–10, was also concentrated in CP 8–10.

Bone marrow transplantation. Autologous bone marrow transplantation was used as an assay for the presence of the pluripotent HSC. Two control monkeys that had been irradiated with 9.0 Gy and given therapeutic support, but not transplanted with autologous bone marrow, survived only 11 and 13 days. These monkeys did not show signs of hemopoietic recovery and had aplastic bone marrow upon necropsy. Monkeys that had been transplanted with autologous unfractioned (*pre*) bone marrow cells (cell doses of 26.1, 29.9, and 80.2 × 10^6 cells/kg) all survived. The peripheral blood granulocyte recoveries that were used to monitor bone marrow engraftment in these animals increased to at least 20% of control levels by days 16–22 after transplantation (Fig. 3). Granulocyte levels increased continuously through 100% control values before reaching a plateau and gradually returning to normal values by day 55. The remaining peripheral blood cells (platelets, lymphocytes, and monocytes) recovered to normal values by approximately day 55 after transplantation.

Two out of three monkeys survived in experiments in which monkeys were transplanted with CP 1–7. The monkey that did not survive died on day 14, did not exhibit a recovery in its peripheral blood granulocytes, and had aplastic marrow. The two surviving monkeys were transplanted with 31.4 and 37.8 × 10^6 nucleated cells/kg, whereas the monkey that died was transplanted with only 21.1 × 10^6 nucleated cells/kg. Granulocyte recoveries of the two surviving monkeys were biphasic and less rapid than those of monkeys transplanted with unfractionated marrow (Fig. 4). In fact, monkeys that had been transplanted with CP 1–7 reached the 20% control level at days 22 and 24, but then maintained a plateau level between 11% and 27% of control for the next 11 days. After days 33–35, the peripheral blood granulocytes began to recover to normal values at a rate similar to that of monkeys transplanted with unfractionated bone marrow. The other peripheral blood cells recovered to normal levels after the granulocytes had recovered.

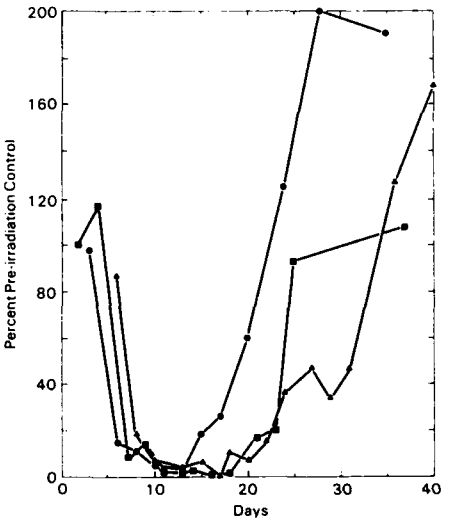

Fig. 3. Rhesus monkey peripheral blood granulocyte recovery curves after a 9.0-Gy dose of irradiation and autologous transplantation of unfractionated bone marrow. Monkeys were transplanted with 80.2 (●), 39.9 (■), and 26.6 (▲) × 10^6 nucleated cells/kg. Granulocytes are expressed as percent of preirradiation control level found in peripheral blood.

All monkeys that had been transplanted with CP 8–10 survived. The monkey that had been transplanted with the lowest number of nucleated cells (23.3 × 10^6 nucleated cells/kg) showed the slowest rate of granulocyte recovery, not reaching the 20% control level until day 27 (Fig. 5). The other two monkeys that had been transplanted with 35.5 and 25.5 × 10^6 nucleated cells/kg showed granulocyte recoveries to the 20% control point on days 20 and 18, respectively. The granulocyte recoveries of all monkeys transplanted with CP 8–10 continued to increase steadily through the 100% level. As was observed with the other transplanted monkeys, the remaining peripheral blood cells recovered to normal values after the granulocytes did so.

Discussion

Two cell populations were separated from rhesus monkey bone marrow with a rapid, gentle, and re-

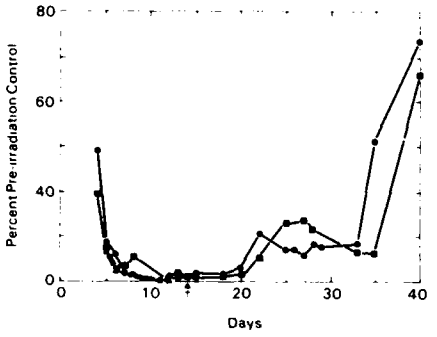

Fig. 4. Rhesus monkey peripheral blood granulocyte recovery curves after a 9.0-Gy dose of irradiation and autologous transplantation of CP 1–7. Monkeys were transplanted with 37.8 (●), 31.4 (■), and 21.1 (▲) × 10^6 nucleated cells/kg. Granulocytes are expressed as percent of preirradiation control level found in peripheral blood.

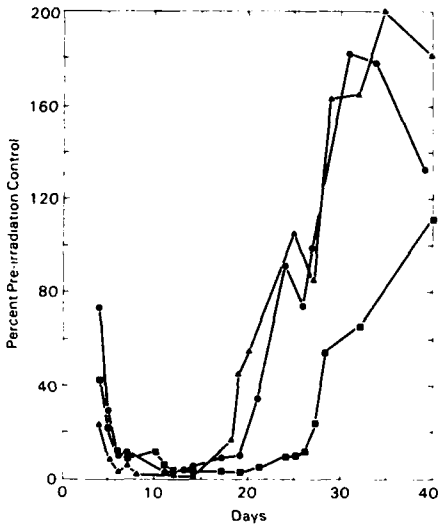

Fig. 5. Rhesus monkey peripheral blood granulocyte recovery curves after 9.0 Gy and autologous transplantation of CP 8–10. Monkeys were transplanted with 35.5 (●), 23.3 (■), and 25.0 (▲) × 10^6 nucleated cells/kg. Granulocytes are expressed as percent of preirradiation control level found in peripheral blood.

producible procedure using the technique of counterflow centrifugation–elutriation (CCE). These two cell populations, designated CP 1–7 and CP 8–10, differed in their proportions of specific cell types and of in vitro colony-forming hemopoietic progenitor cells (GM-CFC, CFU-e, BFU-e, and CFU-mix). CP 1–7 was composed primarily of lymphocytes, and contained less than 6% of the recovered hemopoietic progenitor cell activity. In contrast, CP 8–10 contained almost all the recovered hemopoietic progenitor cell activity, and was composed predominantly of myeloid cells, with only a minor lymphocyte contribution.

The potential of these two cell populations to reconstitute the hemopoeitic system of lethally irradiated autologous recipients served as an assay for the pluripotent hemopoietic stem cell (HSC). After transplantation of either CP 1–7 or CP 8–10, there was an initial increase in the recovery of peripheral-blood granulocytes in monkeys on days 20–25. However, the granulocyte levels of monkeys transplanted with CP 8–10 reached above 100% control levels before achieving a plateau. The granulocyte recovery profiles of these monkeys were similar to those obtained from monkeys transplanted with unfractionated bone marrow. In contrast, there was a biphasic recovery of granulocytes in monkeys transplanted with CP 1–7. A plateau level of 11%–27% of control values was reached and maintained for 11 days (from day 22 to day 33). On days 33–35, there was an increase in granulocytes to control levels. Thus, the transplantation of CP 1–7 led to a slower rate of complete engraftment. The eventual recovery of monkeys transplanted with CP 1–7 can be attributed to the possibility that CP 1–7 contained a small proportion of HSC. In two of the cases, there were enough stem cells to enable engraftment, although delayed. In the third monkey, there were possibly not enough HSC in the cells transplanted to enable engraftment, and death resulted. From the data, we conclude that CP 8–10 demonstrated a greater potential than CP 1–7 in restoring hemopoiesis, and therefore contained a higher concentration of the HSC. In addition, we have demonstrated, using the rhesus monkey model, that there was a good correlation between the in vitro hemopoietic progenitor cell activity and the presence of the HSC.

There appear to be differences in the elutriation position of the HSC in the various large-animal models used in hemopoietic studies. Jemionek et al. [17] isolated three fractions (I, II, and III) in the elutriation of dog bone marrow. In those studies, fraction I was the only fraction shown to have the capability to reconstitute the hemopoietic system of a lethally irradiated dog. The elutriated cell populations, CP 1–7 and CP 8–10, of rhesus marrow were similar both in morphology and progenitor cell activities to dog marrow fractions I and III, respectively. However, unlike the dog model, CP 8–10 (dog fraction III) had the greatest capability to reconstitute the hemopoietic system of a lethally irradiated monkey, while CP 1–7 (dog fraction I) had a lesser capability.

The results presented here for CP 8–10 further expand on the elutriation survey of mammalian bone marrow by Jemionek et al. [6]. In their studies, the GM-CFC activities of both monkey and human bone marrow were elutriated in the larger cell population

of predominantly myeloid cells. De Witte et al. [7], using a combination of Percoll density-gradient centrifugation and CCE, separated cells from human bone marrow that had characteristics similar to those of CP 8–10, as described in the present study. These similarities included enrichment of myeloid progenitor cell activities, composition primarily of immature myeloid cells, and only minor lymphocyte contamination. The isolated human bone marrow cells were evaluated clinically and transplanted into allogeneic bone marrow recipients (HLA-B, C, and D identical siblings). These transplanted donor cells engrafted, and there was a recovery of donor peripheral blood cells in the recipients [18]. Therefore, this separated human cell population contained the necessary HSC to lead to engraftment even in an allogeneic donor–recipient combination. CP 8–10 of the rhesus monkey bone marrow has been shown in this paper to contain a higher proportion of the recovered hemopoietic progenitor cell activity and a concentration of HSC sufficient for hemopoietic reconstitution of a lethally irradiated recipient. Thus, CP 8–10 appears to be analogous to the cell populations separated and transplanted in human transplant studies described by De Witte et al. [7, 18]. A recent report on human bone marrow by Noga et al. [8] further demonstrates the separation of lymphocytes from in vitro hemopoietic progenitor cell activity and immature myeloid cells using CCE.

These comparative reports demonstrate that the progenitor cells and the HSC of the rhesus bone marrow have physical separation characteristics similar to those of cell populations found in human marrow. In addition, the rhesus HSC was concentrated in cell populations that were similar to that of the human HSC, based on morphological and antigenic comparison. In contrast, it was also possible to demonstrate the presence of HSC in the rhesus lymphocyte-rich, progenitor-cell-depleted cell population (CP 1–7); whereas in the human situation, this type of analysis has been impossible to accomplish.

The high degree of cross-reactivity to antihuman monoclonal antibodies to the cell surface antigens on rhesus lymphoid [19–21] and hemopoietic [22, 23] cell types allows this animal to be a useful nonhuman model for the study of hemopoiesis. In the rhesus model, cellular and humoral regulatory requirements of the HSC can be evaluated in vitro concurrently with studies of humans, using available human reagents. A further advantage of the rhesus bone marrow transplantation model is that these requirements can also be evaluated in vivo. Evaluations of this type can address questions on the optimal number of particular cell populations necessary for successful engraftment in the autologous transplantation model. This, in turn, can be extended to the more complex questions associated with the allogeneic situation.

Acknowledgments

The intensive efforts and technical excellence of Carol Feser, Leon Huff, Cathy Hattenburg, and Vic Kieffer, who worked many hours caring for the monkeys, are greatly appreciated. Appreciation is also expressed to the staff of the cobalt source, the staff of the Veterinary Medicine Department, Lisa Hunt, and Gloria Contreras. Special appreciation to John Jemionek for his invaluable training.

References

1. Moore MAS, Williams N, Metcalf D (1972) Purification and characterization of the in vitro colony forming cell in monkey hemopoietic tissue. J Cell Physiol 79:283
2. Wagemaker G, Vriesendorp HM, Van Bekkum DW (1981) Successful bone marrow transplantation across major histocompatibility barriers in rhesus monkeys. Transpl Proc 13:875
3. Reisner Y, Kapoor N, O'Reilly RJ, Good RA (1980) Allogeneic bone marrow transplantation using stem cells fractionated by lectins. VI. In vitro analysis of human and monkey bone marrow cells fractionated by sheep red blood cells and soybean agglutinin. Lancet 2:1320
4. Reisner Y, Kapoor N, Kirkpatrick D, Pollack MS, Cunningham-Rundles S, Dupont B, Hodes MZ, Good RA, O'Reilly RJ (1983) Transplantation for severe combined immunodeficiency with HLA A, B, D, DR incompatible parental marrow cells fractionated by soybean agglutinin and sheep red blood cells. Blood 61:341
5. Monroy RL, Darden JH, MacVittie TJ, Patchen ML, Schwartz GN (1984) Transplantation of a hemopoietic stem cell population isolated by counterflow centrifugation elutriation from monkey bone marrow. Exp Hematol 12:384
6. Jemionek JF, MacVittie TJ, Byrne PJ, Schein PS, Walden DA (1982) Fractionation of mammalian bone marrow by counterflow centrifugation elutriation using a continuous albumin gradient: analysis of granulocyte–macrophage colony forming units. Br J Haematol 50:257
7. De Witte T, Scheltinga-Koekman E, Plas A, Blankenborg G, Salden M, Wessels J, Haanen C (1982) Enrichment of myeloid clonogenic cells by isopycnic density equilibrium centrifugation in percoll gradients and counterflow centrifugation. Stem Cells 2:308
8. Noga SJ, Donnenberg AD, Schwartz CL, Strauss LC, Civin CI, Santos GW (1986) Development of a simplified counterflow centrifugation elutriation procedure for depletion of lymphocytes from human bone marrow. Transplantation 41: 220
9. Hale ML, McCarthy KF (1984) Effects of sublethal ionizing radiation on rat peyer's patch lymphocytes. Rad Res 99:151
10. Weiner MS, Bianco C, Nussenzweiz V (1973) Enhanced binding of neuraminidase treated sheep erythrocytes to human T-lymphocytes. Blood 42:939
11. Pike BL, Robinson WA (1970) Human bone marrow colony growth in agar gel. J Cell Physiol 76:77

12. Fabin I, Douer D, Levitt L, Kletter Y, Greenberg PL (1985) Human spleen cell generation of factors stimulating human pluripotent stem cell erythroid and myeloid progenitor cell growth. Blood 65:990
13. Weinberg SR, McCarthy EG, MacVittie TJ, Baum SJ (1981) Effect of low dose irradiation on pregnant mouse hemopoiesis. Br J Haematol 48:127
14. Ash RC, Detrick RA, Zanjani ED (1981) Studies of human pluripotent hemopoietic stem cell (CFU-GEMM) in vitro. Blood 58:309
15. McLeod DL, Shreeve MM, Axelrad AA (1979) Culture systems in vitro for the assay of erythropoietic and megakaryocytic progenitors. In: Murphy MJ (ed) In vitro aspects of erythropoiesis. New York: Springer, p 31
16. Fauser AA, Messner HA (1979) Identification of megakaryocyte, macrophages, and eosinophils in colonies of human bone marrow containing neutrophilic granulocytes and erythroblasts. Blood 53:1023
17. Jemionek JF, Monroy RL, MacVittie TJ, Conteras TJ, Espy SB (1982) Bone marrow reconstitution of lethally irradiated canines using autologous bone marrow fractions obtained by counterflow centrifugation elutriation. Br J Haematol 51:585
18. De Witte T, Raymakers R, Plas A, Koekman E, Wesels H, Haanen C (1984) Bone marrow repopulation capacity after transplantation of lymphocyte depleted allogeneic bone marrow using counterflow centrifugation. Transplantation 37: 151
19. Haynes BF, Dowell BL, Hensley LL, Gore I, Metzgar RS (1982) Human T-cell antigen expression by primate T-cells. Science 215:298
20. Letvin NL, King NW, Reinherz EL, Hunt RD, Lane H, Schlossman, SF (1983) T-lymphocyte surface antigens in primates. Eur J Immunol 13:345
21. Jonker M, Goldstein G, Balner H (1983) Effects of in vivo administration of monoclonal antibodies specific for human T-cell subpopulation on the immune system in a rhesus monkey model. Transplantation 35:521
22. Letvin NL, Todd III RF, Palley LS, Schlossman SF, Griffin JD (1983) Conservation of myeloid surface antigens on primates' granulocytes. Blood 61:408
23. Pesando JM, Conrad TA (1984) Non-human primates express human leukemia associated antigens. Blood 64:1074

0022-1767/88/1401-0108$02.00/0
THE JOURNAL OF IMMUNOLOGY

Vol. 140, 108-111, No. 1, January 1, 1988
Printed in U.S.A.

INTERDEPENDENCE OF THE RADIOPROTECTIVE EFFECTS OF HUMAN RECOMBINANT INTERLEUKIN 1α, TUMOR NECROSIS FACTOR α, GRANULOCYTE COLONY-STIMULATING FACTOR, AND MURINE RECOMBINANT GRANULOCYTE-MACROPHAGE COLONY-STIMULATING FACTOR[1]

RUTH NETA,* JOOST J. OPPENHEIM,† AND SUSAN D. DOUCHES*

*From the * Department of Experimental Hematology, Armed Forces Radiobiology Research Institute, Bethesda, MD 20814; and the † Laboratory of Molecular Immunoregulation, Biological Response Modifiers Program, National Cancer Institute, Frederick, MD 21701*

Interleukin 1α (IL-1α), tumor necrosis factor α (TNFα), granulocyte-colony-stimulating factor (G-CSF), and granulocyte-macrophage colony-stimulating factor (GM-CSF) are molecularly distinct cytokines acting on separate receptors. The release of these cytokines can be concomitantly induced by the same signal and from the same cellular source, suggesting that they may cooperate. Administered alone, human recombinant (hr)IL-1α and hrTNFα protect lethally irradiated mice from death, whereas murine recombinant GM-CSF and hrG-CSF do not confer similar protection. On a dose basis, IL-1α is a more efficient radioprotector than TNFα. At optimal doses, IL-1α is a more radioprotective cytokine than TNFα in C57BL/6 and B6D2F$_1$ mice and less effective than TNFα in C3H/HeN mice, suggesting that the relative effectiveness of TNFα and IL-1α depends on the genetic makeup of the host. Administration of the two cytokines in combination results in additive radioprotection in all three strains. This suggests that the two cytokines act through different radioprotective pathways and argues against their apparent redundancy. Suboptimal, nonradioprotective doses of IL-1α also synergize with GM-CSF or G-CSF to confer optimal radioprotection, suggesting that such an interaction may be necessary for radioprotection of hemopoietic progenitor cells.

Cytokines are hormone-like polypeptides produced by the cells of the reticuloendothelial system after inflammatory stimuli. Ample evidence exists, based on their described in vivo and in vitro activities, that these molecules serve in host defenses against harmful exogenous challenges (1, 2). Ionizing radiation, originating from natural sources (cosmic rays), represents one such environmental hazard. Our previous observation that a cytokine, interleukin 1 (IL-1)[2] protects mice from radiation-induced death (3, 4) therefore is in accord with the concept of the role of cytokines in host defense and damage repair.

The degree of radioprotection obtained by treatment with IL-1 before irradiation resembles that previously reported for bacterial lipopolysaccharide (LPS) (5–7). Administration of LPS, however, results in induction and release of a number of cytokines, the most prominent of which are IL-1, tumor necrosis factor (TNF), and colony-stimulating factor (CSF) (8). The coordinate release of these cytokines suggests that they may act in concert. Pretreatment with human recombinant (hr) TNFα is also radioprotective, (9, 10). In contrast, we were previously unsuccessful in demonstrating radioprotection using murine recombinant (mr) granulocyte-macrophage (GM)-CSF alone (11). Furthermore, although in our hands hrIL-1 was radioprotective in five strains of mice, C57BL/6, BALB/c, DBA/1, B6D2F$_1$, and CDF$_1$, its radioprotective effect in C3H/HeN mice was minimal (12). It is possible that in the latter strain other cytokines or a combination of IL-1 with other cytokines may be more effective in radioprotection.

To evaluate the above possibilities, we have investigated the radioprotective effect of combinations of hrIL-1α and TNFα, as well as hrIL-1α and mr GM-CSF or hr granulocyte (G)-CSF. These studies were performed using C57BL/6 and B6D2F$_1$ mice, which are high responders to radioprotection with IL-1α, and C3H/HeN mice, and low responders to IL-1-mediated radioprotection.

We now report that combinations of optimally radioprotective doses of IL-1α and TNFα result in additive radioprotection in both high and low responder mice. Suboptimal doses of IL-1α in combinations with nonprotective doses of GM-CSF or G-CSF result in synergistic protection from radiation-induced death.

MATERIALS AND METHODS

Mice. C57BL/6 and B6D2F$_1$ inbred mice were obtained from The Jackson Laboratory, Bar Harbor, ME. C3H/HeN mice were purchased from Animal Genetics and Production Branch, National Cancer Institute, Frederick, MD. The mice were housed in the Veterinary Department Facility at the Armed Forces Radiobiology Research Institute in cages with Micro-Isolation unit tops, 10 mice/cage. Fe-

Received for publication July 23, 1987.
Accepted for publication October 1, 1987.
The costs of publication of this article were defrayed in part by the payment of page charges. This article must therefore be hereby marked *advertisement* in accordance with 18 U.S.C. Section 1734 solely to indicate this fact.

[1] This work was supported by the Armed Forces Radiobiology Research Institute, Defense Nuclear Agency, under Research Work Unit MJB3148. The opinions or assertions contained herein are the private views of the authors; no endorsement by the Defense Nuclear Energy has been given or should be inferred. The research was conducted according to principles enunciated in the "Guide for the Care and Use of Laboratory Animals" prepared by the Institute of Laboratory Animal Resources, National Research Council.

[2] Abbreviations used in this paper: IL-1, interleukin 1; CSF, colony-stimulating factor; G-CSF, granulocyte colony-stimulating factor; GM-CSF, granulocyte-macrophage colony-stimulating factor; hr, human recombinant; LPS, bacterial lipopolysaccharide; mr, murine recombinant; TNF, tumor necrosis factor.

male mice 8 to 12 wk of age were used for all experiments. Standard laboratory chow and HCl-acidified water (pH 2.4) were given ad libitum. All cage-cleaning procedures and injections were carried out in a laminar flow unit.

Cytokines. The hrIL-1α was generously provided by Immunex and Hoffmann-La Roche, Nutley, NJ. The preparations were supplied in phosphate-buffered saline, pH 7.2, and 30 mM Tris-HCl, 400 mM NaCl, pH 7.8, respectively, and used on weight basis. The hrTNFα, lot CP4026POB, specific activity 9.6×10^8 U/mg in phosphate-buffered saline, was a generous gift from Biogen Research Corp., Cambridge, MA. The mrGM-CSF was provided by Immunex as a lyophilized powder with sucrose as a stabilizing agent. The hrG-CSF was a gift from Amgen, Biochemicals, Thousand Oaks, CA. Protein-free phenol-water-extracted endotoxin derived from *Escherichia coli* K235 (LPS) was obtained from Dr. S. N. Vogel, Department of Microbiology, Uniformed Services University of the Health Sciences. All reagents were diluted to the desired concentration in pyrogen-free saline just before i.p. injection of 0.5 ml/mouse. All cytokine preparations were assayed for LPS contamination in a LAL assay and determined to contain less than 0.1 ng/inoculum.

Irradiation. Mice were placed in Plexiglas containers and were given whole body irradiation at 40 rad/min by bilaterally positioned cobalt-60 elements. Mice survival was recorded daily for 30 days.

Statistical analysis. Two survival proportions were compared using a 2×2 contingency table analysis (χ^2). A survival proportion was compared with the sum of two others by assuming that survival has an exponential distribution, i.e., $\exp(-t/\lambda)$. If two survival mechanisms act independently, their mean survival was assumed to add. The survival proportion of the combined mechanism was then compared with the predicted survival proportion of the exponential sum.

RESULTS

Comparison of the radioprotective effects of hrIL-1α and hrTNFα. The effect of increasing doses of hrIL-1α and hrTNFα on the survival of $LD_{100/30}$-irradiated C57BL/6 and $LD_{95/30}$-irradiated B6D2F$_1$ mice, both high responders to radioprotection with IL-1α, was compared. C57BL/6 mice were protected with doses of IL-1α ranging from 100 to 1000 ng (Fig. 1*A*) (doses of 50 ng did not confer significant radioprotective effect; data not shown). Doses of IL-1α ranging from 75 to 1000 ng were similarly radioprotective for B6D2F$_1$ mice (Fig. 1*B*). Equivalent doses of TNFα had no radioprotective effect for these two strains. However, significant radioprotection in these two strains was obtained using 5- to 10-μg doses of TNFα (Fig. 1*A* and *B*). The maximal degree of radioprotection achieved with higher doses of TNFα, however, was less than that observed in both strains with lower doses of IL-1α ($p < 0.001$). Therefore, human TNFα is a less effective radioprotector than human IL-1α in the above two strains.

In our previous studies, C3H/HeN mice were less responsive to the radioprotective effect of IL-1α than C57BL/6, DBA/1 (12), as well as CDF$_1$ or BALB/c mice (R. Neta, unpublished observations). A comparison of the radioprotective effect of IL-1α and TNFα in this mouse strain showed that 5.0- to 7.5-μg doses of TNFα conferred greater protection ($p < 0.05$) than 150- to 500-ng doses of IL-1α (Fig. 1*C*). Therefore, in contrast with C57BL/6 and B6D2F$_1$ mice, TNFα is more radioprotective than IL-1α in C3H/HeN mice. However, TNFα is equally protective in all three strains (Fig. 1*A* to *C*). In doses of 0.2 μg/mouse, mrTNF did not confer protection, 0.5 μg/mouse protected 20%, 1 to 2 μg/mouse 30%, and 5 μg/mouse 40% of mice (n = 10 to 18 mice/group).

The radioprotective effects of the combinations of IL-1α and TNFα. The divergence of the effect of TNFα and IL-1α suggested that they may act differently. It was, therefore, of interest to determine the interactions of these two cytokines in radioprotection. The effect of combinations of IL-1α and TNFα in C57BL/6 mice was additive, as determined from the dose reductor factor (DRF) values (Fig. 2). The DRF were calculated from the ratio of $LD_{50/30}$ of IL-1 treated to control mice. Similarly, combinations of optimal doses of the two cytokines had an additive radioprotective effect ($p < 0.01$) in lethally irradiated B6D2F$_1$ mice (Table I). The radioprotective effect of IL-1α and TNFα in combination was greater in this strain than the radioprotection achieved with optimal doses of LPS ($p < 0.01$), suggesting that combinations of cytokines may be more effective radioprotectants than immunomodulatory substances that induce cytokine release.

Combinations of TNFα and IL-1α also had additive effects in low responder C3H/HeN mice at optimal doses

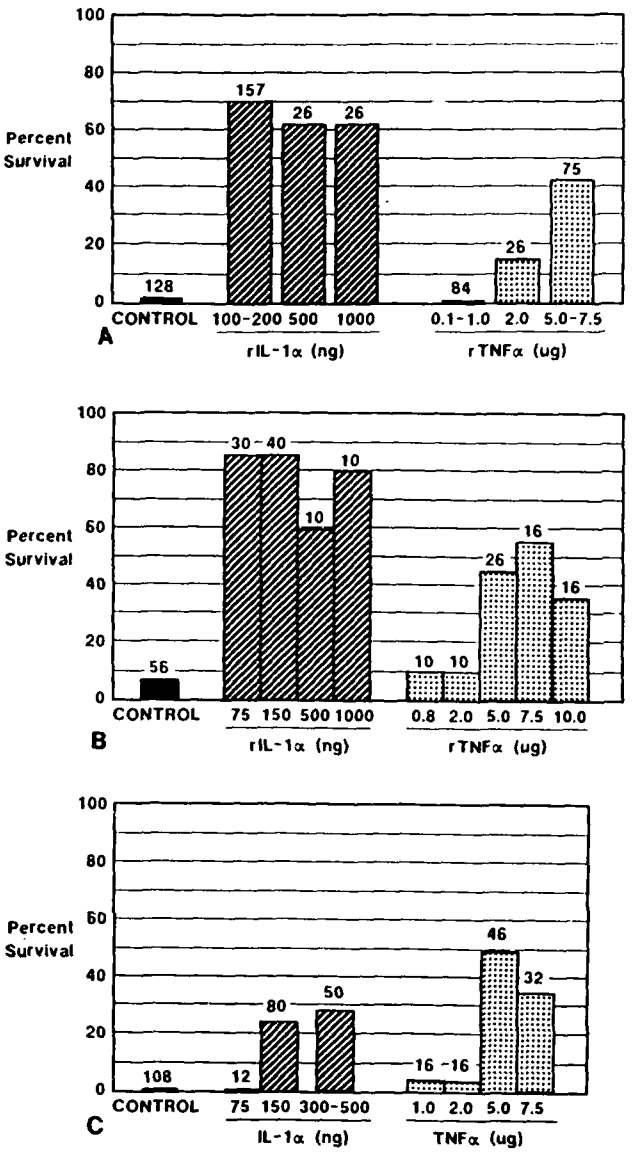

Figure 1. Protective effect of hrTNFα and hrIL-1α in lethally irradiated mice. C57BL/6 (*A*), B6D2F$_1$ (*B*), or C3H/HeN (*C*) mice, 8 to 12 wk old, received i.p. 0.5 ml saline (control) or recombinant cytokines in doses as indicated, 20 hr before whole body irradiation. The radiation doses were 950 rad ($LD_{100/30}$) for C57BL/6 (*A*), 1050 rad ($LD_{95/30}$) for B6D2F$_1$ (*B*), 850 ($LD_{100/30}$ for 8 to 9 wk old), and 900 rad ($LD_{100/30}$ for 10 to 12 wk old) C3H/HeN mice (*C*). The numbers at the top of the bars represent the total number of mice receiving each treatment. TNFα was more radioprotective than IL-1α in C3H/HeN mice ($p < 0.05$) (*C*). TNFα was less radioprotective than IL-1α in C57BL/6 and B6D2F$_1$ mice ($p < 0.001$) (*A*, *B*).

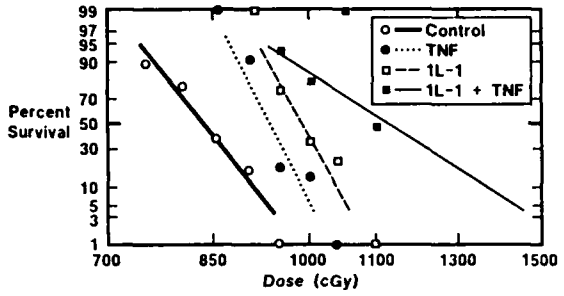

Figure 2. Radioprotective effect on hrTNFα and hrIL-1α, by themselves and in combination, in C57BL/6 mice exposed to increasing doses of radiation. C57BL/6, 8- to 12-wk-old mice, received 5 μg/mouse of hrTNFα, 150 ng/mouse of hrIL-1α, alone or in combination. Each experimental point represents 12 to 70 mice. DRF were calculated from the ratio of $LD_{50/30}$ of treated vs control mice, using probit analysis and were 1.12 (1.08, 1.16) for TNFα; 1.19 (1.16, 1.21) for IL-1α; and 1.38 (1.24, 1.54) for IL-1α + TNFα. The numbers in brackets are 95% confidence limits. Treatment with IL-1α was significantly more radioprotective than treatment with TNFα at 950 rad ($p < 0.001$) and 1000 rad ($p < 0.05$). The effect of combined treatment with IL-1α and TNFα was significantly greater than the sum of effects of treatment with IL-1α or TNFα alone at radiation doses above 1000 rad ($p < 0.01$).

TABLE I

Radioprotection of B6D2F$_1$ mice with rIL-1α, rTNFα, by themselves, and in combination[a]

Treatment	Radiation Dose			
	1050		1150	
	Dead/Total	% Survival	Dead/Total	% Survival
IL-1α				
100 ng	6/22	73	16/22	26
TNFα				
5 μg	12/22	46	21/22	6
IL-1α + TNFα				
100 ng + 5 μg	0/22	100	4/22	82
LPS				
12 μg	3/22	86	14/22	36
Saline	19/22	14	22/22	0

[a] Mice were treated as described in Figure 1. The percentage of survival of mice given 1050 or 1150 rad after treatment with IL-1α was greater than that after treatment with TNFα ($p < 0.05$). IL-1α and TNFα in combination conferred significantly greater protection than the sum of radioprotection with IL-1α and TNFα alone ($p < 0.01$) and also greater than radioprotection with optimal doses of LPS ($p < 0.01$).

TABLE II

Radioprotection of C3H/HeN mice with hrIL-1α or hrTNFα alone and in combination[a]

Treatment	Dead/Total	% Survival
Saline	175/180	2.5
IL-1α		
100 to 200 ng	78/91	15
300 to 500 ng	48/64	25
TNFα		
1.0 to 2.0 μg	32/34	6
5.0 to 7.5 μg	51/88	42
IL-1α + TNFα		
100 ng + 2.0 μg	7/16	55
200 ng + 7.5 μg	6/50	88

[a] C3H/HeN mice were treated as described in Figure 1. TNFα in doses of 5 to 7.5 μg/mouse protected significantly greater numbers of mice than treatment with 150 to 500 ng of IL-1α alone ($p < 0.05$). Treatment with IL-1α and TNFα in combination was significantly more radioprotective than the sum of the radioprotective effects of IL-1α and TNFα administered alone ($p < 0.05$).

of cytokines ($p < 0.01$) (Table II).

The effects of combinations of IL-1α with GM-CSF or G-CSF. The radioprotective effect of IL-1 occurs at radiation dose ranges that suppress hemopoiesis. It has been proposed, therefore, that the effect of IL-1 may be mediated by CSF. However, i.p. administration of GM-CSF 20 hr before irradiation in doses ranging from 1 to 10 μg/mouse had no significant protective effect against lethal doses of radiation (11). To examine further whether GM-CSF contributes to radioprotection, suboptimal doses of IL-1α were administered in combination with GM-CSF or G-CSF. Combinations of these cytokines greatly enhanced the survival of mice in comparison to the effect of each cytokine alone ($p < 0.01$) (Table III). The effect of treatment with combinations of suboptimal doses of IL-1α and GM-CSF or G-CSF equaled that achieved with optimal doses of IL-1α. This effect, however, did not extend to supralethal doses of radiation (Table III).

DISCUSSION

Inflammatory signals induce the release of various cytokines with distinct, as well as overlapping, biologic activities. IL-1α and TNFα represent two such cytokines, which are induced and released by macrophages after the same inflammatory stimulus (LPS as an example) and which also share a number of similar biologic properties, such as induction of fever (13, 14), acute phase proteins (15, 16), or CSF (17–19). Therefore, despite their differing molecular structure and their action on separate receptors, they exhibit apparent redundancy. Our results showing that the two cytokines differ in the extent of their radioprotective effect, that their relative effectiveness may vary depending on the genetic makeup of the host, and that their combined activity is additive independent of the genetic makeup argue against the apparent redundancy of these agents in this context. Higher quantities of TNFα than of IL-1α were required in all strains of mice to confer optimal radioprotection. Although most of these studies utilized hrTNFα, murine TNFα in C3H/HeN mice was also required in doses higher than IL-1 to achieve significant radioprotection.

The radioprotection achieved with optimal doses of IL-1α was greater than that with optimal doses of TNFα in C57BL/6 and B6D2F$_1$ mice, but this situation was reversed in C3H/HeN mice. TNFα, however, was equally protective in all three strains. Although we do not know the basis for the differences in protection of these inbred strains of mice, this observation suggests that different cytokines may achieve similar effects in genetically disparate individuals.

The additive effect of IL-1α and TNFα in radioprotection, independent of genetic makeup or of the dose, sug-

TABLE III

Radioprotection of B6D2F$_1$ mice with combinations of rCSF and rIL-1α[a]

Treatment	Radiation Dose			
	1050		1150	
	Dead/Total	% Survival	Dead/Total	% Survival
IL-1α				
100 ng	9/32	69	16/22	26
33 ng	34/42	19	20/22	9
GM-CSF				
1 μg	35/42	17	22/22	0
G-CSF				
1 μg	8/10	20	ND	
GM-CSF				
1 μg + IL-1α 33 ng	14/42	67	20/22	9
G-CSF				
1 μg + IL-1α 33 ng	3/10	70	ND	
Saline	35/42	17	22/22	0

[a] Mice were treated as described in Figure 1. The radioprotective effect of 33 ng IL-1α or 1 μg of GM-CSF or G-CSF did not differ significantly from treatment with saline. The effects of IL-1α and GM-CSF or IL-1α and G-CSF in combination in mice treated with 1050 rad differed significantly from controls ($p < 0.01$). ND, not determined.

gests that the two cytokines employ different radioprotective pathways. Although the mechanism of action to achieve radioprotection remains unknown, a number of the activities of IL-1α and TNFα may be related to the radioprotective effect. For example, induction of acute phase proteins, some of which (metallothionein and ceruloplasmin) have the capacity to scavenge free radicals (20–23) and other acute phase proteins, may contribute to radioprotection. Although IL-1α induction of bone marrow cell cycling (24) may present yet another critical event in radioprotection, TNFα is not known to have this capability. In fact, TNFα has been reported to be inhibitory to hemopoiesis (25, 26). Several reports exist, however, showing its role in hemopoietic differentiation (27–29). This differentiating effect is most pronounced in synergy with other cytokines. Whether this effect of TNFα on hemopoietic cells contributes to its radioprotective effect remains to be established.

The finding that treatment with TNFα and IL-1α in combination is more effective than treatment with optimal radioprotective doses of LPS (an inducer of the two cytokines) may be explained in two ways. Either the two cytokines are presented in more optimal doses than can be induced with LPS or toxic effect of the LPS molecule itself is circumvented by using the cytokines.

The lack of radioprotective effects of GM-CSF or G-CSF administered alone, and its synergistic effect when combined with suboptimal doses of IL-1α, indicate that these hemopoietic growth factors may be effective only when combined with IL-1α. Possibly, this synergy relates to the recently described hemopoietin-1 (HP-1) activity of IL-1α, because hemopoietin-1/IL-1 has been reported to synergize with GM-CSF in promoting growth of early hemopoietic progenitor cells (30). Furthermore, IL-1α has been shown to induce CSF in vitro as well as in vivo (17, 19). Thus administration of IL-1α generates cytokines with which IL-1α can interact to yield more pronounced biologic effects. Additional possibilities that need to be examined may involve induction by IL-1α of increased expression of CSF receptors.

In all, our observation that combinations of cytokines may be more effective than the administration of each cytokine alone serves as additional evidence that these agents act in concert and despite their apparent redundancy must all be required for normal host defenses.

Acknowledgments. We wish to thank Drs. M. Patchen and E. K. Gallin for reviewing this manuscript and Mr. W. E. Jackson for statistical analysis of the results.

REFERENCES

1. **Oppenheim, J. J., and S. Cohen,** eds. *Interleukins, Lymphokines, and Cytokines.* Academic Press, New York, 1983.
2. **Adelman, N. E., M. E. Hammond, S. Cohen, and H. F. Dvorak.** 1979. Lymphokines as inflammatory mediators. In *Biology of Lymphokines.* S. Cohen, E. Pick, and J. J. Oppenheim, eds. Academic Press, New York, p. 000.
3. **Neta, R., S. D. Douches, and J. J. Oppenheim.** 1986. Interleukin 1 is a radioprotector. *J. Immunol. 136:2483.*
4. **Neta, R., S. D. Douches, and J. J. Oppenheim.** 1987. Radioprotection by interleukin-1. In *Immune Regulation by Characterized Polypeptides.* Alan R. Liss, New York, p. 429.
5. **Mefford, R. B., D. T. Henkel, and J. B. Loeffer.** 1953. Effect of pyromen on survival of irradiated mice. *Proc. Soc. Exp. Biol. Med. 83:54.*
6. **Ainsworth, E. J., and H. B. Chase.** 1959. Effect of microbial antigens on irradiation mortality in mice. *Proc. Soc. Exp. Biol. Med. 102:483.*
7. **Smith, W. W., I. M. Alderman, and R. I. Gillespie.** 1957. Increased survival in irradiated animals treated with bacterial endotoxins. *Am. J. Physiol. 191:124.*
8. **Vogel, S. N., and M. M. Hogan.** 1987. The role of cytokines in endotoxin mediated responses. In *Immunophysiology: Role of Cells and Cytokines in Immunity and Inflammation.* J. J. Oppenheim and E. Shevach, eds. Oxford University Press, New York. *In press.*
9. **Neta, R., S. N. Vogel, J. D. Sipe, J. J. Oppenheim, P. C. Giclas, and S. D. Douches.** 1987. Comparison of the in vivo effects of recombinant IL-1 and recombinant TNF in radioprotection, induction of CSF, and of acute phase reactants. *Fed. Proc. 46:1200 (Abstr.).*
10. **Urbaschek, R., D. N. Mannel, and B. Urbaschek.** 1987. Tumor necrosis factor induced stimulation of granulopoiesis and radioprotection. *Lymphokine Res. In press.*
11. **Neta, R., S. N. Vogel, J. J. Oppenheim, and S. D. Douches.** 1986. Cytokines in radioprotection; comparison of the radioprotective effects of IL-1 to IL-2, GM-CSF, and IFN-gamma. *Lymphokine Res. 5:s105.*
12. **Neta, R., S. D. Douches, and J. J. Oppenheim.** 1986. Strain dependence of mice to radioprotective effect of IL-1. *Sixth International Congress on Immunology,* Toronto, Canada, p. 448 *(Abstr.).*
13. **Kampschmidt, R. F., and H. F. Upchurch.** 1969. Some effects of endotoxin and leukocytic pyrogen on the body temperature of rats. *Proc. Soc. Exp. Biol. Med. 131:864.*
14. **Dinarello, C. A., J. G. Cannon, S. M. Wolf, H. A. Bernheim, B. Beutler, A. Cerami, I. S. Figari, M. A. Palladino, and J. V. O'Connor.** 1986. Tumor necrosis factor (cachectin) is an endogenous pyrogen and induces production of interleukin-1. *J. Exp. Med. 163:1433.*
15. **Ramadori, G., J. D. Sipe, C. A. Dinarello, S. B. Mizel, and H. R. Colten.** 1985. Pretranslational modulation of acute phase hepatic protein synthesis by murine recombinant interleukin-1 (IL-1) and purified human IL-1. *J. Exp. Med. 162:930.*
16. **Sipe, J. D., S. N. Vogel, S. D. Douches, and R. Neta.** 1987. Tumor necrosis factor (cachectin) is a less potent inducer of serum amyloid A synthesis than interleukin-1. *Lymphokine Res. 6:93.*
17. **Zucali, J. R., C. A. Dinarello, D. J. Oblon, M. A. Grass, L. Anderson, and R. S. Weiner.** 1986. Interleukin-1 stimulates fibroblasts to produce granulocyte-macrophage colony-stimulating activity and prostaglandin E2. *J. Clin. Invest. 77:1857.*
18. **Munker, R., J. Gasson, M. Ogawa, and H. P. Koeffler.** 1986. Recombinant human TNF induces production of granulocyte-monocyte colony stimulating factor. *Nature 323:79.*
19. **Vogel, S. N., S. D. Douches, E. N. Kaufman, and R. Neta.** 1987. Induction of colony stimulating factor in vivo by recombinant interleukin-1 and tumor necrosis factor. *J. Immunol. 138: 2143.*
20. **Goldstein, I. M., and I. F. Charo.** 1983. Ceruloplasmin: an acute phase reactant and antioxidant. In *Lymphokines.* E. Pick, ed. Academic Press, New York, *8:383.*
21. **Karin, M., R. J. Imbra, A. Heguy, and G. Wong.** 1985. Interleukin-1 regulates human metallothionein gene expression. *Mol. Cell. Biol. 5:2866.*
22. **Thornalley, P. J., and M. Vajak.** 1985. Possible role for metallothionein in protection against radiation induced oxidative stress: kinetics and mechanism of its reaction with superoxide and hydroxyl radicals. *Biochim. Biophys. Acta 827:36.*
23. **Neta, R., J. J. Oppenheim, S. D. Douches, P. C. Giclas, R. I. Imbra, and M. Karin.** 1986. Radioprotection with interleukin-1: comparison with other cytokines. In *Progress in Immunology. VI.* B. Cinader and R. G. Miller, eds. Academic Press, New York, p. 900.
24. **Neta, R., M. B. Sztein, J. J. Oppenheim, S. Gillis, and S. D. Douches.** 1987. The in vivo effects of interleukin 1. I. Bone marrow cells are induced to cycle after administration of interleukin 1. *J. Immunol. 139:1861.*
25. **Peetre, C., U. Gullberg, E. Nilsson, and I. Olsson.** 1986. Effects of recombinant tumor necrosis factor on proliferation and differentiation of leukemic and normal hemopoietic cells in vitro. *J. Clin. Invest. 78:1694.*
26. **Murase, T., T. Hotta, H. Saito, and R. Ohno.** 1987. Effect of recombinant human tumor necrosis factor on the colony growth of human leukemia progenitor cells and normal hematopoietic progenitor cells. *Blood 69:467.*
27. **Trinchieri, G., M. Kobayashi, M. Rosen, R. Loudon, M. Murphy, and B. Perussia.** 1986. Tumor necrosis factor and lymphotoxin induce differentiation of human myeloid cell lines in synergy with immune interferon. *J. Exp. Med. 164:1206.*
28. **Munker, R., and P. Koeffler.** 1987. In vitro action of tumor necrosis factor on myeloid leukemic cells. *Blood 69:1102.*
29. **Takeda, K., S. Iwamoto, H. Sugimoto, T. Takuma, N. Kawatani, M. Noda, A. Masaki, H. Morise, H. Arimura, and K. Konno.** 1986. Identity of differentiation inducing factor and tumor necrosis factor. *Nature 323:338.*
30. **Moore, M. A. S., and D. J. Warren.** 1987. Synergy of interleukin-1 and granulocyte colony stimulating factor: *In vivo* stimulation of stem cell recovery and hematopoietic regeneration following 5-fluorouracil treatment of mice. *Proc. Natl. Acad. Sci. USA 84:7134.*

ARMED FORCES RADIOBIOLOGY RESEARCH INSTITUTE
SCIENTIFIC REPORT
SR87-44

RADIATION-INDUCED HEMATOLOGIC AND NONSPECIFIC IMMUNOLOGIC EFFECTS IN THE CANINE

M.L. Patchen, T.J. MacVittie, M.M. D'Alessandro

Armed Forces Radiobiology Research Institute
Bethesda, MD 20814-5145 USA

ABSTRACT

A canine model was used to assess the effects of irradiation on bone marrow progenitor cellularity, peripheral blood leukocyte and platelet cellularity, and phagocytosis-induced granulocyte oxidative burst activity. Sexually mature beagles were bilaterally exposed to 2 Gy of cobalt-60 radiation, and at various times postirradiation bone marrow and peripheral blood samples removed. Bone marrow granulocyte-macrophage progenitor cell (GM-CFC) numbers were reduced to ~10% of normal by 24 hours postexposure, and full recovery to normal GM-CFC levels was not seen until day 49 postirradiation. Peripheral blood leukocyte and platelet values were also dramatically reduced postirradiation; by day 49 postexposure, these values had recovered to only ~90% of normal. The ability of percoll-isolated peripheral blood granulocytes to mount an oxidative burst in response to opsonized zymosan also decreased following irradiation. By contrast, the ability of nonisolated peripheral blood granulocytes (i.e., granulocytes in whole blood) to mount an oxidative burst in response to opsonized zymosan increased following irradiation. When sera obtained from dogs at various times postirradiation were assayed for ability to enhance the oxidative burst capacity of normal percoll-isolated peripheral blood granulocytes, stimulatory activity was detected as early as day 2 postirradiation and persisted through day 29 postexposure. These results suggest that, although peripheral blood granulocyte numbers are decreased following radiation injury due to stem cell damage, humoral "factors" may enhance the function of the available granulocytes in irradiated animals.

INTRODUCTION

The exposure of mammals to a single whole-body dose of ionizing radiation results in a complex set of symptoms whose onset, nature, and severity are a function of both total radiation dose and radiation quality. In general, radiation injury can be classified into three syndromes which become evident at progressively higher radiation doses. The hemopoietic syndrome occurs at the lowest radiation doses (< 10 Gy). It is manifest by hemopoietic stem cell depletion and ultimately by depletion of mature hematologic and immune cells, which (whether destroyed directly by the radiation insult or lost naturally through

attrition) cannot be regenerated without hemopoietic stem cells (Broerse and MacVittie, 1984). In turn, the loss of mature functional hematologic and immune cells severely impairs antimicrobial immunity, and ultimately death can ensue due to invasive opportunistic infections (Miller, Hammond, Tompkins, 1951). The data reported here deal specifically with the hematologic and nonspecific immunologic consequences of a 2-Gy (sublethal) radiation exposure in a clinically relevant radiation model, the canine.

METHODS AND MATERIALS

Eight adult beagles were exposed to 2 Gy of bilateral total-body cobalt-60 radiation. At various times postirradiation, peripheral blood and bone marrow were obtained to assay a) peripheral blood white cell and platelet counts, b) zymosan-induced peripheral blood granulocyte oxidative burst activity (Kricka, Stanley, Thorpe, and Whitehead, 1984), c) the capacity of serum to alter normal granulocyte oxidative burst activity, and d) numbers of bone marrow granulocyte-macrophage progenitor cells (GM-CFC) (MacVittie, Monroy, Patchen, and Darden, 1984).

RESULTS

As illustrated in Figure 1, canine bone marrow GM-CFC numbers were reduced to ~10% of normal by 24 hours postirradiation and remained at this level through day 11. At day 14 postirradiation, commencement of GM-CFC recovery was evident. A 60% GM-CFC recovery was observed on day 29 postexposure; however, full GM-CFC recovery was not seen until day 49.

Peripheral blood white cell and platelet values were also reduced postirradiation (Figure 2). The nadirs of these reductions occurred on days 17 and 13, respectively, at which times leukocyte values were ~20% of normal and platelet values were ~1% of normal. By day 49 postexposure, both leukocyte and platelet values had recovered to only ~80% of normal.

In addition to the decreased numbers of peripheral blood white cells observed postirradiation, the functional capacity of percoll-separated peripheral blood granulocytes was also decreased as measured by zymosan-induced oxidative burst capacity (Figure 3). The nadir of this response occurred at day 15 postirradiation, at which time the oxidative burst response was only ~20% of normal. However, it is of interest to note that the ability of nonisolated peripheral blood granulocytes (i.e., granulocytes in whole blood) to mount a zymosan-induced oxidative burst progressively increased following radiation exposure. The peak of this response was observed 15 days postirradiation, at which time it was ~270% of normal (Figure 4).

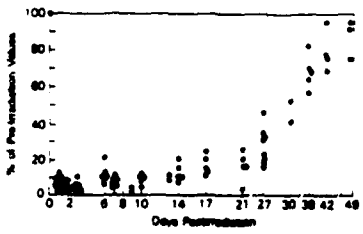

Figure 1. Effect of irradiation on bone marrow-derived GM-CFC. Bone marrow mononuclear cells were isolated by ficoll-hypaque density separation and cultured for GM-CFC using a double-layer agar system. Serum obtained from endotoxin-treated dogs was incorporated (7% v/v) into the lower agar layer as the source of colony-stimulating activity (CSA). GM-CFC colonies ($\geq$ 50 cells) were counted after 10 days of incubation at 37°C and 5% CO2.

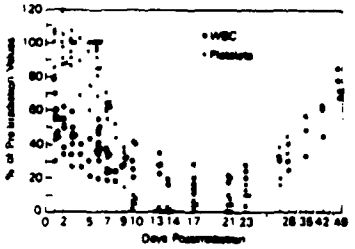

Figure 2. Effect of irradiation on peripheral white blood cell and platelet numbers. White blood cell and platelet counts were performed using a Coulter S-plus automated cell counter.

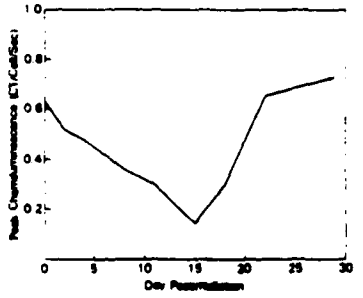

Figure 3. Effect of irradiation on the oxidative burst activity of percoll-separated peripheral blood granulocytes. Granulocytes were assayed 45 minutes for oxidative burst activity using a Picolite 6500 luminometer following stimulation with 50 ul of opsonized zymosan containing luminol (Packard).

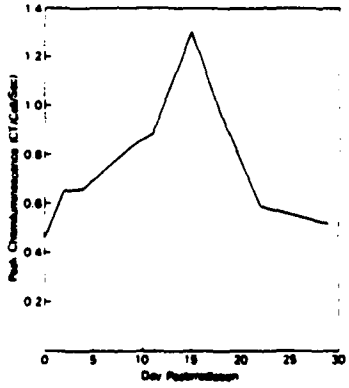

Figure 4. Effect of irradiation on the oxidative burst activity of whole blood granulocytes. Diluted whole blood was assayed 45 minutes for granulocyte oxidative burst activity using a Picolite 6500 luminometer following stimulation with 200 ul of opsonized zymosan containing luminol (Packard).

In addition, when sera obtained from dogs postirradiation were mixed with normal percoll-separated peripheral blood granulocytes and assayed for zymosan-induced oxidative burst activity, oxidative responses significantly greater than those induced by normal sera were consistently observed (Figure 5). The greatest stimulatory activity was observed in sera obtained from dogs 15 days postirradiation.

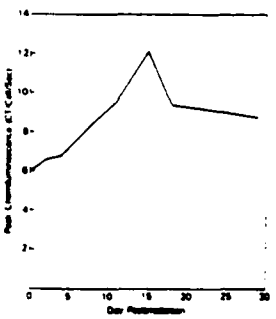

Figure 5. Effect of sera from irradiated canines on the oxidative burst activity of normal canine percoll-separated peripheral blood granulocytes. Fifty ul of normal test sera was added to normal granulocytes and oxidative burst activity was assayed 45 minutes using a Picolite 6500 luminometer following stimulation with 50 ul of opsonized zymosan containing luminol (Packard).

Taken together, these results suggest that although peripheral blood granulocytes are dramatically decreased following even a 2 Gy radiation injury due to hemopoietic stem cell damage, serum "factors" may enhance the function of available granulocytes, and thus aid in host defense postirradiation. Experiments to further identify these serum "factors" are in progress in our laboratory.

REFERENCES

1. J.J. Broerse and T.J. MacVittie, Response of Different Species to Total-Body Irradiation, Martin Nijhoff, Amsterdam (1984).

2. C.P. Miller, C. W. Hammond, and M. Tompkins, J. Lab. Clin. Med., 38, 331 (1951).

3. L.J. Kricka, P.E. Stanley, G.H.G. Thorpe, and T.P. Whitehead, Academic, New York (1984).

4. T.J. MacVittie, R.L. Monroy, M.L. Patchen, and J. H. Darden in Response of Different Species to Total-Body Irradiation, Edited by J.J. Broerse and T.J. MacVittie, pp. 113-129, Martin Nijhoff, Amsterdam (1984).

Supported by the Armed Forces Radiobiology Research Institute, Defense Nuclear Agency, under work unit B3132. Views presented in this paper are those of the authors; no endorsement by the Defense Nuclear Agency has been given or should be inferred. Research was conducted according to the principles enunciated in the "Guide for the Care and Use of Laboratory Animals" prepared by the Institute of Laboratory Animal Resources, National Research Council.

Neuroscience Vol. 23, No. 2, pp. 447–456, 1987
Printed in Great Britain

0306-4522/87 $3.00 + 0.00
Pergamon Journals Ltd

PEROXIDE ALTERS NEURONAL EXCITABILITY IN THE CA1 REGION OF GUINEA-PIG HIPPOCAMPUS *IN VITRO*

T. C. PELLMAR
Physiology Department, Armed Forces Radiobiology Research Institute, Bethesda, MD 20814-5145, U.S.A.

Abstract—Effects of peroxidative damage on neuronal excitability were investigated with electrophysiological techniques in CA1 pyramidal cells of the hippocampal slice preparation. Hydrogen peroxide alone or combined with ferrous ions (peroxide/iron) is likely to produce hydroxyl free radicals through the Fenton reaction.

Intracellularly recorded excitatory postsynaptic potentials and inhibitory postsynaptic potentials were significantly reduced by exposure to peroxide, while responses to iontophoretically applied GABA and glutamate were unaffected. These results suggest that peroxide has presynaptic actions. Peroxide and peroxide/iron also increased frequency adaptation; after exposure, neurons fired fewer action potentials at a lower frequency in response to the same depolarizing current step. A voltage clamp analysis revealed that the potassium currents were unaffected by peroxide/iron. Calcium current was not obviously altered by exposure to peroxide. Sodium spike threshold was also unaffected. Calcium spike threshold was significantly increased by peroxide. This action of peroxide may underlie its presynaptic actions.

It is concluded that peroxide produces both presynaptic and postsynaptic damage. This damage is likely to result from the production of free radicals which have been postulated to underlie a number of pathological states.

Oxygen intermediates such as superoxide and peroxide are normally generated during oxidative metabolism but are well controlled by intrinsic enzyme systems.[11,14,20] Superoxide is converted by superoxide dismutase to hydrogen peroxide which in turn is maintained at low levels by catalase and glutathione peroxidase. Under certain conditions, such as ageing, ischemia, hyperoxia, some toxins, and ionizing radiation, these reactive oxygen species are likely to increase and produce nervous system damage. The damage produced by peroxide is thought to result from interaction with the reduced form of copper or iron (the Fenton reaction) to produce the extremely reactive hydroxyl free radical.[14,20,21] Hydroxyl free radicals attack, among other macromolecules, membrane lipids, initiating lipid peroxidation and disrupting normal membrane integrity.

A previous study in hippocampal pyramidal cells investigated the effects of peroxide on extracellularly evoked potentials in the CA1 region.[30] The study showed that peroxide, either alone or in the presence of ferrous sulfate, substantially reduced the orthodromic field potential. Analysis of the dendritic and the somatic responses revealed that both synaptic efficacy and spike generation mechanisms were impaired. The present study further analyses the deficit caused by peroxide in hippocampal pyramidal cells using intracellular recording and voltage clamp techniques.

Abbreviations: AHP, afterhyperpolarization; EPSP, excitatory postsynaptic potential; GABA, γ-amino butyric acid; IPSP, inhibitory postsynaptic potential; TTX, tetrodotoxin.

EXPERIMENTAL PROCEDURES

Hippocampal slices (400–450 μm thick) were prepared from male Hartley guinea-pigs as previously described.[30,31] The slices were incubated in oxygenated solution at room temperature for at least 1 h to allow recovery from the dissection. One slice was then transferred to a submerged slice recording chamber (Zbicz design[41]) and continually perfused (1–2 ml/min) with a solution containing (in mM): 124 NaCl, 3 KCl, 2.4 $CaCl_2$, 1.3 $MgSO_4$, 1.24 KH_2PO_4, 10 glucose, 26 $NaHCO_3$; pH 7.4, equilibrated with 95% O_2/5% CO_2. In some experiments, barium was used to replace calcium. This required that $MgCl_2$ replace $MgSO_4$ in the bathing solution to prevent a precipitate. Similarly, when manganese was present, replacing calcium, both sulfate and phosphate ions were eliminated from the bathing solution. In the voltage clamp experiments, 0.3 μM tetrodotoxin (TTX) was always present to prevent sodium spiking that cannot be controlled by the single electrode voltage clamp. In a single experiment, control and test solutions always had the same composition, differing only by the addition of peroxide or peroxide/iron to the test solution. All experiments were done at 30 ± 1 °C.

Electrophysiological recordings were obtained through electrodes (20–40 MΩ) filled with either 2 M KCl or 3 M potassium acetate (KAc). Only KCl electrodes were used for voltage clamp recordings. Electrodes were selected for their ability to pass ± 3 nA with minimal rectification. The Axoclamp-I single electrode system was used for all recordings. Switching frequency was set at 4–6 KHz with a 25% duty cycle. Headstage output was continually monitored to ensure accurate adjustment of capacitance feedback and to watch for changes in electrode characteristics. As discussed

Table 1.

	Resting membrane potential (mV)			Membrane resistance (MΩ)		
	Control (mean ± SEM)	Experimental (mean ± SEM)	n	Control (mean ± SEM)	Experimental (mean ± SEM)	n
Peroxide	−69.9 ± 1.1	−69.6 ± 1.1	17	37.3 ± 3.9	35.3 ± 5.0	12
Peroxide/iron	−67.4 ± 1.3	−67.3 ± 1.5	7	32.4 ± 3.5	33.6 ± 2.5	5

previously,[23,31] space clamp limitations in anatomically complex neurons allowed only qualitative analysis of the voltage clamp data. Data were collected on a Gould 2400 chart recorder and Gould 4000 digital storage oscilloscope and stored and analysed on an LSI 11-03 microcomputer.

Neurons were considered acceptable if they had a membrane potential of at least −60 mV (mean ± SEM 68.7 ± 0.5 mV, $n = 60$), membrane resistance of 20 MΩ (35.7 ± 1.9 MΩ, $n = 60$) and an overshooting action potential (amplitude 96.6 ± 1.1 mV, $n = 60$). Neurons were exposed to 0.01% peroxide in normal solution for a minimum of 30 min. In some experiments, where peroxide alone had no effect, 100 μM ferrous sulfate with 0.01% peroxide (peroxide/iron) was also tested. Tissue was, on occasion, reperfused with normal solution (Wash) to test the reversibility of the effects.

The dose of peroxide was chosen on the basis of extracellular field potential studies.[30] A concentration of 0.01% peroxide consistently produced a decrease in the population spike evoked by stimulation of stratum radiatum. The effect was usually near maximal after 30 min. At this dose, reversal was, at best, partial. Lower doses (0.0025–0.0075%) were also effective and more likely to be reversible (Pellmar and Neel, unpublished observations). Because of the variability from tissue to tissue, however, peroxide damage at these lower doses could be relatively slight in some slices. Therefore, to maximize the ability to study and characterize intracellular effects of peroxide, a dose of 0.01% was used.

Stratum radiatum was stimulated with bipolar concentric stainless steel electrodes to evoke excitatory postsynaptic potentials (EPSPs). Stimulation of stratum radiatum or the alveus was used to evoke inhibitory postsynaptic potentials (IPSPs). Both KCl and KAc filled electrodes were used to study the EPSP but, in order to maintain normal chloride concentration gradients, only KAc electrodes were used to study the IPSP. Interstimulus intervals ranged from 5 to 20 s and once established were used throughout the experiment. The synaptic responses were always compared at the same cellular membrane potential.

Glutamate and GABA were applied iontophoretically with a WPI Model 160 iontophoretic unit. A single microelectrode was filled with 0.5 M or 1 M GABA or 1 M glutamate. Currents between 100 and 600 nA for 70–500 ms were used. Bias currents of 0–20 nA were applied to the electrodes to prevent leakage from the pipette. Transmitter was ejected no more frequently than once every 25 s. It was ensured that the response to the transmitter was constant throughout the control period (at least 15 min). Once an interval and currents were established for iontophoresis, they were maintained throughout the experiment.

RESULTS

Membrane properties

Field potential experiments indicated that 0.01% hydrogen peroxide with 100 μM ferrous sulfate (peroxide/iron) impaired both synaptic mechanisms and action potential generation.[30] Two simple explanations for these effects are (1) alteration of membrane potential, or (2) decreased membrane resistance. An intracellular analysis, however, revealed that neither explanation applied. Membrane resistance and membrane potential were not significantly altered by exposure to 0.01% peroxide or peroxide/iron for 30 min or more (Table 1).

Synaptic responses

Peroxidative damage to intracellularly recorded synaptic potentials was evaluated in CA1 hippocampal pyramidal cells. In all five neurons tested, peroxide/iron caused a 30–50% decrease in the EPSP evoked by stimulation of stratum radiatum. As seen in the extracellular experiments, the decrease began approximately 20 min after the beginning of application of the peroxide. Ferrous sulfate (100 μM) alone had minimal effects on the EPSP ($n = 3$). Peroxide alone caused a decrase in the dendritic field potential similar to that of peroxide/iron.[30] Intracellular experiments corroborated this observation. Peroxide alone decreased the EPSP in all four cells tested to approximately the same degree as peroxide/iron (Fig. 1A).

The IPSP was similarly studied in CA1 hippocampal pyramidal cells. IPSPs were evoked by stimulation of stratum radiatum (orthodromic) or stimulation of the alveus (antidromic). Peroxide (0.01%) alone reduced both antidromically and orthodromically evoked IPSPs by 40–60% (Fig. 1B and C). Both the early and late IPSPs were affected, though not always to the same degree. As with the EPSPs, effects were observed with a delay of 20–25 min. Thirty minutes after beginning peroxide perfusion, a decrease in IPSP was invariably observed ($n = 4$).

A decrease in the synaptically evoked potentials could result from either a decrease in transmitter release or a decrease in postsynaptic responsiveness to the neurotransmitter. To differentiate, glutamate and GABA were iontophoretically applied to the neurons. Although the transmitter mediating synaptic excitation in the stratum radiatum of CA1 has not been definitively identified, glutamate is a likely candidate.[10,35] Application of glutamate to the apical dendrites of CA1 pyramidal cells ($n = 3$) resulted in a large depolarization as seen by an intrasomatic electrode. Peroxide added to the bathing solution, for up to an hour, was ineffective in reducing the iontophoretic response to glutamate (Fig. 2A).

The neurotransmitter mediating synaptic inhibition, both antidromic and orthodromic, in the

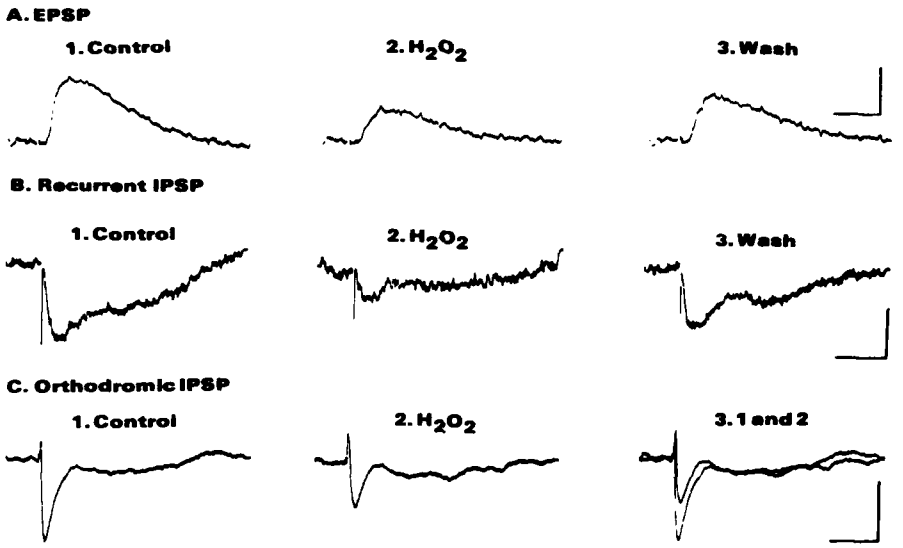

Fig. 1. Peroxide reduces the EPSP and IPSP. (A) EPSP in hippocampal pyramidal cell evoked by stimulation (0.2 Hz) of stratum radiatum. Thirty minutes in 0.01% peroxide alone greatly reduced the EPSP. Thirty-minute wash partially reversed the effect. Membrane potential: −68 mV. Calibration: 10 mV, 10 ms. (B) Antidromic IPSP elicited by subthreshold stimulation (0.2 Hz) of the alveus. Twenty-five minutes in 0.01% peroxide reduced the IPSP. Thirty-minute wash partially reversed the effect. Traces are the average of 20 recordings. Membrane potential: −65 mV. Calibration: 1 mV, 100 ms. (C) Orthodromic IPSP elicited by stimulation of stratum radiatum (0.2 Hz). Thirty-five minutes in 0.01% peroxide reduced the IPSP. Third panel shows superimposition of IPSPs in control and in peroxide. Traces are the average of 15 responses. Membrane potential. −70 mV. Calibration: 0.5 mV, 100 ms.

hippocampus is identified as GABA.[35] External application of GABA to the dendrites of CA1 pyramidal cells produces a depolarizing response with a reversal potential near −40 mV,[1,2] while application of GABA to the soma causes a chloride-dependent hyperpolarization with a reversal potential near −70 mV.[1,2] This latter rsponse more closely resembles the synaptically mediated early inhibiton. The effect of peroxide was tested on both the dendritic ($n = 3$) and somatic ($n = 3$) responses to GABA. Exposure to 0.01% peroxide, up to an hour, never reduced the iontophoretic responses to GABA (Fig. 2B and C).

Frequency adaptation

In addition to the decrease in synaptic efficacy, field potential experiments[30] indicated that peroxide impaired the ability of the neurons to fire action potentials. To investigate the intrinsic neuronal capability for action potential generation, depolarizing current steps of 500 ms were applied to the neurons. A range of depolarizing currents were applied and the total number of action potentials and the early frequency of firing were monitored. Figure 3A illustrates the method of data collection which was used to allow computer acquisition and analysis of action potential data that, otherwise, was too fast to digitize. The depolarizing current step (bottom trace) evoked a train of action potentials. Each time the neuron fired, a Scope Raster/Stepper (WPI) was triggered. The output voltage of the Scope Raster/Stepper incremented by a constant value with each spike (top

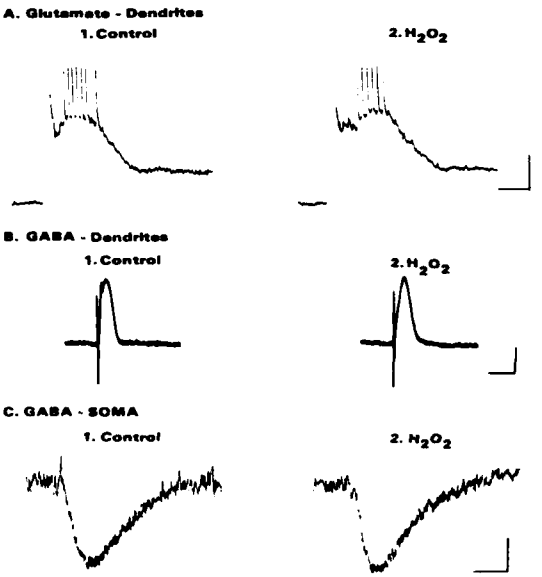

Fig. 2. Peroxide has no effect on iontophoretically applied amino acids. (A) Response to iontophoresis of glutamate (50 ms, 500 nA, 10 nA bias, 1/50 s). Fifty-minute exposure to 0.01% peroxide did not reduce the response. Membrane potential: −80 mV. Calibration: 10 mV, 200 ms. (B) Response to iontophoretic application of GABA (300 ms, 400 nA, 1/35 s) to the dendrites of hippocampal pyramidal cell. Thirty-five-minute exposure to 0.01% peroxide did not affect the response. Membrane potential: −68 mV. Calibration 5 mV, 10 s. (C) Response to iontophoretic application of GABA (400 ms, 600 nA, 10 nA bias, 1/35 s) to soma of hippocampal pyramidal cell. Forty-minute exposure to 0.01% peroxide did not reduce the response. Membrane potential: −68 mV. Calibration: 2.5 mV, 2.5 s.

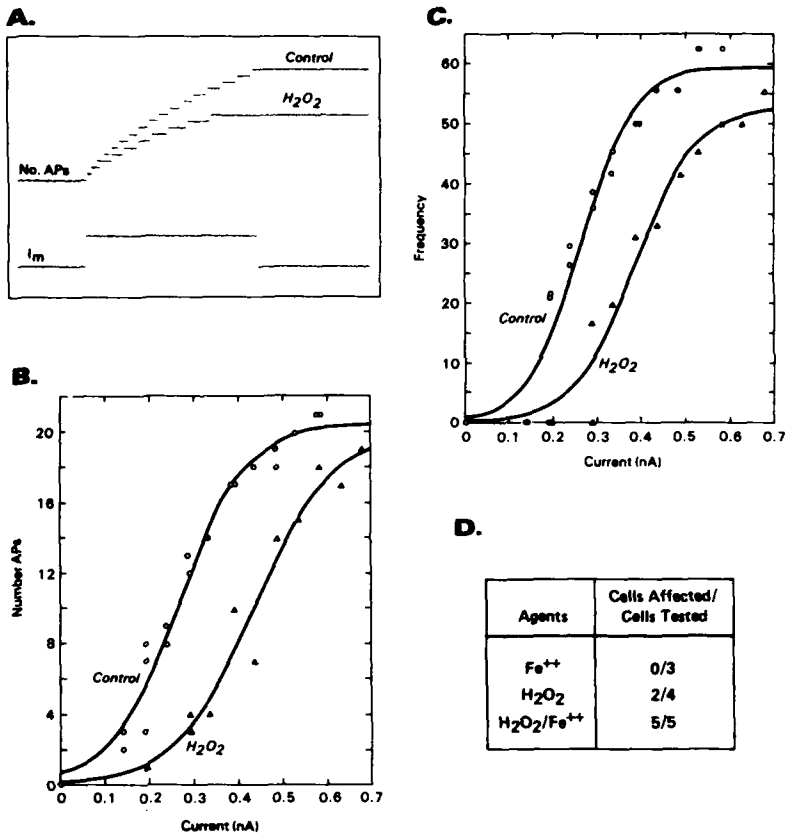

Agents	Cells Affected/ Cells Tested
Fe^{++}	0/3
H_2O_2	2/4
H_2O_2/Fe^{++}	5/5

Fig. 3. Peroxide decreases the frequency and number of action potentials evoked by an intracellular current. (A) Response of neuron to 500-ms current step in control and in 0.01% peroxide (25 min). Bottom trace: current step (0.39 nA). Top trace: with each action potential, the recording steps up one unit. From these traces, the number and the timing of action potentials can be determined. (B) Plot of the number of action potentials elicited by the end of the 500-ms current step versus the current. Peroxide shifted the curve to the right. Curves were computer-fitted to the data by the equation for a sigmoid curve. (C) Plot of the frequency of action potential generation early in the 500-ms step vs current used to elicit the activity. Frequency was measured as the inverse of the interval between the third and fourth action potential in the train. Peroxide shifts the curve to the right. Curves were computer-fitted as in (B). (D) Summary table of experiments done with iron alone, peroxide alone and peroxide/iron. Iron alone never altered the firing response of the cell. Peroxide alone altered the response 50% of the time and peroxide/iron always shifted the curves.

traces). The potential at the end of the trace, therefore, is that incremental value multiplied by the total number of action potentials elicited by the current pulse. Frequency of firing could be calculated from the inverse of the interval between any two consecutive action potentials in the train. In the present study, the third and fourth spikes were used. As described by Madison and Nicoll,[27] a pyramidal cell normally decreases its firing frequency during the course of a depolarizing step. This phenomenon is called frequency adaptation. In 2 of 4 cells tested, 0.01% peroxide appeared to increase adaptation. There was a substantial reduction in the number of evoked action potentials (Fig. 3A) over a range of depolarizing currents (Fig. 3B). In addition, the initial frequency of firing was reduced (Fig. 3C). When 100 μM ferrous sulfate was present in the solution with 0.01% peroxide, all 5 of the neurons tested showed increased adaptation. Iron alone, however, did not alter adaptation ($n = 3$) (Fig. 3D). The potentiating action of iron was necessary to observe the effect consistently. Yet even with iron present, the onset of the response to peroxide could be quite slow and the intensity of the effect variable.

Membrane currents

Potassium currents are likely to underlie neuronal adaptation. Madison and Nicoll[27] found that blocking the calcium-mediated potassium current with cadmium or blocking the M-current with muscarine could reduce adaptation in hippocampal pyramidal cells. Connor[8] has shown that the fast transient outward current (the A-current) can regulate neuronal firing frequency. Enhancement of the potassium currents, therefore, may be a cause of the slowed neuronal firing in peroxide and in peroxide/iron.

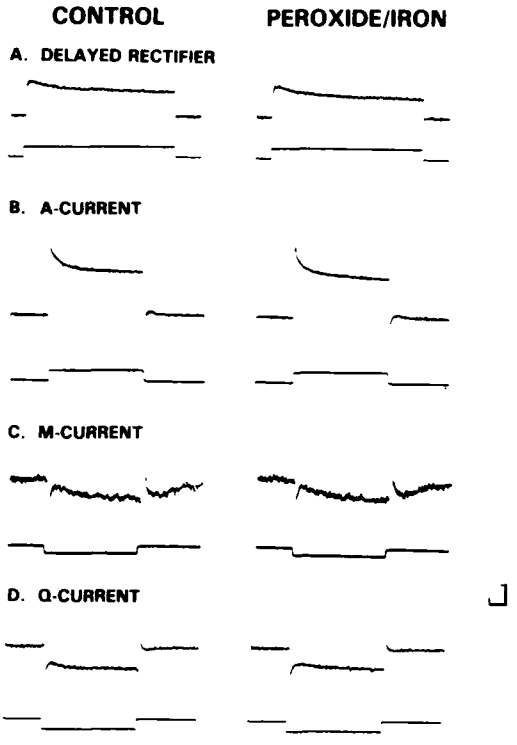

Fig. 4. Potassium currents are not affected by peroxide/iron. (A) Delayed rectifier elicited by a voltage step from −67 to −37 mV. Mn^{2+} replaced Ca^{2+} to prevent contamination with calcium-mediated potassium current. Calibration 0.6 nA, 50 mV; 4 s. (B) A-Current, a fast transient current, appears in response to a voltage step from −69 to −38 mV in the presence of Mn^{2+}. Calibration: 0.6 nA, 50 mV; 100 ms. (C) M-current evoked by a voltage step from −43 to −53 mV. Traces are the average of 4 sweeps. The leak conductance, calculated from the membrane conductance between −60 and −80 mV, was subtracted from current traces to accentuate the M-current. Calibration: 0.3 nA, 50 mV; 100 ms. (D) Q-current evoked in response to voltage command from −67 to −97 mV in the presence of Mn^{2+}. Same cell as in (A). Calibration: 0.6 nA, 50 mV, 100 ms. TTX (0.3 μM) was present in all experiments to prevent contamination with uncontrolled sodium spikes. All cells were exposed to 0.01% peroxide with 100 μM ferrous sulfate for at least 30 min.

These potassium currents are most easily studied under voltage clamp conditions. The potassium currents in hippocampal pyramidal cells were evaluated in 0.01% peroxide with 100 μM iron since peroxide alone only increased adaptation 50% of the time. All observations were made in at least 3 cells. TTX was always present to prevent sodium spiking that could not be controlled by the single electrode voltage clamp. Neurons were held at a potential appropriate (see below) for the current under study. In nearly all cells, a range of depolarizing and hyperpolarizing steps were applied to evaluate the full current–voltage relationship. Sample steps (Fig. 4) are shown as individual examples of time- and voltage-dependent currents.

The delayed rectifier has been described by Segal and Barker[34] in cultured hippocampal pyramidal cells and is also present in pyramidal cells in the slice preparation (31; Zbicz, personal communication). A prolonged step to potentials more depolarized than −50 mV reveals a slow outward current that slowly inactivates as is characteristic of the delayed rectifier (Fig. 4A). These experiments were done in the presence of manganese to block the calcium-mediated potassium current that could contaminate the records. Addition of peroxide/iron for 30 min did not enhance this current ($n = 3$).

Hippocampal pyramidal cells exhibit a fast transient outward current that resembles the A-current of invertebrates.[17,41] If the neuron is held at −70 mV, a voltage command to −30 mV or more positive potentials elicits a quickly inactivating outward current as seen in Fig. 4B. This current was not affected by peroxide/iron ($n = 3$).

A non-inactivating potassium current (M-current) exists at potentials positive to −50 mV. As described by Halliwell and Adams,[19] this current is muscarine sensitive. A voltage step from approximately −40 mV to −50 mV reveals an inward relaxation due to the turning off of the M-current. As seen in Fig. 4C, M-current is unaffected by peroxide/iron ($n = 3$).

At potentials negative to −70 mV, the Q-current turns on.[19] It is revealed by a voltage step from −60 mV to −90 mV and reflected in an inward relaxation due to the opening of potassium and sodium channels. The current is inward because the potential is negative to the reversal potential. This current, also, was not enhanced by peroxide/iron (Fig. 4D) ($n = 5$).

Finally, the calcium-activated potassium current was investigated. Holding at −40 mV inactivates most of the delayed rectifier as well as the A-current.[17,34,41] A positive command from this holding potential produces an outward current that is predominantly calcium-mediated potassium current.[3,41] Again, peroxide with ($n = 4$), or without ($n = 2$), iron did not enhance the current (Fig. 5A). The current–voltage relationship (currents measured at end of 500-ms step) showed no effect of peroxide/iron on late currents throughout the full voltage range ($n = 4$) (Fig. 5B). The actions of peroxide on the calcium-mediated potassium current were further tested by evaluating the slow post-train afterhyperpolarization (AHP) that reflects this current.[22,33,38] A train of 4–5 action potentials was elicited with a series of 4–5 short current pulses (5-ms duration, 10-ms interpulse interval), each of sufficient amplitude to evoke a single action potential. The AHP was evoked at a constant membrane potential. In 4 cells tested, the AHP was not affected by peroxide or peroxide/iron (Fig. 5C).

A review of the current traces produced in these voltage clamp experiments revealed an interesting effect both in the presence and absence of iron. The transient inward current evoked in some of the

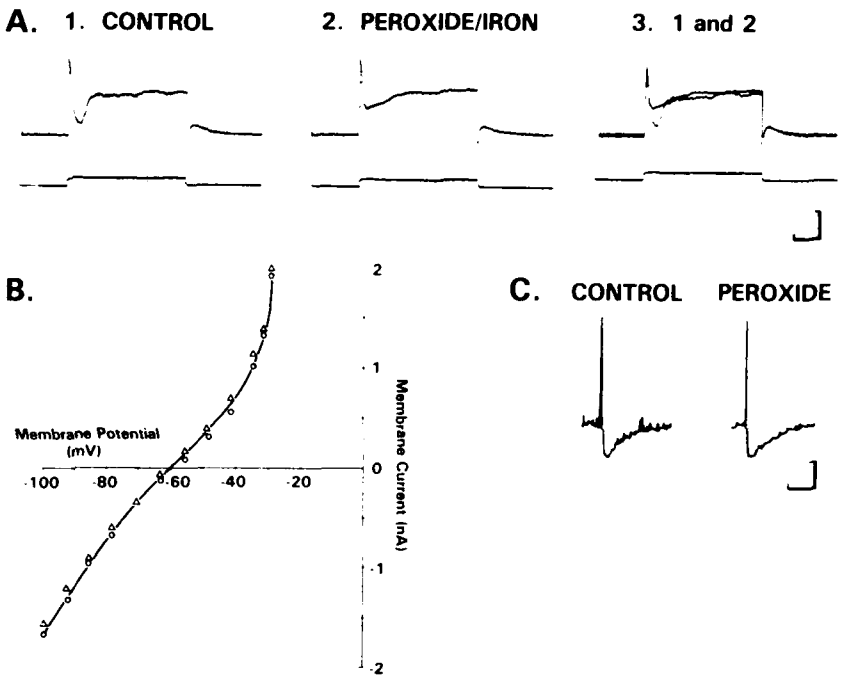

Fig. 5. (A) Exposure of hippocampal pyramidal cell to 0.01% peroxide with 100 μM ferrous sulfate for 37 min did not reduce the outward current evoked by voltage step from -49 to -32 mV. At this holding potential, outward current is predominantly calcium-dependent potassium current.[3] Notice that the transient inward current early in the voltage step appears to be reduced. Traces are the average of 4 sweeps. Calibration: 0.6 nA, 50 mV; 100 ms. (B) Current-voltage curve from same cell as in (A) illustrates absence of effect of peroxide/iron on currents measured at end of 500-ms step. Holding potential: -49 mV. Circles, control; triangles, peroxide/iron. (C) AHP is elicited by train of 4 action potentials at membrane potential of -66 mV. Thirty minutes in peroxide had no effect on the AHP. Action potentials are truncated by the chart recorder. Calibration: 5 mV, 2.5 s.

depolarizing voltage steps appeared to be reduced (Fig. 5). Since this inward current is likely to be calcium (sodium inward current was blocked by TTX), the effects of peroxide on calcium currents were tested. Since calcium current is revealed by blocking outward currents,[4,24] barium, which can carry the slow inward current but does not turn on the calcium-mediated potassium current,[8,16] was used to replace calcium. A holding potential of -40 mV was used to inactivate further remaining potassium currents and to inactivate partially inward currents to improve voltage control. A voltage step from -40 mV to more depolarized potentials produced an inward current. With potassium currents blocked, dendritic calcium spikes, which are often uncontrollable with the single-electrode voltage clamp, appear in the records (see also Ref. 4). The data, therefore, must be evaluated qualitatively. Since voltage control was better near the end of the 500-ms command than at the beginning of the command, only late currents were analysed. It was observed, as might be expected for a transition metal, that iron alone often reduced the inward current (not shown). This necessitated that iron be omitted from the solution in the study of the inward currents. Peroxide alone (0.01%) never reduced the inward current carried by barium ($n = 5$) and did not appear to shift the voltage-dependence of the current (Fig. 6).

Action potentials

Since changes in potassium currents could not explain the increase in adaptation, another explanation was sought. One possibility was that sodium spike threshold was altered. To evaluate this possibility, the sodium action potential was studied in the presence of 2.4 mM manganese (replacing calcium) to eliminate the calcium component of the spikes. A current ramp of 250 ms was provided to the neuron. As membrane potential depolarized, sodium spikes were elicited. A change in threshold would be reflected in a shift in latency of the first action potential. To quantify the change in threshold, 6–10 measurements were made in each cell both in control and following peroxide exposure; average values were compared by the t-test for paired samples. The sodium spike threshold was unaffected by peroxide ($n = 3$; control, 63.7 ± 1.5 mV; peroxide, 63.2 ± 1.1 mV; $P > 0.05$). The shape of the sodium action potential also appeared to be unchanged. The thresh-

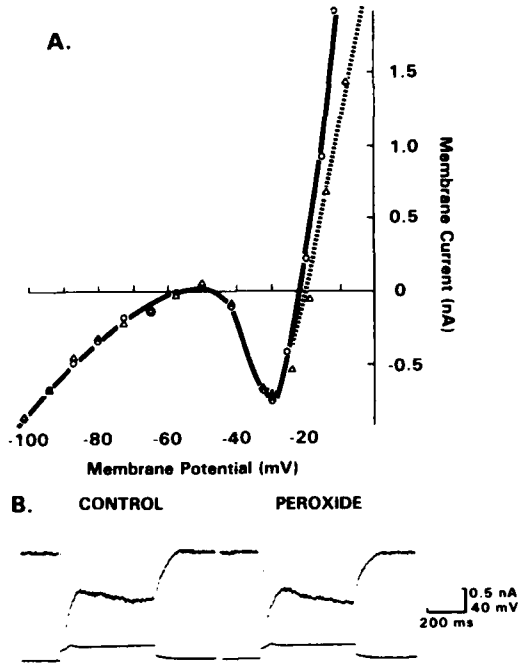

Fig. 6. Inward current carried by divalent cation is not obviously affected by 0.01% peroxide. Graph of current voltage relationship in Ba^{2+} ($0\ Ca^{2+}$) to block the outward current and enhance the inward current. The inward current is unaltered after 30 min in peroxide. Circles, control; triangles, peroxide. The inset shows sample currents in control and after 30 min in peroxide, evoked with a voltage step from −46 to −26 mV. Calibration: 0.5 nA, 40 mV; 200 ms.

old or waveform of the sodium spike were similarly unaffected by peroxide/iron ($n = 2$).

The calcium action potential was examined similarly. In presence of 0.3 μM TTX to block the sodium spike and 15 mM tetraethylammonium to block some of the potassium currents, calcium spikes in CA1 hippocampal pyramidal cells are large overshooting potentials. A 4-s ramp, sufficient in amplitude to evoke several calcium spikes, was applied to the neurons (Fig. 7). Peroxide (0.01%) did not alter the amplitude or waveform of the calcium spikes, but it did shift the latency of the first spike indicating a more positive theshold for the calcium spike ($n = 3$). Four to six measurements of spike threshold were made both before and 30 min after exposure to 0.01% peroxide and averaged for each neuron ($n = 3$). Each individual neuron showed a significant ($P < 0.01$) shift in threshold. Average values for the 3 cells under the two conditions were compared using the t-test for paired samples and found to be significantly different (control, 44.6 ± 3.7 mV; peroxide, 38.4 ± 2.8 mV; $P < 0.05$).

DISCUSSION

Electrophysiological mechanism of peroxide damage

Intracellular analysis of peroxidative damage revealed both presynaptic and postsynaptic effects as suggested by the extracellular field potential experiments.[30] Peroxide/iron decreased evoked neuronal firing. In addition, both EPSPs and IPSPs were blocked by peroxide and peroxide/iron. The decrease

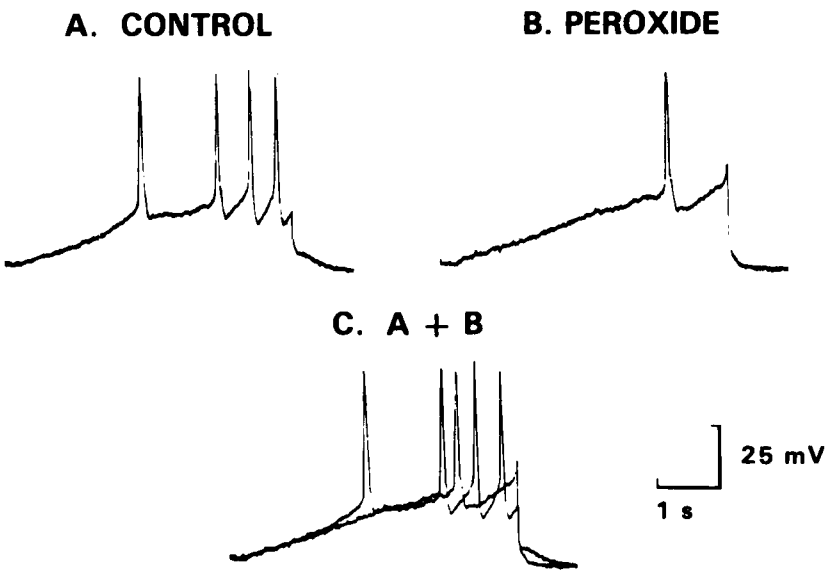

Fig. 7. Sample traces in control and 0.01% peroxide show shift in calcium spike threshold in hippocampal CA1 pyramidal cell. Calcium spikes were evoked by a 4-s ramp in 15 mM TEA and 0.3 μM TTX. (A) Calcium spikes elicited in control conditions. (B) Calcium spikes elicited after 27 min in peroxide. (C) Traces in (A) and (B) superimposed. Notice that the slope of the voltage evoked by the ramp is unchanged as would be expected if membrane resistance was constant. In peroxide, however, the calcium spike occurs later in the trace, at a more depolarized potential, indicating that threshold is increased. Calibration: 25 mV, 1 s.

in the synaptic responses does not appear to be a postsynaptic action since the iontophoretic responses to GABA and glutamate were unaffected by peroxide. The transmitter actions were unchanged in the presence of a concentration of peroxide that severely impaired EPSPs and IPSPs, suggesting that the actions of peroxide are presynaptic. It is possible that the increase in calcium spike threshold could reduce calcium influx in the presynatic terminal and account for the presynaptic action of peroxide.

The mechanism of action of peroxide on calcium currents is, as yet, uncertain. Voltage clamp analysis showed that only in normal solution, with potassium currents unblocked, the early inward current was reduced (as in Fig. 5A). This may be the correlate of increased calcium spike threshold. Yet the analysis of the inward current in barium did not reveal any obvious shift in the voltage-dependence of activation. This absence of effect in barium could be a technical problem such as space clamp limitations preventing the observation of a 6-mV shift. Alternatively, the observation may have a biological basis. Perhaps the site of peroxide damage is a calcium-dependent process for which barium cannot substitute. For instance, peroxide might increase intracellular calcium which causes the inactivation of calcium currents; but barium currents are not similarly affected.[12a] These possibilities require further analysis.

The increase in frequency adaptation produced by peroxide/iron also remains unexplained. Potassium currents are important regulators of adaptation but none of those tested were affected. One possible mechanism is a decrease in recovery from sodium current inactivation during a train of action potentials. However, no evidence for this was seen in the recordings. Another possibility is suggested by the work of McCarren and Alger[28] who have observed that blockers of the Na/K pump increase neuronal excitability and increase calcium spike theshold in the hippocampus. If peroxide enhanced the pump, the opposite effects might be expected to result: a decreased neuronal excitability and a decreased calcium spike threshold. However, an increase in pump activity is contrary to what is hypothesized to occur with free radical damage and lipid peroxidation.[26]

Oxidative mechanisms of peroxide damage

Other methods of producing free radicals in nervous tissue produce effects comparable to those observed here. Oxygen at high pressure and ionizing radiation are both thought to produce nervous system damage through free radicals.[14,15,21] In the hippocampal slice preparation, King and Parmentier[25] observed that hyperbaric oxygen reduced the ability of the afferent volley to evoke a synaptic response. Ionizing radiation (60 Co, 75–200 Gy at 5 Gy/min) also decreased the orthodromic population spike and, at the higher doses, the synaptic response as well.[32]

At the lobster neuromuscular junction, Colton and Colton[5,6] found that hyperbaric oxygen decreased the synaptically evoked excitatory and inhibitory responses without altering the postsynaptic responses to glutamate and GABA, the *intrinsic neurotransmitters*. As in the present study, a presynaptic mechanism was hypothesized. Colton and Gilbert[7] also found that hydrogen peroxide produced similar presynaptic decreases in synaptic activation at the lobster neuromuscular junction. High doses of tertiary butyl hydroperoxide (0.03–3.0%) caused a conduction block in frog nerves accompanied by lipid peroxidation.[18] Similar doses of hydrogen peroxide (0.1%), reduced the antidromic field potential in hippocampal slices.[30]

Free radicals have been postulated to increase muscimol binding reflecting an increase in the affinity of GABA receptors.[13,39] These results might predict an increase in the iontophoretic response to GABA in the present study; but this was not observed. In agreement with the present results, Yoneda *et al.*[39] found that 0.01% peroxide did not alter muscimol binding and that higher doses decreased muscimol affinity. It is likely that 0.01% peroxide, either with or without iron, is not generating the oxygen metabolite effective at the GABA receptors.

Free radicals and other active oxygen species can initiate lipid peroxidation through interaction with unsaturated fatty acids.[12,14,21] Iron reacts with hydrogen peroxide through the Fenton reaction to produce hydroxyl free radicals, perhaps the most reactive of the oxygen intermediates. Addition of iron enhances hyperbaric oxygen damage and the uneven regional distribution of iron may underlie the regional sensitivities in the brain to oxygen damage.[29,40] The potentiating actions of iron on the peroxide-induced increase in adaptation suggest that similar mechanisms may be involved in the present study.

An alternative mechanism for the actions of peroxide in the present study is the oxidation of membrane constituents. In support of this is the observation that the sulfhydryl reducing agent, dithiothreitol, produces effects opposite to those produced by peroxide; field potentials are enhanced,[37] synaptic responses are potentiated and adaptation is decreased.[36] The relative contributions of oxidative and free radical damage to peroxide effects are currently under investigation.

REFERENCES

1. Alger B. E. and Nicoll R. A. (1982) Pharmacological evidence for two kinds of GABA receptor on rat hippocampal pyramidal cells studied in vitro. *J. Physiol., Lond.* **328**, 125–141.
2. Andersen P., Dingledine R., Gjerstad L., Langmoen I. A. and Mosfeldt Laursen A. (1980) Two different responses of hippocampal pyramidal cells to application of gamma-amino butyric acid. *J. Physiol., Lond.* **305**, 279–296.

3. Brown D. A. and Griffith W. H. (1983) Calcium-activated outward current in voltage-clamped hippocampal neurones of the guinea-pig. *J. Physiol., Lond.* **337,** 287–301.
4. Brown D. A. and Griffith W. H. (1983) Persistent slow inward calcium current in voltage-clamped hippocampal neurones of the guinea-pig. *J. Physiol., Lond.* **337,** 303–320.
5. Colton C. A. and Colton J. S. (1982) An electrophysiological analysis of oxygen and pressure on synaptic transmission. *Brain Res.* **251,** 221–227.
6. Colton C. A. and Colton J. S. (1986) The action of oxygen and oxygen at high pressure on inhibitory transmission. *Brain Res.* **364,** 151–158.
7. Colton C. A. and Gilbert D. (1985) Effect of H_2O_2 on excitatory transmission in the lobster neuromuscular junction. *Fedn Proc. Fedn Am. Socs exp. Biol.* **44,** 1273.
8. Connor J. A. (1979) Calcium current in molluscan neurones: measurement under conditions which maximize its visibility. *J. Physiol., Lond.* **286,** 41–60.
9. Connor J. A. (1980) The fast K channel and repetitive firing. In *Molluscan Nerve Cells: From Biophysics to Behavior* (eds Koester J. and Byrne J. H.), pp. 125–133. Cold Spring Harbor Laboratory, New York.
10. Cotman C. W. and Nadler J. V. (1981) Glutamate and aspartate as hippocampal transmitters: biochemical and pharmacological evidence. In *Glutamate: Transmitter in the Central Nervous System* (eds Roberts P. J., Storm-Mathisen J. and Johnson G. A. R.), pp. 117–154. Wiley and Sons, New York.
11. Demopoulos H. B., Flamm E., Seligman M. and Pietronigro D. D. (1982) Oxygen free radicals in central nervous system, ischemia and trauma. In *Pathology of Oxygen* (ed. Autor A. P.), pp. 127–155. Academic Press, New York.
12. Dirks R. C. and Faiman M. D. (1982) Free radical formation and lipid peroxidation in rat and mouse cerebral cortex slices exposed to high oxygen pressure. *Brain Res.* **248,** 355–360.
12a. Eckert R. and Tillotson D. L. (1981) Calcium-mediated inactivation of the calcium conductance in caesium-loaded giant neurones of *Aplysia californica*. *J. Physiol., Lond.* **314,** 265–280.
13. Fatome M. and Roman V. (1984) A study of the mechanism of cerebral hyperexcitability after irradiation. *Int. J. Radiat. Biol.* **46,** 421–424.
14. Fridovich I. (1978) The biology of oxygen radicals. *Science, N.Y.* **201,** 875–880.
15. Gerschman R., Gilbert D. L., Nye S. W., Dwyer P. and Fenn W. O. (1954) Oxygen poisoning and X-irradiation: a mechanism in common. *Science, N.Y.* **119,** 623–625.
16. Gorman A. L. F. and Herman A. (1979) Internal effects of divalent cations on potassium permeability in molluscan neurones. *J. Physiol., Lond.* **296,** 393–410.
17. Gustafsson B., Galvan M., Grafe P. and Wigstrom H. (1982) A transient outward current in a mammalian central neurone blocked by 4-aminopyridine. *Nature* **299,** 252–254.
18. Hall E. D. and Telang F. W. (1985) Characteristics of lipid peroxidative block induced by an organic hydroperoxide in axons of isolated frog nerve. *Cent. nerv. Syst. CNS Trauma* **2,** 161–168.
19. Halliwell J. V. and Adams P. R. (1980) Voltage-clamp analysis of muscarinic excitation in hippocampal neurons. *Brain Res.* **250,** 71–92.
20. Halliwell B. and Gutteridge J. M. C. (1984) Oxygen toxicity, oxygen radicals, transition metals and disease. *Biochem. J.* **219,** 1–14.
21. Halliwell B. and Gutteridge J. M. C. (1985) Oxygen radicals and the nervous system. *Trends Neurosci.* **8,** 22–26.
22. Hotson J. R. and Prince D. A. (1980) A calcium-activated hyperpolarization follows repetitive firing in hippocampal neurons. *J. Neurophysiol.* **43,** 409–419.
23. Johnston D. and Brown T. H. (1983) Interpretation of voltage-clamp measurements in hippocampal neurons. *J. Neurophysiol.* **50,** 464–486.
24. Johnston D., Hablitz J. and Wilson W. A. (1980) Voltage clamp discloses slow inward current in hippocampal burst firing neurones. *Nature, Lond.* **286,** 391–393.
25. King G. L. and Parmentier J. L. (1983) Oxygen toxicity of hippocampal tissue in vitro. *Brain Res.* **260,** 139–142.
26. Kovachich G. B., Mishra O. P. and Clark J. M. (1981) Depression of cortical Na^+, K^+-ATPase activity in rats exposed to hyperbaric oxygen. *Brain Res.* **206,** 229–232.
27. Madison D. V. and Nicoll R. A. (1984) Control of the repetitive discharge of rat CA1 pyramidal neurones *in vitro*. *J. Physiol., Lond.* **354,** 319–331.
28. McCarren M. and Alger B. E. (1985) Epileptiform activity induced by inhibition of the Na/K pump in rat hippocampal slices: Facilitation of calcium spikes. *Soc. Neurosci. Abstr.* **11,** 467.
29. Noda Y., McGeer P. L. and McGeer E. G. (1983) Lipid peroxide distribution in brain and the effect of hyperbaric oxygen. *J. Neurochem.* **40,** 1329–1332.
30. Pellmar T. (1986) Electrophysiological correlates of peroxide damage in guinea pig hippocampus *in vitro*. *Brain Res.* **364,** 377–381.
31. Pellmar T. C. (1986) Histamine decreases calcium-mediated potassium current in guinea pig hippocampal CA1 pyramidal cells. *J. Neurophysiol.* **55,** 727–738.
32. Pellmar T. C. and Tolliver J. M. (1987) Effects of ionizing radiation on hippocampal excitability. In *Brain Slices: Fundamentals, Applications and Implications* (eds Schurr A., Teyler T. J. and Tseng M. T.), pp. 152–156. Karger, Basel.
33. Schwartzkroin P. A. and Stafstrom C. E. (1980) Effect of EGTA on the calcium-activated hyperpolarization in hippocampal CA3 pyramidal cells. *Science, N.Y.* **210,** 1125–1127.
34. Segal M. and Barker J. L. (1984) Rat hippocampal neurons in culture: potassium conductances. *J. Neurophysiol.* **51,** 1409–1433.
35. Storm-Mathisen J. (1977) Localization of transmitter candidates in the brain: the hippocampal formation as a model. *Prog. Neurobiol.* **8,** 119–181.
36. Tolliver J. M. and Pellmar T. C. (1986) Intracellular analysis of dithiothreitol effects on guinea pig CA1 pyramidal cells. *Soc. Neurosci. Abstr.* **12,** 676.
37. Tolliver J. M. and Pellmar T. C. (1987) Dithiothreitol elicits epileptiform activity in CA1 of the guinea pig hippocampal slice. *Brain Res.* **404,** 133–141.
38. Wong R. K. S. and Prince D. A. (1981) Afterpotential generation in hippocampal pyramidal cells. *J. Neurophysiol.* **45,** 86–97.

39. Yoneda Y., Kuriyama K. and Takahashi M. (1985) Modulation of synaptic GABA receptor binding by membrane phospholipids: possible role of active oxygen radicals. *Brain Res.* **333,** 111–122.
40. Zaleska M. M. and Floyd R. A. (1985) Regional lipid peroxidation in rat brain in vitro: Possible role of endogenous iron. *Neurochem. Res.* **10,** 397–410.
41. Zbicz K. L. and Weight F. F. (1985) Transient voltage and calcium-dependent outward currents in hippocampal CA3 pyramidal neurons. *J. Neurophysiol.* **53,** 1038–1058.

(*Accepted* 12 *March* 1987)

Exp. Hematol. 14:963–970 (1986)

Experimental Hematology

Countercurrent Centrifugal Elutriation (CCE) Recovery Profiles of Hematopoietic Stem Cells in Marrow from Normal and 5-FU-Treated Mice

Gretchen N. Schwartz, Thomas J. MacVittie, Rod L. Monroy, and Roy M. Vigneulle

Department of Experimental Hematology, Armed Forces Radiobiology Research Institute, Naval Medical Command, National Capital Region, Bethesda, Maryland, USA

(Received 5 December 1985; in revised form 22 May 1986; accepted 28 May 1986)

Abstract. Data presented in this report describe countercurrent centrifugal elutriation (CCE) recovery profiles of hematopoietic colony-forming cells (CFC) in marrow from normal and 5-fluorouracil-(5-FU) treated mice. Of the total nucleated cells, 75%–95% were recovered, and up to 80% of CFC were recovered after CCE of bone marrow from normal mice. Red blood cells and the majority of lymphocytes were collected in fractions well separated from the CFC. In addition, the CCE recovery profiles of populations of CFC (i.e., BFU-E, CFU-E, GM-CFC, and HPP-CFC) were distinct. The distribution of recovered day 8 CFU-S was different from the distribution of day 12 CFU-S. The CCE recovery profiles of CFC in regenerating marrow from 5-FU-treated mice were shifted to fractions of larger cells, presumably in cell cycle. These data demonstrate that CCE is useful as a method of further characterizing qualitative and quantitative changes in populations of CFC occurring after various hematopoietic-influencing regimens.

Key words: Countercurrent centrifugal elutriation (CCE) — Hematopoietic colony-forming cell (CFC) — Spleen colony-forming unit (CFU-S) — Granulocyte–macrophage colony forming cell (GM-CFC) — High-proliferative-potential colony-forming cell (HPP-CFC)

Countercurrent centrifugal elutriation (CCE) has been used to separate populations of cells on the basis of subtle differences in physical parameters, such as size or density or both [1, 2]. One advantage of CCE is that a large number of cells, 1×10^7–9×10^8, can be separated within the short period of 0.5–2 h [1–3]. A further advantage of CCE is that the flow rates, rotor speeds, and media can be modified in order to optimize conditions for a particular population of cells [1, 2]. As a result, CCE has been used extensively to separate, further characterize, and enrich for subpopulations of cells.

In their functional and physical characteristics, marrow-derived hematopoietic colony-forming cells (CFC) are a heterogeneous population of stem cells. In density-equilibrium and velocity–sedimentation fractionation of murine bone marrow, the peak activity of day 9 spleen colony-forming units (CFU-S) was well separated from that of in vitro granulocyte–macrophage colony-forming cells (GM-CFC) [4]. In addition, distinct subpopulations of GM-CFC [5], erythroid colony-forming units (CFU-E) [6], and day 9 CFU-S [7] have been identified using density-equilibrium and velocity–sedimentation procedures. The recovery profiles of these subpopulations of CFC were shifted when cells or donor animals were pretreated with possible cell-cycle-affecting regimens such as radiation damage [8], 5-fluorouracil (5-FU) [9], or hydroxyurea [7].

Separation of lymphocytes from hematopoietic CFC and fractions of cells enriched for some CFC have been obtained with CCE fractionation of murine bone marrow cells [3, 10]. However, total cell recovery and the recovery of CFC, as well as resolution of subpopulations of CFC after CCE, of bone marrow from normal mice have been poor [3, 10, 11]. Data presented in this report describe the CCE recovery profiles of hematopoietic stem cells, as measured by colony-forming assays in bone marrow from normal mice. With CCE methods described in these studies, more than 90% of the nucleated cells and 50%–80% of populations of CFC were recovered. The distribution of recovered day 8 CFU-S and high-proliferative-potential colony-forming cells (HPP-CFC) was distinct from the distribution of recovered GM-CFC. In addition, the CCE recovery profiles of these populations of CFC were shifted in

Views presented in this paper are those of the authors; no endorsement by the Defense Nuclear Agency has been given or should be inferred.

Address reprint requests to: Dr. G. N. Schwartz, Department of Experimental Hematology, Armed Forces Radiobiology Research Institute, Naval Medical Command, National Capital Region, Bethesda, MD 20814-5145, USA.

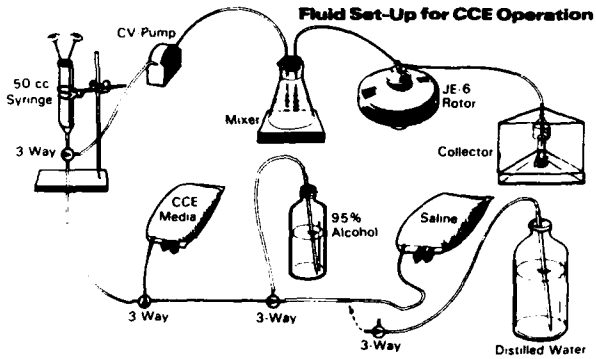

Fig. 1. Schematic representation for separation of bone marrow cells by countercurrent centrifugal elutriation (*CCE*).

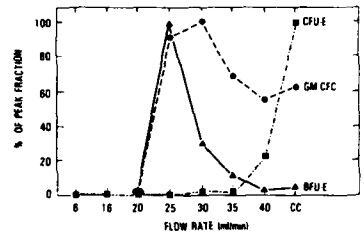

Fig. 2. Percentage of peak fraction for recovery of in vitro colony-forming cells. Bone marrow cells from normal mice were separated by CCE. Fractions of cells collected at individual flow rates were pooled (80–400 ml). The number of *GM-CFC, BFU-E,* and *CFU-E* recovered was determined for each designated flow rate, and the percentage of the maximum number was calculated and plotted.

bone marrow from mice that had been pretreated with 5-FU.

Materials and methods

Mice. (C57Bl/6 × DBA/2)F_1 female mice, purchased from Jackson Laboratories (Bar Harbor, Maine), were used as cell donors or recipients at 12–20 weeks of age. The animals were allowed food (Wayne Rodent Blox) and HCl-acidified water (pH 2.4) ad libitum. Bone marrow from 5-FU-treated mice was obtained from mice that, four days earlier, had been administered 5-FU (Sigma) at a dose of 150 mg/kg body weight by a single intraperitoneal or intravenous injection. Research was conducted according to the principles enunciated in the "Guide for the Care and Use of Laboratory Animals," prepared by the Institute of Laboratory Animal Resources, National Research Council.

Preparation of CCE media. Approximately 1.5 liters of media were needed for each CCE separation procedure. CCE media consisted of Hanks' balanced salt solution with phenol red and without Ca^{2+} and Mg^{2+} (Gibco), 2.0% heat-inactivated fetal calf serum (Hyclone), penicillin–streptomycin solution (Gibco), and 0.1% ethylenediaminetetraacetic acid (Sigma). The media was adjusted to pH 7.4 with 1 *N* NaOH and adjusted with NaCl to an osmolarity of 308 mosmol, which is isotonic to mouse serum [12].

CCE separation methods. Cells for CCE were flushed from excised femurs with "CCE media," dispersed through a 25-gauge needle, and filtered through 41-μm nylon mesh (Spectromesh; Spectrum Medical Industries). Cell suspensions before and during the CCE procedures were maintained at room temperature (18–20°C). A ZM Coulter particle counter with a Coulter ACCU-Comp/C-100 system (Coulter Electronics, Hialeah, Florida) was used to determine the size distribution of cells collected after CCE.

Cells were separated using a J-21B centrifuge with JE6 rotor with a Sanderson chamber (Beckman Instruments). The CCE set up for the separation cells was as illustrated in Figure 1. The rotor speed was set to 3000 ± 10 rpm, and the fluid flow rate through the chamber was calibrated for each desired flow rate with a variable transformer (type 39N1010; Newark Electronics) attached to a cardiovascular pump (Surns). From 5 × 10^7 to 3 × 10^8 cells in 25 ml CCE media were introduced into the system by injecting them into an inverted syringe [3] and allowed to enter the chamber at a flow rate of 6.5 ± 0.5 ml/min. Once all of the cells had entered the chamber, the collection of fractions was started: two 40-ml fractions were collected at the entry flow rate. Cells were then collected at each desired flow rate until the top portion of the chamber cleared (80–400 ml). The chamber contents consisted of two 40-ml fractions collected as soon as the rotor was turned off and the cells remaining in the chamber after the rotor had stopped.

Hematopoietic colony-forming assays. CFU-S determinations were done basically as described by Till and McCulloch [13]. Recipient mice were exposed bilaterally to a cobalt-60 irradiation source for a whole-body dose of 9.75 Gy at a dose rate of 0.40 Gy/min. This dose was sufficient to reduce background day-8 and day-12 macroscopic colonies to an average of less than 1/spleen. Animals were injected with cells within 5 h after irradiation. Cell suspensions were diluted to give 1 × 10^4 to 1 × 10^5 cells in 0.2 ml media and injected into a caudal vein of each mouse. After eight or 12 days, the spleens were removed, placed into Bouin's fixative, and the number of macroscopic colonies were counted.

CFU-E and burst-forming unit, erythroid (BFU-E) determinations were made, using a plasma-clot culture system described in detail by Weinberg et al. [14]. Cells were plated at a final concentration of 5 × 10^5 cells/ml with 0.25 U/ml (CFU-E) or 3.0 U/ml (BFU-E) anemic sheep plasma, step III erythropoietin (Connaught Labs, lot 3079-2) as 0.4-ml plasma clots in four-well Nunclone culture dishes (Nunc). Cultures were placed into a 37°C incubator with 5% CO_2 for 2.5 days for CFU-E and 8 days for BFU-E, fixed, harvested, stained, and evaluated as described by McLeod et al. [15].

GM-CFC and HPP-CFC were assayed by the double-layer agar technique, basically as described by Hagan et al. [16]. The agar medium was plated into 35-mm and 60-mm plastic petri dishes for GM-CFC and HPP-CFC assays, respectively. The respective colony-stimulating assay (CSA) was added to each dish, followed by the addition of a 1:1 mixture of double-strength culture medium (CMRL-1066) and 1% agar (Bactoagar; Difco), 1 ml to the 35-mm dishes and 2 ml to the 60-mm dishes. CSA for GM-CFC was 50 μl of pregnant mouse uterine tissue (PMUE) [17], and CSA for HPP-CFC was 250 μl of PMUE plus 250 μl of rat-spleen-conditioned media [18]. The CMRL-1066 medium, made as described for GM-CFC, contained 25% heat-inactivated, pooled human serum for culture of HPP-CFC. Marrow cells were plated and incubated at 37°C in 5% humidified CO_2 in air. GM-CFC were scored on day 10 and HPP-CFC were scored on day 14. An eyepiece reticule was used to assess colony size to distinguish HPP-CFC from GM-CFC. All colonies greater than 2 mm in size were considered to be derived from HPP-CFC. Optimal amounts

of CSA were determined by dose–response curves. HPP-CFC-derived colonies were observed only under conditions using the complete assay of colony-stimulating factors (CSFs) and accessory factors. Preliminary experiments were also used to determine the cycling characteristics of the HPP-CFC relative to those of the GM-CFC. The femoral content of each cell type was determined 2 h after the injection of mice with hydroxyurea (900 mg/kg body weight). The assay procedure was considered to be valid if the HPP-CFC were found to be relatively insensitive to the action of hydroxyurea.

Statistics. Student's *t*-test, two-tailed, was used to determine significant differences between groups of mice.

Results

Distribution of colony-forming cells in marrow from normal mice

In preliminary studies, cells were collected from CCE at media flow rates ranging from 6.5 to 40 ml/min. Fractions of cells collected at each flow rate were pooled, and the recovery of nucleated cells and in vitro colony-forming cells was determined. The peak fractions of recovered BFU-E, CFU-E, and GM-CFC were well separated (Fig. 2).

The peak fraction of BFU-E was collected at a flow rate of 25 ml/min. Approximately 70% of the recovered BFU-E was collected at this flow rate. In addition, there was a 2.6-fold enrichment for BFU-E, from $21 + 7.1/10^5$ nucleated cells in the pre-CCE sample to $55 \pm 1.7/10^5$ cells collected at a flow rate of 25 ml/min.

There was a twofold enrichment of CFU-E in cells from the chamber contents (designated as flow rates >40 ml/min); this was also the peak fraction for recovered CFU-E. No CFU-E were detected in fractions collected at a flow rate of 25 ml/min, and only 2% were collected at flow rates of less than 40 ml/min.

There was a broad distribution of recovery for GM-CFC. Approximately 50% of the recovered GM-CFC were collected at flow rates of 25 and 30 ml/min, with the peak fraction at 30 ml/min. There was no enrichment of GM-CFC at these flow rates. However, in the chamber contents, the number of GM-CFC/10^5 cells increased from 87 ± 13, in the pre-CCE sample, to 573 ± 120—a four- to sixfold enrichment.

These data demonstrate that the described stepwise CCE fractionation of marrow from normal mice can be used to separate populations of hematopoietic colony-forming cells. There was a higher recovery of colony-forming activity when media flow rates did not exceed 40 ml/min; thus, in subsequent studies, cells were collected at flow rates of 14, 16, 25, and 35 ml/min and chamber contents (>35 ml/min).

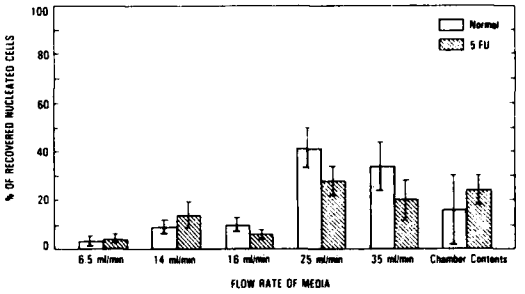

Fig. 3. CCE recovery profiles of nucleated cells of marrow from normal and 5-FU-pretreated mice. The number of nucleated cells recovered at each flow rate was determined, and the percentage of the total cells recovered was calculated. The values represent the mean ± SD of five studies of marrow from *normal* mice and the mean ± SD of four studies of marrow from *5-FU*-pretreated mice.

Cell recovery profiles from normal and 5-FU-treated mice

The number, volume, and type of cells collected at each flow rate were determined for marrow from normal and 5-FU-treated mice. The number of nucleated cells entered into the CCE chamber was 2.5 ± 0.59 ($\times 10^8$) from normal mice and 8.14 ± 0.93 ($\times 10^7$) from 5-FU-treated mice. The decreased number of cells for CCE of marrow from 5-FU-treated mice was due to the low number of nucleated cells (0.1% of normal) in the femurs from these mice. The average recovery of nucleated cells was 84% for both groups, and, at a particular flow rate, approximately the same percentage of cells ($p > 0.05$) was recovered from both types of marrow (Fig. 3).

Mean cell volumes and cell types in fractions collected at a particular flow rate were similar for marrow from both normal and 5-FU-treated mice. At a flow rate of 14 ml/min, primarily red blood cells and nonviable cells were collected. Cell viability was at least 90% in fractions collected at the other flow rates. Cells collected at 16 ml/min were mainly small lymphocytes, and consisted of a population of cells with a mean cell volume of 135 μm^3. Most of the cells collected at 25 ml/min were granulocytes (bands), with a small proportion of lymphocytes. There were two peaks of cell volume at 25 ml/min: one with a mean of 148 μm^3, and a larger peak with a mean cell volume of 244 μm^3. At 35 ml/min, the peak of smaller cells was gone, and there was a shift toward larger cells with a mean volume of 260 μm^3. In the chamber contents, three peaks of cell volume were evident. There was a small peak of cells with a mean volume of 148 μm^3 and a small peak at 260 μm^3; there was a new peak of cells with a mean volume of 477 μm^3.

Table 1. Summary of recovery of hematopoietic colony-forming cells after CCE of marrow from normal and 5-FU-pretreated B6D2F$_1$ mice[a]

Assay	No. in pre-CCE sample	% Recovered after CCE	Peak fraction of recovery	% of recovered in peak fraction	No./10^5 cells (pre)	No./10^5 cells (peak/pre)[b]
Cell number						
Normal	2.5 ± 0.59 (×10^8)	84 ± 13.7				
5-FU	0.8 ± 0.09 (×10^8)	84 ± 12.2				
GM-CFC						
Normal	3.3 ± 2.31 (×10^5)	73 ± 13.9	35 ml/min	41 ± 5.2	126 ± 54.7	1.3–2.0
			CC[c]	41 ± 10.0		2.0–4.5
5-FU	2.0 ± 1.89 (×10^5)	75 ± 8.4	CC	74 ± 9.1	161 ± 90.0	1.6–2.5
HPP-CFC						
Normal	19.7 ± 11.55 (×10^4)	74 ± 17.7	35 ml/min	56 ± 8.1	61 ± 31.1	1.2–2.0
5-FU	4.9 ± 4.48 (×10^4)	29 ± 18.5	35 ml/min	42 ± 8.7	43 ± 21.2	1.2–1.9
			CC	48 ± 9.9		1.2
Day-8 CFU-S						
Normal	5.4 ± 1.05 (×10^4)	65 ± 24.2	25 ml/min	53 ± 3.3	25 ± 9.2	1.3–1.6
5-FU	2.1 ± 3.02 (×10^4)	40 ± 9.1	35 ml/min	47 ± 15.0	18 ± 16.7	1.3–1.7
			CC	47 ± 13.4		1.3–1.5
Day-12 CFU-S						
Normal	5.7 ± 1.90 (×10^4)	79 ± 29.3	35 ml/min	50 ± 2.8	26 ± 1.4	1.2–1.8
5-FU	1.1 ± 0.12 (×10^4)	63 ± 18.0	35 ml/min	57 ± 12.3	35 ± 16.4	1.5

[a] Normals represent the means ± SD of values from five CCE fractionations, and 5-FU the mean ± SD of $n = 4$.
[b] Enrichment.
[c] Chamber contents.

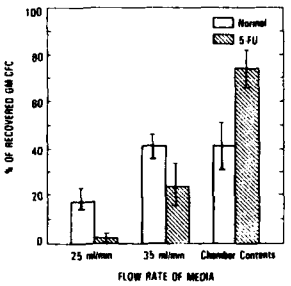

Fig. 4. CCE recovery profiles of granulocyte–macrophage colony-forming cells (GM-CFC). Cells were collected at 6.5, 14, 16, 25, and 35 ml/min and chamber contents. The number of GM-CFC recovered at each flow rate was calculated, and the percentage of total recovery was calculated for each flow rate. No GM-CFC were observed in fractions of cells collected at flow rates <25 ml/min. The values represent the mean ± SD of four studies of marrow from *normal* mice and the mean ± SD of three studies of marrow from *5-FU*-pretreated mice.

Recovery of colony-forming cells from normal and 5-FU-treated mice

The first evidence of hematopoietic colony-forming cells in bone marrow cell suspensions was not observed until the media flow rate was increased to 25 ml/min. The peak fraction, or the flow rate at which the largest number of CFC was collected, and the percentage of total recovered CFC at each flow rate were determined for GM-CFC, HPP-CFC, day-8 CFU-S, and day-12 CFU-S. Table 1 presents a summary of the recovery, peak fractions, and enrichment of these colony-forming cells in bone marrow separated by CCE. In contrast to bone marrow cells from normal mice, a shift was observed in CCE recovery profiles of hematopoietic CFC in marrow from 5-FU-treated mice.

Recovery of granulocyte–macrophage colony-forming cells (GM-CFC)

In five studies, the number of GM-CFC recovered after CCE of marrow from normal mice was 2.2 ± 0.87 (×10^5), or approximately 73% of the pre-CCE marrow sample. Only about 45%, or 4.1 ± 2.98 (×10^4) ($n = 4$), of the GM-CFC measured in the pre-CCE sample were recovered in marrow from 5-FU-treated mice (Table 1). In contrast to marrow from normal mice, a shift in CCE recovery profiles of GM-CFC was observed in marrow from 5-FU-treated mice (Fig. 4). Of the GM-CFC recovered after CCE fractionation of marrow from normal mice, 19% were collected at a flow rate of 25 ml/min, and the number of GM-CFC/10^5 cells was about one-third of the concentration found in the pre-CCE samples. There was an equal distribution of GM-CFC recovered at 35 ml/min and in the chamber

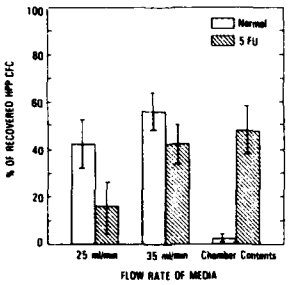

Fig. 5. CCE recovery profiles of high-proliferative-potential colony-forming cells (HPP-CFC). Cells were collected at 6.5, 14, 16, 25, and 35 ml/min and chamber contents. The number of HPP-CFC recovered at each flow rate was calculated, and the percentage of total recovery was calculated for each flow rate. No HPP-CFC were observed in fractions of cells collected at flow rates <25 ml/min. The values represent the mean ± SD of four studies of marrow from *normal* mice and the mean ± SD of two studies of marrow from *5-FU*-pretreated mice.

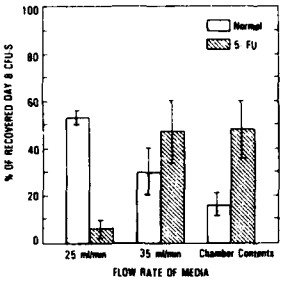

Fig. 6. CCE recovery profiles of day-8 spleen colony-forming units (day-8 CFU-S). Cells were collected at 6.5, 14, 16, 25, and 35 ml/min and chamber contents. The number of day-8 CFU-S recovered at each flow rate was calculated, and the percentage of total recovery was calculated for each flow rate. No CFU-S were observed in fractions of cells collected at flow rates <25 ml/min. The values represent the mean ± SD of the mean CFU-S (n = 5/group) of four studies of marrow from *normal* mice and the mean ± SD of four studies of marrow from *5-FU*-pretreated mice.

contents with only a 1.6-fold enrichment in both fractions. Of the total GM-CFC recovered in marrow from 5-FU-treated mice, only 2% were collected at 25 ml/min, and approximately 23% were collected at 35 ml/min. The peak fraction of GM-CFC in marrow from 5-FU mice was shifted to the chamber contents, in which 74% of the recovered GM-CFC were collected with a two- to threefold enrichment of GM-CFC/10^5 cells.

Recovery of HPP-CFC

As was determined for the recovery of GM-CFC, the recovery of HPP-CFC after CCE of marrow from 5-FU-treated mice was significantly lower (p = 0.04) than the 79%, or 1.5 ± 1.10 (×10^5), recovered in marrow from normal mice (Table 1). Only about 29%, or 1.0 ± 0.40 (×10^4), of the HPP-CFC in marrow from 5-FU-pretreated mice were recovered after CCE. In addition, as contrasted to marrow from normal mice, HPP-CFC recovery in marrow from 5-FU-pretreated mice was shifted to fractions collected at faster media flow rates (Fig. 5). For example, of the HPP-CFC recovered after CCE of bone marrow from normal mice, approximately 42% were found in fractions collected at 25 ml/min, 56% at 35 ml/min, and only 4% were found in the chamber contents. However, in marrow from 5-FU-pretreated mice, 48% of the recovered HPP-CFC were collected in the chamber contents, and only 15% were found in fractions collected at 25 ml/min. Compared to the number of HPP-CFC/10^5 nucleated cells in pre-CCE samples, there was a 1.2- to twofold enrichment of HPP-CFC in the peak fractions for marrow from both normal and 5-FU-pretreated mice (Table 1).

Table 2. CCE recovery of day-8 and day-12 CFU-S in marrow from normal and 5-FU-treated mice

CCE[a] flow rate	CFU-S/10^5 nucleated cells		
	Day 8	Day 12	p values =
	Normal		
Pre CCE[b]	30 ± 7.9	30 ± 9.9	1.00
25 ml/min	45 ± 11.3	44 ± 10.5	0.14
35 ml/min	16 ± 3.3	26 ± 6.7	0.02
Chamber	21 ± 7.2	25 ± 9.7	0.49
	5-FU		
Pre CCE[b]	10 ± 7.1	47 ± 29.0	0.0001
25 ml/min	2 ± 2.5	6 ± 3.2	0.06
35 ml/min	22 ± 6.6	49 ± 9.2	0.001
Chamber	31 ± 11.5	47 ± 9.6	0.04

[a] Fractions collected from CCE are mean ± SD from one study each, with five mice per group.

[b] Normal, Pre: mean ± SD of mean CFU-S from nine studies with five mice per group in each.

[c] 5-FU, Pre: mean ± SD of mean CFU-S from four studies with five mice per group in each study.

Recovery of CFU-S

The CCE recovery profiles of CFU-S giving rise to spleen colonies by day 8 (day-8 CFU-S) and by day 12 (day-12 CFU-S) were determined for marrow from normal and 5-FU-pretreated mice. There was no significant difference in the percentage of day-8 and day-12 CFU-S recovered after CCE of marrow from normal and 5-FU-pretreated mice (Table 1). However, as was observed for GM-CFC and HPP-CFC, there was a shift in the recovery profiles (Fig. 6). More than 50% of the day-8 CFU-S recovered from normal mice were found in fractions collected at 25 ml/min, with a 1.3- to 1.6-fold enrichment.

Only 6% of the day-8 CFU-S from 5-FU-pretreated mice were collected at this flow rate, and approximately 47% were recovered at both 35 ml/min and in the chamber contents, with a 1.4-fold enrichment in both fractions.

For pre-CCE marrow and for cells recovered after CCE of marrow from 5-FU-treated mice, the number of day-12 CFU-S was 2–16 times greater than the number of day-8 CFU-S (Table 2). Thus, many additional CFU-S appeared after day 8. This was not observed for marrow from normal mice. No significant differences in the number of day-8 and day-12 CFU-S were observed for cells recovered at 25 ml/min and in the chamber contents. However, the number of day-12 CFU-S was 2.1 ± 0.1 ($n = 3$ studies) times greater than the number of day-8 CFU-S for marrow from normal mice collected at a flow rate of 35 ml/min.

Discussion

The primary objective of the present report was to evaluate countercurrent centrifugal elutriation (CCE) as a technique for separating and further characterizing subpopulations of hematopoietic colony-forming cells (CFC). Total cell recovery and the recovery of CFC, as well as resolution of subpopulations of CFC after CCE of bone marrow from normal mice, have been poor [3, 10]. In studies described in the present report, with several modifications to previously described procedures and without prior removal of red blood cells, 75%–95% of the total nucleated cells and up to 80% of the CFC were recovered after CCE of bone marrow from normal mice. In addition, the CCE recovery profiles of GM-CFC, HPP-CFC, and CFU-S were distinct from marrow for normal mice.

A major problem described by others was a significant loss of cells due to clumping as cells were entered into the CCE chamber. Another problem described was a further nonselective loss of cells from the chamber during the entry process before fractionation procedures were initiated [3, 10]. In the studies described in the present report, only minimal cell clumping occurred when cells, media, and CCE procedures were maintained at room temperatures [2]. Less than 2% of the total cells were collected at the entry flow rate of 6.5 ml/min with the rotor speed at 3000 rpm, rather than the 2000 rpm generally used [3, 10]. However, at the higher rotor speed used, it was necessary to use faster media flow rates. This was a problem, in that damage to some cells may occur at the faster flow rates. Persidsky and Olson [19] observed that an increase in the flow rates at which granulocytes were collected was correlated with a significant decrease in their bactericidal ability. One possible reason for the low recovery of CFC activity after CCE of marrow from 5-FU-pretreated mice may be that these cells are more susceptible to damage due to the physical stress of the high rotor speed and flow rates of the CCE procedure [1].

An advantage of CCE is that flow rates, rotor speeds, and media can be modified in order to optimize conditions for a particular population of cells [1, 2]. Another advantage of CCE is that a large number of cells, 1×10^7–9×10^8, can be separated within the short period of 0.5–2 h [1–3]. Velocity–sedimentation and density-equilibrium separation procedures are generally limited to the separation of 2×10^8 total cells [5, 7–9]. In conditions such as those found in the marrow from 5-FU-pretreated mice, the high proportion of red cells further limits the number of nucleated cells that can be processed for the separation of populations of CFC unless the red cells are first removed [9]. With CCE, the red cells can be washed from the chamber by means of proper adjustments of the media flow rate, leaving the nucleated cells in the CCE rotor chamber for further separation or for use in other separation procedures [1, 2]. In the present report, approximately 84% of the total nucleated cells and 65%–80% of CFC were recovered after CCE of marrow from normal mice. These recoveries were comparable to velocity–sedimentation and density-equilibrium procedures used for the separation of cells from bone marrow of normal mice [5, 7, 8].

With CCE procedures described in the present report, there was some enrichment for populations of CFC, as compared with unfractionated bone marrow cells. When media flow rates were increased to 40 ml/min, there was a four- to sixfold increase in the number of GM-CFC and a twofold increase in the number of CFU-E per 10^5 nucleated cells in the chamber contents. There was only a 1.5- to threefold increase in the concentrations of day-8 CFU-S, day-12 CFU-S, HPP-CFC, GM-CFC, and BFU-E in various fractions collected after CCE. Other one-step separation procedures with marrow from normal mice gave fractions of cells enriched two- to sixfold for populations of CFC [2, 9, 10]. Multiple-step separation procedures used with marrow or spleen from normal or treated mice provided fractions of cells enriched six to 220-fold for populations of CFC [11, 20, 21]. For example, Visser et al. [20] were able to obtain fractions of cells with a 120- to 220-fold enrichment for day-8 and day-12 CFU-S.

In their studies, low-density cells were collected after separation in a discontinuous metrizamide gradient, followed by two separations, using a fluorescence-activated cell sorter to isolate cells labeled with wheat germ agglutinin and H-2K antibody.

Populations of CFC have been separated on the basis of changes in cell size and density that occurred as they progressed through stages of the cell cycle. For example, velocity sedimentation studies have demonstrated that CFU-S in proliferative phases of the cell cycle (i.e., S, G_2, and M) sediment at a faster rate than nonproliferating (G_0 and G_1) populations of CFU-S [7, 8]. The increase in sedimentation rate is primarily the result of a slight increase in cell density, from 1.070 g/cm^3 for CFU-S in G_0 to 1.075 g/cm^3 for populations of proliferating CFU-S. CCE has been shown to be a rapid and reproducible technique for separating proliferating and nonproliferating populations of human marrow-derived CFC [22].

Data described in the present report indicate that CCE recovery profiles of CFC in marrow from normal and 5-FU-pretreated mice are similar to the recovery profiles observed with other cell separation procedures. For example, 80% of the recovered day-8 CFU-S were collected at media flow rates of 25 and 35 ml/min (Fig. 6). Only 16% were recovered in the chamber contents. This is similar to the 10%–20% of day-8 CFU-S reported by others to be in S phase of the cell cycle, and recovered in fractions of large, dense cells after velocity–sedimentation or density-equilibrium separation procedures [7, 8]. Others have reported that the majority of CFC recovered in the chamber contents were large cells, presumably in cell cycle [22]. Less than 10% of the HPP-CFC and approximately 41% of GM-CFC in marrow from normal mice were collected in the chamber contents, comparable to the 9% HPP-CFC [16] and 35% GM-CFC [23] reported to be in S phase of the cell cycle. The proportion of proliferating CFC was shown to have increased to as much as 80% in regenerating bone marrow [8, 22], and these CFC were recovered in fractions of larger cells after velocity–sedimentation or density-equilibrium separation procedures [7–9]. In the present report, 50%–80% of CFU-S, GM-CFC, and HPP-CFC in regenerating marrow from 5-FU-pretreated mice were recovered in the chamber contents after CCE, with a concomitant decrease in the percentage of CFC recovered at 25 ml/min. These studies indicate that CCE is useful as a cell-separation procedure to further characterize qualitative and quantitative changes occurring in populations of CFC after various hematopoietic-influencing regimens.

Acknowledgments

We are grateful to Vic Kieffer, James Atkinson, Brenda Bell, and Rita Hardy for their excellent technical assistance, and to Dr. Charles L. Dorian for his assistance in setting up the computer-based data-analysis system used in these studies.

References

1. Figdor GC, Leemans JMM, Bint WS, De Vries JE (1983) Theory and practice of centrifugal elutriation (CE): factors influencing the separation of human blood cells. Cell Biophys 5:105
2. Sanderson RF, Bird K (1977) Cell separation by counterflow centrifugation. In: Prescott DM (ed) Methods in cell biology, vol 15. New York: Academic Press, p 1
3. Jemionek JF, MacVittie TJ, Byrne PJ, Shein PS, Walden DA (1982) Fractionation of mammalian bone marrow by counterflow centrifugation elutriation using a continuous albumin gradient analysis of granulocyte–macrophage colony-forming units. Br J Haematol 50:257
4. Worton RG, McCulloch EA, Till JE (1969) Physical separation of hemopoietic stem cells from cells forming colonies in culture. J Cell Physiol 74:171
5. Bol S, Visser J, Van den Engh G (1979) The physical separation of three subpopulations of granulocyte–macrophage progenitor cells from mouse bone marrow. Exp Hematol 7: 541
6. Heath DS, Axelrad AA, McLeod DL, Shreeve MM (1976) Separation of the erythropoietin responsive progenitors BFU-E and CFU-E in mouse bone marrow by unit gravity sedimentation. Blood 47:787
7. Monette FC, Gilio MJ, Chalifoux P (1974) Separation of proliferating CFU from G_0 cells of murine bone marrow. Cell Tissue Kinet 7:443
8. Visser J, Van den Engh G, Williams N, Mulder D (1976) Physical separation of the cycling and noncycling compartments of murine hematopoietic stem cells. In: Baum SJ, Ledney GD (eds) Experimental hematology today. New York: Springer, p 21
9. Bertoncello I, Bradley TR, Hodgson GS (1981) Characterization and enrichment of macrophage progenitor cells from normal and 5-fluorouracil treated mouse bone marrow by unit gravity sedimentation. Exp Hematol 9:604
10. Attwood PA, Bertoncello I, Bradley TR, Hodgson GS (1982) A comparison of counterflow centrifugation and unit gravity sedimentation in the separation of mouse bone marrow progenitor cells. Aust J Exp Biol Med 60:707
11. Inoue T, Carsten AL, Cronkite EP, Kelley JET (1981) Separation and concentration of murine hematopoietic stem cells (CFU-S) using a combination of density gradient sedimentation and counterflow centrifugal elutriation. Exp Hematol 9:563
12. Williams N, Kroft N, Shortman K (1972) The separation of different cell classes from lymphoid organs. VI. The effect of osmolarity of gradient media on the density distribution of cells. Immunology 22:885
13. Till JE, McCulloch EA (1961) A direct measurement of the radiation sensitivity of normal bone marrow cells. Radiat Res 14:213
14. Weinberg SR, McCarthy EG, MacVittie TJ, Baum SJ (1981) Effect of low-dose irradiation on pregnant mouse haemopoiesis. Br J Heamatol 48:127

15. McLeod DL, Shreeve MM, Axelrad AA (1974) Improved plasma system for production of erythrocytic colonies in vitro: quantitative assay method for CFU-E. Blood 44:517
16. Hagan MP, MacVittie TJ, Dodgen DP (1985) Cell kinetics of GM-CFC in the steady state. Exp Hematol 13:532
17. Bradley TR, Stanley ER, Sumner MA (1971) Factors from mouse tissues stimulating colony growth of mouse bone marrow cells in vitro. Aust J Exp Biol Med Sci 49:595
18. Metcalf D, Johnson GR (1981) Production by spleen and lymph node cells of conditioned medium with erythroid and haemopoietic colony-stimulating activity. Br J Haematol 48: 147
19. Persidsky MD, Olson LS (1978) Granulocyte separation by modified centrifugal elutriation system. Proc Soc Exp Biol Med 157:599
20. Visser JWM, Bauman JGJ, Mulder AH, Eliason JF, De Leeuw AM (1984) Isolation of murine hemopoietic stem cells. J Exp Med 59:1576
21. Nijhof W, Wierenga PK (1984) The isolation of murine splenic pluripotent stem cells. Exp Hematol [Suppl] 12:10
22. De Witte T, Plas A, Koekman E, Blankenbor G, Salden M, Wessels J, Haanen C (1984) Separation of human bone marrow by counterflow centrifugation monitored by DNA-flow cytometry. Br J Haematol 58:249
23. Iscove NN, Till JE, McCulloch EA (1970) The proliferative states of mouse granulopoietic progenitor cells. Proc Soc Exp Biol Med 134:33

From: PROSTAGLANDIN AND LIPID METABOLISM
IN RADIATION INJURY
Edited by Thomas L. Walden, Jr. and Haywood N. Hughes
(Plenum Publishing Corporation, 1987)

EFFECTS OF NEUTRON IRRADIATION ON PGE_2 AND TxB_2 LEVELS IN BIOLOGICAL FLUIDS: MODIFICATION BY WR-2721

L. K. Steel[1] and G. D. Ledney[2]

Departments of [1]Radiation Biochemistry and [2]Experimental Hematology
Armed Forces Radiobiology Research Institute
Bethesda, Maryland 20814-5145

ABSTRACT

Whole-body fission neutron irradiation of mice results in changes in plasma and urinary prostaglandin levels. No relationship was found between urinary TxB_2 excretion and the neutron dose. Elevated plasma PGE_2 at 2-4 days postexposure coincides with increased PGE_2 in the urine. A second increase in urinary PGE_2 occurred 6-10 days postirradiation, and was dose dependent up to 3.85 Gy. Plasma PGE_2 levels at this time were normal. WR-2721 administration markedly increased (24 hr) and then reduced (2-4 days) PGE_2 excretion in nonirradiated animals. The urinary PGE_2 of WR-2721-pretreated, irradiated mice paralleled those of drug-treated, nonirradiated animals for the first 5 days. However, WR-2721 injection did not modify the elevation of PGE_2 occurring 6-10 days postexposure. Urinary TxB_2 from nonirradiated groups was not altered by WR-2721, but the combination of drug and radiation resulted in increased levels 1-7 days postexposure. These results further implicate prostaglandins in the biological response to radiation exposure and suggest another mechanism of WR-2721 radioprotection.

INTRODUCTION

A role for prostaglandins (PG) as modulators of radiation-induced tissue injury is becoming increasingly evident. Antagonistic as well as cytoprotective effects of PG have been demonstrated in radiation injuries (reference 1 and references therein). To date most reports have focused on alterations in arachidonic acid metabolites as a consequence of low-LET (linear energy transfer, i.e., X or gamma) radiation exposure (2). The higher density of ionization produced by neutrons, compared to that of gamma rays, may intensify the interaction between free radicals and unsaturated fatty acids in membrane lipids. This could result in greater membrane damage from lipid peroxidation than observed from gamma or X rays. The effect of fission neutrons on the synthesis of these compounds has recently been addressed (1).

The present study reviews the *in vivo* effect of whole-body exposure to fission neutrons on plasma PGE_2, urinary TxB_2, and urinary PGE_2 in mice. In addition, the phosphorothioate compound WR-2721 was examined for its radioprotective efficacy against fission neutron irradiation, and its effect on urinary PG synthesis/excretion. The results further implicate PG's in the biological response to ionizing radiation, and suggest a role for PG's in the mechanism of radioprotection by WR-2721.

METHODS

The radioprotective compound WR-2721 was provided by COL David E. Davidson, Jr., Division of Experimental Therapeutics, Walter Reed Army Institute of Research. The drug was dissolved in normal saline (pH 7.6) immediately before use and administered intraperitoneally (i.p.) in a single 0.5-ml dose of 453 mg/kg of body weight. Control mice received saline only.

Animal Irradiation

Neutron irradiations were conducted using the AFRRI TRIGA Mark-F reactor as previously described (1,3). A minimum of 27 mice were used at each dose (2.0-5.0 Gy). Whole-body radiation was delivered at a midline tissue (MLT) dose rate of 0.4 Gy/min. The gamma component of the MLT dose was approximately 4.5% of the total dose (neutron-to-gamma ratio of approximately 21). The average neutron and gamma energies are estimated to be 0.68 MeV and 1.8 MeV, respectively (4).

Urine and Plasma

B6D2F1 (C57BL♀ x DBA/2J♂) female mice (Jackson Labs, Bar Harbor, ME) were housed in lucite metabolic cages, three animals per cage, for 7 days before initiating urine collection. Urine was collected from each cage at 24-hr intervals beginning 7 days before exposure and continuing to 30 days postirradiation. Urine samples were quantitated, aliquoted, organically extracted, and chromatographed on individual silica columns as described (1). Immunoreactive PGE_2 and TxB_2 in the column extracts were measured by radioimmunoassay as described (5,6).

Urine was collected daily for 7 days prior to drug injection. On the seventh day, mice were administered either WR-2721 or saline, and urine was collected daily for 7 days postinjection. In radiation experiments, WR-2721 or saline was administered 30 min before whole-body irradiation (4 Gy). Following exposure, animals were returned to their metabolic cages, and urine was collected up to 30 days postexposure.

Blood was obtained via cardiac puncture on anesthetized animals and plasma isolated by centrifugation at 4°C (7). PGE_2 was extracted from individual mouse plasma samples using solid phase C-18 extraction columns (8), and quantitated by radioimmunoassay (1,8). Radioactivity was measured in an LKB gamma counter,

and PGE_2 concentrations were determined by extrapolation from standard curves (1,5,6,8).

Statistical Analyses

Student's t test for paired samples (9) was applied to determine significance between postirradiation and/or postinjection values and baseline (postirradiation and/or preinjection) values. Thirty-day and 100-day survival results were analyzed by probit analysis (10) to determine the radiation $LD_{50/30}$ or $LD_{50/100}$. Survival data were compared by the method of Finney (10). Correlations across postirradiation time, within each radiation dose [Spearman's rank correlation (11)] or across radiation doses (12), were examined for each sampling day postirradiation. Other statistical analyses and comparison tests were performed as described previously (1).

RESULTS

Radiation-Induced Changes in Plasma and Urinary PG

Urine excretion rate during the 7 days prior to irradiation averaged 1.17 ± 0.05 ml/24 hr/mouse (M ± SE; range 0.8 to 1.35 ml). Urinary PGE_2 and TxB_2 averaged 311.79 ± 25.65 and 472.86 ± 29.70 pg/24 hr/mouse, respectively (range, 211.12-416.67 pg PGE_2 and 390.67-643.17 pg TxB_2). Preirradiation excretion rates were relatively constant within each radiation group (see legends to Figures 1 and 2). No correlation was found between PGE_2, TxB_2, and urine volume excretion rates ($p > 0.05$).

Total-body exposure to fission neutrons resulted in biphasic elevations in PGE_2 excretion (Figure 1). Urinary PGE_2 levels at days 2-3 were 1.5-fold to threefold

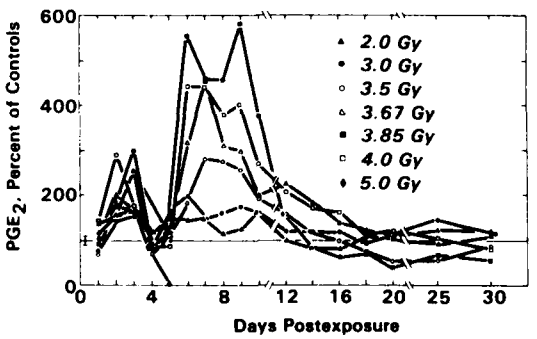

Fig. 1. Urinary excretion of PGE_2 from mice exposed to fission neutrons. Data are % of preirradiation baseline excretion rates (pg/24 hr/mouse: 2.0 Gy, 426.7 ± 25.6; 3 Gy, 253.0 ± 22.8; 3.5 Gy, 389.9 ± 31.2; 3.67 Gy, 277.0 ± 16.6; 3.85 Gy, 334.5 ± 33.5; 4.0 Gy, 211.1 ± 23.2; 5.0 Gy, 312.1 ± 15.6). I, overall preirradiation excretion at day 0.

higher than controls, but this elevation was not dose dependent. A second increase in urinary PGE_2 occurred days 6-10 postexposure. Increases in radiation dose up to 3.85 Gy were associated with increasingly elevated PGE_2 excretion. At day 10 postirradiation, urinary PGE_2 was still elevated, but there was no significant difference in excretions between radiation doses. Days 12-16 were characterized by declining urinary PGE_2; by 18 days postexposure, most groups were within control levels.

Plasma levels of PGE_2 were examined on days 1-5, 7, 9 and 11 following exposure to 3.0-Gy fission neutrons (Figure 2). Nearly a threefold increase in PGE_2 concentrations occurred 3-4 days after exposure, declining to control levels on the 5th day. Thereafter, the levels of PGE_2 in plasma from irradiated mice were similar to those of controls.

The levels of thromboxane B_2 positively correlated with urine excretion only in those animals exposed to 2.0 Gy ($p < 0.01$). Urinary TxB_2 concentrations were unchanged or reduced (3.67 or 3.85 Gy) during the first 3 days postexposure (Figure 3). Groups that received 3.67-3.86 Gy had reduced TxB_2 levels between days 4 and 8, while 4.0-Gy-exposed animals exhibited elevated TxB_2 excretion. The second week postexposure, urinary TxB_2 was transiently elevated in animals exposed to 2.0 Gy, while higher doses resulted in unchanged or transiently reduced levels. On days 14-16 postexposure, patterns of excretion were not statistically different across doses. Variable transient increases in urinary TxB_2 occurred 18-30 days postexposure in mice exposed to ≤ 3.0 Gy. Those that received ≥ 3.5 Gy had unchanged or reduced (3.85 Gy) urinary TxB_2.

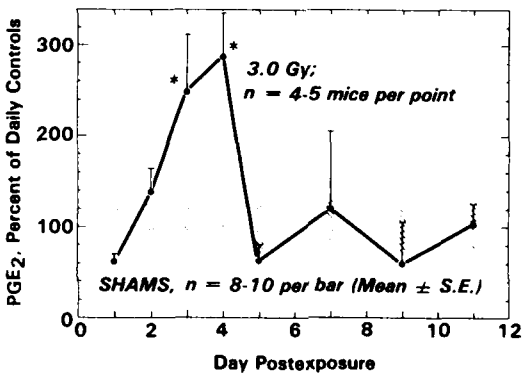

Fig. 2. PGE_2 in mouse plasma after whole-body fission neutron irradiation (3.0 Gy). Data are presented as percentage of control (nonirradiated) levels (▓). Mean control plasma levels were 30 ± 5 pg PGE_2/ml.

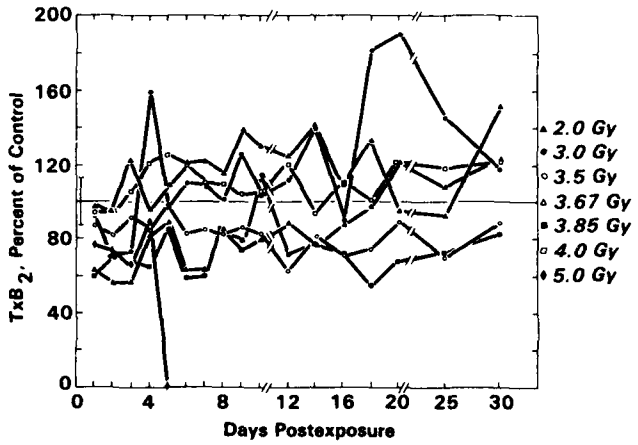

Fig. 3. Urinary excretion of TxB_2 from mice exposed to fission neutrons. Data are presented as percentage of preirradiation baseline excretion rates (pg/24 hr/mouse: 2.0 Gy, 390.7 ± 27.4; 3.0 Gy, 422.4 ± 54.9; 3.5 Gy, 463.0 ± 32.4; 3.67 Gy, 643.2 ± 45.0; 3.85 Gy, 571.8 ± 45.7; 4.0 Gy, 523.9 ± 21.0; 5.0 Gy, 399.9 ± 20.0). I, overall preirradiation excretion illustrated at day 0.

WR-2721 Administration

Under the conditions of these studies, the $LD_{50/30}$ value for female mice exposed to fission neutrons is 3.97 Gy (95% C.I., 3.92, 4.02 Gy) (1). Administration of WR-2721 (453 mg/kg, i.p.) 30 min prior to irradiation extends the $LD_{50/30}$ to 4.87 Gy (4.50, 5.83 Gy), with a DMF of 1.23 (1.17, 1.29) (39).

Administration of WR-2721 (453 mg/kg, i.p.) to nonirradiated mice resulted in nearly a threefold increase in urinary PGE_2 excretion during the first 24 hr (Figure 4). On the second day postinjection, PGE_2 levels were significantly reduced; PGE_2 excretion was 38 ± 5% of control (saline-treated) values. WR-2721-treated animals also exhibited reduced urinary PGE_2 concentrations 3 and 4 days postadministration (61% and 65% of controls, respectively), which returned to control levels by the 5th day (Figure 4). Urine volume and urinary TxB_2 excretion were not altered by WR-2721 administration 1-7 days postinjection, compared to saline-treated controls (data not shown). In the present studies, no toxic deaths occurred following a single i.p. injection of 453 mg/kg WR-2721.

Urinary excretion of PGE_2 from mice administered WR-2721 30 min prior to whole-body fission neutron irradiation (4.0 Gy) is shown in Figure 5. Pretreated, irradiated animals exhibited increased PGE_2 excretion at 24 hr and reduced excretion 48 hr postirradiation to the same extent as nonirradiated mice injected with WR-2721 (Figure 4). WR-2721 eliminated the expected elevation in urinary PGE_2 between 2 and 3 days postirradiation (Figures 1,5), but not the second PGE_2 elevation at days 6-10 postexposure (Figure 5).

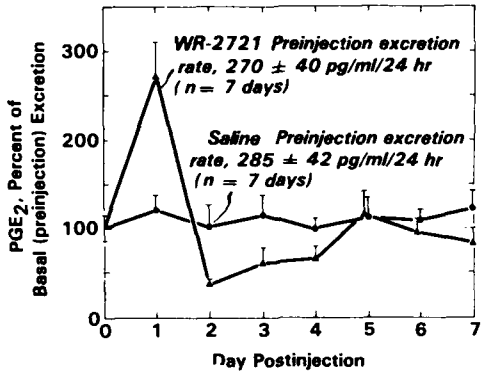

Fig. 4. Urinary PGE_2 from mice after i.p. injection of saline or WR-2721 (453 mg/kg). Data are presented as percent of preinjection excretion rates. ▲—▲, WR-2721 (preinjection excretion, 270 ± 40 pg PGE_2/ml/24 hr). ●—●, saline (preinjection excretion, 285 ± 42 pg PGE_2/ml/24 hr).

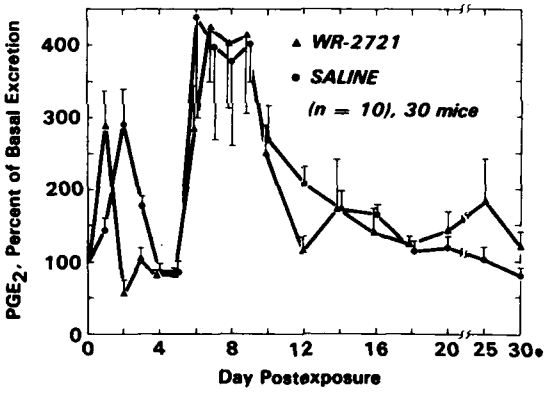

Fig. 5. Urinary PGE_2 from mice after i.p. injection of WR-2721 (453 mg/kg) and whole-body fission neutron irradiation (4 Gy). Data are presented as a percentage of preirradiation excretion rates. ▲—▲, WR-2721; ●—●, control.

Although WR-2721 did not modify urinary TxB_2 levels in nonirradiated animals, the combination of drug and fission neutron irradiation (4 Gy) resulted in increased urinary TxB_2 1-7 days postexposure (Figure 6). Mice that received 4 Gy but no drug pretreatment exhibited a modest elevation (20%-26%) in TxB_2 excretion on days 4-6 only. On these same days, urinary TxB_2 levels from WR-2721-injected, irradiated animals were 80%-121% higher than control (preirradiation) excretion. TxB_2 levels were within normal values in both WR-2721-treated and nontreated groups 8-30 days postexposure.

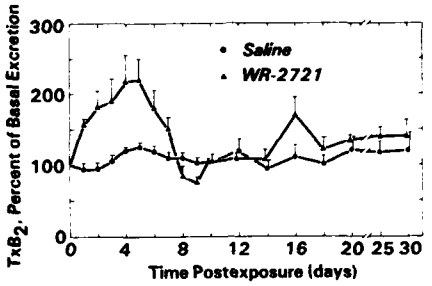

Fig. 6. Urinary TxB_2 from mice after i.p. injection of WR-2721 (453 mg/kg) and whole-body fission neutron irradiation (4 Gy). Data are presented as a percentage of preirradiation excretion rates. ▲—▲, WR-2721; ●—●, control.

DISCUSSION

Biphasic increases in mouse urinary excretion of PGE_2 occurred following whole-body exposure to fission neutrons (1). The initial transient elevation 2-3 days postexposure was not correlated with radiation dose. The second elevation occurring 6-10 days postexposure was dose dependent up to 3.85 Gy (Figure 7). These results suggest that urine PGE_2 may be a useful indicator of radiation exposure.

PGE_2 in urine is normally a reflection of renal production (13). Increases in urine PGE_2 levels may indicate a direct effect of radiation on the kidney. The fact that plasma PGE_2 was normal 6-10 days postexposure suggests that the increase in urine is primarily of renal origin. However, radiation exposure alters PG levels *in vivo* and *in vitro* in a variety of tissues and fluids (1,2,5,6,14,15-23), and the elevated plasma PGE_2 2-4 days postexposure (3 Gy) doses coincide with the initial increase observed in the urine. Thus, the extra-renal contribution of elevated circulating PGE_2 to urinary levels is a distinct possibility. Tanner and co-workers (14) have reported an increase in plasma PG-like material in patients treated with synchronous radiotherapy and chemotherapy for head and neck cancer. Conversely, Lifshitz et al. (24) found no elevation in plasma PG's and no correlation between radiation dosage and PG levels in patients undergoing pelvic irradiation for gynecologic cancer. Neither of these studies examined plasma PG concentrations within the first 7 days following radiotherapy, and urinary PG's were not measured. Several investigations (15-17) have reported increases in PG activity in rat and mouse tissues after exposure to ionizing radiation. These increases were found to occur 3-4 and 7-8 days postexposure, markedly similar to the biphasic elevations seen in urinary PGE_2 excretion. Conversely, Eisen and Walker examined PG-like activity (bioassay, reference 25) in whole blood and kidneys of mice 1-7 days after irradiation with 7 Gy X rays, and found no significant changes (15).

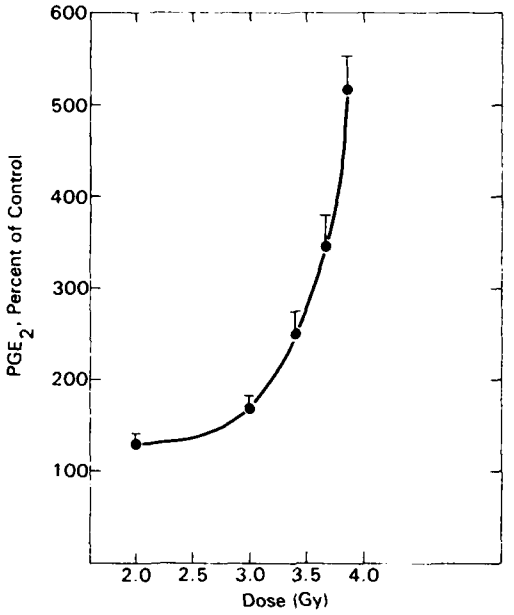

Fig. 7. Urinary excretion of PGE_2 6-9 days postexposure. Data are presented as means ± S.E.M. (% of controls) of mean urinary levels of days 6, 7, 8, and 9 postexposure, for each radiation dose.

Sublethal neutron irradiation (2-3 Gy) resulted in unchanged or transiently elevated TxB_2 excretion, while intermediate doses (3.5-3.85 Gy) resulted in transient reductions. We and others have found dose-related increases in guinea pig lung tissue (5) and rat urine (18,19) TxB_2 concentrations after whole-body gamma irradiation. These differences may be due to species and radiation quality.

Intraperitoneal administration of WR-2721 (453 mg/kg) to nonirradiated mice results in nearly a threefold increase in PGE_2 excretion the first 24 hr, reduced excretion 2-4 days postinjection, and normal levels on the 5th day. Urinary TxB_2 levels in these animals were not altered by WR-2721 treatment. Trocha and Catravas (20) have reported no change in PGE_2 and PGF_2 content in rat spleen or liver tissues 1 hr to 3 days after WR-2721 administration. Similarly, Donlon et al. (21) did not observe a change in PG excretion rates in WR-2721-treated rats. However, Pryanishnikova and co-workers (22) demonstrated increased PGE_2 and PGF_2 synthesis in mouse cerebral and testicular cystolic fractions and hepatic microsomes incubated *in vitro* with WR-2721. Furthermore, these increases could be inhibited by the addition of indomethacin.

Biodistribution studies have shown that WR-2721 has a short half-life in the body, being rapidly distributed to the kidneys and excreted in the urine (26). High levels of the compound (or its metabolites) and long retention times (>2 hr) are seen in kidney tissues (27). The most frequent adverse effects of WR-2721 include

nausea, vomiting, hypotension, and hypocalcemia (reviewed in reference 28). These same symptoms also occur with PG administration. The observed increase in PGE_2 synthesis/excretion following WR-2721 administration suggests that PG's may contribute to these side effects. Further work is required to determine whether PGE_2 acts as a modulator or a necessary component. One logical approach is premedication with a PG inhibitor (i.e., indomethacin) before WR-2721 injection.

The combination of WR-2721 (453 mg/kg, i.p.) and radiation (4 Gy) resulted in 100% animal survival. Urinary PGE_2 levels in WR-2721-pretreated and irradiated mice paralleled those of drug-treated nonirradiated animals for 5 days postinjection/irradiation. The radioprotectant did not modify the elevation of PGE_2 occurring 6-10 days postexposure. In comparison, neither drug nor fission neutron exposure (4 Gy) markedly altered TxB_2 excretion, but in combination, TxB_2 synthesis/excretion was elevated for 7 days. These results further implicate PG's in the biological response to ionizing radiation and suggest another mechanism of phosphorothioate radioprotection. Both natural and synthetic PGE_2 (16,16-dimethyl PGE_2) have been shown to provide radioprotection when given before irradiation, but are ineffective when given after irradiation (29,30). Simultaneous administration of synthetic PGE_2 (5 μg, subcutaneously) and WR-2721 (200 mg/kg, i.p.) to mice 15 min prior to exposure to gamma radiation from a ^{60}Co source additively increases the DMF (T. Walden, personal communication). Although acetylsalicylate has been shown to effectively control many gastrointestinal symptoms occurring in patients postradiotherapy (31), neither dexamethasone nor indomethacin premedication (400 μg or 100 μg, intramuscularly, respectively, every 12 hr for 3 days prior to 3.9-5.0 Gy fission neutron irradiation) modified animal weight loss or mortality (Steel, unpublished observations). These findings suggest that elevated PGE_2 levels at the time of radiation exposure (either by endogenous stimulation with WR-2721 or by exogenous addition) contribute to radioresistance. The potential mechanism(s) of PG-induced radioprotection (i.e., through modulation of intermediary substances such as cAMP, erythropoietin, glutathione, superoxide dismutase, nonprotein sulfhydryls, or other physiological changes) is currently under examination.

Renal production of Tx is normally low, but many pathological and inflammatory conditions are associated with increased biosynthesis and excretion (reviewed in reference 32). Free radicals formed by radiation exposure (33) may potentiate changes in arachidonate metabolism. The extent of radical and peroxide formation may determine the magnitude and direction of arachidonate metabolism. Lipid peroxides and H_2O_2 activate cyclooxygenase in a dose-dependent manner (34-37); however, high concentrations of hydroperoxide or free radicals inactivate cyclooxygenase (35,38). The addition of free radical scavengers has been shown to prevent this inactivation (37). Elevated urinary TxB_2 following WR-2721 administration and fission neutron irradiation may reflect the ability of the radioprotectant to effectively trap free radicals and thereby inhibit cyclooxygenase inactivation. Enhanced Tx synthesis/release may also be the result of direct or indirect stimulation of one or more of the enzyme systems participating in endoperoxide intermediate conversions.

ACKNOWLEDGMENTS

Supported by the Armed Forces Radiobiology Research Institute, Defense Nuclear Agency, under Research Work Units MJ 00064 and B2152. The views presented in this paper are those of the authors; no endorsement by the Defense Nuclear Agency has been given or should be inferred. Research was conducted according to the principles enunciated in the "Guide for the Care and Use of Laboratory Animals," prepared by the Institute of Laboratory Animal Resources, National Research Council. The authors gratefully acknowledge the secretarial assistance of Mrs. M. J. Waldbillig; the AFRRI Reactor Facilities staff for the performance of animal irradiations; Cpt M. Dooley, Radiological Physics Division, for performance of dosimetry techniques; and the technical expertise of Mr. W. Wolfe, Ms. M. Rafferty, and Ms. D. A. Kennedy. The authors also thank LCDR H. N. Hughes and T. L. Walden, Jr., for their critical evaluation and advice in the preparation of this manuscript.

REFERENCES

1. Steel, L. K., Rafferty, M. A., Wolfe, W. W., Egan, J. E., Kennedy, D. A., Catravas, G. N., Jackson, W. E., III, and Dooley, M. A. Urinary excretion of cyclic nucleotides, creatinine, prostaglandin E_2 and thromboxane B_2 from mice exposed to whole-body irradiation from an enhanced neutron field. Int. J. Radiat. Biol. 50: 695-715, 1986.
2. Polgar, P., Hahn, G., and Taylor, L. Radiation effects on eicosanoid formation. In: "Biochemistry of Arachidonic Acid Metabolism." W. E. M. Lands, ed. Martin Nijhoff Publishing, Boston, 1985, pp. 161-173.
3. Stewart, D. A., Ledney, G. D., Baker, W. H., Daxon, E. G., and Sheehy, P. A. Bone marrow transplantation of mice exposed to a modified fission neutron (N/G-30:1) field. Radiat. Res. 92: 268-279, 1982.
4. Zeman, G. H., and Ferlic, K. P. Paired ion chamber constants for fission gamma-neutron fields. Technical Report TR84-8. Armed Forces Radiobiology Research Institute, Bethesda, Maryland, 1984.
5. Steel, L. K., and Catravas, G. N. Radiation-induced changes in production of prostaglandins $F_{2\alpha}$, E, and TxB_2 in guinea pig parenchymal lung tissues. Int. J. Radiat. Biol. 42: 517-530, 1982.
6. Steel, L. K., Sweedler, I. K., and Catravas, G. N. Effects of ^{60}Co radiation on synthesis of prostaglandins $F_{2\alpha}$, E and thromboxane B_2 in lung airways of guinea pigs. Radiat. Res. 94: 156-165, 1983.
7. Ledney, G. D., Steel, L. K., Exum, E. D., and Gelston, H. M. Pathophysiologic responses in mice after neutron irradiation combined with either wound or burn trauma. In: "The Pathophysiology of Combined Injury and Trauma: Management of Infectious Complications in Mass Casualty Situations." D. Gruber, R. I. Walker, T. J. MacVittie, and J. J. Conklin, eds. Academic Press, Inc., Orlando, Florida, 1987.

8. El-Bayer, H., Steel, L., Montcalm, E., Danquechin-Dorval, E., Dubois, A., and Shea-Donohue, T. The role of endogenous prostaglandins in the regulation of gastric secretion in Rhesus monkeys. Prostaglandins 30: 401-419, 1985.
9. Snedecor, G. W., and Cochran, W. G. The comparison of two samples. In: "Statistical Methods." Iowa State University Press, Ames, Iowa, 1980, pp. 85-86.
10. Finney, D. J. In: "Statistical Method in Biological Assay." Third Edition. Macmillan Publishing Co., Inc., New York, 1978, pp. 349-390.
11. Conover, W. J. In: "Practical Nonparametric Statistics." Second Edition. John Wiley and Sons, Inc., New York, 1980, pp. 144-151.
12. Snedecor, G. W., and Cochran, W. G. Analysis of variance. In: "Statistical Methods." Iowa State University Press, Ames, Iowa, 1980, pp. 235-237.
13. Frölich, J. C., Wilson, T. W., Sweetman, B., Smigel, M., Nies, A. S., Carr, K., Watson, J. T., and Oates, J. A. Urinary prostaglandins. Identification and origin. J. Clin. Invest. 55: 763-770, 1975.
14. Tanner, N. S. B., Stamford, I. F., and Bennett, A. Plasma prostaglandins in mucositis due to radiotherapy and chemotherapy for head and neck cancer. Brit. J. Cancer 43: 767-771, 1981.
15. Eisen, V., and Walker, D. I. Effect of ionizing radiation on prostaglandin-like activity in tissues. Br. J. Pharmacol. 57: 527-532, 1976.
16. Trocha, P. J., and Catravas, G. N. Prostaglandin levels and lysosomal activities in irradiated rats. Int. J. Radiat. Biol. 38: 503-522, 1980.
17. Päusescu, E., Chirvasie, R., Teodosiu, T., and Päun, C. Effect of ^{60}Co γ-radiation on the hepatic and cerebral levels of some prostaglandins. Radiat. Res. 65: 163-171, 1976.
18. Donlon, M., Steel, L., Helgeson, E. A., Shipp, A., and Catravas, G. N. Radiation-induced alterations in prostaglandin excretion in the rat. Life Sci. 32: 2631-2639, 1983.
19. Schneidkraut, M. J., Kot, P. A., Ramwell, P. W., and Rose, J. C. Urinary prostacyclin and thromboxane levels after whole-body gamma irradiation in the rat. Adv. in Prostaglandin, Thromboxane, and Leukotriene Res. 12: 107-112, 1983.
20. Trocha, P. J., and Catravas, G. N. Effects of WR-2721 on cyclic nucleotides, prostaglandins and liposomes. Radiat. Res. 94: 239-251, 1983.
21. Donlon, M. A., Steel, L. K., Helgeson, E. A., Wolfe, W. W., and Catravas, G. N. WR-2721 inhibition of radiation-induced prostaglandin excretion in rats. Int. J. Radiat. Res. 47: 205-212, 1985.
22. Pryanishnikova, E. N., Zhulanova, Z. I., and Romantsev, E. F. Effect of S-[N-(3)aminopropyl)-2-aminoethyl]thiophosphoric acid on prostaglandin synthetase activity in mouse tissues (in Russian). Vopr. Med. Khim. 26: 685-688, 1980.
23. Dubois, L. A., Dorvall, E. D., Steel, L., O'Connell, L., and Durakovic, A. Do prostaglandins mediate radiation-induced suppression of gastric acid output? 33rd Annual Meeting of Radiation Research Society, Los Angeles, CA. May 5-9, 1985. Abstr. Jf-4, p. 133.
24. Lifshitz, S., Savage, J. E., Taylor, K. A., Tewfik, H. H., and VanOrden, D. E. Plasma prostaglandin levels in radiation-induced enteritis. Int. J. Radiat. Oncol. Biol. Phys. 8: 275-277, 1982.

25. Jaffe, B. M., Behrman, H. R., and Parker, C. W. Radioimmunoassay measurement of Prostaglandins E, A and F in human plasma. J. Clin. Invest. 52: 398-405, 1972.
26. Utley, J. F., Marlowe, C., and Waddell, W. J. Distribution of ^{35}S-labeled WR-2721 in normal and malignant tissues of the mouse. Radiat. Res. 68: 284-291, 1976.
27. Rasey, J. S., Nelson, N. J., Mahler, P., Anderson, K., Krohn, K. A., and Menard, T. Radioprotection of normal tissues against gamma rays and cyclotron neutrons with WR-2721: LD_{50} studies and ^{35}S-WR-2721 biodistribution. Radiat. Res. 68: 284-291, 1976.
28. Kligerman, M. M., Glover, D. J., Turrisi, A. T., Norfleet, A. L., Yuhas, J. M., Coia, L. R., Simone, C., Glick, J. H., and Goodman, R. L. Toxicity of WR-2721 administered in single and multiple doses. Int. J. Radiat. Oncol. Biol. Phys. 10: 1733-1776, 1984.
29. Hanson, W. R., and Thomas, C. 16,16-dimethyl prostaglandin E_2 increases survival of murine intestinal stem cells when given before photon radiation. Radiat. Res. 96: 393-398, 1983.
30. Walden, T. L., Snyder, S. L., Patchen, M. L., and Steel, L. K. Enhanced LD 50/30 survival in mice by 16,16 dimethyl prostaglandin E_2. 34th Annual Meeting of Radiation Research Society, Las Vegas, Nevada, April 12-17, 1986. Abstract Cl-11, p. 41.
31. Mennie, A. T., Dalley, V. M., Dinneen, L. C., and Collier, H. O. J. Treatment of radiation-induced gastrointestinal distress with acetylsalicylate. Lancet 2: 942-943, 1975.
32. Granström, E., Diczfalusy, U., and Hamberg, M. The thromboxanes. In: "Prostaglandins and Related Substances." C. Pace-Asciak and E. Granström, eds. Elsevier Science Publishers, Amsterdam, The Netherlands, 1983, pp. 45-93.
33. Granger, D. N., and Parks, D. A. Role of oxygen radicals in the pathogenesis of intestinal ischemia. Physiologist 26: 159-164, 1983.
34. Taylor, L., and Polgar, P. Stimulation of prostaglandin synthesis by ascorbic acid via hydrogen peroxide formation. Prostaglandins 19: 693-700, 1980.
35. Taylor, L., Menconi, M. J., and Polgar, P. The participation of hydroperoxides and oxygen radicals in the control of prostaglandin synthesis. J. Biol. Chem. 258: 6855-6857, 1983.
36. Seregi, A., Serfozo, P., and Mergl, Z. Evidence for the localization of hydrogen peroxide-stimulated cyclooxygenase activity in rat brain mitochondria: A possible coupling with monoamine oxidase. J. Neurochem. 40: 407-413, 1983.
37. Hemler, M. E., Cook, H. W., and Lands, W. E. M. Prostaglandin biosynthesis can be triggered by lipid peroxides. Arch. Biochem. Biophys. 193: 340-345, 1979.
38. Egan, R. W., Paxton, J., and Kuehl, F. A., Jr. Mechanism for irreversible self-destruction of prostaglandin synthetase. J. Biol. Chem. 251: 7329-7335, 1976.
39. Steel, L. K., Jacobs, A. J., Giambarresi, L. I., and Jackson, W. E., III. Protection of mice against fission neutron irradiation by WR-2721 or WR-151327. Radiat. Res. 109: 469-478, 1987.

RADIATION RESEARCH 112, 555–563 (1987)

Ionizing Radiation Alters Neuronal Excitability in Hippocampal Slices of the Guinea Pig[1]

J. M. TOLLIVER AND T. C. PELLMAR

Physiology Department, Armed Forces Radiobiology Research Institute, Bethesda, Maryland 20814-5145

TOLLIVER, J. M. AND PELLMAR, T. C. Ionizing Radiation Alters Neuronal Excitability in Hippocampal Slices of the Guinea Pig. *Radiat. Res.* **112**, 555–563 (1987).

To investigate the effects of ionizing radiation on an isolated neuronal network without complicating systemic factors, slices of hippocampus from the guinea pig were isolated and studied *in vitro*. Slices were irradiated with a ^{60}Co source and compared to paired, sham-irradiated controls. Electrophysiological activity in the CA1 population of pyramidal cells was evoked by stimulation of the stratum radiatum. Analysis of the somatic and dendritic responses suggested sites of radiation damage. Orthodromically evoked activity was significantly decreased in slices receiving greater than 75 Gy γ radiation. The effects were dose and dose-rate dependent. At 20 Gy/min, doses of 50 Gy and greater produced synaptic impairment while doses of 75 Gy and greater also produced postsynaptic damage (i.e., the ability of the synaptic response to generate an action potential). A lower dose rate, 5 Gy/min, reduced the sensitivity of synaptic damage to radiation exposure; synaptic impairment required a dose of 100 Gy or greater at the lower dose rate. In contrast, postsynaptic damage was not sensitive to dose rate. This study demonstrates that ionizing radiation can directly affect the integrated functional activity of neurons.

INTRODUCTION

Ionizing radiation alters the excitability of the mammalian nervous system. It has been known for some time that exposure to 4–10 Gy X rays modifies electroencephalographic activity in a variety of brain areas (*1–3*). One of the most sensitive areas is the hippocampus where spiking activity develops (*1–3*). Bassant and Court (*4*) examined the cellular response of the hippocampus to γ radiation and found that 4 Gy altered neuronal firing patterns.

Several factors can contribute to the acute nervous system damage *in vivo*. Systemic blood pressure is reduced following exposure to 25–100 Gy γ radiation (*5, 6*) and cerebral blood flow decreases in a variety of brain regions including the hippocampus (*7*). The ischemia produced by decreased blood flow is likely to affect neuronal activity (*8*). The blood–brain barrier is thought to be disrupted by ionizing radiation (*9,*

[1] This work was supported by the Armed Forces Radiobiology Research Institute, Defense Nuclear Agency, under work unit 00105. Views presented in this paper are those of the authors; no endorsement by the Defense Nuclear Agency has been given or should be inferred. Research was conducted according to the principles enunciated in the "Guide for the Care and Use of Laboratory Animals" prepared by the Institute of Laboratory Animal Resources, National Research Council.

0033-7587/87 $3.00

10). This would allow radiation-released neuromodulatory substances such as neurotensin, histamine, and serotonin, as well as other circulating factors, abnormal access to the neurons.

The present study was initiated to determine the effects of radiation directly on neuronal properties. To do this brain tissue was isolated from the animal and irradiated *in vitro*. Hippocampus was chosen because of its particular sensitivity to ionizing radiation. In addition, the hippocampal slice provides an excellent preparation (*11*) where neural pathways are maintained and input/output relationships of a relatively homogenous population of neurons can be analyzed.[2]

METHODS

Male guinea pigs were anesthetized with halothane inhalation and killed by cervical dislocation. The brain was quickly removed from the skull and chilled in iced solution containing (in m*M*): NaCl, 124; KCl, 3.0; $CaCl_2$, 2.4; $MgSO_4$, 1.3; KH_2PO_4, 1.24; glucose, 10; and $NaHCO_3$, 26, equilibrated with 95% O_2/5% CO_2. The hippocampus from the left hemisphere was dissected free and slices approximately 400–450 μm thick were cut with a McIlwain tissue chopper. Keeping the tissue chilled during this phase of preparation has been shown to enhance tissue viability (*12*). Adjacent slices were alternated between two beakers filled with the iced solution. Since the shape of the slices varied through the length of the hippocampus, physical appearance was used later to pair adjacent slices for analysis. Hippocampal slices were incubated for approximately 2 h in normal solution at room temperature (22–26°C) bubbled constantly with 95% O_2/5% CO_2. Incubation at room temperature allows recovery from the trauma of dissection. These methods, as developed in a number of laboratories, provide healthy slices of hippocampus (*12*).

Beakers containing slices were removed to an exposure room where one beaker was placed in the radiation field and the other beaker (containing control slices) was positioned in a shielded area. Transportation to the exposure room required only 2 to 3 min, at which time both beakers were again oxygenated with 95% O_2/5% CO_2. The beakers contained Plexiglas lining to minimize radiation scatter during the exposure. Doses of 6.25 to 200 Gy γ radiation at dose rates of either 5 or 20 Gy/min were supplied through a ^{60}Co source. Dose rate, calibrated with a 50-cc ionization chamber, was controlled by adjusting the distance between the tissue and the bilateral ^{60}Co source. After radiation exposure, slices were returned to the laboratory for electrophysiological recording.

Slices were placed sequentially in a submerged slice recording chamber maintained at 30 ± 1°C. This temperature permitted accurate recordings of electrophysiological events. The tissue in the chamber was constantly perfused with normal solution at a rate of approximately 1 ml/min. Usually two pairs of control and irradiated slices were tested for each animal. Data were collected within 15 min of placing a slice in the recording chamber. Data collection was always complete within 1.5 h of radiation exposure. Nonradiated tissue stays healthy and responsive for more than 8 h.

The hippocampal brain slice maintains a high degree of organization that can be visualized through a dissecting microscope. The organization of the slice and the arrangement of the stimulating and recording

---

[2] In this paper several neurophysiological terms are used repeatedly. For easy reference these terms, some synonyms, and their definitions are listed here: *Orthodromic pathway*, afferent pathway, synaptic pathway—a pathway providing input to the neurons through a synapse. *Antidromic pathway*—pathway consisting of the axons of the neurons studied. *Population spike*, PS, somatic response—the summated action potential recorded extracellularly from a population of neurons in response to stimulation of a synaptic pathway. *Population synaptic potential*, pop PSP, dendritic response—the summated response to stimulation of a synaptic pathway, recorded extracellularly from the dendritic region, stratum radiatum. *Afferent volley*, volley—summated action potential of the fibers in the afferent pathway. *Spiking*—firing of action potentials. *Single unit*—a single neuron whose electrical activity is studied with extracellular recording. *Stratum radiatum*, dendritic layer—layer of hippocampus containing dendrites of CA1 neurons and afferent pathways (see Fig. 1). *Stratum pyramidale*, cell body layer, somatic layer—layer of hippocampus containing the cell bodies of CA1 neurons.

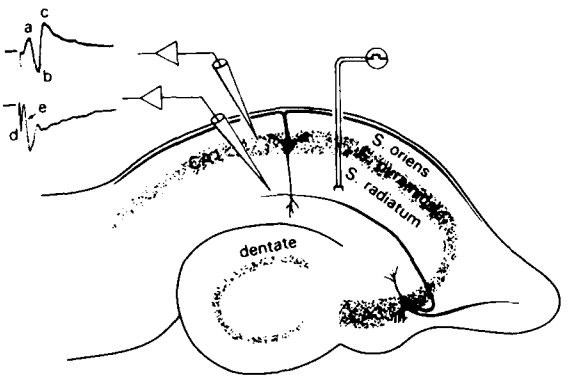

FIG. 1. Schematic of hippocampal brain slice. Stimulating electrode is positioned in stratum radiatum which contains afferent fibers to CA1 pyramidal cells. Recording electrodes are placed in cell body layer of CA1 region, stratum pyramidale, and in the dendritic region, stratum radiatum. Traces show typical recordings of population spike from stratum pyramidale (top) and pop PSP from stratum radiatum (bottom). PS amplitude is calculated from potentials at points a, b, and c; $(a + c)/2 - b$. Afferent volley is at point d. Pop PSP is quantitated from the slope at point e.

electrodes are illustrated in Fig. 1. A stimulating electrode (concentric bipolar, stainless steel, DKI) was placed in the stratum radiatum to stimulate the orthodromic pathway (i.e., synaptically mediated input). A glass recording electrode filled with 2 *N* NaCl was placed in the stratum pyramidale to record the population spike (PS). This response (Fig. 1, top trace) results from the synchronous firing of action potentials in the neuronal cell bodies near the microelectrode (*13*). The amplitude of the PS is measured as the difference between the greatest negativity (point b on Fig. 1, top trace) and the average of the early (point a) and the late (point c) positivity. A second glass recording electrode was positioned in the stratum radiatum to record the dendritic response. The population synaptic potential (pop PSP) (Fig. 1, lower trace) is the summated extracellular response of the dendrites to synaptic input (*14*). The maximum early slope (at point e) of the pop PSP was measured to quantitate the dendritic response. The afferent volley (point d), a measure of the number of presynaptic axons that are stimulated by the stimulus (Fig. 1c), was also recorded with the electrode in the stratum radiatum.

Electrical recordings were obtained through the glass microelectrodes, amplified with a high gain extracellular amplifier, and monitored on an oscilloscope. The recordings were digitized, stored, and analyzed on an LSI 11-03 microcomputer. An isolated constant current source was used to provide stimuli ranging from 0 to 1.5 mA, 200 μs duration at 0.2 Hz to the stimulating electrodes. Four traces at each stimulus intensity from both the dendritic and the somatic recording sites were averaged and used to generate input-output curves. These curves consisted of three relationships: (1) afferent volley vs population spike, (2) afferent volley vs pop PSP, and (3) pop PSP vs population spike. The first (volley vs PS) reflects the ability of presynaptic activity to elicit an action potential in the postsynaptic neurons. This encompasses both synaptic and postsynaptic mechanisms. The second curve (volley vs pop PSP) reflects primarily synaptic mechanisms: effectiveness of the presynaptic axons to produce a postsynaptic potential. The third curve (pop PSP vs PS) reflects postsynaptic mechanisms: effectiveness of a postsynaptic depolarization to evoke an action potential. Analysis of these curves can therefore provide information on the site of radiation damage.

Composite input-output curves were constructed for control and radiated slices at each radiation dose as previously described (*15*). Averages and standard errors at each stimulus strength were computed for the volley amplitude, PS amplitude, and pop PSP slope for both treated slices and the paired controls. The input-output data for each radiation dose were plotted and computer fit with the equation for a sigmoid curve. Differences between the control and treated curves were tested for significance by comparing the residual sum of squares for the individual curves with the residual sum of squares for a curve fit to a composite of control and test data. Significance was accepted at $P < 0.05$.

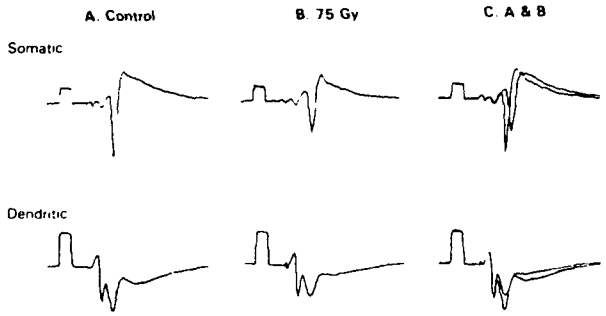

FIG. 2. Effect of 75 Gy γ radiation at 20 Gy/min on PS and pop PSP. (A) Recordings from control slice. (B) Recordings from a paired irradiated slice at same stimulus intensity. (C) Superimposition of records in A and B to accentuate the radiation effect. PS (somatic response) and pop PSP are reduced but afferent volley is not changed. Square wave preceding each trace is calibration pulse of 1 mV, 2 ms. Stimulus artifact has been deleted from the traces.

Dose–response curves were constructed for each of the three input–output curves developed for each radiation dose. For each input–output curve, a parameter was calculated from the ratio of the maximal y value and the x value at half-maximal y. This ratio was found to provide reliable quantification for the curves, showing significant differences between control and radiated curves consistent with the residual sum of squares method described above. Radiation effect was expressed as the percentage decrease in this ratio. Standard errors for the ratios were computed from the errors associated with the parameters of the fitted curves. Data for both dose rates (20 and 5 Gy/min) were plotted and compared using these ratios. Significance was determined for the differences between the effects at the two rates. $P < 0.05$ was considered significant.

Preliminary results have been reported previously (*16*).

RESULTS

Stimulation of the stratum radiatum in hippocampal slices produces an orthodromic response that can be recorded in the cell body layer (PS) and the dendritic layer (pop PSP). Although the responses from animal to animal could vary substantially, using paired slices from the same animal and attempting to position the electrodes reproducibly could minimize variability. Examples of recorded responses are illustrated in Fig. 2. The population spike in the control slice was evoked with a stimulus strength of 0.25 mA. The pop PSP was recorded simultaneously. In the paired slice, exposed to 75 Gy γ radiation at a dose rate of 20 Gy/min, the population spike evoked with the same stimulus intensity was substantially smaller (by 25%). The afferent volley, visible in the recording of the dendritic response, was unchanged. The pop PSP, however, was also significantly reduced. Similar recordings were obtained at 16 stimulus intensities in both control and irradiated slices. At this dose and dose rate, nine slice pairs were examined.

From these data, input–output curves (Fig. 3) were constructed as described under Methods. The first curve (volley vs PS, Fig. 3A) shows the net effect of radiation on the population spike. At 75 Gy, 20 Gy/min, radiation significantly decreased the population spike at most stimulus intensities. The maximum amplitude for the averaged PS was smaller (by 24%) in irradiated slices. The afferent volley amplitude re-

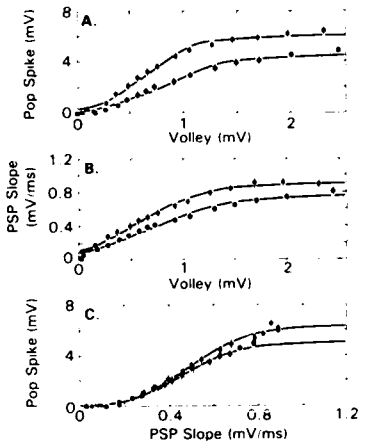

FIG. 3. Input–output curves for slices irradiated at 75 Gy, 20 Gy/min (circles) and their paired controls (squares). Error bars represent standard error of the mean of PS amplitude in A and C and standard error of the mean of pop PSP slope in B. Irradiated slices $n = 9$; paired controls $n = 9$. (A) For equivalent volley size, the PS is smaller in amplitude following radiation. Maximum amplitude of PS is decreased. (B) Volley is less efficient in evoking pop PSP after radiation. (C) At this dose and rate, the radiation-induced decrease in the ability of the pop PSP to elicit a PS is not significant.

quired to evoke a half-maximal PS was increased by 33%. Figure 3B illustrates the effect of this radiation exposure on the dendritic response. The afferent volley produced smaller pop PSPs in slices exposed to radiation than in control. In contrast, Fig. 3C shows that the ability of the pop PSP to evoke a PS was essentially unchanged by radiation exposure of 75 Gy at 20 Gy/min. Analysis of these curves suggests, therefore, that the effect of γ radiation (75 Gy at 20 Gy/min) on the population spike amplitude was due to impairment of synaptic function.

This analysis was done for six doses (doses in Gy, 6.25 $n = 8$, 50 $n = 12$, 75 $n = 7$, 100 $n = 10$, 150 $n = 6$, and 200 $n = 4$) at 5 Gy/min and four doses (50 $n = 6$, 75 $n = 9$, 100 $n = 17$, and 200 $n = 5$) at 20 Gy/min. From the three input–output curves constructed at each dose, three dose–response curves were constructed (Fig. 4). From these curves one can determine the degree and site of damage at each dose for the two dose rates. The dose–response curve in Fig. 4A was constructed from the first of the input–output curves and reflects the net effect of radiation on the amplitude of the population spike. It encompasses effects of radiation on both synaptic and postsynaptic mechanisms. The dose–response curve in Fig. 4B shows the dose-dependent decrease in the synaptic response. It was constructed from the input–output curve of volley vs pop PSP. The third dose–response curve (Fig. 4C) illustrates the dose dependence of postsynaptic effects reflecting the ability of the pop PSP to evoke the population spike.

At a dose rate of 5 Gy/min, a dose of 75 Gy produced a significant decrease in the population spike (Fig. 4A). Higher doses produced an effect of greater magnitude. At 200 Gy the population spike was completely blocked in the irradiated slices. The dose–response curve was shifted to the left with a higher dose rate (20 Gy/min). At

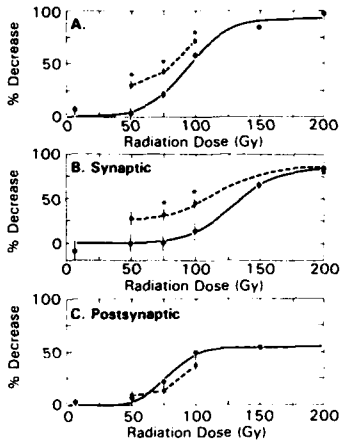

FIG. 4. Dose-response curves for ^{60}Co radiation at dose rates of 5 Gy/min (circles) or 20 Gy/min (squares). Asterisks indicate significant differences between the effects of the two dose rates at the same dose. See text for details of construction and analysis of dose-response curves. (A) Net effect of radiation on population spike. Higher dose-rate shifts curve to the left. (B) Curve for radiation effect on synaptic mechanisms is also shifted left by higher dose rate. (C) Postsynaptic deficits caused by γ radiation are not significantly dose-rate dependent.

50 Gy where a dose rate of 5 Gy/min produced no significant decrease in the population spike, the dose rate of 20 Gy/min caused significantly more damage. The decrease in the population spike by 200 Gy at 20 Gy/min was so complete, a sigmoid curve could not be fitted to the experimental data, and therefore a percentage decrease at this dose could not be calculated. It is for this reason that only the three doses at 20 Gy/min are represented in Fig. 4A.

Figure 4B shows the dose response for the effect of radiation on synaptic effects. At 5 Gy/min only 150 and 200 Gy produced statistically significant decreases in the pop PSP. Even at these high doses the maximal reduction in the synaptic response is 75%. A dose rate of 20 Gy/min shifted the dose-response curve to the left and produced a significant decrease in synaptically evoked dendritic responses as low as 75 Gy. As at the lower dose rate, a dose of 200 Gy caused 75% decrease. Close examination of the figure reveals an interesting, although not statistically significant, trend. At 5 Gy/min doses less than 75 Gy actually showed small increases in the synaptic response. This is most evident at 6.25 Gy. It is possible that lower doses at similar or lower dose rates will reveal an excitatory effect.

The dose dependence of the postsynaptic response is shown in Fig. 4C. Unlike the synaptic damage caused by the radiation, postsynaptic damage was not dose-rate dependent. At both 5 and 20 Gy/min there was a significant decrease at 75 Gy. At 100 Gy the effects appear to be maximal at a 55% decrease in the ability of the dendritic response to evoke a population spike. Increasing the dose to 150 Gy at 5 Gy/min did not increase the damage. The effect at 200 Gy for both dose rates could not be included in Fig. 4C because the synaptic responses at this dose were too limited in range to allow curves to be fit to the experimental data.

DISCUSSION

This study is the first to demonstrate that moderate doses of radiation can *directly* affect the integrated functional activity of neurons. At a dose rate of 5 Gy/min, 75 Gy of ^{60}Co radiation significantly decreases the orthodromic population spike. At this dose, the radiation damage is primarily due to a postsynaptic mechanism. Synaptic impairment only contributes to the damage at 150 Gy and greater. A higher dose rate of 20 Gy/min more effectively decreases the orthodromic response. This results from the dose-rate effect on synaptic damage. At 20 Gy/min, synaptic deficits occur at doses as low as 50 Gy. In contrast, the increased dose rate does not significantly modify postsynaptic damage.

The differences in dose-rate dependence of postsynaptic and synaptic effects may indicate that different mechanisms underlie the two steps involved in eliciting the orthodromic population spike. Lipid peroxidation, a consequence of ionizing radiation that modifies membrane properties and might contribute to neuronal dysfunction, is more readily produced at lower dose rates. This inverse dose-rate relationship is most dramatic at rates less than 1 Gy/min and less steep at higher rates (*17*). If this holds true in our experiments on hippocampal tissue, lipid peroxidation would be an unlikely mechanism for the deficits that are seen at the synapse, but might underlie the damage observed at the postsynaptic site.

Although several studies have addressed the effect of radiation on EEG activity and evoked potentials, investigations of radiation damage on a more cellular level in neurons of the brain are limited. Single unit activity has been recorded in rat olfactory bulb (*18*) and rabbit hippocampus (*4*) *in vivo*. Very short exposures to X radiation (2–8 cGy) at low rates (90 cGy/min) altered the activity of neurons in the olfactory bulb, most typically increasing firing rate during exposure but decreasing activity after termination of exposure (*18*). A more recent study by Bassant and Court (*4*) showed that activity of single units in the hippocampus was greatly reduced by 4.5 Gy γ radiation at 14 cGy/min. Similarly, Popova and Shlyafer (1968 as quoted in (*4*)) found that 7 Gy X radiation at 17 cGy/min decreased the number of hippocampal units responding to a sensory stimulus.

In these *in vivo* studies, many factors can influence the neuronal activity following radiation. Ionizing radiation (25–100 Gy ^{60}Co) decreases brain–blood flow and blood pressure (*5–7*). Ischemic episodes are known to alter spontaneous and evoked activity (*19*). Since radiation can break down the blood–brain barrier (*9, 10*), circulating factors that are increased by radiation, such as histamine, or other plasma constituents may come in contact with neurons and influence their excitability. To eliminate these influences, neural tissue can be irradiated *in vitro*. Peimer *et al.* (*20*) irradiated hippocampal slices with 0.7–86 cGy X rays and ^{137}Cs at dose rates of 8.4–258 cGy/min. Spontaneously bursting single units in the CA1 region (possibly interneurons because of their firing pattern (*21, 22*)) increased their burst rate with radiation exposure. However, the very low doses and dose rates used by Peimer *et al.* (*20*) make comparisons with the present study difficult.

The effects of ionizing radiation reported here are very similar to those of hydrogen peroxide (and of peroxide with ferrous sulfate) in hippocampal slices (*23*). Like ^{60}Co radiation, peroxide and peroxide/iron reduce the orthodromic population spike

through both synaptic and postsynaptic mechanisms. Hydrogen peroxide interacts with iron to produce hydroxyl free radicals, one of the more reactive oxygen species generated by ionizing radiation. An electrophysiological analysis of peroxide damage (*24*) indicated that resting membrane potential, membrane resistance, and directly evoked action potentials are unchanged. Yet the cells are less capable than normal of maintaining a train of action potentials. Excitatory postsynaptic potentials and inhibitory postsynaptic potentials, however, are decreased. This effect is likely to be presynaptic since the neurons respond normally to exogenously applied neurotransmitter. An increase in the depolarization required to evoke the calcium component of the action potential was observed and may be responsible for this presynaptic action of peroxide. It is possible that similar changes in neuronal electrophysiology occur with radiation. Preliminary intracellular recordings support this possibility. A recording from a neuron in a hippocampal slice exposed to 100 Gy γ radiation showed normal directly evoked action potentials, resting membrane potential, and membrane resistance. Yet, evoked synaptic potentials were smaller than normal and failed to elicit action potentials (J. M. Tolliver and T. C. Pellmar, unpublished observations).

In summary, our results indicate that ionizing radiation can alter neuronal excitability in isolated brain tissue. Damage occurs both synaptically and postsynaptically, probably through different molecular mechanisms. The ionic and molecular mechanisms involved in the actions of radiation are currently under investigation.

ACKNOWLEDGMENTS

The authors thank Mr. H. L. Leikin, Mr. W. E. Jackson, and Dr. G. L. King for helpful discussions.

RECEIVED: April 8, 1987; REVISED: July 10, 1987

REFERENCES

1. H. GANGLOFF, Acute effects of X-irradiation on brain electrical activity in cats and rabbits. In *Effects of Ionizing Radiation on the Nervous System*, pp. 123–135. International Atomic Energy Agency, Vienna, 1962.
2. T. J. HALEY, Changes induced in brain activity by low doses of X-irradiation. In *Effects of Ionizing Radiation on the Nervous System*, pp. 171–185. International Atomic Energy Agency, Vienna, 1962.
3. R. L. SCHOENBRUN, E. CAMPEAU, and W. R. ADEY, Electroencephalographic and behavioral effects from x-irradiation of the hippocampal system. In *Response of the Nervous System to Ionizing Radiation, Second International Symposium* (T. J. Haley and R. S. Snider, Eds.), pp. 411–428. Little, Brown, Boston, 1964.
4. M. H. BASSANT and L. COURT, Effects of whole-body γ irradiation on the activity of rabbit hippocampal neurons. *Radiat. Res.* **75**, 593–606 (1978).
5. P. H. CHAPMAN and R. J. YOUNG, Effect of cobalt-60 gamma irradiation on blood pressure and cerebral blood flow in the *Macaca mulatta*. *Radiat. Res.* **35**, 78–85 (1968).
6. L. G. COCKERHAM, T. J. CERVANY, and J. D. HAMPTON, Postradiation regional cerebral blood flow in primates. *Aviat. Space Environ. Med.* **57**, 578–582 (1986).
7. L. G. COCKERHAM, E. L. PAUTLER, and J. D. HAMPTON, Radiation-induced hippocampal ischemia altered with antihistamines and disodium cromoglycate. *Fed. Proc.* **44**, 1357 (1985).
8. T. KIRINO, A. TAMURA, and K. SANO, Selective vulnerability of the hippocampus to ischemia—Reversible and irreversible types of ischemic cell damage. *Prog. Brain Res.* **63**, 39–58 (1985).

9. T. W. GRIFFIN, J. S. RASEY, and W. A. BLEYER, The effect of photon irradiation on blood brain barrier permeability to methotrexate in mice. *Cancer* **40,** 1109–1111 (1977).
10. T. SCHETTLER and C. N. SHEALY, Experimental selective alteration of blood–brain barrier by x-irradiation. *J. Neurosurg.* **32,** 89–94, (1970).
11. P. ANDERSON, Brain slices—A neurobiological tool of increasing usefulness. *Trends Neurosci.* **4,** 53–56 (1981).
12. B. E. ALGER, S. S. DHANJAL, R. DINGLEDINE, J. GARTHWAITE, G. HENDERSON, G. L. KING, P. LIPTON, A. NORTH, P. A. SCHWARTZKROIN, T. A. SEARS, M. SEGAL, T. S. WHITTINGHAM, and J. WILLIAMS, Brain slice methods. In *Brain Slices* (R. Dingledine, Ed.), pp. 381–437. Plenum Press, New York, 1984.
13. P. ANDERSON, T. V. P. BLISS, and K. K. SKREDE, Unit analysis of hippocampal population spikes. *Exp. Brain Res.* **13,** 208–221 (1971).
14. P. ANDERSON, H. SILFVENIUS, S. H. SUNDBERG, O. SVEN, and H. WIGSTROM, Functional characteristics of unmyelinated fibers in the hippocampal cortex. *Brain Res.* **144,** 11–18 (1978).
15. J. M. TOLLIVER and T. C. PELLMAR, Dithiothreitol elicits epileptiform activity in CA1 of the guinea pig hippocampal slice. *Brain Res.* **404,** 133–141 (1987).
16. T. C. PELLMAR and J. M. TOLLIVER, Effects of ionizing radiation on hippocampal excitability. In *Brain Slices: Fundamentals, Applications and Implications* (A. Schurr, T. J. Teyler, and M. T. Tseng, Eds.), pp. 152–156, Karger, Basel, 1987.
17. J. A. RALEIGH, W. KREMERS, and B. GABOURG, Dose-rate and oxygen effects in models of lipid membranes: Linoleic acid. *Int. J. Radiat. Biol.* **31,** 203–213 (1977).
18. G. P. COOPER and D. J. KIMELDORF, The effect of X-rays on the activity of neurons in the rat olfactory bulb. *Radiat. Res.* **27,** 75–86 (1966).
19. R. SUZUKI, T. YAMAGUCHI, C. L. LI, and I. KLATZO, The effects of 5-minute ischemia in Mongolian gerbils. II. Changes of spontaneous neuronal activity in cerebral cortex and CA1 sector of hippocampus. *Acta Neuropathol. (Berlin)* **60,** 217–222 (1983).
20. S. I. PEIMER, A. O. DUDKIN, and A. G. SWERDLOV, Response of hippocampal pacemaker-like neurons to low doses of ionizing radiation. *Int. J. Radiat. Biol.* **49,** 597–600 (1986).
21. M. MUHLETHALER, S. CHARPAK, and J. J. DREIFUSS, Contrasting effects of neuropophysial peptides on pyramidal and non-pyramidal neurones in the rat hippocampus. *Brain Res.* **308,** 97–107 (1984).
22. W. D. KNOWLES and P. A. SCHWARTZKROIN, Local circuit synaptic interactions in hippocampal brain slices. *J. Neurosci.* **1,** 318–322 (1981).
23. T. C. PELLMAR, Electrophysiological correlates of peroxide damage in guinea pig hippocampus in vitro. *Brain Res.* **364,** 377–381 (1986).
24. T. C. PELLMAR, Peroxide alters neuronal excitability in the CA1 region of guinea pig hippocampus in vitro. *Neuroscience* (1987), in press.

From: PROSTAGLANDIN AND LIPID METABOLISM IN RADIATION INJURY
Edited by Thomas L. Walden, Jr. and Haywood N. Hughes
(Plenum Publishing Corporation, 1987)

A PARADOXICAL ROLE FOR EICOSANOIDS: RADIOPROTECTANTS AND RADIOSENSITIZERS

T. L. Walden, Jr.

Department of Radiation Biochemistry
Armed Forces Radiobiology Research Institute
Bethesda, Maryland 20814-5145

ABSTRACT

Understanding the radiobiology of eicosanoids is complicated by their ability to act as mediators of damage and recovery and as radioprotective agents. Changes in the tissue concentrations of eicosanoids following irradiation are dependent on several factors, including the type of eicosanoid, time postirradiation, radiation dose, and other contributing mediators and enzyme changes in the surrounding microenvironment. Many of these same prostaglandins and the leukotrienes have been shown to be radioprotective when given before irradiation.

INTRODUCTION

The eicosanoids are a group of biological mediators that have received attention in the field of radiobiology as mediators of radiation injury (1-3) and recently as radioprotective agents (4-6). They are metabolites of arachidonic acid (Figure 1), an essential 20-carbon fatty acid containing four unsaturated double bonds (7). Arachidonic acid is primarily esterified in the second position of the glycerol backbone of phospholipids in the cell membranes. Ultraviolet and ionizing radiation stimulate the release of free arachidonic acid through the action of phospholipases (8-10). Increased calcium concentrations also stimulate the phospholipase release of arachidonic acid. Following arachidonic acid release, one of three events occurs (outlined in Figure 1): (a) re-esterification of the free arachidonic acid back into the cell membrane, or (b) and (c) metabolism through the arachidonic acid cascade. Arachidonic acid is metabolized (Figure 1) through either the cyclooxygenase pathway (B), leading to the formation of prostaglandins, thromboxane, and prostacyclin, or the lipoxygenase pathway (C), leading to the formation of leukotrienes, lipoxins, and hydroxy fatty acids. These compounds have a number of important physiological roles in vasoregulation, smooth muscle regulation, electrolyte balance, and neuroregulation, as well as pathological roles in inflammation, fever, pain, and shock (reviewed in reference 7).

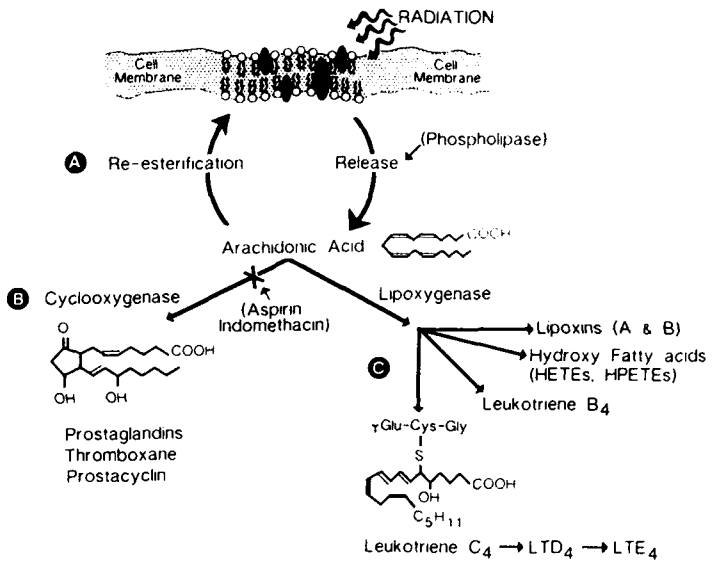

Fig. 1. Arachidonic acid cascade. Radiation stimulates release of free arachidonic acid from phospholipids of cell membrane. Once released, arachidonic acid may be (a) re-esterified back into cell membrane, (b) metabolized through cyclooxygenase pathway, or (c) metabolized through lipoxygenase pathway. Compounds that block either pathway may be exerting a beneficial effect by inhibiting production of a particular eicosanoid or by shunting more arachidonic acid into products of other pathway.

PROSTAGLANDINS IN RADIATION INJURY

The role of prostaglandins in radiation injury has been recently reviewed (11). Irradiation has been shown to alter tissue prostaglandin levels, producing both elevations (12-17) and decreases (1,17,18). The response following irradiation depends on dose received (18,19), tissue irradiated (1,13-19), and time of determination postirradiation (1). Some radiation-induced alterations in prostaglandin synthesis may persist for months after exposure to radiation or, conversely, may not become altered until several months postexposure (12). Prostaglandin changes following irradiation have been demonstrated *in vitro* in fibroblasts (11), endothelial cells (20), tissue slices, homogenates (21,22), and urine (23). Several effects of radiation on prostaglandin metabolism in the blood vessels are summarized in Figure 2. Alteration of tissue prostaglandin levels may result from either anabolic or catabolic processes, or from combinations of the two. Exposure of minipig skin to X radiation results in the increased production of prostaglandin E_2 (PGE_2) over the first 24 hours postirradiation (13). Early PGE_2 elevation in X-irradiated minipig skin is followed by a progressive decrease in PGE_2, which corresponds to an increase in prostaglandin F_2 (PGF_2) tissue levels. These latter processes are the result of an increase in 9-keto prostaglandin reductase, an enzyme that converts PGE_2 to PGF_2. There is an association between alterations in the spleen prostaglandin levels of

irradiated mice and alterations in the activity of prostaglandin dehydrogenase (24), an enzyme responsible for prostaglandin inactivation. Increases in prostaglandin E_1 (PGE_1) in the spleen postirradiation are caused by decreased enzymatic catabolism, leading to accumulation.

A role for prostaglandins as mediators of radiation injury has been suggested in experiments using cyclooxygenase-inhibiting drugs, such as indomethacin (3) or aspirin (2,25), to reduce specific radiation-induced inflammatory responses. These experiments indicate that prostaglandins contribute to radiation-induced ocular tissue inflammation in rabbits (2), mucositosis in humans (14), esophagitis in opossums (3), and gastrointestinal syndrome in mice (26). Prostaglandins may mediate inflammation through increased extravasation, vasoregulation, and fever and as chemotactic factors for phagocytic white blood cells (reviewed recently in references 7,27). Radiation may also affect the ability of the receptor to bind the prostaglandin and induce a specific function. The specific binding of prostaglandin E_2 is decreased in the spleens and small intestines of irradiated mice (28). The effects of indomethacin on alteration of whole animal survival are contradictory, and have been shown to either enhance survival (29) or have no effect (30). The reasons for the different responses to nonsteroidal anti-inflammatory drugs are not

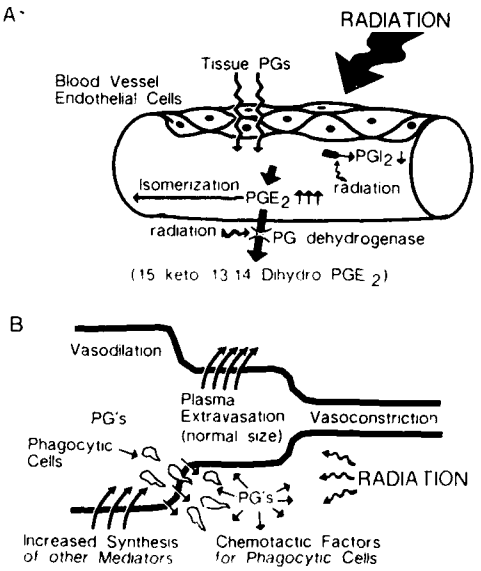

Fig. 2. A: Effects of radiation on prostaglandin metabolism by blood vessels. This figure presents a brief summary and is based on observations observed in human umbilical arteries (ref. 18) and in mouse spleen (ref. 24). B: Prostaglandin effects on blood vessels. Radiation induces an alteration of prostaglandin concentrations. These compounds may be either vasodilatory or vasoconstrictive, depending on class of prostaglandin released, particular vascular site, and prostaglandin concentration. As indicated, they may induce synthesis of other mediators or act as chemotactic agents.

known, but one may speculate that they are related to the dosage and schedule of administration.

PROSTAGLANDINS AND LEUKOTRIENES IN RADIOPROTECTION

Paradoxically, the prostaglandins have pathological roles in damage, but they also function as radioprotectants for cells in culture (6,31) and hematopoietic and intestinal stem cells (4) *in vivo,* and also enhance whole animal survival (5). Several studies on prostaglandin-induced modification of radiosensitivity in cell culture provide evidence that protection may be associated with elevations in cyclic AMP (6,31). These studies have centered on the use of PGE_1, a potent cAMP stimulus. For prostaglandin enhancement of whole animal survival from otherwise lethal exposure to ionizing radiation, the processes are more complicated, and the basic underlying mechanism(s) remains unknown. The most effective prostaglandin in terms of whole animal survival (31; Walden et al., submitted) is 16,16-dimethyl prostaglandin E_2 ($DiPGE_2$) (Figure 3), an analog of the naturally occurring prostaglandin E_2. Misoprostil, an analog of PGE_1, appears to be more effective for protection of the intestinal crypt cells (32). $DiPGE_2$ has a biological half-life in the tens of minutes (5), as illustrated and explained in Figure 3. The naturally occurring prostaglandin E_2 has a half-life of 2 minutes (7). Forty μg of $DiPGE_2$/mouse (1.6 mg/kg body weight) enhances the LD50/30 of mice exposed to cobalt-60 gamma radiation, providing a dose modification factor of 1.72 (5). Radioprotection by eicosanoids is both time and dose dependent, and must be

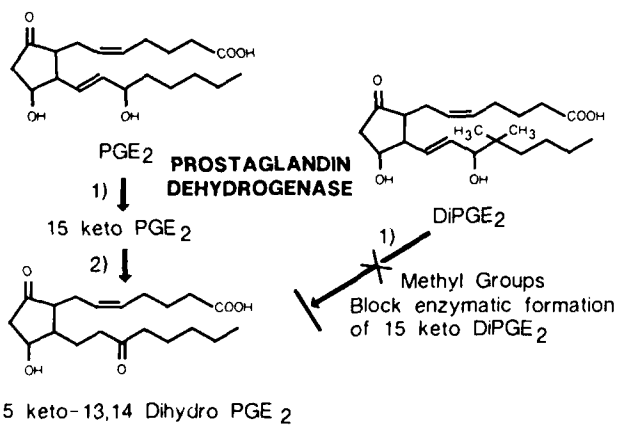

Fig. 3. Inactivation of prostaglandin E_2 but not 16,16-dimethyl prostaglandin E_2 ($DiPGE_2$). Prostaglandin E_2 in vasculature is normally inactivated by lung through action of prostaglandin dehydrogenase. Methyl groups in 16 position of $DiPGE_2$ prevent this inactivation step from occurring at 15 position, extending biological half-life. $DiPGE_2$ is primarily inactivated by liver (ref. 39).

administered just prior (approximately 15 min) to irradiation (5,33; Walden et al., submitted). There does not appear to be a common vascular end point induced by radioprotective eicosanoids, since some are vasodilatory and others are vasoconstrictive, and there is no general effect on the hematocrit (Walden et al., submitted). Pharmacological studies indicate that the $DiPGE_2$ protection results from the parent analog rather than a metabolite. However, the optimal period of radioprotection does not correlate with the optimal concentrations of $DiPGE_2$ in the tissue (5).

A decrease in locomotor activity (33) is produced by radioprotective concentrations of $DiPGE_2$. The optimal time for protection (5-60 min) is shorter than the duration of the locomotor behavior decrement (33). A marked depression of the locomotor activity occurred within 5 min postadministration of 10 μg $DiPGE_2$/mouse or greater. The behavior of $DiPGE_2$-treated mice returns to control levels by 6 hours following a 10-μg $DiPGE_2$ dose and 30 hours following a 40-μg dose (33). Diarrhea is another undesirable effect of some but not all of the radioprotective eicosanoids (Walden et al., submitted). It may be possible in the future to separate the detrimental effects without a decrease in protective efficacy.

Most work on the radiobiology of arachidonic acid metabolites to date has centered on the prostaglandins, primarily because the standards and radioimmunoassay kits for analyses are commercially available. Arachidonic acid may also be metabolized by the lipoxygenase pathway (Figure 1) to form leukotrienes and hydroxy fatty acids. Ultraviolet-B irradiation of human skin produced a threefold elevation of 12-hydroxy eicosatetraenoic acid 24 hours postirradiation, although no changes in leukotriene B_4 levels were observed (34). Leukotriene C_4, a thiol ether of glutathione and the triene-containing 20-carbon backbone, is elevated in the plasma of mice receiving hematoporphyrin derivative-induced phototherapy (400- to 410-nm wavelength radiation) and may be related to mast cell degranulation (35). Leukotriene C_4 modifies the radiosensitivity of V79A03 Chinese hamster cells in culture (36). Two-hour pretreatment with 2.5 μM leukotriene C_4 doubles the number of cells surviving a subsequent X irradiation (reproductive survival, based on colony formation). This protection is concentration dependent and appears to be associated with specific leukotriene C4-binding sites on the cell surface. Leukotriene C_4 also induces radioprotection and enhances the LD50/30 of mice (Walden, submitted).

Future research directions in eicosanoid radioprotection need to focus on the mechanism of action for this novel class of biological mediators/radioprotective agents. Effective radioprotective concentrations of arachidonic acid metabolites are in the μg/animal range (1.6 μg/kg body weight) (4,5), compared to mg/mouse (200-800 mg/kg body weight) required for the classical thiol radioprotectants. Several mechanisms may be involved in protection. The role of specific receptor activation provides the opportunity to enhance and control the protection. If a primary component of protection is receptor mediated, it may be possible to selectively protect all normal tissues that have receptors, but not those normal and tumor tissues that lack the receptor. Eicosanoid-induced events mediated on the cellular level by a receptor may enhance their effects on these cells and also other tissues

through systemic responses to eicosanoids that might occur through the cardiovascular system. Actions at these higher levels may play significant roles in the radioprotection. The success of the long-lived $DiPGE_2$, an analog of PGE_2, as a protective agent points to the need to develop other biologically stable eicosanoid analogs that retain radioprotective efficacy with minimal side effects.

Tumors secreting biological mediators with protective activity may modify the efficacy of the therapy. This appears to be the case for several of the prostaglandin-secreting tumors (37). The prostaglandin may conceivably protect the tumor at the cellular level by elevation of cyclic AMP (5,31) or glutathione (38), or at a systemic level by suppression of the immune system (1). An interesting set of experiments relating to this issue were conducted using the HSDM1C1 mouse fibrosarcoma cell line, which has been shown to secrete high levels of PGE_2 (38). Radiation clonogenic survival curves were performed in the presence or absence of flurbiprofen, a cyclooxygenase inhibitor. The two survival curves do not significantly differ, and may indicate that the PGE_2 produced by this tumor cell line does not feed back and modify its own cellular radiosensitivity. It is not known whether this cell line has receptors to PGE_2, and if the radioprotection is receptor mediated, then the lack of PGE_2 receptors may explain the inability of PGE_2 to act as a radioprotectant in this cell line.

ACKNOWLEDGMENTS

This research was supported by the Armed Forces Radiobiology Research Institute (AFRRI), Defense Nuclear Agency, under Research Work Unit 000153. The views presented in this paper are those of the authors; no endorsement by the Defense Nuclear Agency has been given or should be inferred. Any AFRRI research included in this review was performed according to the principles enunciated in the "Guide for the Care and Use of Laboratory Animals," prepared by the Institute of Laboratory Animal Resources, National Research Council.

REFERENCES

1. Trocha, P. J., and Catravas, G. N. Prostaglandins, lysosomes, and radiation injury. In: "Advances in Prostaglandin and Thromboxane Research," Volume 7. B. Sammuelsson, P. W. Ramwell, and R. Paoletti, eds. Raven Press, New York, 1980, pp. 851-856.
2. Bito, L. Z., and Klein, E. M. The role of arachidonic acid cascade in the species-specific X-ray-induced inflammation of the rabbit eye. Invest. Opthalmol. Vis. Sci. 22: 579-587, 1982.
3. Northway, M. G., Libshitz, H. I., Osborne, B. M., Feldman, M. S., Mamel, J. J., West, J. H., and Szwarc, I. A. Radiation esophagitis in the opossum: Radioprotection with indomethacin. Gastroenterology 78: 883-892, 1980.

4. Hanson, W. R., and Ainsworth, E. J. 16,16-Dimethyl prostaglandin E2 induces radioprotection in murine intestinal and hematopoietic stem cells. Radiat. Res. 103: 196-203, 1985.
5. Walden, T. L., Jr., Patchen, M. L., and Snyder, S. L. 16,16-Dimethyl prostaglandin E_2 increases survival in mice following irradiation. Radiat. Res. 109: 440-448, 1987.
6. Prasad, K. N. Radioprotective effect of prostaglandin and an inhibitor of cyclic nucleotide phosphodiesterase on mammalian cells in culture. Int. J. Radiat. Biol. 22: 187-189, 1972.
7. Ogburn, P. L., and Brenner, W. E."The Physiologic Actions and Effects of Prostaglandins." UpJohn, Kalamazoo, 1981.
8. Camp, R. D., Greaves, M. W., Hensby, C. N., Plummer, N. A., and Warin, A. P. Irradiation of human skin by short wavelength ultraviolet radiation (100-290 nm) (u.v.C): Increased concentrations of arachidonic acid and prostaglandins E2 and F2a. Br. J. Clin. Pharmac. 6: 145-148, 1978.
9. Black, A. K., Greaves, M. W., Hensby, C. N., Plummer, N. A., and Warin, A. P. The effects of indomethacin on arachidonic acid and prostaglandins E2 and F2a levels in human skin 24 hours after u.v.B. and u.v.C. irradiation. Br. J. Clin. Pharmac. 6: 261-266, 1978.
10. Snyder, D. S. Effect of topical indomethacin on UVR-induced redness and prostaglandin E levels in sunburned guinea pig skin. Prostaglandins 11: 631-643, 1976.
11. Polgar, P., Hahn, G., and Taylor, L. Radiation effects on eicosanoid formation. In: "Biochemistry of Arachidonic Acid Metabolism." W. E. M. Lands, ed. Kluwer Academic Publishers, Boston, 1985, pp. 161-173.
12. Ts'Ao, C. H., Ward, W. F., and Port, C. D. Radiation injury in rat lung. I. Prostacyclin (PGI2) production, arterial perfusion and ultrastructure. Radiat. Res. 96: 284-293, 1983.
13. Ziboh, V. A., Mallia, C., Morhart, E., and Taylor, J. R. Induced biosynthesis of cutaneous prostaglandins by ionizing radiation. Proc. Soc. Exp. Biol. Med. 169: 386-391, 1982.
14. Tanner, N. S., Stamford, I. F., and Bennett, A. Plasma prostaglandins in mucositis due to radiotherapy and chemotherapy for head and neck cancer. Br. J. Cancer 43: 767-771, 1981.
15. Eisen, V., and Walker, D. I. Effect of ionizing radiation on prostaglandin-like activity in tissues. Br. J. Pharmac. 57: 527-532, 1976.
16. Steel, L. K., Rafferty, M. A., Wolfe, W. W., Egan, J. E., Kennedy, D. A., Catravas, G. N., Jackson, W. E., III, and Dooley, M. A. Urinary excretion of cyclic nucleotides, creatinine, prostaglandin E2, and thromboxane B2 from mice exposed to whole-body irradiation from an enhanced neutron field. Int. J. Radiat. Biol. 50: 695-715, 1986.
17. Trocha, P. J., and Catravas, G. N. Effect of radioprotectant WR2721 on cyclic nucleotides, prostaglandins, and lysosomes. Radiat. Res. 94: 239-251, 1983.
18. Allen, J. B., Sagerman, R. H., and Stuart, M. J. Irradiation decreases vascular prostacyclin formation with no concomitant effect on platelet thromboxane production. Lancet 2: 1193-1195, 1981.

19. Pausescu, E., Chirvasie, R., Popescu, M.-V., and Tedodsiu, T. Dynamics of the changes in the cerebral amounts of cyclic AMP and some prostaglandins during cobalt-60 gamma-radiation-induced brain edema. Physiologie 14: 283-289, 1977.
20. Rubin, D. B., Drab, E. A., Ts'Ao, C. H., Gardner, D., and Ward, W. F. Prostacyclin synthesis in irradiated endothelial cells cultured from bovine aorta. J. Appl. Physiol. 58: 592-597, 1985.
21. Steel, L. K., Sweedler, I. K., and Catravas, G. N. Effects of ^{60}Co radiation on synthesis of prostaglandins F2a, E, and thromboxane B2 in lung airways of the guinea pigs. Radiat. Res. 94: 156-165, 1983.
22. Gal, D., Strickland, D. M., Lifshitz, S., Buchsbaum, H. J., and Mitchell, M. D. Effect of radiation on prostaglandin production by human bowel *in vitro*. Int. J. Radiat. Oncol. Biol. Phys. 10: 653-657, 1984.
23. Donlon, M., Steel, L. K., Helgeson, E. A., Shipp, A., and Catravas, G. N. Radiation induced alterations in prostaglandin excretion in the rat. Life Sci. 32: 2631-2639, 1983.
24. Walker, D I., and Eisen, V. Effect of ionizing radiation on 15-hydroxy prostaglandin dehydrogenase (PGDH) activity in tissue. Int. J. Radiat. Biol. 36: 399-407, 1979.
25. Mennie, A. T., and Dalley, V. M. Aspirin in radiation-induced diarrhea. Lancet 1: 1131, 1973.
26. Borowska, A., Sierakowski, S., Mackowiak, J., and Wisiniewski, K. A prostaglandin-like activity in small intestine and postirradiation gastrointestinal syndrome. Experientia 35: 1368-1370, 1979.
27. Weissman, G. "Prostaglandins in Acute Inflammation." UpJohn, Kalamazoo, 1980.
28. Prianishikova, E. N., Zhulanova, Z. I., and Agaf'eva, V. S. Effect of different doses of ionizing radiation on the binding of prostaglandin E2 in mouse tissues. Radiobiologiia (USSR) 26: 652-655, 1986.
29. Popisil, M., Netikova, J., and Kozubik, A. Enhancement of hematopoietic recovery by indomethacin after sublethal whole-body gamma irradiation. Acta Radiol. Oncol. 25: 195-198, 1987.
30. Steel, L. K., and Ledney, G. D. Effects of neutron irradiation on PGE2 and TXB2 levels in biological fluids: Modification by WR-2721. In: "Prostaglandins and Lipid Metabolism in Radiation Injury." T. L. Walden and H. N. Hughes, eds. Plenum Press, New York, 1987 (this volume).
31. Lehnert, S. Modification of postirradiation survival of mammalian cells by intracellular cyclic AMP. Radiat. Res. 62: 107-116, 1975.
32. Hanson, W. R., Houseman, K. A., and Collins, P. W. *In vivo* radiation protection by prostaglandins and related compounds of the arachidonic acid cascade. Pharmacol. Ther., in press.
33. Landauer, M. R., Walden, T. L., Davis, H. D., and Dominitz, J. A. Alterations in locomotor activity induced by radioprotective doses of 16,16-dimethyl prostaglandin E2. In: "Prostaglandins and Lipid Metabolism in Radiation Injury." T. L. Walden and H. N. Hughes, eds. Plenum Press, New York, 1987 (this volume).

AD-A194 461 AFRRI (ARMED FORCES RADIOBIOLOGY RESEARCH INSTITUTE) 3/3
REPORTS OCTOBER NOVEMBER AND DECEMBER 1987(U) ARMED
FORCES RADIOBIOLOGY RESEARCH INST BETHESDA MD MAR 88
UNCLASSIFIED F/G 22/1 NL

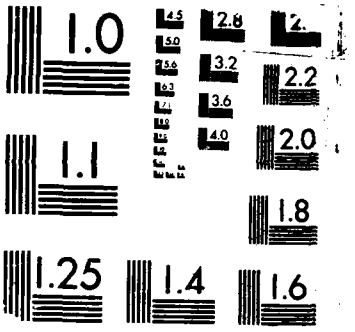

MICROCOPY RESOLUTION TEST CHART

BUREAU OF STANDARDS-1963-A

34. Black, A. K., Barr, R. M., Wong, E., Brain, S., Greaves, M. W., Dickinson, R., Shroot, B., and Hensby, C. N. Lipoxygenase products of arachidonic acid in human inflamed skin. Br. J. Clin. Pharmacol. 20: 185-190, 1985.
35. Kerdel, F. A., Soter, N. A., and Lim, H. W. *In vivo* mediator release and degranulation of mast cells in hematoporphyrin derivative-induced phototoxicity in mice. J. Invest. Dermatol. 88: 277-280, 1987.
36. Walden, T. L., Jr., Holahan, E. V., and Catravas, G. N. Development of a model system to study leukotriene-induced modification of radiation sensitivity in mammalian cells. Prog. Lipid Res. 25: 587-590, 1986.
37. Bennett, A. Cancer. In: "Biological Protection With Prostaglandins," Volume I. M. M. Cohen, ed. CRC Press, Boca Raton, Florida, 1986, pp. 73-80.
38. Millar, B. C., and Jinks, S. Do prostaglandins affect cellular radiosensitivity *in vitro?* Int. J. Radiat. Biol. 46: 367-373, 1984.
39. Weeks, J. R., Ducharme, D. W., Magee, W. E., and Miller, W. L. The biological activity of the (15S)-15-methyl analogs of prostaglandin E2 and F2. J. Pharmac. Exp. Ther. 186: 67-74, 1973.

AFRRI TECHNICAL REPORT

Comparison of AFRRI and ETCA dosimetry measurements at AFRRI TRIGA reactor

M. Dooley

G. H. Zeman

AFRRI TR87-1

DEFENSE NUCLEAR AGENCY

ARMED FORCES RADIOBIOLOGY RESEARCH INSTITUTE

BETHESDA, MARYLAND 20814-5145

REVIEWED AND APPROVED

GARY H. ZEMAN
Commander, MSC, USN
Chairman
Radiation Sciences Department

RICHARD I. WALKER
Commander, MSC, USN
Acting, Scientific Director

GEORGE W. IRVING, III
Colonel, USAF, BSC
Director

CONTENTS

INTRODUCTION

A team of physicists from the Etablissement Technique Central de l'Armament (ETCA), a component of the French Ministry of Defense, performed a series of dosimetric measurements at the Armed Forces Radiobiology Research Institute (AFRRI) TRIGA (Training Research Isotopes General Atomic) reactor on 10-12 September 1985. The purpose of the experiment was to begin the process of comparing results from radiobiology research, done at high dose rates close to the source, to battlefield effects studies, performed at low dose rates far from the source.

The ETCA group used several types of personnel dosimeters (diodes, thermoluminescent dosimeters [TLD's], radiophotoluminescent glass [RPL], fission track detectors, and activation foils) to measure the kerma free in air (FIA) and the dose inside an anthropomorphic dosimetry phantom (a lucite cylinder 30 cm in diameter and 60 cm tall) in exposure room 1 of the AFRRI TRIGA reactor. As reference dosimetry, the ETCA group measured the FIA kerma rate with fission chambers, and AFRRI dosimetrists used ionization chambers to measure the FIA kerma rate and the dose rate midline in the phantom. All measurements were performed in exposure room 1 with the 15-cm shield in place with the center of all arrays set at 70 cm from the tank wall and 120 cm above the floor. Results of ETCA and AFRRI measurements were reported in references 1 and 2, respectively. This report compares the results obtained by the two groups and discusses some of the relevant problems met and the dosimetric information deduced from the experiment.

FIA MEASUREMENTS

The AFRRI group made ionization chamber measurements FIA at the array center point (70 cm from the tank wall and 120 cm above the floor), and the ETCA group made several measurements with fission chambers and passive dosimeters in a styrofoam array that covered the same volume as the AFRRI phantom. The results of these measurements are compared in Tables 1 and 2 and Figures 1 and 2. Table 1A shows that the FIA kerma measured with ionization chambers, fission chambers, and the Np foil all agree exceptionally well (within 5%). However, the diode data are about 10% lower than the AFRRI ionization chamber data. Table 1B shows that the FIA gamma-ray kerma measured by AFRRI ionization chambers and ETCA TLD's and RPL glass do not compare as well as the neutron kerma, with the TLD and RPL results 20%-25% higher than the AFRRI ionization chamber results. However, this large discrepancy in gamma-ray kerma did not affect the comparison of the total kerma, as shown in Table 1C. The total kerma measured by AFRRI and ETCA differs by only about $\pm$ 3%.

The measurements of distance and field size are compared in Table 2. In Table 2A, the AFRRI and ETCA distance measurements show the same trend, but the ETCA-measured neutron kerma falls off more rapidly with distance from the tank wall. Both the AFRRI and ETCA data in Table 2B indicate that laterally the field is fairly symmetrical about the center position.

Table 1. FIA Kerma Measurements in ER1: 15 cm Pb, 70 cm From Tank Wall

A. Neutron kerma

Nominal Reactor Power	AFRRI Ion chambers (cGy/kW - min)	ETCA Fission chambers (cGy/kW - min)
0.3 kW	6.00	6.00
1.0 kW	6.00	5.72
Precision	± 1%	± 3%

	Ion chambers (Gy)	Fission chambers (Gy)	Np foil (Gy)	Diodes (Gy)
5.0 kW	4.1	3.9	4.1	3.7

B. Gamma kerma (Gy)

	AFRRI	ETCA	
	Ion chambers	TLD's	RPL glass
5.0 kW	0.41	0.51	0.49

C. Total kerma (Gy)

	AFRRI	ETCA			
		Fission chambers		Np foil	
	Ion chambers	TLD's	RPL	TLD's	RPL
5.0 kW	4.51	4.41	4.39	4.61	4.59

Table 2. Spatial Variation Measurements in ER1

A. Normalized neutron kerma versus distance from tank wall

Detector	Distance From Tank Wall (cm): 55	70	85
AFRRI Rh	1.54	1.00	0.65
AFRRI S	1.53	1.00	0.68
ETCA FC[1]	1.62	1.00	0.66
ETCA diodes	1.65	1.00	0.60

B. Normalized neutron kerma versus lateral distance from center at 70 cm from tank wall

	Distance From Center (cm): (Left, facing core)		(Right)
Detector	15	0	15
AFRRI Rh	1.02	1.00	1.00
AFRRI S	1.01	1.00	0.98
ETCA FC	--	1.00	0.97
ETCA diodes	0.99	1.00	0.97

[1] Fission chambers

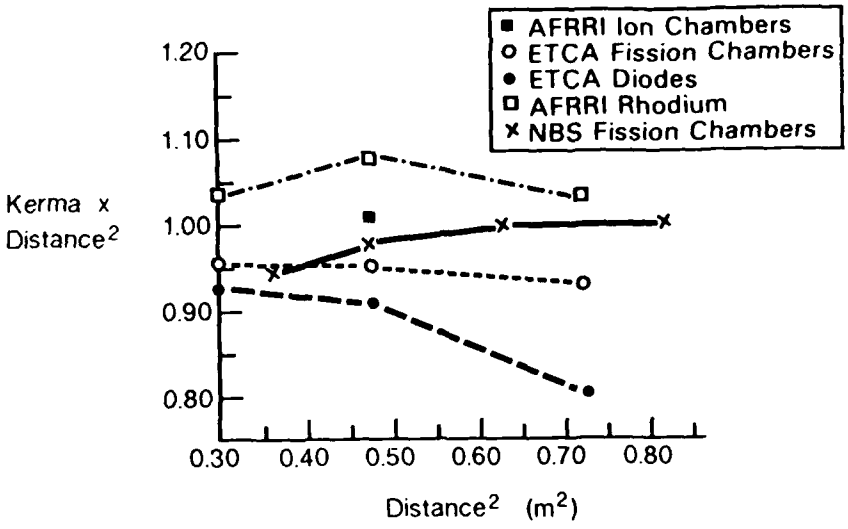

Figure 1. Measurements made in exposure room 1 with 15-cm-Pb shield. Distances were referenced to the reactor tank wall as source center. See text for details.

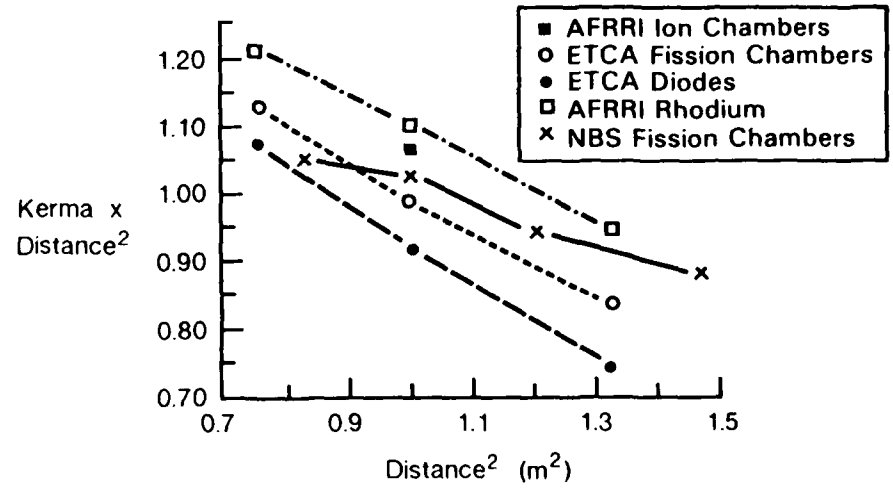

Figure 2. Measurements made in exposure room 1 with 15-cm-Pb shield. Distances were referenced to the center of the reactor core as source center. See text for details.

IN-PHANTOM MEASUREMENTS

Two irradiations were performed with dosimeters inside the anthropomorphic dosimetry phantom. The AFRRI ionization chambers were placed in hollow plastic tubes and inserted in the phantom about 6 cm above the ETCA dosimeters (diodes, TLD's, and RPL glass). Small holes were machined into solid plastic rods so that the ETCA detectors could be placed every 3 cm through the centerline of the phantom. In the first run, the phantom was positioned with the dosimeters parallel to the core centerline so that the depth dose through the phantom was measured. The phantom was rotated 90 degrees for the second run. At that time the dosimeters were perpendicular to the core centerline, and the lateral variation across the midline of the phantom was measured. Note that AFRRI made ionization chamber measurements midline in the phantom only during the second run. The dose for the first run was calculated from the readings of a monitor chamber attached to the lead shield. Table 3 compares the results at the center point in the phantom. The ETCA data are plotted in Figures 3 and 4.

The results of the in-phantom runs show poorer agreement than do the FIA results. ETCA-measured neutron doses at the center of the phantom are 12%-28% higher than those measured with AFRRI ionization chambers. The gamma-ray dose measured by the ETCA TLD's and RPL glass differed from the gamma-ray dose measured by the AFRRI ionization chamber by -25% to +27%. In addition, the TLD and RPL data differed from each other by as much as 40%.

Table 3. Absorbed Dose (Gy) Midline in AFRRI Anthropomorphic Dosimetry Phantom

AFRRI			ETCA				
Ion chambers			n	g		Total	
n	g	Total	Diodes	TLD's	RPL	TLD's	RPL
0.34	1.18	1.52	0.38[1]	0.88	1.50	1.26	1.88
			0.435[2]	1.10	0.99	1.54	1.43

[1] Detectors parallel to core (depth dose)

[2] Detectors perpendicular to core (lateral variation)

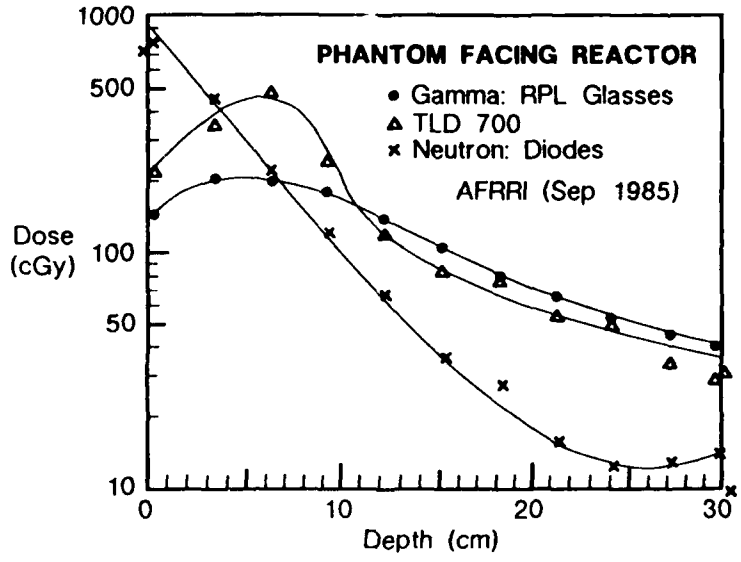

Figure 3. ETCA-measured depth dose through AFRRI anthropomorphic dosimetry phantom (ref. 2)

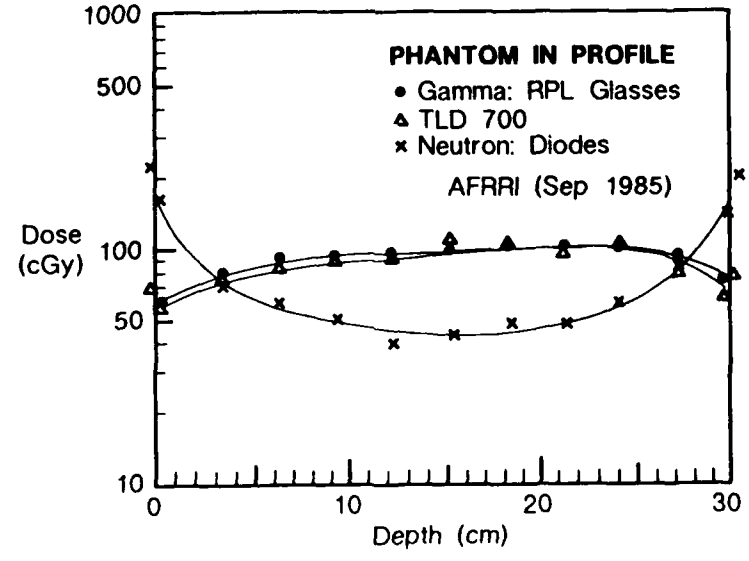

Figure 4. ETCA-measured lateral (side to side) dose through midline of AFRRI anthropomorphic dosimetry phantom (ref. 2)

DISCUSSION

FIA RESULTS

The agreement between AFRRI and ETCA measurements of neutron kerma was excellent at the FIA reference point (70 cm from the tank wall and 120 cm above the floor). This is especially encouraging considering that the methods of dosimetry used by each group were based on fundamentally different physical principles. Note also that the AFRRI ionization chamber results, which indicated a neutron kerma rate of 1.003 mGy/kW·sec, agreed very well with the 1.027 mGy/kW·sec measured at low nominal power levels in the ion chamber intercomparison between the National Bureau of Standards (NBS) and AFRRI for this same configuration (3). The FIA gamma-ray measurements did not compare as well, with as much as a 25% difference between the ETCA and AFRRI data. This difference may be due in part to the sensitivity of the TLD 700's and RPL glass to thermal and fast neutrons.

IN-PHANTOM RESULTS

As indicated above, the in-phantom measurements of the ETCA and AFRRI groups did not show good agreement. Several concerns about the experiment that may have contributed are discussed below.

(a) The positioning of the phantom and the dosimeters inside the phantom is extremely critical. The ETCA dosimeters were placed 15.2 cm inside the phantom, and the AFRRI chambers were centered 15 cm inside the phantom. Although this is a very small difference, Figure 3 shows that the dose is changing very rapidly in this region, on the order of 15% per cm. A small positioning error could translate into a much larger discrepancy in the measured neutron dose.

(b) Differences were also seen in the radiation geometry between the AFRRI ionization chambers and the ETCA detectors. The ionization chambers were placed in hollow plastic tubes and inserted into the phantom, whereas the ETCA insert rod was made of solid plastic with small holes for the dosimeters. It is possible that these subtle geometry differences altered the neutron scattering and absorption in the vicinity of the detectors.

(c) The neutron dose measured by the diodes was not consistent for the two phantom runs. The diode response may be dependent on orientation, or this discrepancy could have been due to the positioning problem mentioned above. Unfortunately, ionization chamber data were available for only the second run, so the positioning theory cannot be corroborated. More work needs to be done to resolve this disparity.

(d) The two types of ETCA gamma-ray dosimeters did not agree well with the AFRRI ionization chambers in the phantom, nor did they agree with each other. These dosimeters may have a fast neutron sensitivity dependent on neutron energy as well as a sensitivity to thermal neutrons. In addition, ETCA has attributed the disagreement in part to calibration procedures (2), and further studies by ETCA are under way to clarify this discrepancy.

FIA SPATIAL VARIATION

Figures 1 and 2 depict how well the neutron kerma follows an inverse square relationship with distance from the tank wall (Figure 1) and the core center (Figure 2). Plotted on the ordinate is the neutron kerma multiplied by the distance squared (mGy · m^2/kW·sec), and on the abscissa is the distance squared (m^2). The data are normalized to the AFRRI ion chamber measurements at 0.7 m from the tank wall (1.0 m from the core center). A horizontal line in these curves means that the neutron kerma decreases with distance proportionally to the inverse of the distance squared, as expected from a point source. The data from Figures 1 and 2 indicate that the effective source center is close to the reactor tank wall, not at the core center. This same trend was demonstrated by fission chamber measurements obtained by NBS at AFRRI in March 1985 (4), and these data are included in Figures 1 and 2.

DEPTH DOSE MEASUREMENTS

The results of the ETCA in phantom measurements are summarized in Figures 3-5. In Figure 3, the uncorrected depth dose data are plotted. In Figure 5, the inverse square portion of the data is removed so that only attenuation in the phantom is considered. Also provided in Figure 5 are similar data taken by ETCA at the SILENE reactor (5). The neutron depth dose data show exponential attenuation until about 26 cm into the phantom, with an approximate half-value layer of about 4.5 cm (using the corrected data). These data agree with previous large-phantom studies at AFRRI (6-8). The exponential attenuation indicates that the shape of the neutron energy spectrum does not change much through a hydrogenous phantom. However, at the exit side of the phantom, the neutron dose seems to increase slightly. This was also seen in previous work and has been attributed to the incidence of scattered neutrons on the backside of the phantom (5,7).

As noted earlier, a large discrepancy was seen between data for the TLD and the RPL glass gamma-ray depth dose, especially in the first few centimeters in the phantom (see Figure 3). The ETCA group attributed this to the thermal neutron sensitivity of the TLD's, and it considers the RPL glass to be more accurate (2). The RPL glass data indicate that the gamma-ray dose increases until about 5 cm into the phantom and then decreases approximately exponentially through the rest of the phantom. This is probably because in the first few centimeters of the plastic, the production of gamma rays ($H[n, \gamma]^2H$) dominates over attenuation, but as the neutron flux decreases, the production rate also decreases and attenuation becomes more significant.

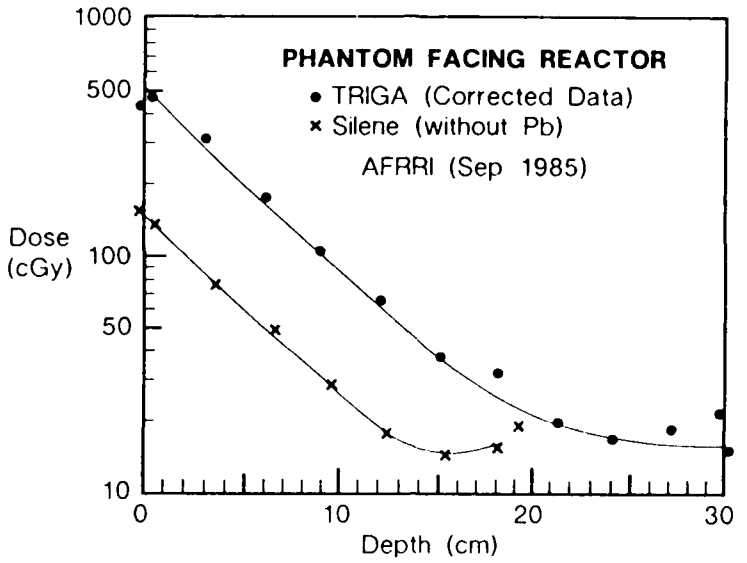

Figure 5. ETCA-measured neutron depth dose, corrected for inverse square (ref. 2)

In Figure 4, the lateral variation of the neutron and gamma-ray doses across the midline of the phantom is plotted. The data indicate that the dose is not symmetric about the center of the phantom. Because the FIA data indicated at most a 3% difference between the right and left sides, the asymmetry is probably a manifestation of the positioning difficulties mentioned above. In any event, the neutron dose decreases by a factor of about 5 from the outside edge of the phantom to the center, while the gamma-ray dose increases by about 50%.

SUMMARY

Using fundamentally different dosimetry techniques, ETCA and AFRRI obtained close agreement of the measured FIA kerma in exposure room 1 of the AFRRI TRIGA reactor. Many valuable data were collected concerning depth dose in an anthropomorphic phantom and also the spatial variation in the exposure room. However, more work is required to resolve some of the discrepancies found in the in-phantom measurements. This experiment was an important first step in relating mixed-field radiobiology studies to research concerning military applications on the nuclear battlefield.

REFERENCES

1. AFRRI Form 60, Dosimetry Report RUR#85-129, dated 19 September 1985. Armed Forces Radiobiology Research Institute, Bethesda, MD.

2. Serbat, A., Dhermain, J., and Le Teurnier, D. Rapport Preliminaire Concernant L'Experimentation a L'Army Force Radiobiology Research Institute en Septembre 1985. Establissement Technique Central de l'Armament, Centre D'Etudes Du Bochet, October 1985.

3. NBS Annual Progress Report on Program Support of Neutron Dosimetry, Work Unit Code 00078. DNA IACRO 83-847, October 1, 1984.

4. Dooley, M., Goodman, L. J., Zeman, G. H., Schwartz, R. B., Eisenhauer, C. M., and Blake, P. K. Ionization chamber intercomparison in mixed neutron and gamma-ray radiation fields by National Bureau of Standards and Armed Forces Radiobiology Research Institute. Technical Report TR86-3. Armed Forces Radiobiology Research Institute, Bethesda, MD, 1986.

5. Barry, F., and Lemaire, G. Silene. A typical solution-fueled irradiation facility. Proceedings of 1985 Workshop of Research Study Group on Assessment of Ionizing Radiation Injury in Nuclear Warfare. Published for NATO RSG.5 by Defense Research Establishment, Ottawa, Canada, September 1985, pp. 1-13.

6. Monroy, R. L., Zeman, G. H., Patchen, M. L., Darden, J. D., Feser, C. L., and MacVittie, T. J. Re-evaluation of the neutron effectiveness in the canine model. Proceedings of 1985 Workshop of Research Study Group on Assessment of Ionizing Radiation Injury in Nuclear Warfare. Published for NATO RSG.5 by Defense Research Establishment, Ottawa, Canada, September 1985, pp. 151-184.

7. Verrelli, D. M. Dosimetry for neutron radiation studies in miniature pigs. AFRRI Technical Note TN71-2. Armed Forces Radiobiology Research Institute, Bethesda, MD, 1971.

8. Verrelli, D. M., and Shosa, D. W. Comparison of dose patterns in a miniature pig exposed to neutron and to gamma radiation. AFRRI Technical Note TN71-5. Armed Forces Radiobiology Research Institute, Bethesda, MD, 1971.

END

DATE

FILMED

8-88

DTIC